The application of environmental isotopes in understanding of process in river catchments

Zibo Zhou

(*BSc, MSc*)

A thesis submitted for the degree of

Doctor of Philosophy

at Monash University in 2023

School of Earth, Atmosphere and Environment

Faculty of Science

Copyright notice

Contents

Abstract 1
Publications during enrolment 3
Thesis including published works declaration 4
Plain language summary 6
Acknowledgements 7
Chapter 1 Introduction 9
1.1 Research background and aims 9
1.2 Understanding the location and flux of baseflow to rivers 13
1.3 Timescales of water flow 16
1.4 Contrasts in catchment behavior between perennial and intermittent streams 18
1.5 Research methodology 20
1.6 Thesis structure 21
References 24
Chapter 2 Using geochemistry to identify and quantify the sources, distribution, and fluxes of baseflow to an intermittent river impacted by climate change: The upper Wimmera River, southeast Australia 37
Abstract 38
2.1 Introduction 39
2.1.1 Documenting baseflow inputs 41
2.1.2 Objectives 43
2.2 Study area 44
2.3 Materials and methods 47
2.3.1 Sampling 47
2.3.2 Analytical techniques 47
2.3.3 Radon (^{222}Rn) mass balance 48
2.3.4 Water mass balance 50
2.4 Results 51
2.4.1 Streamflow 51
2.4.2 Regional groundwater geochemistry 52
2.4.3 Stream water geochemistry 53

2.4.4 Radon emanation rates ... 57
2.4.5 Baseflow estimates from radon (^{222}Rn) ... 57
2.4.6 Baseflow estimates from water mass balance ... 61
2.5 Discussion and conclusion ... 62
2.5.1 Sources of water contributing to the stream ... 62
2.5.2 Controls on the temporal and spatial variations of baseflow discharge ... 64
2.5.3 Implications ... 64
References ... 67
Chapter 3 Sources and mean transit times of stream water in an intermittent river system: the upper Wimmera River, southeast Australia ... 83
Abstract ... 84
3.1 Introduction ... 85
3.1.1 Documenting mean transit times ... 86
3.1.2 Understanding water sources ... 89
3.1.3 Objectives ... 90
3.2 Study area ... 91
3.3 Materials and methods ... 93
3.3.1 Sampling ... 93
3.3.2 Analytical techniques ... 94
3.3.3 Mean transit times ... 95
3.3.4 Volumes of groundwater ... 97
3.4 Results ... 97
3.4.1 Streamflow ... 97
3.4.2 EC and major ion geochemistry ... 100
3.4.3 Stable isotopes ... 101
3.4.4 ^{3}H and ^{14}C activities ... 103
3.5 Discussion ... 106
3.5.1 Identification of water sources ... 106
3.5.2 Mean transit times of river water ... 108
3.5.3 Groundwater transit times ... 111
3.5.4 Comparison with perennial streams ... 112

3.6 Conclusions 113
References 115
Chapter 4 Integrating major ion geochemistry, stable isotopes (^{18}O, ^{2}H) and radioactive isotopes (^{222}Rn, ^{14}C, ^{36}Cl, ^{3}H) to understand the interaction between catchment waters and an intermittent headwater stream: the upper Avoca River, southeast Australia 130
Abstract 131
4.1 Introduction 133
4.2 Study area 136
4.3 Materials and methods 138
4.3.1 Sampling 138
4.3.2 Analytical techniques 139
4.3.3 Mean residence and mean transit times 141
4.4 Results 142
4.4.1 Streamflow 142
4.4.2 Major ion geochemistry and radon (^{222}Rn) 144
4.4.3 Stable isotopes 146
4.4.4 Radioactive isotopes (^{3}H, ^{14}C, and ^{36}Cl) 147
4.5 Discussion 151
4.5.1 Baseflow discharge to the river 151
4.5.2 Sources of water contributing to streamflow 152
4.5.3 $R^{36}Cl$ as a tracer of the solutes 153
4.5.4 Mean transit and residence times 154
4.6 Conclusions and summary 156
References 158
Chapter 5 Summary and conclusions 170
5.1 Research aims and methods 170
5.1.1 Integration of environmental tracers to understand intermittent streams 171
5.1.2 Limitations of environmental tracers 172
5.2 Baseflow discharge in intermittent streams 173
5.3 Timescales of water flow in intermittent streams 175
5.4 Implications for water resources management 176

5.5 Future research directions 177
References 179
Appendix 185

List of figures and tables

Figure 1. 1. Google Earth image of the upper Wimmera River and upper Avoca River (main channel). Inset shows location of study area in Australia. Red dashed lines represent the catchment boundaries. MDB = Murray-Darling Basin. The arrows show the flow directions and there are few perennial tributaries. 11

Figure 1. 2. Schematic diagram of multiple water sources sustaining the river flow in intermittent streams 12

Figure 1. 3. Schematic diagram of water components in perennial (a) and intermittent streams (b). GW = groundwater, NRW = near-river water. Bold arrow indicates that the contribution of NRW is more important in intermittent streams. 20

Figure 2.1. Summary geological and hydrogeological map of the upper Wimmera River. Stream water sampling sites and groundwater bores are indicated by numbers and letters, respectively. Gauging station and site numbers are: EVER = Eversley (415207), MCC = Mount Cole Creek (415245), CON = Concongella Creek (415237), GLYN = Glynwylln (415206), GLEN = Glenorchy (415201). Data from Robinson et al. (2006), Department of Environment, Land, Water and Planning (2020), Department of Jobs, Precincts and Regions (2020). 46

Figure 2.2. (a) Variations in streamflow and EC of the upper Wimmera River at Glynwylln (missing data are due to malfunction of measurement equipment). Sampling times are indicated by the diamond symbols. A and B represent high streamflow events in 2019 (Fig. 2.3). 2b. Flow duration curves for Eversley, Glynwylln and Glenorchy (Fig. 2.1) in 2019 and between 2000 and 2019. Line arrows show the conditions during the 2019 sampling campaigns. Data from the Department of Environment, Land, Water and Planning (2020). 52

Figure 2.3. EC vs streamflow hysteresis loops for high streamflow events in 2019 (A and B in Figure 2.2). Arrows show changes with time. Data from the Department of Environment, Land, Water and Planning (2020). 54

Figure 2.4. Downstream variations in ^{222}Rn activities (a) and Cl concentrations and ^{3}H activities (individual symbols) (b) in 2019 with inferred zones of high baseflow discharge (purple shading) and lower baseflow discharge (red shading). Shaded area indicates the range of ^{3}H activities in regional groundwater. (c) Topography variations along the river (topography data from International Agricultural Research Consortium database). Data from Table 2.1. 55

Figure 2.5. ^{3}H activities and EC of stream water at different flow conditions. Strong inverse correlations between ^{3}H activities and EC in September and November sampling rounds. Data from Table. 2.1.. 56

Figure 2.6. Baseflow influxes of each sampling period calculated from ^{222}Rn mass balance. Error bars represent the variations caused by net uncertainty (σ_t) based on uncertainty propagation (a). Cumulative baseflow and variations (dot lines) of overall uncertainty for the upper Wimmera River (b).. 59

Figure 3.1. Summary geological and hydrogeological map of the upper Wimmera River. Stream water sampling sites and groundwater bores are indicated by numbers and letters, respectively. The sites that have radioactive isotope data are shown in solid symbols. Gauging stations with site number are Eversley (EVER; 415207), Glynwylln (GLYN; 415206), and Glenorchy (GLEN; 415201). Background geological map from Department of Jobs, Precincts and Regions (2021) (© State Government of Victoria 1996-2021); other information from Robinson et al. (2006), Department of Environment, Land, Water and Planning (2021), and Zhou and Cartwright (2021). Boxes show ^{14}C (red) and ^{3}H activities (black) of groundwater (data from Table 3.2). 93

Figure 3.2. (a) Variations in daily rainfall, daily actual evapotranspiration, and temperature and (b) EC at Glynwylln (missing data are caused by measurement errors of equipment) and streamflow at Eversley, Glynwylln, and Glenorchy (Fig. 3.1) in the upper Wimmera River in 2019. Variations in EC at Glynwylln (missing data are caused by measurement errors of equipment) and streamflow at Eversley, Glynwylln, and Glenorchy (Fig.3.1) in the upper Wimmera River in 2019. Sampling times are indicated by arrowed lines. Shaded areas represent the zero-flow periods. Data from Department of Environment, Land, Water and Planning (2021) and Bureau of Meteorology (2021). 99

Figure 3.3. Trilinear diagram summarising molar major ion ratios of the different water sources in the upper Wimmera River (data from Table S1 and S2). GW=groundwater; PW= Pool Water; NRW=Near River Water; SW=Stream Water. Inserts show details of the data......................... 101

Figure 3.4. Stable isotope ratios of water samples in the upper Wimmera River. GMWL=Global Meteoric Water Line ($\delta^2H = 8.2 \times \delta^{18}O + 11.3$ ‰, as defined by Rozanski et al., 1993); MMWL= Melbourne Meteoric Water Line ($\delta^2H = 7.4 \times \delta^{18}O + 8.6$ ‰, as defined by Hughes and Crawford,

2012). GW=regional groundwater; PW=pool water; NRW=Near-river water; SW=stream water. The dashed line is the best fit for the pool water data. Data from Table S1 and S2. 102
Figure 3.5. ^{3}H activities vs. ^{14}C activities of groundwater from the upper Wimmera River. Curved lines are the predicted covariance in the radioisotopes predicted by the Exponential Mixing, Exponential-Piston (EPM ratio = 1), and Dispersion (DP=0.5) lumped parameter models. Solid arrowed lines show schematically the effects of mixing between old regional groundwater (low ^{14}C and ^{3}H free) and modern or recently recharged water (high ^{14}C and ^{3}H). Calcite dissolution lowers the predicted ^{14}C activities (dashed lines are used to display 10% calcite dissolution).. 104
Figure 3.6. (a) Variation of ^{3}H activities and δ^{2}H values and (b) ^{3}H activities and TDS of stream water, pool water and groundwater (GW) in the upper Wimmera catchment. arrows show trends expected from evaporation and mixing. Data from Table S1 and S2. 105
Figure 3.7. Variation of ^{3}H activities and streamflow. Pool water represents a time of zero streamflow. Shaded areas show ^{3}H range of modern rainfall and regional groundwater. Data from Table 3.1. 106
Figure 3.8. (a) Impacts of varying the ^{3}H activity of modern rainfall from 2.8 to 3.2 TU on MTTs calculated using the Exponential-Piston Flow Model (EPM ratio = 0.33). (b) Impacts of varying ^{3}H activity of rainfall between 90% and 110% of its assumed values on mean transit time calculated using the Exponential-Piston Flow Model (EPM ratio = 0.33). 110
Figure 3.9. (a) Comparison of ^{3}H activities and runoff coefficients at low and zero flow conditions and (b) volumes of water sustaining streamflows between the upper Wimmera River and other intermittent and perennial streams in southeast Australia. Error bars represent the uncertainty of annual rainfall in the upper Wimmera Catchment. Perennial streams are the Ovens, Latrobe, Yarra, and Gellibrand (data from Cartwright et al., 2020); intermittent streams are Deep Creek and Gatum (data from Cartwright and Morgenstern, 2016 and Barua et al., 2022). 113

Figure 4.1. Summary geological and hydrogeological map of the upper Avoca River. Stream water sampling sites and groundwater bores are indicated by numbers and letters, respectively. The inset shows the location in Victoria (VIC) and the Murry-Darling Basin (MDB). The sites that have ^{14}C, ^{3}H, and/or ^{36}Cl data are shown in solid symbols. Gauging stations with site number are Amphitheatre (AMPH; 408202), Archdale Junction (ARCH; 408206), and Coonooer (CONER;

408200). Background geological map from Department of Jobs, Precincts and Regions (2022). 138
Figure 4.2. (a) Variations in rainfall in the upper Avoca River and EC and Q (streamflow) at Amphitheatre (b) and Coonooer (c) (Fig. 4.1) in the upper Avoca River in 2019 (missing data during the flow period are caused by equipment failure). Shaded areas indicate the cease-to-flow period. Data from Department of Environment, Land, Water and Planning (2022) and Bureau of Meteorology (2022). 143
Figure 4.3. Downstream variations in ^{222}Rn (a) and Cl concentrations (b) during different flow conditions in the Avoca River. Solid symbols represent pool water samples and open symbols were tributaries samples. 144
Figure 4.4. Trilinear diagram summarising molar major ion ratios of the different water sources in the Avoca River (data from Table S3 and S4). GW=groundwater; PW= pool water; SW=stream water... 146
Figure 4.5. Stable isotope ratios of water samples in the Avoca catchment. MMWL = Melbourne Meteoric Water Line ($\delta^2H = 7.4 \times \delta^{18}O + 8.6$ ‰, as defined by Hughes and Crawford, 2012). GW = regional groundwater; PW = pool water; SW = stream water. The dashed line is the best fit for the pool water data. LEL=local evaporation line. Data from Table S4. 147
Figure 4.6. (a) ^{3}H activities vs. R^{36}Cl of groundwater (GW), pool water (PW), and stream water (SW) from the upper Avoca River and modern rainfall in the region. The curved line shows schematically the effects of mixing between young and old water end members. The shaded area represents the modern rainfall in the region. (b) ^{3}H activities vs. ^{14}C activities of groundwater from the upper Avoca River. Curved lines are the predicted covariance in the radioisotopes predicted by the Exponential Mixing, Exponential-Piston (EPM ratio = 1), and Dispersion (D_P=0.5) lumped parameter models. Solid lines show schematically the effects of mixing between old regional groundwater (low ^{14}C and ^{3}H free) and modern or recently recharged water (high ^{14}C and ^{3}H). Calcite dissolution lowers the predicted ^{14}C activities (dashed lines display trends with 10% calcite dissolution).. 150
Figure 4.7. (a) R^{36}Cl vs. Cl concentrations of groundwater (GW), pool water (PW), and stream water (SW) in July and August from the upper Avoca River. (b) R^{36}Cl vs. distance in PW and SW. Shaded areas represent the range of R^{36}Cl values in modern rainfall....................................... 151

Table 2.1. Streamflow and geochemistry of stream water from the upper Wimmera River 78
Table 2.2. Geochemistry of groundwater from the upper Wimmera Catchment 80
Table 2.3. Radon emanations from the upper Wimmera River alluvial sediments 81
Table 2.4. Parameters used for calculating net baseflow influxes by water mass balance (I_{net}) with net uncertainty (σ_t) between different gauges and comparison to ^{222}Rn mass balance (I_{RMB}) 82

Table 3.1. ^{3}H activities and calculated mean transit times (MTTs) from pool water and stream water of upper Wimmera River 128
Table 3. 2. ^{3}H, ^{14}C activities, and calculated MTTs by EPM (ratio=0.33) of groundwater from the upper Wimmera River... 129

Table 4.1. ^{3}H, ^{14}C activities, and calculated MTTs by exponential piston-flow model (EPM; ratio=0.33) of groundwater from the upper Avoca Catchment. letters in brackets represent location site in Fig 4.1... 148
Table 4.2. ^{3}H activities, $R^{36}Cl$ values and calculated mean transit times (MTTs) from pool water and stream water of upper Avoca River. Numbers in brackets represent location site in Fig 4.1. 149

S1-Geochemistry of stream water (SW), pool water (PW), and near-river water (NRW) in the upper Wimmera River... 185
S2-Geochmistry of regional groundwater in the upper Wimmera Catchment 190
S3-Geochemistry of stream water (SW), pool water (PW) in the upper Avoca River............... 191
S4-Geochemistry of regional groundwater in the upper Avoca Catchment 194

Abstract

Understanding the multiple water sources with different ages derived from within catchments that can contribute to streamflow is essential for the efficient management of water resources and the protection of riverine ecosystems. However, our knowledge of the sources of water that contribute to intermittent streams remains incomplete compared to perennial streams. Considering that catchment intermittency is forecasted to increase in the future due to changes of climate and increased groundwater pumping, it is necessary to understand the sources of water that sustains streamflow in intermittent streams at different hydrological conditions and how these catchments respond to climate and land use changes. This study uses major ion geochemistry, stable isotopes (^{18}O and ^{2}H), and radioisotopes (^{222}Rn, ^{3}H, ^{14}C, and ^{36}Cl) together with EC (electrical conductivity), and streamflow measurements to identify the contributions of different water sources in the intermittent upper Wimmera and Avoca Rivers in the southern Murray-Darling Basin in southeast Australia.

Along-stream variations in ^{222}Rn activities and Cl concentrations suggest that baseflow inflows are most important in the upper and middle reaches that have steep topography and high hydraulic gradients; however, the contribution from groundwater is limited. Rather, less saline younger water (up to 15 years in the upper Wimmera and 7 years in the upper Avoca River) from small-volume near-river stores such as bank storage and return flows, soil water, and/or interflow are more important component in maintaining the streamflow. Older saline regional groundwater may only contribute to these streams at the initial flows following rainfall. This is contrast to comparable perennial streams that are sustained by older water (mean transit times of up to several hundreds of years old). The residence times of regional groundwater in these catchments are much longer

compared than the stream water (up to 5690 years in the Wimmera and 12900 years in the Avoca catchment) and there is little indication of river water recharging the groundwater.

The conclusion that intermittent streams in southeast Australia are mainly connected to small near-river water stores rather than the large regional groundwater system implies that it is important to protect those water stores from potential contaminants. While the intermittent streams are probably less impacted by regional groundwater pumping, because the near-river water stores have small volumes, they will be more vulnerable to short-term changes in climate and land use.

Mean transit times (MTTs) in intermittent streams are difficult to estimate using seasonal tracers such as Cl and stable isotopes. This study provides an example of using tritium in determining MTTs via lumped parameter models (LPMs) in Southern Hemisphere intermittent streams and is one of only a few studies to estimate MTTs in such streams globally. This study also demonstrates the need to integrate a wide range of tracers to understand water sources and demonstrates that ^{36}Cl is a viable tracer of the sources of Cl solute to the river and may be especially useful in detecting small inflows of saline regional groundwater.

Publications during enrolment

Zhou, Z., Cartwright, I., Morgenstern, U., 2022. Sources and mean transit times of stream water in an intermittent river system: the upper Wimmera River, southeast Australia. Hydrology and Earth System Sciences, 26, 4497-4513.

Zhou, Z., Cartwright, I., 2021. Using geochemistry to identify and quantify the sources, distribution, and fluxes of baseflow to an intermittent river impacted by climate change: The upper Wimmera River, southeast Australia. Science of The Total Environment, 801, 149725.

Thesis including published works declaration

I hereby declare that this thesis contains no material which has been accepted for the award of any other degree or diploma at any university or equivalent institution and that, to the best of my knowledge and belief, this thesis contains no material previously published or written by another person, except where due reference is made in the text of the thesis.

This thesis includes two original papers published in peer reviewed journals. The core theme of the thesis is application of geochemical/environmental tracers in groundwater-surface water interaction study. The ideas, development and writing up of all the papers in the thesis were the principal responsibility of myself, the student, working within the School of Earth, Atmosphere and Environment under the supervision of Professor Ian Cartwright.

The inclusion of co-authors reflects the fact that the work came from active collaboration between researchers and acknowledges input into team-based research.

In the case of Chapters 2, 3, and 4 my contribution to the work involved the following:

Thesis Chapter	Publication Title	Status	Nature and % of student contribution	Co-author name(s) Nature and % of Co-author's contribution*	Co-author(s), Monash student
2	Using geochemistry to identify and quantify the sources, distribution, and fluxes of baseflow to an intermittent river impacted by climate change: The upper Wimmera River, southeast Australia	Published	75%. Concept and collecting data and data interpretation, manuscript writing	25%. Ian Cartwright. Supervisory role, concept, field work, collecting data, manuscript review.	No
3	Sources and mean transit times of	Published	70%. Concept and collecting	20%. Ian Cartwright.	No

	stream water in an intermittent river system: the upper Wimmera River, southeast Australia		data and data interpretation, manuscript writing	Supervisory role, concept, field work, collecting data, manuscript review. 10%. Uwe Morgenstern. Sample analysis, review.	
4	Using geochemistry to understand the interaction between catchment waters and an intermittent headwater stream: the upper Avoca River, southeast Australia	Ready to submit	65%. Concept and collecting data and data interpretation, manuscript writing	15%. Ian Cartwright. Supervisory role, concept, field work, collecting data, manuscript review. 10%. Uwe Morgenstern. Sample analysis, review. 10%. Keith Fifield Sample analysis, review.	No

I have renumbered sections of submitted or published papers in order to generate a consistent presentation within the thesis.

Student name: Zibo Zhou

Student signature: **Date: 03/05/2023**

I hereby certify that the above declaration correctly reflects the nature and extent of the student's and co-authors' contributions to this work. In instances where I am not the responsible author I have consulted with the responsible author to agree on the respective contributions of the authors.

Main Supervisor name: Ian Cartwright

Main Supervisor signature: **Date: 03/05/2023**

Plain language summary

Streams may receive water from different sources in their catchments. There is limited understanding of which water stores intermittent streams are connected to. Using environmental tracers, we show that the intermittent streams in southeast Australia are connected to younger smaller near-river water stores rather than regional groundwater and contributions of regional groundwater to the streams are relatively limited even during the dry seasons. On one hand, this makes these streams more vulnerable to the impacts of climate change and requires management of the riparian zone for their health and protection. On the other hand, the near-river water stores could act as a buffer zone to prevent the ecosystems from potentially contaminated groundwater.

Acknowledgements

During my PhD journey, many people provided me with a wealth of support and I could never finish this project just by myself. First and foremost, I would like to express my gratitude to my supervisor Professor Ian Cartwright for his continuous support, guidance, and encouragement, which are absolutely invaluable. Ian, sending the first PhD inquiring email to you on 7th August 2018 was the best decision I have ever made. It is lucky and such a great honour to ride this journey with you. I have learned a lot from you, not only about groundwater and surface water.

I also want to thank my co-supervisor, Associate Professor Oliver Nebel who always supported me and taught me not only knowledge of stable isotopes but how to make a good presentation and respond to tricky and hard questions. I would like to thank my milestone panel members, Associate Professor Vanessa Wong, Associate Professor Ruth Reef, and Professor Joel Brugger. Vanessa, thank you for inviting me to your group meeting during the lockdown periods. This gave me a lot of mental support and helped me recall my previous life as a soil scientist. This was always a great time when I learned a lot about soils in Australia from you and your group. Ruth and Joel, thank you for the constructive suggestions for my milestone reports and the project. Special thanks to Dr. Massimo Raveggi and Rachelle Pierson for their generous help with the analytical work and for being lifesavers in the lab. It was a pleasure to work with you both. I also thank the whole professional team at EAE, Emily, Silvana, Christine, Yuzhou, Rob, Junnel, and Leigh.

To my peer students at EAE: Although about 40% of our time was stolen by the pandemic, you guys still make EAE a great place to work. Shovon and Ture, thank you for your support either in the field or in the lab. Such a great time to study and work together in the hydro-group. Shovon, thank you so much for your help and good conversations about water science. Ture, you still owed me a hat of Golden State Warriors (hope you could see this sentence someday when you download my thesis). Adriana, Jonas, Hoseong, and Afiq, thank you for making our office the best place with lots of chats and laughs every single day. Shout out to Jonas, thank you for showing me the secret recipe of carrot cake ×3 (you understand what I am saying). Thanks to great friends who made life fun at EAE: Sophia, Qiushi, Dawn, Xueying, Yanlu, and Matt.

Finally, thank you mom, dad, and sister in China for endless love and support throughout my entire studies. Lu, thank you so much for everything you have done for me and our family. Lucas, thank you for being a good boy when I was writing.

前方的路，依然海阔天空，一起走过的日子，都是光辉岁月! (Whilst there is still a long future in front of me, the time that we have shared together has been rich and invaluable for me).

I acknowledge the support from the Co-funded Monash Graduate Scholarship, Faculty of Science Dean's International Postgraduate Research Scholarship, Graduate Research Completion Award, and Monash University Postgraduate Publication Award. This research was further supported by the Australian Research Council Special Research Initiative Grant (0800001) awarded to Ian Cartwright.

Chapter 1

Chapter 1 Introduction

1.1 Research background and aims

Considering the rapidly growing human population and increasing industrial activity, more stress is being placed on global water resources including surface water and groundwater (Green et al., 2011; Irvine et al., 2017). Upper catchments are critical to the health of riverine systems as they commonly contribute a significant proportion of total river flow and so are the sources of water used downstream for agriculture, industry, or domestic supply (Freeman et al., 2007; Cartwright and Morgenstern, 2018). Additionally, due to the low salinity and nutrient concentration, water from upper catchments also plays a vital role in maintaining river health. The better elucidation of upper catchment functioning allows us to understand the transport of nutrients and sediments, and predict the response to future land use or climate change (Kingston et al. 2010; Howcroft et al., 2019). Previous studies have commonly focused on investigating upper catchment of perennial streams (Wu et al., 2008; Duvert et al., 2016; Cartwright and Morgenstern, 2018; Howcroft et al., 2018), Intermittent (also referred to as non-perennial) streams, which constitute over half of the world's stream network length, are less well understood (Datry et al., 2014; Costigan et al., 2016; Shanafield et al., 2021). The intermittency of streams is predicted to increase due to global climate change and water use (Messager et al., 2021), which will have a great influence on water availability for domestic or agriculture use, and health of riverine ecosystems. Hence, detailed investigations of the water sources sustaining streamflow in intermittent streams and the interaction between intermittent rivers and the underlying groundwater at different flow conditions are required complete our understanding of hydrological processes and will have broad implications for water resources management and understanding how intermittent streams respond to changes in climate and land use (Gutiérrez-Jurado et al., 2019; Barua et al., 2022).

Several approaches can be used to investigate the interaction between rivers and water stored within catchments at different spatial and temporal scales (Sophocleous, 2002; Kalbus, et al. 2006; Fleckenstein et al., 2010; Cook et al., 2018; Ntona et al., 2022). Those techniques include analysis of river hydrographs (Eckhardt et al., 2005; Aksoy et al., 2009; Zhang et al., 2013; Cartwright et al., 2014; Cartwright, 2022), heat tracers (Hatch et al., 2006; Atkinson et al., 2015) and environmental tracers (McCallum et al., 2012; Cook, 2013; Gue et al., 2018; Adyasari et al., 2023). Because of contrasting geochemical signatures, environmental tracers can be used to identify different water components in the river at variable flow conditions (Kalbus, et al. 2006; Martinez et al., 2015; Joshi et al. 2018; Freitas et al., 2019; Cartwright et al., 2020a; Adyasari et al., 2023).

This study focuses on geochemical study of two intermittent upper catchment streams in southeast Australia (the Wimmera and Avoca Rivers). These are adjacent catchments in the southern Murray-Darling Basin (Fig. 1.1) that have a similar landscape and topography. Studying the two catchments allows comparisons and assessment of the generality of the conclusions. The overarching aims of this thesis are to better understand:

- the multiple sources of water contributing to intermittent streams at different flow conditions
- the timescale of water flow through the catchments into these intermittent streams
- Whether regional groundwater inflows are important in sustaining these intermittent rivers comparing to perennial streams
- the suitability and uncertainty of different environmental tracers for discerning multiple water sources within the catchment

The results of this study will improve the understanding of catchment functioning that are vital to water resource protection and management. The sources of water and timescales of flow in perennial upper catchment streams in southeast Australia have also been intensively studied (e.g., Tweed et al., 2009; Ralph and Hesse, 2010; Yu et al., 2013; Duvert et al., 2016; Cartwright et al., 2020a), which allows the differences in functioning between intermittent and perennial catchments to be identified.

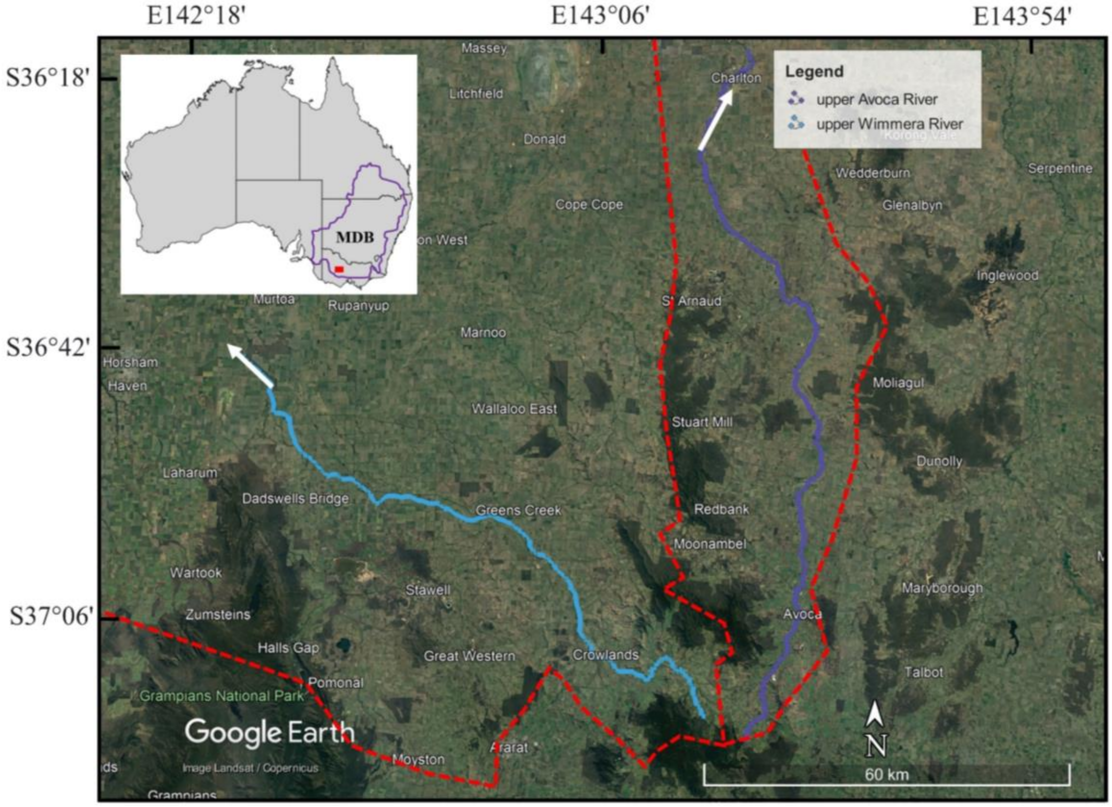

Figure 1. 1. Google Earth image of the upper Wimmera River and upper Avoca River (main channel). Inset shows location of study area in Australia. Red dashed lines represent the catchment boundaries. MDB = Murray-Darling Basin. The arrows show the flow directions and there are few perennial tributaries.

Between high rainfall events, streamflow is sustained by subsurface water stored within catchments. Although these water stores are commonly "thought of as comprising groundwater", there are multiple other catchment water sources with different residence times that can contribute to rivers at different flow conditions. These include short-lived transient water sources (e.g., bank storage, perched groundwater in the riparian zone, and soil water (Cartwright et al., 2014; Peters et al., 2014; Duvert et al., 2016; Howcroft et al., 2019). The relative importance of these sources may vary both seasonally and following storm events. For example, bank storage represents water that infiltrates into adjacent aquifers at high river stage and subsequently returns to the river as bank return flows as the river stage declines (Chen and Chen, 2003; McCallum et al., 2010). Depending on antecedent conditions, bank return waters may contribute to streamflow for several months or years (McCallum et al., 2010). Soil water may contribute most to streamflow when the catchments become saturated immediately following rainfall (Stelzer et al., 2014; Cartwright and Morgenstern, 2018; Stewart et al., 2022). Riparian groundwater inputs are likely contributors to streamflow especially during the low flow periods (Peters et al., 2014). Regional groundwater, which represents the oldest, deepest, and largest volume water component, is probably most important in sustaining streamflow during prolonged low-flow conditions when the shorter-lived water stores have largely drained (Atkinson et al., 2015; Duvert et al., 2016; Jung et al., 2019; Cartwright et al, 2020a) (Fig. 1.2).

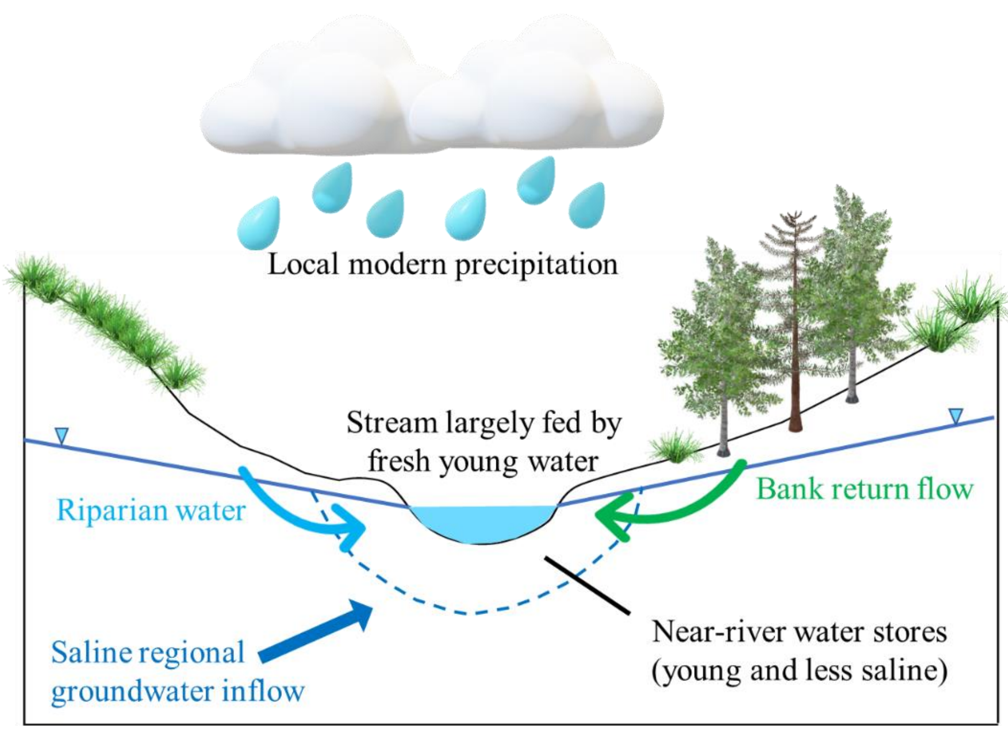

Figure 1. 2. Schematic diagram of multiple water sources sustaining the river flow in intermittent streams

Geochemistry may be used to discern where in the catchments water contributing to streamflow is derived from as different sources of water may have contrasting geochemistry (e.g., Duvert et al., 2016; Cartwright and Morgenstern, 2018; Jung et al., 2019). For example, stable isotopes and major ion geochemistry help identify the presence of relatively young water (less than 50 years old) in riverbanks (Murgulet et al., 2016; Howcroft et al., 2018). Higher nitrate and organic carbon are recorded in soil water due to organic matter breakdown (Stelzer et al., 2014) and the inflow of soil water can increase the concentrations of these solutes in the rivers (e.g., Cartwright and Morgenstern, 2018). Regional groundwater in southeast Australia generally has moderate to high salinities (EC values typically 5,000 to >50,000 μS/cm) and the inflows of saline regional groundwater will increase river salinity concentrations (e.g., Ortega et al., 2015; Zhou and Cartwright, 2021). Using multiple environmental tracers provides a more complete view of the different water stores contributing to rivers, which improves our understanding of catchment functioning.

1.2 Understanding the location and flux of baseflow to rivers

As discussed above, the water that sustains streamflow between rainfall events may have a variety of sources. A non-generic categorization of streamflow following rainfall is the division into quick flow and baseflow (Nathan and McMahon, 1990; Yu and Schwartz, 1999; Eckhardt, 2005; Brodie et al., 2007; Cartwright et al., 2014; Stewart, 2015). Quick flow is the water that contributes to river flow immediately after rainfall and is likely to be mainly recent rainfall. As noted above, baseflow includes all water stored in the catchment that sustains the river between rainfall events. Baseflow includes regional groundwater and transient stores of water such as interflow, bank return waters, perched riparian groundwater, and water from the soil (McCallum et al., 2010;

Miller et al., 2015; Lott and Stewart, 2016; Saraiva et al., 2018). The locations of baseflow inputs are mainly controlled by basin topography, hydraulic gradients adjacent to river channels, and the hydraulic conductivity of the near-river aquifers (Sophocleous, 2002; Pritchard, 2005; Yu et al., 2013). For example, higher baseflow inputs are commonly recorded in incised river reaches due to high hydraulic gradients that increase the baseflow fluxes.

Several methods have arisen to estimate the location and magnitude of baseflow fluxes; these include analysis of river hydrographs, geochemical methods and other techniques.

Hydrograph methods are based on several decades or longer streamflow (river discharge) records from one or more gauges in catchments (Brodie et al., 2007; Cartwright et al., 2014; Duncan, 2019; Cartwright, 2022). Automated baseflow separation methods assume that the baseflow flux is the minimum streamflow that occurs within a specified period of time that varies with catchment area (Aksoy et al, 2009; Cartwright et al, 2014). The digital filtering techniques consider quick flow to have a high-frequency response while baseflow varies at lower frequencies. Filtering out the high-frequency signals from the hydrograph allows the baseflow to be estimated (Eckhardt, 2005). The flow duration curve (FDC) interprets the baseflow from magnitude and frequency of streamflows. Baseflow is estimated as the ratio of low flows to median flows (Brodie et al., 2005, 2007). Hydrograph methods are straightforward, automated and relatively simply applied, however, they can only be used in gauged rivers that are not highly regulated. While they provide valuable information on the temporal variability of baseflow, they do not help in understanding the spatial distribution of baseflow inputs (Brodie and Hostetler, 2005). Also, they do not distinguish the various stores of water that make up baseflow as the baseflow estimates aggregate all delayed waters (such as bank return flow and interflow) not just groundwater inputs (Nathan and McMahon, 1990; Brodie et al., 2007).

Where baseflow and river water have contrasting geochemistry, environmental tracers can be used to detect baseflow inputs to rivers (McCallum et al., 2012; Cook, 2013; Miller et al., 2015; Cartwright, 2022). A wide range of environmental tracers have been used including electrical conductivity (EC), major ions, stable isotopes and radioactive isotopes (especially ^{222}Rn) (Oxtobee and Novakowski, 2003; Cook, 2013; Atkinson et al., 2015; Cook et al., 2018; Jung et al., 2019; Adyasari et al., 2023). Time series of EC data can be used to understand the temporal variation of baseflow at a single gauge (e.g., Yu and Schwartz; 1999; Gonzales et al., 2009; Cartwright et al., 2014). River chemistry surveys allow mapping of the distribution and amount of baseflow inflows at specific dates (e.g., Cook, 2013). Environmental tracers are relatively easy to measure and can be used in regulated or unregulated catchments. Additionally, these techniques can be used to estimate the groundwater inflow rather than the total baseflow flux due to some of delayed sources including bank storage and return flows that have similar geochemistry to surface runoff (McCallum et al., 2010). There are some concerns with these techniques. Major ion concentrations may be affected by in-river evaporation, mineral precipitation or biochemical processes (Cook, 2013; Cook et al., 2018). Additionally, overlapping δ^2H and $\delta^{18}O$ values in groundwater and river water makes their usage difficult (Bourke et al., 2015; Qin et al., 2021). The use of ^{222}Rn can be complicated by production in the hyporheic zone and uncertainties in the degree of degassing (Mullinger et al., 2009; Cartwright et al., 2014; Adyasari et al., 2023). While these factors complicate the use environmental tracers in quantifying baseflow, they can still be reliably used to identify zones of relatively high baseflow contributions in rivers (Tetzlaff and Soulsby, 2008; Zhang et al., 2013).

Other techniques such as modelling (GSFLOW, HydroGeoSphere and SWATMOD) and temperature records have been adopted in recent years (Hatch et al., 2006; Kalbus et al., 2006;

Tian et al., 2015). Detailed knowledge of parameters, such as hydraulic conductivity, groundwater elevations and runoff data, that are required in those models are not always well known. For interpreting temperature records the variability of thermal conductivity in heterogeneous sediments may be problematic (Duque et al., 2016).

1.3 Timescales of water flow

Many rivers are sustained by inflows of water that are a few years to centuries old (McGuire and McDonnell, 2006; Morgenstern et al., 2010; Duvert et al., 2016; Jung et al., 2019). However, relatively little is known about the timescales of water flow in most catchments and whether water of different ages contributes to river flow at different conditions (Soulsby et al., 2000; McGuire and McDonnell, 2006; Stewart et al., 2010). The mean transit times (MTTs) represent the average time taken for water flowing through the catchment from the recharge area to discharges area (McDonnell, 2010; Cartwright and Morgenstern, 2018). Understanding the transit time of water is vital in protecting and managing riverine systems as it impacts the lag time of contaminant transport (Morgenstern et al, 2015). In addition, the variations of transit time may affect water salinity, temperature, microbial activity and attenuation and dispersion of nutrients in rivers (Kirchner et al., 2000).

Many methods can be utilized to estimate the transit time of water including ^{3}H, ^{14}C, chloride, gaseous tracers, and stable isotopes (^{18}O and ^{2}H) (McGuire and McDonnell, 2006; Hrachowitz et al., 2010). The different methods for estimating transit time have potential advantages and disadvantages. ^{3}H is an ideal tracer as it is part of the water molecule and geochemical or biogeochemical reactions in the soils or aquifers do not affect its abundance. Especially in the southern hemisphere, it can be applied to estimate transit times of up to 100 years (Morgenstern et al., 2010; Cartwright and Morgenstern, 2018). ^{14}C has a half-life of 5730 years and is commonly used to estimate transit time of regional groundwater as discussed in detail by Cartwright et al., 2020b. It is less useful for waters less than 100 years due to high ^{14}C activities of recharge following the atmospheric nuclear tests in 1950s and 1960s and is difficult to use in surface water due to the exchange with the atmosphere and the decay of organic matter (Clark and Fritz, 1997; Clark, 2015). ^{36}Cl has a half-life of 301,000 years and has most applications in understanding very old groundwater up to 1 Ma (Phillips, 2000).

$R^{36}Cl$ values of precipitation are a function of both ^{36}Cl fallout and Cl deposition. Generally, $R^{36}Cl$ values increase with distance from the ocean due to chloride concentrations decreasing inland (Bentley et al., 1982; Keywood et al., 1998). Hence, $R^{36}Cl$ values of precipitation at a given locality will be higher when sea levels were lower and the climate is more continental. This may result in groundwater recharged during the Holocene having higher $R^{36}Cl$ values than modern rainfall (Howcroft et al., 2019). In addition, elevated $R^{36}Cl$ values were recorded during the atmospheric nuclear tests in the 1950s and 1960s (Phillips, 2000). Because of the long half-life of ^{36}Cl, these variations in $R^{36}Cl$ values are preserved and can be used to identify water that was recharged at different times over the last few ka.

Gaseous tracers, such as $^{3}H/^{3}He$, SF_6, or chlorofluorocarbons are effective tracers of younger water, but gas exchanges with the atmosphere limit their application in surface waters (Cartwright et al., 2017; Chambers et al., 2019). The attenuation of stable isotope and major ion variations in rainfall can be used to calculate transit times (e.g., McGuire and McDonnell, 2006), however, those tracers become ineffective when transit times are in excess of 4-5 years as temporal variations are smoothed out (Stewart et al., 2010), which makes them less suitable for Australian upper catchments as many have transit times >10 years (e.g., Cartwright et al., 2020a). Also, this method usually assumes catchments are at a steady state, which is not realistic (Kirchner, 2016). Other techniques such as ensemble hydrographs (Kirchner, 2019), flux tracking (Hrachowitz et al., 2013), and StorAge Selection Functions (Rinaldo et al., 2015) can determine transit times from shorter stable isotope time-series and do not assume steady-state conditions. However, these methods still require intensive measurements (such as frequent tracer data for rainfall and streams) that are not commonly available.

Lumped parameter models (LPM), which estimate the distribution of water with different ages and tracer concentrations in aquifers with homogeneous hydraulic properties, simplified geometries, and uniform recharge rates can be used to estimate the transit time from ^{3}H activities (Małoszewski and Zuber, 1982; Maloszewski, 2000; McGuire and McDonnell, 2006; Cartwright et al., 2020a). The bomb-pulse ^{3}H activities in the Southern Hemisphere were relatively low (~60 TU in Melbourne: Tadros et al., 2014) compared with those in the Northern Hemisphere (up to several thousand TU: Clark and Fritz, 1997). This bomb-pulse ^{3}H has now largely decayed and water stored in catchments has lower ^{3}H activities than modern rainfall, which permits MTTs to be estimated from individual ^{3}H measurements (Morgenstern et al., 2010). Even where MTTs cannot be reliably estimated, ^{3}H activities provide an indication of relative age as older water will have lower ^{3}H activities.

1.4 Contrasts in catchment behavior between perennial and intermittent streams

Unlike the perennial streams that have continuous river flow at all conditions, intermittent catchments only flow part of time throughout the year (Datry et al., 2014; Costigan et al., 2016; Gutiérrez-Jurado et al., 2019; Shanafield et al., 2021). Some intermittent streams dry up entirely during low rainfall periods. However, other intermittent streams contain a series of laterally-disconnected persistent pools during the cease-to-flow periods (Bestland et al., 2017; Bourke et al., 2023), commonly referred to as a chain-of-ponds. These pools are important as they provide habitats for a number of species of flora and fauna (Williams et al., 2020). In some cases, these pools may be groundwater-fed (Cartwright and Morgenstern, 2016, Williams et al., 2020; Lamontagne et al., 2021; Bourke et al., 2023). However, a recent study in western Victoria in southeast Australia showed that during the dry seasons, young and fresh water stores from perched aquifers in the riparian zone locally make significant contributions to these pools (Barua et al., 2022).

Most previous studies of MTTs have focused on perennial streams (Hrachowitz et al., 2010; Morgenstern et al., 2010; Gusyev et al., 2016; Howcroft et al., 2018; Cartwright et al., 2020a). In southeast Australia, these perennial streams are commonly sustained by water with MTTs that are typically years to several decades and the MTTs typically increase at low streamflows. The volume of the water stores sustaining streamflow is proportional to the MTTs (Małoszewski and Zuber, 1982), implying the perennial streams are fed by relatively large water stores, probably including regional groundwater during the low flow conditions (Fig. 1.3a). Being sustained by large volume water stores makes perennial streams more resilient to short-term changes in climate or landuse.

There are more limited studies of MTTs in intermittent streams (e.g., Cartwright and Morgenstern, 2016; Bansah and Ali, 2019; Barua et al., 2022). These studies have shown that the MTTs of water sustaining intermittent streams are generally much shorter (typically on the order of a few years). This difference in MTTs agrees with the idea that transient near-river water (NRW) are expected to be more important in maintaining intermittent streams than perennial ones and the contribution from regional groundwater is limited (Fig. 1.3b).

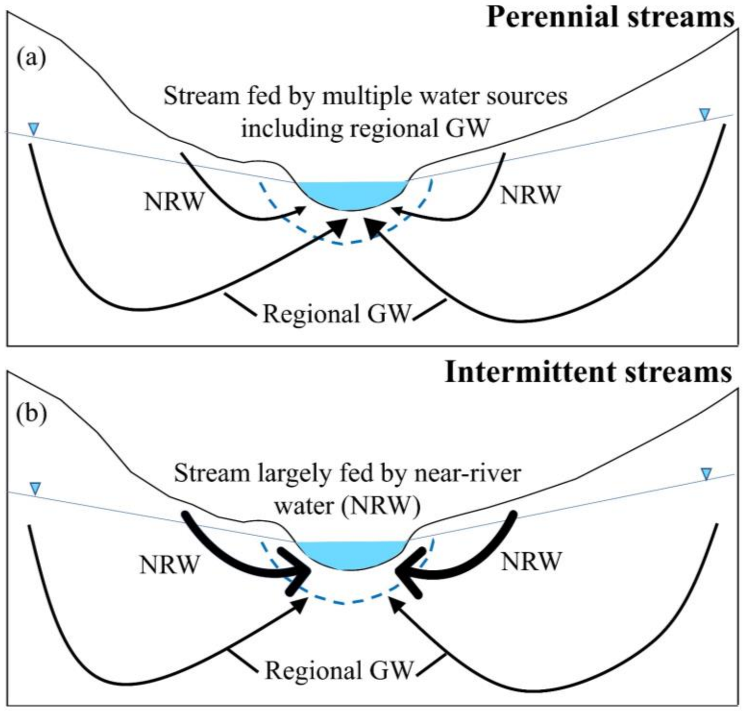

Figure 1. 3. Schematic diagram of water components in perennial (a) and intermittent streams (b). GW = groundwater, NRW = near-river water. Bold arrow indicates that the contribution of NRW is more important in intermittent streams.

Due to the significant contributions from transient near-river water stores, intermittent streams may be more vulnerable to shorter-timescale changes of climate and landuse compared to perennial streams. They also will be more impacted by changes to landuse and groundwater extraction that occurs on the floodplain rather than further away. This emphasizes the importance of protecting those transient stores for the health of intermittent catchments as river health may be at risk if these water stores are contaminated or depleted by multiple years of drought.

1.5 Research methodology

This study is based on the upper Wimmera and Avoca Rivers, in the southern Murry-Darling Basin (MDB) in southeast Australia (Fig. 1.1). These rivers are endorheic and discharge into terminal lakes and wetlands near the Murray River. Rainfall ranges from 505 to 709 mm in the upper

Wimmera and 420 to 536 mm in the upper Avoca River respectively and the wet periods are in winter and spring whereas summer months are the driest. These rivers also have similar topography with confined valleys in their upper reaches and lower reaches that occupy broad alluvial floodplains.

The geochemistry of the pool water, stream water and regional groundwater from those two catchments is used to investigate the relative importance of young water components (e.g. modern rainfall, stream water, bank storage and soil water) and older deep regional groundwater to these rivers.

Environmental tracers have been successfully applied to the research on groundwater and river water interactions in catchments globally (McGuire and McDonnell, 2006; Cartwright et al., 2014, 2017; Cook et al., 2018; Gue et al., 2018; Freitas et al., 2019; Zhou and Cartwright, 2021). Multiple tracers and combined methods could reduce some of the uncertainties in understanding the locations and sources of baseflow inputs. For example, incorporating cosmogenic isotopes (e.g., ^{3}H and ^{36}Cl) may better help distinguish sources of water and solutes in streams. Also, the application of multiple tracers in pools potentially allows the composition of near-river water stores that actually interacts with the river to be better understood.

1.6 Thesis structure

The main outcomes of this study are discussed in Chapters 2-4, which have been prepared for publication in peer-reviewed journals. The thesis structure is:

Chapter 2: Using geochemistry to identify and quantify the sources, distribution, and fluxes of baseflow to intermittent rivers: the upper Wimmera River, southeast Australia

Chapter 1

Chemical mass balance (^{222}Rn) and water mass balance models together with major ion geochemistry and ^{3}H were used to estimate the distribution, sources and fluxes of baseflow discharge into the upper Wimmera River. The chapter was published in Science of the Total Environment (Zhou and Cartwright, 2021).

Chapter 3: Sources and mean transit times of stream water in an intermittent river system: the upper Wimmera River, southeast Australia

Radioisotopes (^{3}H and ^{14}C) combined with stable isotopes and major ion geochemistry were used to distinguish water sources with different ages sustaining the intermittent upper Wimmera River during different flow conditions. This work was published in Hydrology and Earth System Sciences (Zhou et al., 2022).

Chapter 4: Integrating major ion geochemistry, stable isotopes (^{18}O, ^{2}H) and radioactive isotopes (^{222}Rn, ^{14}C, ^{36}Cl, ^{3}H) to understand the interaction between catchment waters and an intermittent headwater stream: the upper Avoca River, southeast Australia

Major ion geochemistry, stable isotopes (^{18}O and ^{2}H), and radioisotopes (^{222}Rn, ^{3}H, ^{14}C, and ^{36}Cl) were used in this study to investigate the sources and transit times of water in the intermittent upper Avoca River and the interaction of the stream water with the underlying regional groundwater. This work will be submitted to Science of the Total Environment.

Chapter 5: Summary and Conclusions.

This chapter summarizes the key results of the research and outlines the broader implications for understanding processes in intermittent catchments.

Overall the combined data permit a detailed understanding of the functioning of these catchments. Taken together, the information is critical in understanding the location and origin of baseflow and the timescales of water flow in the catchments.

Chapter 1

References

Adyasari, D., Dimova, N. T., Dulai, H., Gilfedder, B. S., Cartwright, I., McKenzie, T., Fuleky, P., 2023. Radon-222 as a groundwater discharge tracer to surface waters. Earth-Science Reviews, 104321, https://doi.org/10.1016/j.earscirev.2023.104321

Aksoy, H., Kurt, I., Eris, E., 2009. Filtered smoothed minima baseflow separation method. Journal of Hydrology, 372, 94-101, https://doi.org/10.1016/j.jhydrol.2009.03.037.

Atkinson, A.P., Cartwright, I., Gilfedder, B.S., Hofmann, H., Unland, N.P., Cendón, D.I., Chisari, R., 2015. A multi-tracer approach to quantifying groundwater inflows to an upland river; assessing the influence of variable groundwater chemistry. Hydrological Processes, 29, 1-12. https://doi.org/10.1002/hyp.10122.

Bansah, S., Ali, G., 2019. Streamwater ages in nested, seasonally cold Canadian watersheds. Hydrological processes, 33, 495-511, https://doi.org/10.1002/hyp.13373.

Barua, S., Cartwright, I., Dresel, P. E., Morgenstern, U., McDonnell, J. J., Daly, E., 2022. Sources and mean transit times of intermittent streamflow in semi-arid headwater catchments, Journal of Hydrology, 604, 127208, https://doi.org/10.1016/j.jhydrol.2021.127208.

Bentley, H.W., Phillips, F.M., Davis, S.N., Gifford, S., Elmore, D., Tubbs, L.E., Gove, H.E., 1982. Thermonuclear ^{36}Cl pulse in natural water. Nature, 300, 737-740, https://doi.org/10.1038/300737a0.

Bestland, E., George, A., Green, G., Olifent, V., Mackay, D., Whalen, M., 2017. Groundwater dependent pools in seasonal and permanent streams in the Clare Valley of South Australia. Journal of Hydrology: Regional Studies, 9, 216-235, https://doi.org/10.1016/j.ejrh.2016.12.087.

Chapter 1

Bourke, S. A., Cook, P. G., Dogramaci, S., Kipfer, R., 2015. Partitioning sources of recharge in environments with groundwater recirculation using carbon-14 and CFC-12. Journal of Hydrology, 525, 418-428, https://doi.org/10.1016/j.jhydrol.2015.03.061.

Bourke, S. A., Shanafield, M., Hedley, P., Chapman, S., Dogramaci, S., 2023. A hydrological framework for persistent pools along non-perennial rivers. Hydrology and Earth System Sciences, 27, 809-836, https://doi.org/10.5194/hess-27-809-2023.

Brodie, R. S., Hostetler, S., 2005. A review of techniques for analysing baseflow from stream hydrographs. In Proceedings of the NZHS-IAH-NZSSS 2005 conference (Vol. 28). Auckland New Zealand.

Brodie, R., Sundaram, B., Tottenham, R., Hostetler, S., Ransley, T., 2007. An overview of tools for assessing groundwater-surface water connectivity. Bureau of Rural Sciences, Canberra, Australia.

Cartwright, I., 2022. Implications of variations in stream specific conductivity for estimating baseflow using chemical mass balance and calibrated hydrograph techniques. Hydrology and Earth System Sciences, 26, 183-195, https://doi.org/10.5194/hess-26-183-2022.

Cartwright, I., Cendón, D., Currell, M., Meredith, K., 2017. A review of radioactive isotopes and other residence time tracers in understanding groundwater recharge: Possibilities, challenges, and limitations. Journal of Hydrology, 555, 797-811, https://doi.org/10.1016/j.jhydrol.2017.10.053.

Cartwright, I., Currell, M. J., Cendón, D. I., Meredith, K. T., 2020b. A review of the use of radiocarbon to estimate groundwater residence times in semi-arid and arid areas. Journal of Hydrology, 580, 124247, https://doi.org/10.1016/j.jhydrol.2019.124247.

Chapter 1

Cartwright, I., Gilfedder, B., Hofmann, H., 2014. Contrasts between estimates of baseflow help discern multiple sources of water contributing to rivers. Hydrology and Earth System Sciences, 18, 15-30. https://doi.org/10.5194/hess-18-15-2014.

Cartwright, I., Morgenstern, U., 2016. Using tritium to document the mean transit time and sources of water contributing to a chain-of-ponds river system: implications for resource protection. Applied Geochemistry, 75, 9-19, https://doi.org/10.1016/j.apgeochem.2016.10.007.

Cartwright, I., Morgenstern, U., 2018. Using tritium and other geochemical tracers to address the “old water paradox” in headwater catchments. Journal of hydrology, 563, 13-21, https://doi.org/10.1016/j.jhydrol.2018.05.060.

Cartwright, I., Morgenstern, U., Howcroft, W., Hofmann, H., Armit, R., Stewart, M., Irvine, D., 2020a. The variation and controls of mean transit times in Australian headwater catchments. Hydrological Processes, 34, 4034-4048, https://doi.org/10.1002/hyp.13862.

Chambers, L. A., Gooddy, D. C., Binley, A. M., 2019. Use and application of CFC-11, CFC-12, CFC-113 and SF6 as environmental tracers of groundwater residence time: A review. Geoscience Frontiers, 10, 1643-1652, https://doi.org/10.1016/j.gsf.2018.02.017.

Clark, I.D., 2015. Groundwater geochemistry and isotopes, CRC Press Boca Raton, FL, USA

Clark, I.D., Fritz, P., 1997. Environmental Isotopes in Hydrogeology, Lewis, New York, p. 328.

Chen, X., Chen, X., 2003. Stream water infiltration, bank storage, and storage zone changes due to stream-stage fluctuations. Journal of Hydrology, 280, 246-264. https://doi.org/10.1016/S0022-1694(03)00232-4.

Cook, P.G., 2013. Estimating groundwater discharge to rivers from river chemistry surveys. Hydrological Processes, 27, 3694–3707. https://doi.org/10.1002/hyp.9493.

Chapter 1

Cook, P.G., Rodellas, V., Stieglitz, T.C., 2018. Quantifying Surface Water, Porewater, and Groundwater Interactions Using Tracers: Tracer Fluxes, Water Fluxes, and End-member Concentrations. Water Resources Research, 54, 2452-2465. https://doi.org/10.1002/2017WR021780.

Costigan, K.H., Jaeger, K.L., Goss, C.W., Fritz, K.M., Goebel, P.C., 2016. Understanding controls on flow permanence in intermittent rivers to aid ecological research: integrating meteorology, geology and land cover. Ecohydrology, 9, 1141-1153. https://doi.org/10.1002/eco.1712

Datry, T., Larned, S.T., Tockner, K., 2014. Intermittent rivers: a challenge for freshwater ecology. BioScience, 64, 3, 229-235. https://doi.org/10.1093/biosci/bit027.

Duncan, H. P., 2019. Baseflow separation–A practical approach. Journal of Hydrology, 575, 308-313, https://doi.org/10.1016/j.jhydrol.2019.05.040.

Duque, C., Müller, S., Sebok, E., Haider, K., Engesgaard, P., 2016. Estimating groundwater discharge to surface waters using heat as a tracer in low flux environments: the role of thermal conductivity. Hydrological Processes, 30, 383-395, https://doi.org/10.1002/hyp.10568.

Duvert, C., Stewart, M.K., Cendón, D.I., Raiber, M., 2016. Time series of tritium, stable isotopes and chloride reveal short-term variations in groundwater contribution to a stream, Hydrology and Earth System Sciences, 20, 257-277, https://doi.org/10.5194/hess-20-257-2016.

Eckhardt, K., 2005. How to construct recursive digital filters for baseflow separation. Hydrological Processes: An International Journal, 19, 507-515, https://doi.org/10.1002/hyp.5675.

Fleckenstein, J. H., Krause, S., Hannah, D. M., Boano, F., 2010. Groundwater-surface water interactions: New methods and models to improve understanding of processes and dynamics. Advances in Water Resources, 33, 1291-1295, https://doi.org/10.1016/j.advwatres.2010.09.011.

Chapter 1

Freeman, M. C., Pringle, C. M., Jackson, C. R., 2007. Hydrologic connectivity and the contribution of stream headwaters to ecological integrity at regional scales 1. JAWRA Journal of the American Water Resources Association, 43, 5-14, https://doi.org/10.1111/j.1752-1688.2007.00002.x.

Freitas, J. G., Furquim, S. A. C., Aravena, R., Cardoso, E. L., 2019. Interaction between lakes' surface water and groundwater in the Pantanal wetland, Brazil. Environmental Earth Sciences, 78, 139, https://doi.org/10.1007/s12665-019-8140-4.

Gonzales, A. L., Nonner, J., Heijkers, J., Uhlenbrook, S., 2009. Comparison of different base flow separation methods in a lowland catchment. Hydrology and Earth System Sciences, 13, 2055-2068, https://doi.org/10.5194/hess-13-2055-2009.

Green, T. R., Taniguchi, M., Kooi, H., Gurdak, J. J., Allen, D. M., Hiscock, K. M., Aureli, A., 2011. Beneath the surface of global change: Impacts of climate change on groundwater. Journal of Hydrology, 405, 532- 560, https://doi.org/10.1016/j.jhydrol.2011.05.002.

Gue, A., Grasby, S. E., Mayer, B., 2018. Influence of saline groundwater discharge on river water chemistry in the Athabasca oil sands region–A chloride stable isotope and mass balance approach. Applied Geochemistry, 89, 75-85, https://doi.org/10.1016/j.apgeochem.2017.10.004.

Gusyev, M. A., Morgenstern, U., Stewart, M. K., Yamazaki, Y., Kashiwaya, K., Nishihara, T., and Iwami, Y., 2016. Application of tritium in precipitation and baseflow in Japan: a case study of groundwater transit times and storage in Hokkaido watersheds, Hydrology and Earth System Sciences, 20, 3043-3058, https://doi.org/10.5194/hess-20-3043-2016.

Gutiérrez-Jurado, K.Y., Partington, D., Batelaan, O., Cook, P., Shanafield, M., 2019. What triggers streamflow for intermittent rivers and ephemeral streams in low-gradient catchments in Mediterranean climates. Water Resources Research, 55, 9926-9946. https://doi.org/10.1029/2019WR025041

Chapter 1

Hatch, C. E., Fisher, A. T., Revenaugh, J. S., Constantz, J., Ruehl, C., 2006. Quantifying surface water–groundwater interactions using time series analysis of streambed thermal records: Method development. Water Resources Research, 42, https://doi.org/10.1029/2005WR004787

Howcroft, W., Cartwright, I., Cendón, D.I., 2019. Residence times of bank storage and return flows and the influence on river water chemistry in the upper Barwon River, Australia. Applied Geochemistry, 101, 31-41, https://doi.org/10.1016/j.apgeochem.2018.12.026.

Howcroft, W., Cartwright, I., Morgenstern, U., 2018. Mean transit times in headwater catchments: Insights from the Otway Ranges, Australia. Hydrology and Earth System Sciences, 22, 635-653, https://doi.org/10.5194/hess-22-635-2018.

Hrachowitz, M., Savenije, H., Bogaard, T. A., Tetzlaff, D., Soulsby, C., 2013. What can flux tracking teach us about water age distribution patterns and their temporal dynamics?. Hydrology and Earth System Sciences, 17, 533-564, https://doi.org/10.5194/hess-17-533-2013.

Hrachowitz, M., Soulsby, C., Tetzlaff, D., Speed, M., 2010. Catchment transit times and landscape controls—does scale matter?. Hydrological Processes: An International Journal, 24, 117-125, https://doi.org/10.1002/hyp.7510.

Irvine, D. J., Kurylyk, B. L., Cartwright, I., Bonham, M., Post, V. E., Banks, E. W., Simmons, C. T., 2017. Groundwater flow estimation using temperature-depth profiles in a complex environment and a changing climate. Science of the Total Environment, 574, 272-281, https://doi.org/10.1016/j.scitotenv.2016.08.212.

Joshi, S. K., Rai, S. P., Sinha, R., Gupta, S., Densmore, A. L., Rawat, Y. S., Shekhar, S., 2018. Tracing groundwater recharge sources in the north-western Indian alluvial aquifer using water isotopes (δ18O, δ2H and 3H). Journal of hydrology, 559, 835-847, https://doi.org/10.1016/j.jhydrol.2018.02.056.

Chapter 1

Jung, Y. Y., Koh, D. C., Yoon, Y. Y., Kwon, H. I., Heo, J., Ha, K., Yun, S. T., 2019. Using stable isotopes and tritium to delineate groundwater flow systems and their relationship to streams in the Geum River basin, Korea, Journal of Hydrology, 573, 267-280, https://doi.org/10.1016/j.jhydrol.2019.03.084.

Kalbus, E., Reinstorf, F., Schirmer, M., 2006. Measuring methods for groundwater? surface water interactions: a review. Hydrology and Earth System Sciences, 10, 873-887, https://doi.org/10.5194/hess-10-873-2006.

Keywood, M.D., Fifield, L.K., Chivas, A.R., Cresswell, R.G., 1998. Fallout of chlorine 36 to the Earth's surface in the southern hemisphere. Journal of Geophysical Research, 103 (D7), 8281-8286, https://doi.org/10.1029/97JD03125.

Kingston, D. G., Taylor, R. G., 2010. Sources of uncertainty in climate change impacts on river discharge and groundwater in a headwater catchment of the Upper Nile Basin, Uganda. Hydrology and Earth System Sciences, 14, 1297-1308, https://doi.org/10.5194/hess-14-1297-2010.

Kirchner, J. W., 2016. Aggregation in environmental systems–Part 2: Catchment mean transit times and young water fractions under hydrologic nonstationarity. Hydrology and Earth System Sciences, 20, 299-328, https://doi.org/10.5194/hess-20-299-2016.

Kirchner, J. W., 2019. Quantifying new water fractions and transit time distributions using ensemble hydrograph separation: theory and benchmark tests. Hydrology and Earth System Sciences, 23, 303-349, https://doi.org/10.5194/hess-23-303-2019.

Kirchner, J. W., Feng, X., Neal, C., 2000. Fractal stream chemistry and its implications for contaminant transport in catchments. Nature, 403, 524, https://doi.org/10.1038/35000537

Lamontagne, S., Kirby, J., Johnston, C., 2021. Groundwater–surface water connectivity in a chain-of-ponds semiarid river. Hydrologica Processes, 35, e14129, https://doi.org/10.1002/hyp.14129.

Chapter 1

Lott, D. A., Stewart, M. T., 2016. Base flow separation: A comparison of analytical and mass balance methods. Journal of Hydrology, 535, 525-533, https://doi.org/10.1016/j.jhydrol.2016.01.063.

Maloszewski, P., 2000. Lumped-parameter models as a tool for determining the hydrological parameters of some groundwater systems based on isotope data, in: Tracer and Modelling in Hydrogeology – Proceetings of the TraM'2000 Conference, IAHS Publ. no. 262, Liege, Belgium, 271-276.

Małoszewski, P., Zuber, A., 1982. Determining the turnover time of groundwater systems with the aid of environmental tracers: 1. Models and their applicability, Journal of Hydrology, 57, 207-231, https://doi.org/10.1016/0022-1694(82)90147-0.

Martinez, J. L., Raiber, M., Cox, M. E., 2015. Assessment of groundwater–surface water interaction using long-term hydrochemical data and isotope hydrology: Headwaters of the Condamine River, Southeast Queensland, Australia. Science of the Total Environment, 536, 499-516, https://doi.org/10.1016/j.scitotenv.2015.07.031.

McCallum, J. L., Cook, P. G., Berhane, D., Rumpf, C., McMahon, G. A., 2012. Quantifying groundwater flows to streams using differential flow gaugings and water chemistry. Journal of Hydrology, 416, 118-132, https://doi.org/10.1016/j.jhydrol.2011.11.040.

McCallum, J.L., Cook, P.G., Brunner, P., Berhane, D., 2010. Solute dynamics during bank storage flows and implications for chemical base flow separation. Water Resources Research, 46, W07541. https://doi.org/10.1029/2009WR008539

McDonnell, J. J., McGuire, K., Aggarwal, P., Beven, K. J., Biondi, D., Destouni, G., Lyon, S., 2010. How old is streamwater? Open questions in catchment transit time conceptualization, modelling and analysis. Hydrological Processes, 24, 1745-1754, https://doi.org/10.1002/hyp.7796.

Chapter 1

McGuire, K. J., McDonnell, J. J., 2006. A review and evaluation of catchment transit time modelling, Journal of Hydrology, 330, 543-563, https://doi.org/10.1016/j.jhydrol.2006.04.020.

Messager, M. L., Lehner, B., Cockburn, C., Lamouroux, N., Pella, H., Snelder, T., Datry, T., 2021. Global prevalence of non-perennial rivers and streams, Nature, 594, 391-397, https://doi.org/10.1038/s41586-021-03565-5.

Miller, M. P., Johnson, H. M., Susong, D. D., Wolock, D. M., 2015. A new approach for continuous estimation of baseflow using discrete water quality data: Method description and comparison with baseflow estimates from two existing approaches. Journal of Hydrology, 522, 203-210, https://doi.org/10.1016/j.jhydrol.2014.12.039.

Morgenstern, U., Daughney, C. J., Leonard, G., Gordon, D., Donath, F. M., Reeves, R., 2015. Using groundwater age and hydrochemistry to understand sources and dynamics of nutrient contamination through the catchment into Lake Rotorua, New Zealand. Hydrology and Earth System Sciences, 19, 803-822, https://doi.org/10.5194/hess-19-803-2015.

Morgenstern, U., Stewart, M.K., Stenger, R., 2010. Dating of stream water using tritium in a post nuclear bomb pulse world: continuous variation of mean transit time with streamflow, Hydrology and Earth System Sciences, 14, 2289-2301, https://doi.org/10.5194/hess-14-2289-2010.

Mullinger, N. J., Pates, J. M., Binley, A. M., Crook, N. P., 2009. Controls on the spatial and temporal variability of 222Rn in riparian groundwater in a lowland Chalk catchment. Journal of hydrology, 376, 58-69, https://doi.org/10.1016/j.jhydrol.2009.07.015.

Murgulet, D., Murgulet, V., Spalt, N., Douglas, A., Hay, R. G., 2016. Impact of hydrological alterations on river-groundwater exchange and water quality in a semi-arid area: Nueces River, Texas. Science of the Total Environment, 572, 595-607, https://doi.org/10.1016/j.scitotenv.2016.07.198.

Nathan, R. J., McMahon, T. A., 1990. Evaluation of automated techniques for base flow and recession analyses, Water Resource. Research., 26, 1465–1473, https://doi.org/10.1029/WR026i007p01465.

Ntona, M. M., Busico, G., Mastrocicco, M., Kazakis, N., 2022. Modeling groundwater and surface water interaction: An overview of current status and future challenges. Science of The Total Environment, 157355, https://doi.org/10.1016/j.scitotenv.2022.157355.

Ortega, L., Manzano, M., Custodio, E., Hornero, J., Rodríguez-Arévalo, J., 2015. Using 222Rn to identify and quantify groundwater inflows to the Mundo River (SE Spain). Chemical Geology, 395, 67–79. https://doi.org/10.1016/j.chemgeo.2014.12.002.

Oxtobee, J. P., Novakowski, K. S., 2003. Ground water/surface water interaction in a fractured rock aquifer. Groundwater, 41, 667-681, https://doi.org/10.1111/j.1745-6584.2003.tb02405.x.

Peters, N. E., Burns, D. A., Aulenbach, B. T., 2014. Evaluation of high-frequency mean streamwater transit-time estimates using groundwater age and dissolved silica concentrations in a small forested watershed. Aquatic Geochemistry, 20, 183-202, https://doi.org/10.1007/s10498-013-9207-6.

Phillips, F.M., 2000. Chloribe-36. In: Cook, P., Herczeg, A. (Eds.), Environmental Tracers in Subsurface Hydrology. Kluwer Academic Publishers, Boston, pp. 299-348.as

Pritchard, J. L., 2005. Dynamics of stream and groundwater exchange using environmental tracers. Flinders University, School of Chemistry, Physics and Earth Sciences.

Qin, W., Han, D., Song, X., Liu, S., 2021. Environmental isotopes (δ18O, δ2H, 222Rn) and hydrochemical evidence for understanding rainfall-surface water-groundwater transformations in a polluted karst area. Journal of Hydrology, 592, 125748, https://doi.org/10.1016/j.jhydrol.2020.125748.

Ralph, T. J., Hesse, P. P., 2010. Downstream hydrogeomorphic changes along the Macquarie River, southeastern Australia, leading to channel breakdown and floodplain wetlands. Geomorphology, 118, 48-64, https://doi.org/10.1016/j.geomorph.2009.12.007

Rinaldo, A., Benettin, P., Harman, C. J., Hrachowitz, M., McGuire, K. J., Van Der Velde, Y., Botter, G., 2015. Storage selection functions: A coherent framework for quantifying how catchments store and release water and solutes, Water Resources Research, 51, 4840-4847, https://doi.org/10.1002/2015WR017273.

Saraiva Okello, A. M. L., Uhlenbrook, S., Jewitt, G. P., Masih, I., Riddell, E. S., Van der Zaag, P., 2018. Hydrograph separation using tracers and digital filters to quantify runoff components in a semi-arid mesoscale catchment. Hydrological processes, 32, 1334-1350, https://doi.org/10.1002/hyp.11491.

Shanafield, M., Bourke, S.A., Zimmer, M.A., Costigan, K.H., 2021. An overview of the hydrology of non-perennial rivers and streams. Wiley Interdisciplinary Reviews: Water, 8, e1504. https://doi.org/10.1002/wat2.1504.

Sophocleous, M., 2002. Interactions between groundwater and surface water: the state of the science. Hydrogeology Journal, 10, 52-67. http://dx.doi.org/10.1007/s10040-014-1215-0.

Stelzer, R. S., Thad Scott, J., Bartsch, L. A., Parr, T. B., 2014. Particulate organic matter quality influences nitrate retention and denitrification in stream sediments: evidence from a carbon burial experiment. Biogeochemistry, 119, 387-402, https://doi.org/10.1007/s10533-014-9975-0.

Stewart, B., Shanley, J. B., Kirchner, J. W., Norris, D., Adler, T., Bristol, C., Li, L., 2022. Streams as mirrors: Reading subsurface water chemistry from stream chemistry. Water Resources Research, 58(1), e2021WR029931, https://doi.org/10.1029/2021WR029931.

Stewart, M. K., 2015. Promising new baseflow separation and recession analysis methods applied to streamflow at Glendhu Catchment, New Zealand. Hydrology and Earth System Sciences, 19, 2587-2603, https://doi.org/10.5194/hess-19-2587-2015.

Stewart, M. K., Morgenstern, U., McDonnell, J. J., 2010. Truncation of stream residence time: how the use of stable isotopes has skewed our concept of stream water age and origin. Hydrological Processes, 24, 1646-1659, https://doi.org/10.1002/hyp.7576.

Tadros, C.V., Hughes, C.E., Crawford, J., Hollins, S.E., Chisari, R., 2014. Tritium in Australian precipitation: A 50-year record. Journal of Hydrology, 513, 262-273. https://doi.org/10.1016/j.jhydrol.2014.03.031.

Tetzlaff, D., Soulsby, C., 2008. Sources of baseflow in larger catchments–Using tracers to develop a holistic understanding of runoff generation. Journal of Hydrology, 359, 287-302, https://doi.org/10.1016/j.jhydrol.2008.07.008.

Tian, Y., Zheng, Y., Wu, B., Wu, X., Liu, J., Zheng, C., 2015. Modeling surface water-groundwater interaction in arid and semi-arid regions with intensive agriculture. Environmental Modelling & Software, 63, 170-184, https://doi.org/10.1016/j.envsoft.2014.10.011.

Tweed, S., Leblanc, M., Cartwright, I., 2009. Groundwater–surface water interaction and the impact of a multi-year drought on lakes conditions in South-East Australia. Journal of Hydrology, 379, 41-53, https://doi.org/10.1016/j.jhydrol.2009.09.043

Williams, R.T., Fryirs, K.A. Hose, G.C., 2020. The hydrological function of a large chain-of-ponds: a wetland system with intermittent surface flows. Aquat Sci 82, 61., https://doi.org/10.1007/s00027-020-00735-x.

Wu, W., Yang, J., Xu, S., Yin, H., 2008. Geochemistry of the headwaters of the Yangtze River, Tongtian He and Jinsha Jiang: silicate weathering and CO2 consumption. Applied Geochemistry, 23, 3712-3727, https://doi.org/10.1016/j.apgeochem.2008.09.005.

Chapter 1

Yu, M.C.L., Cartwright, I., Braden, J.L., De Bree, S.T., 2013. Examining the spatial and temporal variation of groundwater inflows to a valley-to-floodplain river using ^{222}Rn, geochemistry and river discharge: The Ovens River, southeast Australia. Hydrology and Earth System Sciences, 17, 4907. https://doi.org/10.5194/hess-17-4907-2013.

Yu, Z., Schwartz, F. W., 1999. Automated calibration applied to watershed-scale flow simulations. Hydrological Processes, 13, 191-209, https://doi.org/10.1002/(SICI)1099-1085(19990215)13:2<191::AID-HYP706>3.0.CO;2-N.

Zhang, R., Li, Q., Chow, T. L., Li, S., Danielescu, S., 2013. Baseflow separation in a small watershed in New Brunswick, Canada, using a recursive digital filter calibrated with the conductivity mass balance method. Hydrological Processes, 27, 2659-2665, https://doi.org/10.1002/hyp.9417.

Zhou, Z., Cartwright, I., 2021. Using geochemistry to identify and quantify the sources, distribution, and fluxes of baseflow to an intermittent river impacted by climate change: The upper Wimmera River, southeast Australia, Science of the Total Environment, 149725, https://doi.org/10.1016/j.scitotenv.2021.149725.

Zhou, Z., Cartwright, I., Morgenstern, U., 2022. Sources and mean transit times of stream water in an intermittent river system: the upper Wimmera River, southeast Australia. Hydrology and Earth System Sciences, 26, 4497-4513, https://doi.org/10.5194/hess-26-4497-2022.

Chapter 2

Chapter 2 Using geochemistry to identify and quantify the sources, distribution, and fluxes of baseflow to an intermittent river impacted by climate change: The upper Wimmera River, southeast Australia

Science of the Total Environment 801 (2021) 149725

Contents lists available at ScienceDirect

Science of the Total Environment

journal homepage: www.elsevier.com/locate/scitotenv

Using geochemistry to identify and quantify the sources, distribution, and fluxes of baseflow to an intermittent river impacted by climate change: The upper Wimmera River, southeast Australia

Zibo Zhou *, Ian Cartwright

School of Earth, Atmosphere and Environment, Monash University, Clayton, VIC 3800, Australia

HIGHLIGHTS

- Intermittent rivers less well connected to regional groundwater system
- Distributions, sources and fluxes of baseflow investigated using geochemistry
- Significant contribution of near-river storage (e.g., bank return flow and/or interflow)
- Protection of near-river environment is important in maintaining catchment health and responding to climate variability.

GRAPHICAL ABSTRACT

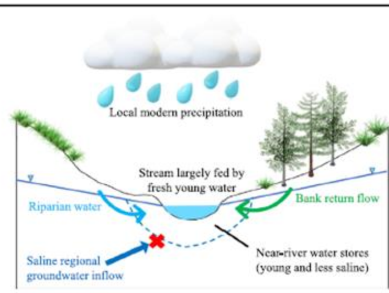

ARTICLE INFO

Article history:
Received 24 May 2021
Received in revised form 12 August 2021
Accepted 13 August 2021
Available online 18 August 2021

Editor: José Virgílio Cruz

Keywords:
Baseflow
^{222}Rn
^{3}H
Geochemistry
Intermittent rivers

ABSTRACT

Documenting the distribution, sources and fluxes of baseflow discharge into rivers is important for their management and for maintaining ecosystem health. This study uses major ion geochemistry, ^{222}Rn, and ^{3}H to differentiate between the input of low-salinity near-river waters (bank storage and return waters and/or interflow) and regional groundwater in an intermittent river from southeast Australia that is undergoing long-term changes in flow resulting from climate change. Baseflow discharge calculated by ^{222}Rn mass balance was up to 1.3 m^3/m/day in the high flow period in July 2019 and up to 0.1 m^3/m/day at low flow conditions in November 2019. The distribution of ^{222}Rn activities implies higher baseflow fluxes in the upper and middle reaches that have relatively steep topography and higher hydraulic gradients. The lower reaches received less baseflow due to subdued topography and fine-grained sediments. The observation that Cl concentrations did not increase uniformly downstream, however, implies that much of the baseflow may comprise bank return flow or interflow. This conclusion is also consistent with water mass balance calculations and the observation that ^{3}H activities (1.85–3.00 TU) in the river were higher than in the groundwater (<0.45 TU). Intermittent streams are likely to be less well connected to regional groundwater, and thus near-river water stores will be more important in sustaining streamflow during dry periods than regional groundwater. These rivers and their ecosystems may be less susceptible to the impacts of groundwater extraction and the near-river waters will provide a buffer zone from potentially contaminated regional groundwater. However, these near river stores are vulnerable to short-term climate variability, and changes to flow regimes resulting from climate change may significantly impact water supplies and ecosystem health.

Chapter 2

Abstract

Documenting baseflow the distribution, sources and fluxes of baseflow discharge into rivers is important for their management and for maintaining ecosystem health. This study uses major ion geochemistry, ^{222}Rn, and ^{3}H to differentiate between the input of low-salinity near-river waters (bank storage and return waters and/or interflow) and regional groundwater in an intermittent river from southeast Australia that is undergoing long-term changes in flow resulting from climate change. Baseflow discharge calculated by ^{222}Rn mass balance was up to 1.3 m^3/m/day in the high flow period in July 2019 and up to 0.1 m^3/m/day at low flow conditions in November 2019. The distribution of ^{222}Rn activities implies higher baseflow fluxes in the upper and middle reaches that have relatively steep topography and higher hydraulic gradients. The lower reaches received less baseflow due to subdued topography and fine-grained sediments. The observation that Cl concentrations did not increase uniformly downstream, however, implies that much of the baseflow may comprise bank return flow or interflow. This conclusion is also consistent with water mass balance calculations and the observation that ^{3}H activities (1.85-3.00 TU) in the river were higher than in the groundwater (<0.45 TU). Intermittent streams are likely to be less well connected to regional groundwater, and thus near-river water stores will be more important in sustaining streamflow during dry periods than regional groundwater. These rivers and their ecosystems may be less susceptible to the impacts of groundwater extraction and the near-river waters will provide a buffer zone from potentially contaminated regional groundwater. However, these near river stores are vulnerable to short-term climate variability, and changes to flow regimes resulting from climate change may significantly impact water supplies and ecosystem health.

Chapter 2

2.1 Introduction

Understanding the water balance in rivers is required for protecting water resources and riverine ecosystems and predicting their response to changing climate, land use, and water extraction (Sophocleous, 2002; Cook., 2013; Van Dijk et al., 2013; Gleeson et al., 2016; Segura et al., 2019). Baseflow represents water stored within a catchment that sustains streamflow between high rainfall periods when surface runoff is limited. In semi-arid areas, baseflow is critical for maintaining rivers and their ecosystems during times of low streamflow (Kalbus et al., 2006; Cartwright and Gilfedder, 2015; Ortega et al., 2015). Baseflow includes regional groundwater, however, other younger sources of water (e.g., perched riparian water, bank return flows, and interflow) may contribute to rivers at different hydrological conditions (McCallum et al., 2010; Cartwright et al., 2014a, Cartwright and Hofmann, 2016; Cook et al., 2018). In many cases, those near-river water stores may contribute a significant proportion of river flows over several weeks to months following high flow events (Cranswick and Cook, 2015; Rhodes et al., 2017; Gilfedder et al., 2019; Cartwright and Irvine, 2020). This may explain the observations that a significant portion of global stream water is less than a few months old (Jasechko et al., 2016) and that stream salinities are commonly significantly below those of regional groundwater even in catchments with prolonged dry seasons (e.g., Simpson and Herczeg, 1991; Howcroft et al., 2019). Near-river water stores are also important in sustaining riparian vegetation (Baillie et al., 2007; Costigan et al., 2016; Riis et al., 2020).

While intermittent streams constitute more than 50% of global river network and are especially common in semi-arid areas, their hydrogeology is far less well understood than that of perennial streams (Datry et al., 2014; Costigan et al., 2016; Gutiérrez-Jurado et al., 2019, Shanafield et al., 2021). Perennial streams are likely to be connected to regional groundwater, which may form a substantial component of baseflow during low flow periods (Tetzlaff and Soulsby, 2008; Cartwright et al., 2014b, 2018; Duvert et al., 2016). On the contrary, intermittent streams are less well connected to regional groundwater, especially during and close to cease-to-flow periods when the water table falls. This means that regional groundwater is less likely to be a major component of baseflow in intermittent streams, which may lead to these streams responding differently to stresses. For example, if much of the baseflow is derived from near-river stores, these may provide a buffer to inflows of contaminated regional groundwater and lessen the impacts of regional groundwater extraction.

The near river-stores are dominated by relatively young water that is vulnerable to short-term changes to climate and streamflow. For example, the high streamflow that generates bank storage waters is diminished during low rainfall years, which can result in significant year-on-year variability in the volume of bank return flows. While regional groundwater is a longer-lived store of water that is less diminished by short-term climate change, prolonged periods of low rainfall can reduce regional water tables which will lessen its connection with rivers (Boulton et al., 2010; Peterson et al., 2021).

Understanding what constitutes baseflow, is also important for calculating baseflow discharge from river geochemistry. Because many of the near-river water stores are derived from recent rainfall, their geochemistry is more similar to surface runoff than regional groundwater and chemical mass balance methods may underestimate the total baseflow discharge (Gonzales et al., 2009, Cartwright et al., 2014a; Rhodes et al., 2017).

Chapter 2

2.1.1 Documenting baseflow inputs

Several methods have been adopted to investigate the location and magnitude of baseflow inputs in rivers (Brodie et al., 2007; Gonzales et al., 2009; Cook, 2013; Hagedorn, 2020). When there are sufficient groundwater bores and river elevation data, baseflow could be determined using Darcy's Law (Lamontagne et al., 2014; Martinez et al., 2015). However, the paucity of bores and gauges in most catchments makes this difficult (McCallum et al., 2012; Cook, 2013). Water mass balance (also referred to as differential flow gauging) estimates baseflow from the difference in streamflow between upstream and downstream points along the river (McCallum et al., 2012; Unland et al., 2013; Rhodes et al., 2017). This technique, however, requires a high density of river discharge measurements and it is difficult to determine small exchange fluxes.

Because baseflow and river water are likely to have contrasting geochemistry, longitudinal changes in river geochemistry can be used to estimate baseflow discharge (e.g., Cook, 2013). A wide range of geochemical tracers have been applied to map the distribution and quantify the amount of baseflow, including electrical conductivity (EC), major ions, stable isotopes and radioactive isotopes (especially radon-222) (Oxtobee and Novakowski, 2003; Brodie et al., 2007; Smerdon et al., 2012; Cook, 2013; Unland et al., 2013; Cartwright and Gilfedder, 2015; Ortega et al., 2015; Cartwright and Hofmann, 2016; Cook et al., 2018). Various factors affect the utility of different tracers, such as: the difference in concentrations between stream water and baseflow; the spatial and temporal heterogeneity of the baseflow component; and processes that may change the concentration of chemical tracers in the river (e.g., evaporation, radioactive decay, degassing and biochemical reactions). However, while such factors need to be considered, geochemical tracers remain useful in estimating baseflow contributions in regulated or unregulated catchments.

^{222}Rn is an important tracer for quantifying baseflow fluxes to rivers. ^{222}Rn, which has a half-life of 3.8 days, is part of the ^{238}U to ^{206}Pb decay series. Because the concentration of U in minerals is significantly higher than that in surface water, ^{222}Rn activities in groundwater are commonly 2 to 3 orders of magnitude higher than those of stream water (Cecil and Green, 2000; Burnett and Dulaiova, 2006; Burnett et al., 2010). Because of radioactive decay and degassing to the atmosphere, high ^{222}Rn activities generally occur only around zones of baseflow input (Genereux and Hemond, 1992; Cook, 2013).

While it is a successful tracer of baseflow discharge, there are several uncertainties in using ^{222}Rn. The ^{222}Rn activities in the baseflow may be poorly defined or spatially and temporally heterogeneous (Mullinger et al., 2007; Cook, 2013; Atkinson et al., 2015; Cartwright and Hofmann, 2016). In particular, ^{222}Rn activities measured in groundwater from bores that are several kilometres from the river may not be the same as those of the near-river groundwater. In addition, the rate of ^{222}Rn degassing is difficult to quantify (Genereux and Hemond, 1992; Lamontagne and Cook, 2007; Cook, 2013). Lastly, estimating the ^{222}Rn produced in the hyporheic zone is required to calculate baseflow fluxes (Bourke et al., 2014; Cartwright et al., 2014b; Cartwright and Hofmann, 2016). These factors lead to uncertainties in quantifying baseflow inputs, although the variation in ^{222}Rn activities in rivers may still be used to map zones of baseflow inputs. Another radioactive tracer tritium (^{3}H) with a half-life of 12.32 years can also be employed to understand the sources of water in streams (e.g., Morgenstern et al., 2010; Duvert et al., 2016; Howcroft et al., 2019). Following the decline of the high ^{3}H activities produced during the atmospheric nuclear tests in the 1950s and 1960s, ^{3}H activities in older water in the southern hemisphere are lower than those in younger water (Morgenstern et al., 2010). This makes ^{3}H valuable for distinguishing between younger near-river stores and older regional groundwater (Tardros et al., 2014; Cartwright et al., 2018; Howcroft et al., 2019).

The combined use of geochemical tracers can help resolve whether regional groundwater dominates baseflow or if near-river sources of water are also important. Because ^{222}Rn activities achieve secular equilibrium with minerals in the aquifer matrix over much shorter timescales (approximately 3 weeks; Cecil and Green, 2000) than those over which changes to major ion geochemistry by mineral dissolution or evapotranspiration occurs (Genereux and Hemond, 1992), the combined use of ^{222}Rn and major ions could be able to distinguish between these water stores. In addition, ^{3}H activities directly indicate the residence time of the water that contributes to baseflow at different locations or times.

2.1.2 Objectives

This study determines the sources, location, and magnitude of baseflow discharge in the upper Wimmera River, southeast Australia using ^{222}Rn, ^{3}H activity, major ion geochemistry, and water mass balance. Specially, the study addresses: 1) whether the combination of geochemical tracers can distinguish between the input of baseflow from near-river stores (e.g., bank storage and return flows) and regional groundwater; 2) the controls on the spatial and temporal variation of baseflow, and 3) whether estimates of baseflow using ^{222}Rn activities from regional groundwater or emanations from near-river sediments are more appropriate to apply in ^{222}Rn mass balance studies. As with many rivers globally, climate change has altered streamflow in the upper Wimmera River and the results have broad implications for the study of baseflow in intermittent rivers and streams that will aid in managing and protecting these critical environments.

2.2 Study area

The Wimmera River (Fig. 2.1) is an intermittent river in the Murray-Darling Basin of southeast Australia with a catchment area of approximately 24000 km^2 (Department of Environment, Land, Water and Planning, 2020). It is an endorheic system that discharges to a series of terminal lakes and wetlands in northern Victoria. The lower and middle Wimmera River is an important water source for dryland agriculture in semi-arid north-west Victoria (Fletcher, 2015; Department of Environment, Land, Water and Planning, 2020). The study area in the little utilised upper Wimmera River catchment (Fig. 2.1) is approximately 3000 km^2 and includes two intermittent tributaries: Mount Cole Creek and Concongella Creek (Wimmera Catchment Management Authority, 2013). Although an important tributary to the Murray-Darling system there have been no published studies of the hydrogeology of the Wimmera River aside from an analysis of stratified groundwater-fed pools in the lower reaches of the Wimmera River (Western et al., 1996).

The geology of the area consists of several Palaeozoic basement formations (Fig. 2.1) including metamorphosed shales and schists of the St Arnaud Group, indurated sandstones of the Glenthompson and Grampians Groups, and Devonian granites (Department of Jobs, Precincts and Regions, 2020). Overlying these are several Palaeogene to Recent formations of alluvial and lacustrine sediments that were deposited by the current rivers and which consist of rounded gravels, coarse sands, silts and clays (Cayley and McDonald, 1995; Robinson et al., 2006). Most of the catchment is covered by dryland pasture with remnant native eucalypt woodlands on some of the hills in the upper reaches (Fletcher, 2015; Department of Environment, Land, Water and Planning 2020). The upstream reaches of the upper Wimmera River occupy a broad valley surrounded by hills while the downstream reaches are open alluvial flood plains. Those plains receive flows from ephemeral tributaries and are prone to flooding in wet periods (Robinson et al., 2006; Department of Environment, Land, Water and Planning, 2020).

Average annual rainfall of this area ranges from 709 mm in the southeast of the area to 505 mm in the northwest (Bureau of Meteorology, 2019). The wettest months are from May to August whereas January and April are the driest. Monthly potential evaporation ranged from 27 to 218 mm in 2019 and rainfall is only higher than evaporation during the winter months (Bureau of Meteorology, 2019). High streamflow occurs in the winter and spring and the river commonly ceases to flow during the summer months and consists of disconnected pools. Unlike the larger pools in the lower Wimmera River (Western et al., 1996), these are not stratified. Average annual streamflow between 2000 and 2019 ranged from 3.6×10^4 to 3.2×10^7 m^3/year at Eversley, 2.6×10^4 to 1.2×10^8 m^3/year at Glynwylln, and from 4.4×10^4 to 1.5×10^8 m^3/year at Glenorchy (Department of Environment, Land, Water and Planning, 2020).

Wimmera River streamflow has declined and the duration of cease-to-flow periods have increased since the 1980s especially during the prolonged Millennium drought in southeast Australia (1996 to 2009) and the subsequent frequent hotter and drier than average years (Vertessy et al., 2019; Bureau of Meteorology, 2019; Department of Environment, Land, Water and Planning, 2020). Groundwater elevations in the upper Wimmera River have also fallen by up to a few metres since the 1980s (Department of Environment, Land, Water and Planning, 2020). These changes suggest that, like many streams in southeast Australia, the Wimmera river has become progressively less connected to regional groundwater and is more intermittent (Peterson et al., 2021).

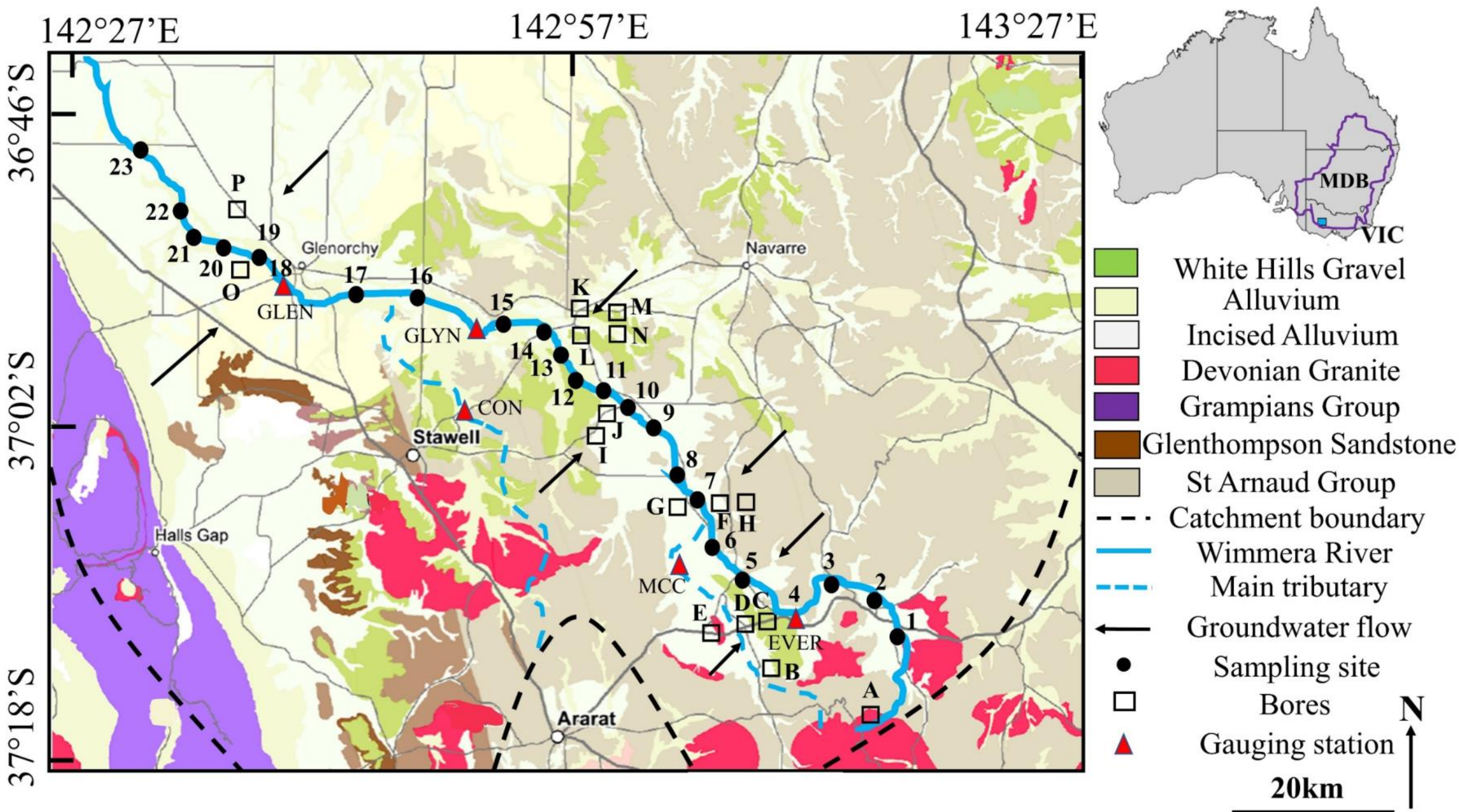

Figure 2.1. Summary geological and hydrogeological map of the upper Wimmera River. Stream water sampling sites and groundwater bores are indicated by numbers and letters, respectively. Gauging station and site numbers are: EVER = Eversley (415207), MCC = Mount Cole Creek (415245), CON = Concongella Creek (415237), GLYN = Glynwylln (415206), GLEN = Glenorchy (415201). Data from Robinson et al. (2006), Department of Environment, Land, Water and Planning (2020), Department of Jobs, Precincts and Regions (2020).

2.3 Materials and methods

2.3.1 Sampling

Three rounds of stream water sampling took place between July and November 2019 in the upper Wimmera River. The July and September periods represent generally high and intermediate streamflow periods whereas the November 2019 sampling was just prior to the river ceasing to flow. Each sampling campaign involved sampling 23 sites (Fig. 2.1, Table 2.1) from the centre of flowing sections using an open collector. The samples were collected from ~1m below the surface (or just above the riverbed where the river was shallower). Groundwater samples were collected using an impeller pump in November 2019 from bores installed on the river bank and floodplain (Fig. 2.1, Table 2.2). 32 samples of river bed sediments along the river were also collected (Table 2.3).

Distances (Table 2.1) were measured relative to the first sampling site at Elmhurst (0 km). Streamflow is measured continuously at three gauging stations along the river (Eversley, Glynwylln and Glenorchy; Fig. 1) (Department of Environment, Land, Water and Planning, 2020). Intermediate streamflow data was estimated by linear interpolation and extrapolation. Mount Cole Creek and Concongella Creek also have continuous streamflow measurements.

2.3.2 Analytical techniques

A calibrated TPS meter and electrode was used to measure EC values in the field. Cation concentrations were measured on a ThermoFischer quadrupole ICP-OES at Monash University on samples filtered through 0.45μm cellulose nitrate filters and acidified to pH <2. A Thermo Fischer ion chromatograph at Monash University was used to measure anions on filtered unacidified samples. The precision of major ion concentrations based on replicate analyses is 2-5 %. EC values, Cl concentrations, and Na concentrations are presented in Tables 2.1 and 2.2; a full suite of geochemistry is in the Supplement. Portable radon-in-air detectors (Durridge Corporation RAD-7) were used to measure ^{222}Rn activities in groundwater and surface water following Burnett and Dulaiova (2006). ^{222}Rn was degassed from 500 ml of water for 5 min into a closed air loop of known volume. Counting times were 2 hours and ^{222}Rn activities are reported in becquerels per m^3 of water (Bq/m^3). The precision of ^{222}Rn activities is ~3% at 10,000 Bq/m^3 and ~10% at 100 Bq/m^3. ^3H activities were analysed at GNS, New Zealand following Morgenstern and Taylor (2009) by liquid scintillation using Quantulus counters following vacuum distillation and electrolytic enrichment. ^3H activities are expressed in tritium units (TU) and the detection limit is 0.02 TU with a precision of ~2%.

^{222}Rn emanation rates (γ in $Bq/m^3/day$) were determined from the sediment samples by sealing a known dry weight of sediment in airtight containers with water and allowing ^{222}Rn to accumulate (Lamontagne and Cook, 2007). After 4-5 weeks incubation, the rate of ^{222}Rn production and decay has reached steady state. The ^{222}Rn activities were measured from 100-150 mL of water using the same method as above but with counting times of 6-12 hours. γ was calculated from the ^{222}Rn produced per unit mass of sediment (E_m in Bq/kg), sediment density (ρ_s in kg/m^3), and porosity (φ) by (Lamontagne and Cook, 2007; Cartwright et al., 2014b)

$$\gamma = \frac{E_m(1-\varphi)\rho_s\lambda}{\varphi} \tag{1}$$

where λ is the decay constant ($0.181 day^{-1}$).

2.3.3 Radon (^{222}Rn) mass balance

The baseflow flux I (in $m^3/m/day$) was estimated from

$$I=\frac{Q\frac{dCr}{dx}-wECr-F_h+kdwC_r+\lambda dwC_r}{C_{bf}-C_r} \tag{2}$$

(Mullinger et al., 2007; Cook, 2013). In equation 2, Q is streamflow (m^3/day), C_r and C_{bf} are the ^{222}Rn activities in the river and baseflow respectively (Bq/m^3), x is distance along the river (m), w is river width (m), d is river depth (m), E is the evaporation rate (m/day), F_h is the input of ^{222}Rn resulting from exchange with the hyporheic zone (Bq/m/day), k is the gas-transfer coefficient (day^{-1}), and λ is the decay constant.

River depth and width were measured in the field and evaporation rates were obtained from the Bureau of Meteorology (2019). The regional groundwater bores are located a few hundreds of meters to several kilometres from the river. As mentioned above, it is not certain whether regional groundwater contributes significantly to streamflow. Furthermore, even if regional groundwater does discharge into rivers, its ^{222}Rn activities are controlled by the emanation rates in the aquifers immediately adjacent to the river (Avery et al., 2018; Gilfedder et al., 2019). Hence, C_{bf} was estimated in this study from the average radon emanation from the sediments (Table 3). The input of ^{222}Rn from the hyporheic zone (F_h in Bq/m/day) was estimated via a one-dimensional exchange model (Lamontagne and Cook, 2007; Cartwright et al., 2014b):

$$F_h=\frac{\gamma w_h d_h \varphi}{1+\lambda t_h}-\frac{\lambda w_h d_h \varphi}{1+\lambda t_h}C_r \tag{3}$$

In equation (3), w_h is the width of the hyporheic zone and d_h is the thickness of the hyporheic zone. The residence time of water in the hyporheic zone (t_h) is relatively short and usually ranges from 0.05 to 0.2 days in relatively fine-grained sediments (Lamontagne and Cook, 2007; Sawyer and Cardenas, 2009; Zarnetske et al., 2011). F_h is relatively insensitive to t_h where t_h is less than one day (Lamontagne and Cook, 2007).

The gas-transfer coefficient (k) was estimated using the empirical equations:

$$k=9.301\times10^{-3}\left(\frac{v^{0.5}}{d^{1.5}}\right) \tag{4}$$

and

$$k=4.87\times10^{-4}\left(\frac{v}{d}\right)^{0.85} \tag{5}$$

(O'Connor and Dobbins, 1958; Negulescu and Rojanski, 1969; Mullinger et al., 2007) where d is river depth (m) and v is river velocity (m/day). Other empirical formulations (e.g., Genereux and Hemond, 1992) generally yield estimates of k between those from equations (4) and (5) (Mullinger et al., 2007). Values of k were estimated for each reach using the interpolated streamflow and average depth and widths.

2.3.4 Water mass balance

Assuming steady state conditions, net baseflow (I_{net}) can be estimated from the water mass balance between two gauging stations:

$$I_{net}=Q_d - Q_u - Q_t + E_{net} - P \tag{6}$$

(Lerner et al., 1990; McCallum et al., 2012; Rhodes et al., 2017). In Eq. (6), Q_d is the streamflow at the downstream gauge, Q_u is the streamflow at the upstream gauging station, Q_t is tributary streamflow, and P is the direct precipitation on the river, and E_{net} is the net evaporation rate. All parameters have units of m^3/day.

2.4 Results

2.4.1 Streamflow

The streamflow between January 2018 and June 2020 at the Glynwylln gauging station in the middle of the studied section of the Wimmera River is shown in Fig. 2.2a (Department of Environment, Land, Water and Planning, 2020). Streamflow was less than 200 m^3/day in 2018 (Fig. 2.2a), whereas in 2019, which had higher rainfall compared to 2018, streamflow was up to 6.5×10^6 m^3/day. Between January and March 2019, the river periodically ceased to flow and consisted of disconnected water pools. The streamflow significantly increased from June and peaked in August at 6.5×10^6 m^3/day. During the sampling periods, the average values of daily streamflow at Glynwylln were 71,100 m^3/day in July, 24,580 m^3/day in September and 133 m^3/day in November 2019 (Fig. 2.2a); these varied by < 15% over each sampling periods. Maximum streamflow increased downstream from Eversley to Glenorchy (Fig. 2.2b). While all stations recorded cease-to-flow periods, these were more prevalent at Glenorchy (45% of the time between 2000 and 2019) than at Eversley (28%) or Glynwylln (14%).

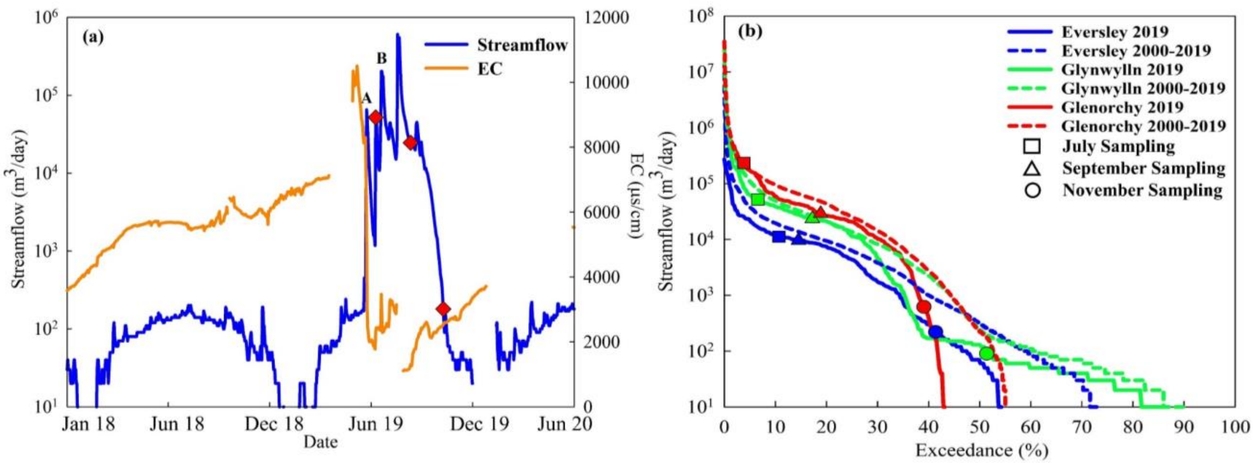

Figure 2.2. (a) Variations in streamflow and EC of the upper Wimmera River at Glynwylln (missing data are due to malfunction of measurement equipment). Sampling times are indicated by the diamond symbols. A and B represent high streamflow events in 2019 (Fig. 2.3). 2b. Flow duration curves for Eversley, Glynwylln and Glenorchy (Fig. 2.1) in 2019 and between 2000 and 2019. Line arrows show the conditions during the 2019 sampling campaigns. Data from the Department of Environment, Land, Water and Planning (2020).

2.4.2 Regional groundwater geochemistry

Regional groundwater from the upper Wimmera had EC values of 1045-20,750 µS/cm (mean = 7482 ± 5729 µS/cm). These are within the range generally reported for this part of the catchment (10,000-22,000 µS/cm: Department of Environment, Land, Water and Planning, 2020). Na and Cl concentrations were 156-4281 mg/L (mean = 1238 ±1026 mg/L) and 460-8400 mg/L (mean = 2581 ± 2285 mg/L), respectively (Table 2.2). The Cl concentrations of groundwater were lower (2010 ±1871 mg/L, n=14) in the upper catchment (A to I on Fig. 2.1) than in the lower part of the catchment (3308 ± 2635 mg/L, n=11) (J to P on Fig. 2.1). EC values and the concentration of other major ions showed a similar distribution (Table 2.2). ^{222}Rn activities of groundwater varied between 3700 and 99,700 Bq/m^3 (mean = 30,389 ± 23,225 Bq/m^3, n=23). The ^{222}Rn activities of groundwater from the various alluvium deposits ranged from 3900 to 99,700 Bq/m^3 (mean = 32,996 ± 26,475 Bq/m^3, n=16), ^{222}Rn activities of groundwater from the White Hill gravel varied from 3700 to 35,100 (mean = 20,925 ± 11,985 Bq/m^3, n=4); one sample of groundwater from the granite had a ^{222}Rn activity of 23,900 Bq/m^3, and the ^{222}Rn activities of two samples of groundwater in the St Arnaud Group were 4980 and 18,500 Bq/m^3. Regional groundwater had ^{3}H activities of 0.02-0.45 TU (Table 2.2).

2.4.3 Stream water geochemistry

In 2018, the EC values were relatively high (3580 to 6500 μS/cm) throughout the entire year (Fig.2.2a), whereas in 2019 EC values peaked at 10,500 μS/cm in late May and decreased to 1780 μS/cm in June. The lowest EC values of 1100 μS/cm in 2019 occurred during the high streamflow in August and EC values subsequently increased to 5520 μS/cm in June 2020 as streamflow declined. The high EC values of stream water were most likely caused by inflows of saline regional groundwater; however, they were always below the EC values of this groundwater (typically between 10,000 and 22,000 μS/cm) even during the low rainfall periods.

EC values and streamflow defined clockwise hysteresis loops (i.e. the EC on the rising limb of the hydrograph was higher than for the same streamflow on the falling limb) (Fig. 2.3). Similar hysteresis loops have been interpreted to indicate dilution of saline baseflow by surface runoff at the start of the flow event followed by the input of low salinity waters such as bank return flows and/or interflow after the high flow event (Batlle-Aguilar et al., 2014; Rhodes et al., 2017; Howcroft et al., 2019).

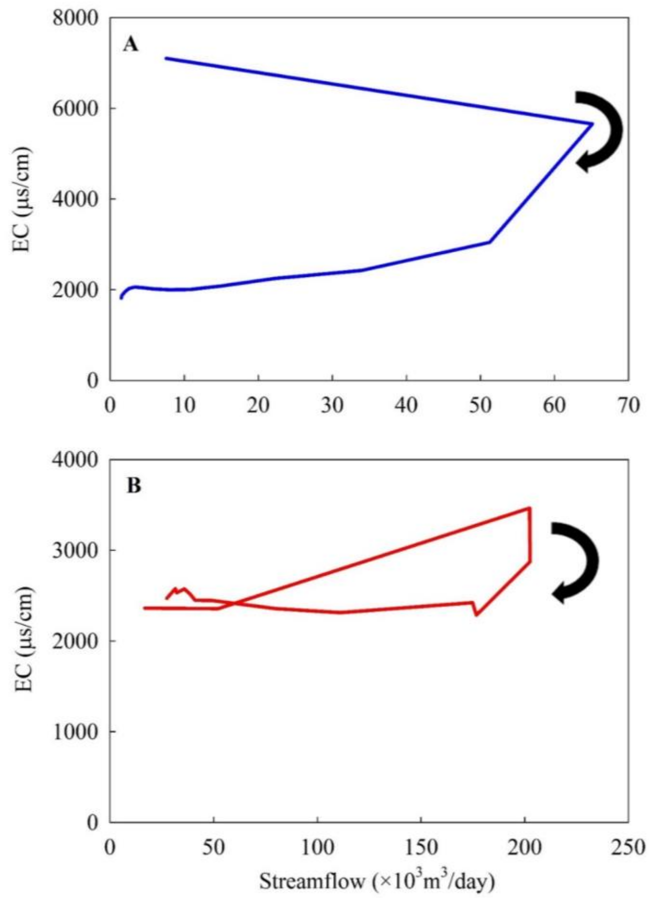

Figure 2.3. EC vs streamflow hysteresis loops for high streamflow events in 2019 (A and B in Figure 2.2). Arrows show changes with time. Data from the Department of Environment, Land, Water and Planning (2020).

Radon activities along the river were variable (Fig. 2.4a, Table 2.1). The highest ^{222}Rn activities in each sampling round (up to 2860 Bq/m^3 in November) occurred in the upper reaches at Elmhurst (0 km). Between 0 to 20 km ^{222}Rn activities declined irregularly to as low as 366 Bq/m^3 in July. In November, a zone of higher ^{222}Rn activities (up to 1500 Bq/m^3) occurred between 32 km and 44 km but ^{222}Rn activities in this area were less variable (421-700 Bq/m^3) in July and September. There were peaks in ^{222}Rn activities (up to 1160 Bq/m^3) in all three sampling periods between 53 km and 70 km. The reaches downstream of 80 km had ^{222}Rn activities ranging from 150 to 600 Bq/m^3 with higher activities recorded in November (Table 2.1, Fig. 2.4a).

Unlike many rivers that receive groundwater inflows where Cl concentrations increase uniformly downstream (Unland et al., 2013; Ortega et al., 2015), Cl concentrations in the upper Wimmera River were spatially variable (Fig. 2.4b). Cl concentrations between 0 km and 32 or 39 km increased irregularly from 370 to 1100 mg/L in July, 200 to 550 mg/L in September and 310 to 870 mg/L in November. Cl concentrations in September and November then gradually decreased downstream to as low as 317 and 605 mg/L, respectively. In July, Cl concentrations downstream of 32 km were more irregular with locally high concentrations of 1200 and 1280 mg/L recorded at 53 and 98 km, respectively; Cl concentrations in the remaining reaches were as low as 79 mg/L (Fig. 4b). EC values and concentrations of other major ions, such as Na, had similar trends (Table 1).

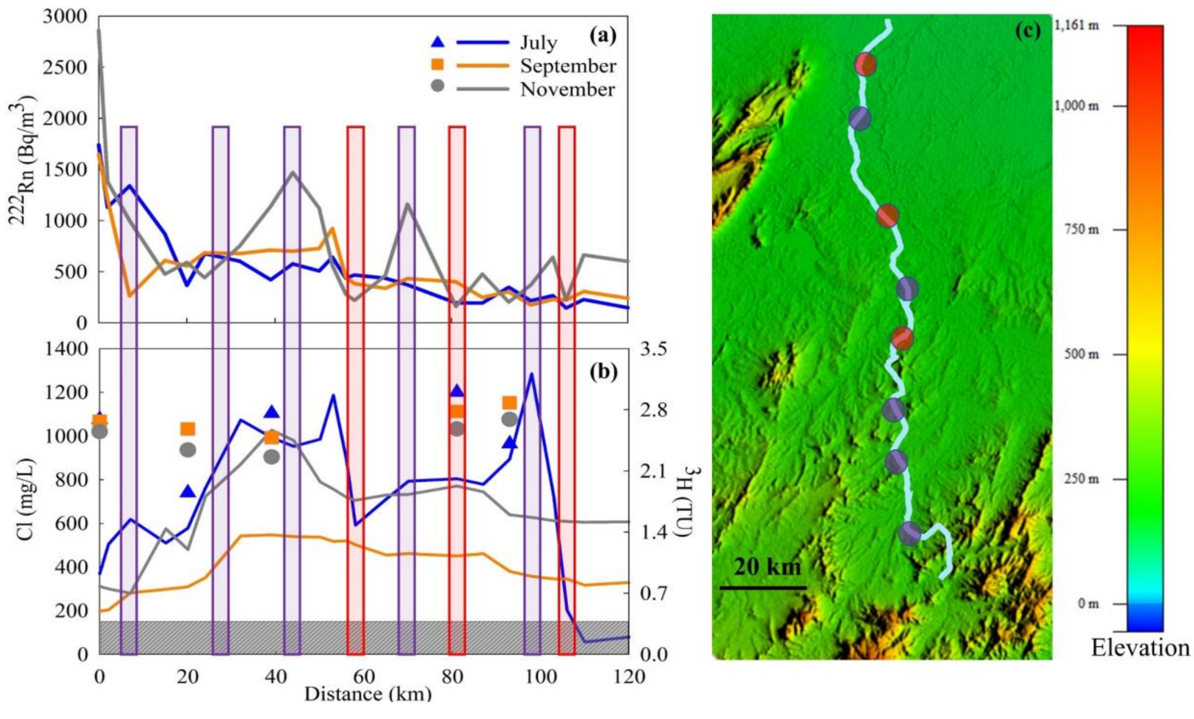

Figure 2.4. Downstream variations in ^{222}Rn activities (4a) and Cl concentrations and ^{3}H activities (individual symbols) (b) in 2019 with inferred zones of high baseflow discharge (purple shading) and lower baseflow discharge (red shading). Shaded area indicates the range of ^{3}H activities in regional groundwater. (c) Topography variations along the river (topography data from International Agricultural Research Consortium database). Data from Table 2.1.

The average ^3H activity in local precipitation in this region is 3.0±0.2 TU (Tadros et al., 2014; Howcroft et al., 2019). The ^3H activities of stream water were lower than those of rainfall and ranged from 1.85 to 3.00 TU in July, 2.48 to 2.88 TU in September, and 2.26 to 2.69 TU in November (Table. 2.1 and Fig. 2.4). The ^3H activities of river water were, however, significantly higher than those of regional groundwater (< 0.45TU) at all flow conditions. The ^3H activities in the lower reaches (Camb and Glen on Fig. 2.1) were higher (2.41-3.00 TU) than in the upper and middle reaches. The ^3H activities and EC in the high-flow period (July) were uncorrelated. In the intermediate (September) and low flow periods (November) the ^3H activities were higher at lower EC values (Fig. 2.5), although the correlation is weak (R^2 ~0.1).

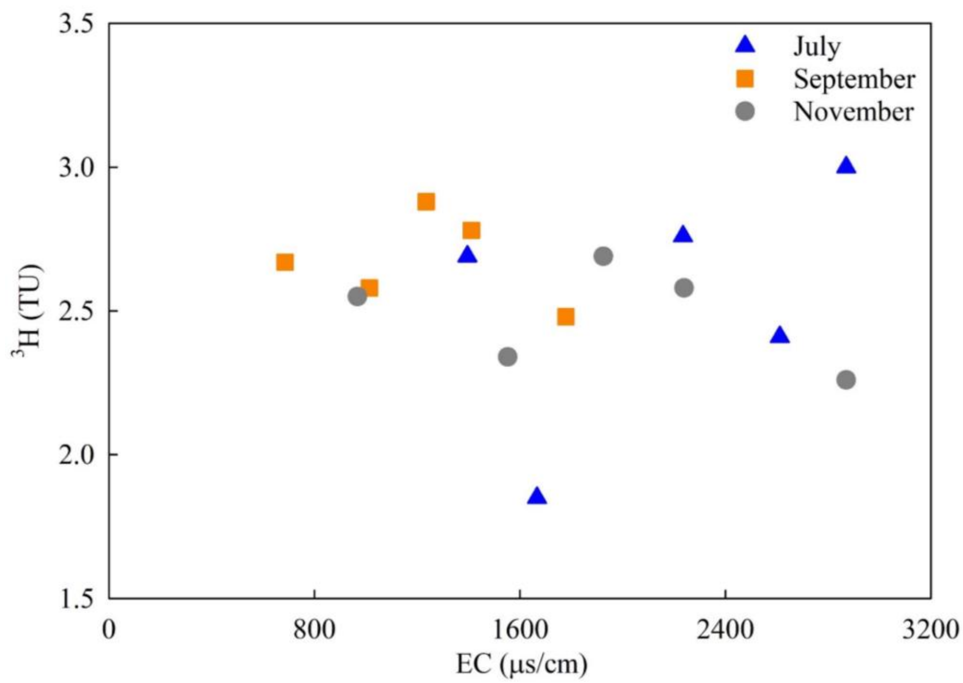

Figure 2.5. ^3H activities and EC of stream water at different flow conditions. Strong inverse correlations between ^3H activities and EC in September and November sampling rounds. Data from Table. 2.1.

2.4.4 Radon emanation rates

The ^{222}Rn emanation rates of the river bank sediments (Table 2.3) were determined via Eq. (1) using a matrix density of 2700 kg/m^3, which is suitable for quartz-dominant sediments, and a porosity of 0.4, which is suitable for unconsolidated sediments (Lamontagne and Cook, 2007; Cartwright and Gilfedder, 2015). γ values ranged from 1041-12,624 Bq/m^3/day with a mean value of 4274 ± 2872 Bq/m^3/day (n=32). Radon activities of water in equilibrium with the sediment calculated from γ/λ (Cecil and Green, 2000) were 5751 to 69,747 Bq/m^3 (mean = 23,615 ± 15,866 Bq/m^3) (Table 3). These ^{222}Rn activities were lower than those measured in the groundwater (30,389 ± 23,225 Bq/m^3), but this difference was not significant (p-value from a two-tailed T-test = 0.2).

2.4.5 Baseflow estimates from radon (^{222}Rn)

Baseflow fluxes were estimated using Eq. (2). The mean radon emanation rate (γ) of 4274 Bq/m^3/day (Table 2.3) yields an average ^{222}Rn activity of baseflow of 23615 Bq/m^3 (Table 2.3). The input of ^{222}Rn from hyporheic zone exchange (Eq. 3) assumed that the hyporheic zone is as wide as the river with a thickness of 0.1 m (appropriate in relatively fine-grained sediments) and a porosity of 0.2, which is also appropriate for fine-grained sediments (Lamontagne and Cook, 2007; Sawyer and Cardenas, 2009; Zarnetske et al., 2011). t_h was assigned as 0.1 days. Average evaporation rates for the sampling periods were 8.1×10^{-4} m/day in July 2019, 1.9×10^{-3} m/day in September, and 5.5×10^{-3} m/day in November 2019 (Bureau of Meteorology, 2019). Gas-transfer coefficients (k) estimated from Eqs (4) and (5) were 1, 0.6 and 0.2 day^{-1} in the July, September, and November sampling rounds respectively. These values are relatively low compared with those in other rivers (e.g. Cook et al., 2006; Mullinger et al, 2007, 2009; Unland et al., 2013; Yu et al., 2013; Cartwright et al., 2014b; Atkinson et al., 2015). However, this is consistent with the upper Wimmera River being dominated by slow-flowing pool sections, especially during November, and the lack of fast-flowing turbulent reaches. The impact of ^{222}Rn contributions from tributaries was assessed using ^{222}Rn activities and tributary streamflow data. Because the tributaries had similar ^{222}Rn activities to the main river, they had little impact on the ^{222}Rn budget.

Baseflow fluxes were irregularly distributed along the river and were up to 1.3 m^3/m/day (Fig. 2.6a), increasing with streamflow. Given that ^{222}Rn reaches secular equilibrium with aquifer sediments in approximately three weeks, these fluxes likely represent total baseflow rather than just the regional groundwater inflows. In November 2019, baseflow inputs were lowest (<0.12 m^3/m/day). The zones of little or no baseflow inputs are in the middle reaches (58 to 81 km) implying that these may have been losing. During high flow periods in July 2019, the baseflow fluxes were relatively high with several zones of high baseflow inputs (1.0 and 1.1 m^3/m/day) between 20 to 53 km and 81 to 98 km, respectively. In the lower reaches between 103 and 106 km, baseflow inputs in July were < 0.7 m^3/m/day. Baseflow inputs in September were up to 0.4 m^3/m/day and had a similar distribution to those in November (Fig. 2.6a). The cumulative baseflow inputs in the upper Wimmera River were 72,800 m^3/day (51% of total streamflow) in July, 15,180 m^3/day (42% of total streamflow) in September, and 5120 m^3/day in November (Fig. 2.6b). The cumulative baseflow input exceeded the total streamflow under low flow conditions in November. This is because sampling occurred just prior to the cease-to-flow period and several reaches were probably losing at that time. Geochemical tracers, such as ^{222}Rn, only quantify baseflow discharge and not losses from rivers with alternating gaining and losing reaches. Nevertheless, the distribution of ^{222}Rn still allows the distribution of gaining and losing reaches to be identified.

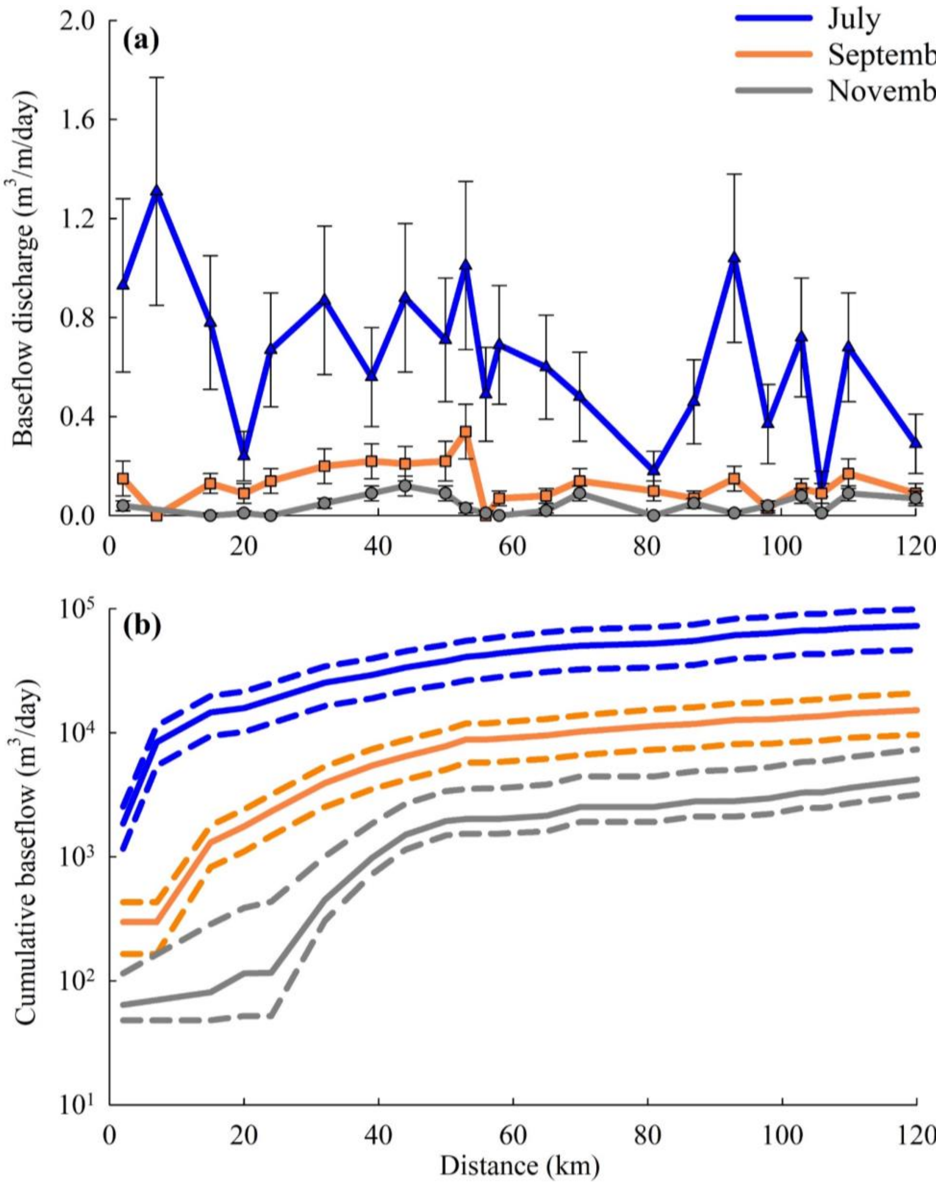

Figure 2.6. Baseflow influxes of each sampling period calculated from ^{222}Rn mass balance. Error bars represent the variations caused by net uncertainty (σ_t) based on uncertainty propagation (a). Cumulative baseflow and variations (dot lines) of overall uncertainty for the upper Wimmera River (b).

2.4.5.1 Uncertainties

The variability of radon activities in the baseflow end member (C_{bf}), values of the gas-transfer coefficient (k) and the effects of hyporheic zone exchange (F_h) are the main uncertainties in the ^{222}Rn mass balance. Assuming that the uncertainties are uncorrelated and normally distributed, the net uncertainty (σ_t) is $\sqrt{\sigma_{c_{bf}}{}^2+\sigma_{Fh}{}^2+\sigma_k{}^2}$.For the baseflow end member, the 95% confidence interval of ^{222}Rn emanation rates from near river sediments (5720 Bq/m^3 in Table 2.3) was used to estimate uncertainty. This resulted in 26%, 24%, and 24% of variations in all baseflow discharge estimates. The gas transfer constant (k) varies with river turbulence, velocities and depth (Genereux and Hemond, 1992; Mullinger et al., 2007, 2009) and is difficult to estimate. Other empirical formulations (e.g., Genereux and Hemond, 1992) yield similar k values to those from Eq. (4) and Eq. (5). Direct measurement of k values over small river sections is possible (Cook et al., 2006; Bourke et al., 2014) but these may not be applicable to all river reaches and different flow conditions. The uncertainty in k is difficult to robustly assess but previous studies have estimated it at 25% (Cartwright and Gilfedder, 2015). A 25% uncertainty of k values led to 27%, 24%, and 29% variations during different flow stages, similar to that resulting from variations in the ^{222}Rn activity of the baseflow end-member. Because the thickness of hyporheic zone is likely to be only a few centimetres in these fine-grained sediments, uncertainties in F_h had a limited impact on baseflow estimates and even assuming no hyporheic exchange just increased the baseflow influxes by less than 10%. The variability of F_h represents a minor source of uncertainty as is the case in other studies (e.g., Tonina and Buffington, 2011; Cranswick et al., 2014; Avery et al., 2018).

The overall uncertainties of baseflow discharge estimates in three sampling rounds ranged from 33 to 102 % in July, 32 to 82 % in September, and 33 to 307 % in November respectively (Fig. 2.6a). The higher relative uncertainties are in reaches that had little baseflow inputs, especially in November; these have little impact on the estimated total baseflow. For the studied section of the Wimmera River, the uncertainties in cumulative discharge were 40% in July, 36% in September, and 200% in November (Fig. 2.6b). The high uncertainty in November reflects the low baseflow influxes that have high relative errors. While there are significant uncertainties in the ^{222}Rn mass balance, these do not alter the conclusions of the distribution of gaining and losing reaches or the relative baseflow inflows within and between sampling campaigns.

2.4.6 Baseflow estimates from water mass balance

The net baseflow flux to the river was calculated using Eq. (6). The water mass balance is most easily applied to rivers without major storages. The weir at Glenorchy moderates streamflow at Glenorchy gauge (Department of Environment, Land, Water and Planning, 2020), hence, this technique was applied to the section of the river between the Eversley and Glynwylln gauges (Fig. 1) using the parameters in Table 4. The streamflow ranged from 203 to 16,210 m^3/day at Eversley and 133 to 71,100 m^3/day at Glynwylln. Mount Cole Creek is the only major tributary between Eversley and Glynwylln and the contribution of streamflow from Mount Cole Creek is 70 to 11,690 m^3/day. The baseflow discharge was highest in July 2019 at 42,879 m^3/day and it decreased to 9017 m^3/day in September and 2729 m^3/day in November (Table 2.4). The water mass balance and the ^{222}Rn mass balance yielded similar estimates of baseflow for this part of the river (Table 2.4).

Previous studies have shown that most of the uncertainty using this method stems from the uncertainty in measuring streamflow of rivers when rating curves are used (McCallum et al., 2012; Coxon et al., 2015; Rhodes et al., 2017). The median uncertainties of daily river streamflow measurements in Australia are typically ± 4.5 % (McMahon and Peel, 2019). Applying those uncertainties to streamflow data at the upstream, downstream, and tributary gauging station resulted in net uncertainties (σ_t) in baseflow discharge of 8.6% (July), 15.1% (September) and 0.5%

(November). Those net uncertainties yielded ranges of baseflow of 39,537-46,211m^3/day (July), 8314-9720 m^3/day (September), and 2516-2942 m^3/day (November) (Table 2.4).

2.5 Discussion and conclusion

The combined geochemical data allow the spatial pattern, sources, and volumes of baseflow discharge to the upper Wimmera River, which were previously unknown, to be determined.

2.5.1 Sources of water contributing to the stream

The variations in streamflow and EC values (Fig. 2.2a) suggested that high salinity regional groundwater contributed to streamflow in 2018 and during some flow periods in 2019. EC values were lower during the high flow events in 2019 probably due to the greater contribution of surface runoff. The persistence of lower EC values following the high flow events in 2019 together with the observation that EC values and streamflow defined clockwise hysteresis loops (Fig. 2.3) probably reflects the input of low salinity water such as bank return flow or interflow as flows decline (Cartwright et al., 2014a; Howcroft et al., 2019; Liang et al., 2020).

A significant contribution of low salinity near-river water stores also explains the observations that the Cl concentrations of the upper Wimmera River did not uniformly increase downstream (Fig. 2.4b) and that the EC of the river water was always lower than that of regional groundwater. Reaches where Cl concentrations increase (e.g. in the upper catchment) probably receive higher volumes of higher salinity regional groundwater. In the middle and lower reaches, the fluctuating Cl concentrations were probably caused by the limited input of regional groundwater and lower salinity water from near-river stores. The observation that ^{3}H activities were always significantly higher than those of regional groundwater (Fig. 2.4, 2.5) is also consistent with this hypothesis. The higher ^{3}H activities during the intermediate and low flow periods imply the significant input of low salinity young water derived from recent rainfall via bank return flows or interflow at those times. The broad inverse correlation between ^{3}H activities and EC values implies there is some input of older more saline regional groundwater, although the high ^{3}H activities imply that the volume of groundwater is limited. Because regional groundwater is saline, the input of relatively small volumes will influence the major ion geochemistry of the stream. The poor correlation between ^{3}H and EC during the high flow period may reflect the inflows of water from multiple sources (e.g. surface runoff, displaced soil water, regional groundwater and riparian water) at that time.

The observation that the water mass balance and the ^{222}Rn mass balance yielded similar estimates of baseflow is consistent with both estimating total baseflow rather than solely groundwater inflows. ^{222}Rn reaches secular equilibrium with aquifer sediments within a few weeks, which is a much shorter timescale to that over which major ion geochemistry changes due to evapotranspiration and/or mineral dissolution. The combined use of ^{222}Rn and major ion geochemistry is thus useful in discriminating between baseflow derived from regional groundwater and near-river sources. A mixture of regional groundwater and near water stores contributing to baseflow discharge over prolonged periods have been identified elsewhere, such as the Brazons River, USA (Rhodes et al., 2017), the Mitchell River in northern Australia (Batlle-Aguilar et al., 2014), the Oven, Gellibrand, Barwon, Avon, and Tambo Rivers in southeast Australia (Unland et al., 2014; Cartwright et al., 2014a; Atkinson et al., 2014; Gilfedder et al., 2019; Howcroft et al., 2019; Cartwright and Irvine, 2020), and the Cedar River, USA (Squillace, 1996). Additionally, modelling studies suggest that transient water sources such as bank storage and interflow may contribute to streamflow for several weeks and months following high flow events (e.g. Chen and Chen, 2003; McCallum et al., 2010; Cranswick and Cook, 2015; Cartwright and Irvine, 2020).

2.5.2 Controls on the temporal and spatial variations of baseflow discharge

The high fluxes of baseflow (up to 43,250 m^3/day) in July were probably due to the rise in the water table following increased rainfall and recharge. The rising groundwater would have increased the hydraulic gradient resulting in high inputs of baseflow. As the water table fell baseflow reduced to 2729 m^3/day in November and some reaches became losing as the river disconnected with the regional groundwater.

The distributions of total baseflow influxes estimated from the ^{222}Rn activities were irregular (Fig. 2.6a). High baseflow discharge up to 1.3 m^3/m/day was recorded in the upper reaches between 7 and 15 km where the river is located near steeper hillslopes and flows through coarse sediments (Fig. 2.1 and Fig. 2.4c). Likewise, the reaches from 24 to 53 km where baseflow was up to 1.1 m^3/m/day are where the river flows through a region of relatively steep topography. The high baseflow influxes that occurred in the lower reaches between 93 and 103 km are where the river occupies a narrow valley that is several meters deep (Fig. 2.4c). In all of these localities, there are likely to be steep hydraulic gradients that promote baseflow discharge. In contrast, low baseflow inputs or losing conditions between 53-58 km, 70-87 km and, 106-120 km are in areas of subdued topography (flat alluvial floodplain) where hydraulic gradients are also likely to be lower (Fig. 2.4c). The river at those reaches was likely to recharge the adjacent aquifers and river bank, which again emphasized the importance of near-river water. Overall, topography and hydraulic gradients control the location and volume of baseflow discharge.

2.5.3 Implications

This is the first study to discuss the hydrogeology of the upper Wimmera River and the conclusions help assess the locations, sources, and magnitudes of baseflow in this catchment. These data are vital for managing water resources in this area, especially understanding the potential impacts of groundwater extraction and migration of contaminants (e.g., from agricultural activity). More broadly, this study adds to the understanding that rivers may largely be connected to relatively young near-river water stores rather than old regional groundwater (e.g., Rhodes et al., 2017). This also accounts for the common presence of relatively young water in rivers (Jasechko et al., 2016) and observations that river salinities even in semi-arid areas with long dry seasons are often significantly lower than those of regional groundwater (e.g., Simpson and Herczeg, 1991; Howcroft et al., 2019). Globally, intermittent rivers, such as the upper Wimmera River, may be less well connected to regional groundwater than perennial rivers and are therefore likely to receive a high proportion of water from near-river stores in the alluvial sediments.

The results of this study highlight the difficulty in defining the baseflow end member for chemical mass balance calculations. If rivers receive significant quantities of water from near-river stores, using the geochemistry of regional groundwater in chemical mass balance calculations may not be suitable. In the case of ^{222}Rn, using emanation rates from sediments adjacent to the river rather than data from groundwater bores may be a more viable way of constraining the composition of the baseflow endmember. Other geochemical parameters may be measured from shallow near-river piezometers; however, the likely spatial and temporal variation of geochemistry in the dynamic near-river environment is challenging. Specifically, for ^{222}Rn, the water would need to have been resident in the banks for several weeks for secular equilibrium to be reached.

The exchange of water between the river and adjacent aquifers is important for river functioning and riverine ecosystems. If near-river stores are an important component of baseflow, the impact of extracting regional groundwater on the river is likely to be lower. Additionally, the bank storage zone may act as a buffer zone from potentially contaminated regional groundwater, reducing the rate of contaminant transport into the river. However, to maintain catchment health and river water quality, it is essential to protect the near-river environment.

Streamflow and water table elevations in southeast Australia have declined following the numerous low rainfall years recorded since 1996 and many rivers are becoming increasingly intermittent. Around 30% of catchments in southeast Australia have not recovered following multiple drought years (Peterson et al., 2021). The Wimmera River provides an example of a system that has become more intermittent over time where currently short-term near-river water stores are an important component of baseflow. This results in this river being sensitive to year-on-year variations in precipitation, which may significantly impact river flows and riverine ecosystems in dry years. Determining not only the spatial and temporal variations of baseflow but the sources of the baseflow is important in understanding catchment behaviour.

Chapter 2

References

Atkinson, A.P., Cartwright, I., Gilfedder, B.S., Hofmann, H., Unland, N.P., Cendón, D.I., Chisari, R., 2015. A multi-tracer approach to quantifying groundwater inflows to an upland river; assessing the influence of variable groundwater chemistry. Hydrological Processes, 29, 1-12. https://doi.org/10.1002/hyp.10122

Avery, E., Bibby, R., Visser, A., Esser, B., Moran, J., 2018. Quantification of groundwater discharge in a subalpine stream using radon-222. Water, 10. https://doi.org/10.3390/w10020100

Baillie, M.N., Hogan, J.F., Ekwurzel, B., Wahi, A.K., Eastoe, C.J., 2007. Quantifying water sources to a semiarid riparian ecosystem, San Pedro River, Arizona. Journal of Geophysical Research: Biogeosciences, 112, G03S02. https://doi.org/10.1029/2006JG000263

Batlle-Aguilar, J., Harrington, G.A., Leblanc, M., Welch, C., Cook, P.G., 2014. Chemistry of groundwater discharge inferred from longitudinal river sampling. Water Resources Research, 50, 1550-1568. https://doi.org/10.1002/2013WR013591

Boulton, A.J., Datry, T., Kasahara, T., Mutz, M., Stanford, J.A., 2010. Ecology and management of the hyporheic zone: stream–groundwater interactions of running waters and their floodplains. Journal of the North American Benthological Society, 29, 26-40. https://doi.org/10.1899/08-017.1

Bourke, S.A., Cook, P.G., Shanafield, M., Dogramaci, S., Clark, J.F., 2014. Characterisation of hyporheic exchange in a losing stream using radon-222. Journal of Hydrology, 519, 94-105. https://doi.org/10.1016/j.jhydrol.2014.06.057

Brodie, R., Sundaram, B., Tottenham, R., Hostetler, S., Ransley, T., 2007. An overview of tools for assessing groundwater-surface water connectivity. Bureau of Rural Sciences, Canberra, Australia. http://www.affashop.gov.au/product.asp?prodid=13674

Chapter 2

Bureau of Meteorology, 2019. Commonwealth of Australia Bureau of Meteorology Australian landscape water balance. http://www.bom.gov.au/water/landscape/ (Accessed 20 December 2019).

Burnett, W.C., Dulaiova, H., 2006. Radon as a tracer of submarine groundwater discharge into a boat basin in Donnalucata, Sicily. Continental Shelf Research, 26, 862-873. https://doi.org/10.1016/j.csr.2005.12.003

Burnett, W.C., Peterson, R.N., Santos, I.R., Hicks, R.W., 2010. Use of automated radon measurements for rapid assessment of groundwater flow into Florida streams. Journal of Hydrology, 380, 298-304. https://doi.org/10.1016/j.jhydrol.2009.11.005

Cartwright, I., Gilfedder, B., 2015. Mapping and quantifying groundwater inflows to Deep Creek (Maribyrnong catchment, SE Australia) using ^{222}Rn, implications for protecting groundwater-dependant ecosystems. Applied Geochemistry, 52, 118-129. https://doi.org/10.1016/j.apgeochem.2014.11.020

Cartwright, I., Hofmann, H., 2016. Using radon to understand parafluvial flows and the changing locations of groundwater inflows in the Avon River, southeast Australia. Hydrology and Earth System Sciences, 20, 3581. https://doi.org/10.5194/hess-20-3581-2016

Cartwright, I., Irvine, D., 2020. The spatial extent and timescales of bank infiltration and return flows in an upland river system: Implications for water quality and volumes. Science of the Total Environment, 140748. https://doi.org/10.1016/j.scitotenv.2020.140748

Cartwright, I., Atkinson, A.P., Gilfedder, B.S., Hofmann, H., Cendón, D.I., Morgenstern, U., 2018. Using geochemistry to understand water sources and transit times in headwater streams of a temperate rainforest. Applied Geochemistry, 99, 1-12. https://doi.org/10.1016/j.apgeochem.2018.10.018

Chapter 2

Cartwright, I., Gilfedder, B., Hofmann, H., 2014a. Contrasts between estimates of baseflow help discern multiple sources of water contributing to rivers. Hydrology and Earth System Sciences, 18, 15-30. https://doi.org/10.5194/hess-18-15-2014

Cartwright, I., Hofmann, H., Gilfedder, B., Smyth, B., 2014b. Understanding parafluvial exchange and degassing to better quantify groundwater inflows using ^{222}Rn: The King River, southeast Australia. Chemical Geology, 380, 48-60. https://doi.org/10.1016/j.chemgeo.2014.04.009

Cayley, R.A., McDonald, P.A., 1995. Beaufort 1:100,000 Map Geological Report, Geological Survey of Victoria, Melbourne, Australia.

Cecil, L.D., Green, J.R., 2000. Radon-222. In: Cook P.G., Herczeg A.L. (Eds.), Environmental Tracers in Subsurface Hydrology. Springer, Boston, MA,175-194, 2000. https://doi.org/10.1007/978-1-4615-4557-6_6

Chen, X., Chen, X., 2003. Stream water infiltration, bank storage, and storage zone changes due to stream-stage fluctuations. Journal of Hydrology, 280, 246-264. https://doi.org/10.1016/S0022-1694(03)00232-4

Cook, P.G., 2013. Estimating groundwater discharge to rivers from river chemistry surveys. Hydrological Processes, 27, 3694-3707. https://doi.org/10.1002/hyp.9493

Cook, P.G., Lamontagne, S., Berhane, D., Clark, J.F., 2006. Quantifying groundwater discharge to Cockburn River, southeastern Australia, using dissolved gas tracers ^{222}Rn and SF6. Water Resources Research, 42. https://doi.org/10.1029/2006WR004921

Cook, P.G., Rodellas, V., Stieglitz, T.C., 2018. Quantifying Surface Water, Porewater, and Groundwater Interactions Using Tracers: Tracer Fluxes, Water Fluxes, and End-member Concentrations. Water Resources Research, 54, 2452-2465. https://doi.org/10.1002/2017WR021780

Chapter 2

Costigan, K.H., Jaeger, K.L., Goss, C.W., Fritz, K.M., Goebel, P.C., 2016. Understanding controls on flow permanence in intermittent rivers to aid ecological research: integrating meteorology, geology and land cover. Ecohydrology, 9, 1141-1153. https://doi.org/10.1002/eco.1712

Coxon, G., Freer, J., Westerberg, I. K., Wagener, T., Woods, R., Smith, P.J., 2015. A novel framework for discharge uncertainty quantification applied to 500 UK gauging stations. Water Resources Research, 51, 5531-5546. https://doi.org/10.1002/2014WR016532

Cranswick, R.H., Cook, P.G., 2015. Scales and magnitude of hyporheic, river–aquifer and bank storage exchange fluxes. Hydrological Processes, 29, 3084-3097. https://doi.org/10.1002/hyp.10421

Cranswick, R.H., Cook, P.G., Lamontagne, S., 2014. Hyporheic zone exchange fluxes and residence times inferred from riverbed temperature and radon data. Journal of Hydrology, 519, 1870-1881. https://doi.org/10.1016/j.jhydrol.2014.09.059

Datry, T., Larned, S.T., Tockner, K., 2014. Intermittent rivers: a challenge for freshwater ecology. BioScience, 64, 3, 229-235. https://doi.org/10.1093/biosci/bit027.

Department of Environment Land Water and Planning, 2020. State Government Victoria Department of Environment, Land, Water and Planning Water Monitoring. http://data.water.vic.gov.au/monitoring.htm (Accessed 20 August 2020).

Department of Jobs, Precincts and Regions, 2020. Energy and Earth Resources. Geovic: Geology of Victoria online. http://www.energyandresources.vic.gov.au/earth-resources/maps-reports-and-data/geovic (Accessed 20 August 2020).

Duvert, C., Stewart, M.K., Cendón, D.I., Raiber, M., 2016. Time series of tritium, stable isotopes and chloride reveal short-term variations in groundwater contribution to a stream. Hydrology and Earth System Sciences, 20, 257-277. https://doi.org/10.5194/hess-20-257-2016

Chapter 2

Fletcher, G., 2015. Environmental Water Management Plan-Wimmera River System. Government of Victoria Wimmera Catchment Management Authority. http://wcma.vic.gov.au

Genereux, D.P., Hemond, H.F., 1992. Determination of gas exchange rate constants for a small stream on Walker Branch Watershed, Tennessee. Water Resources Research, 28, 2365-2374. https://doi.org/10.1029/92WR01083

Gilfedder, B.S., Cartwright, I., Hofmann, H., Frei, S., 2019. Explicit Modelling of Radon-222 in HydroGeoSphere During Steady State and Dynamic Transient Storage. Groundwater, 57, 36-47. https://doi.org/10.1111/gwat.12847

Gleeson, T., Befus, K.M., Jasechko, S., Luijendijk, E., Cardenas, M.B., 2016. The global volume and distribution of modern groundwater. Nature Geoscience, 9, 161-167. https://doi.org/10.1038/ngeo2590

Gonzales, A.L., Nonner, J., Heijkers, J., Uhlenbrook, S., 2009. Comparison of different base flow separation methods in a lowland catchment. Hydrology and Earth System Sciences, 6, 2055–2068. https://doi.org/10.5194/hess-13-2055-2009

Gutiérrez-Jurado, K.Y., Partington, D., Batelaan, O., Cook, P., Shanafield, M., 2019. What triggers streamflow for intermittent rivers and ephemeral streams in low-gradient catchments in Mediterranean climates. Water Resources Research, 55, 9926-9946. https://doi.org/10.1029/2019WR025041

Hagedorn, B., 2020. Hydrograph separation through multi objective optimization: Revealing the importance of a temporally and spatially constrained baseflow solute source. Journal of Hydrology, 125349. https://doi.org/10.1016/j.jhydrol.2020.125349

Chapter 2

Howcroft, W., Cartwright, I., Cendón, D.I., 2019. Residence times of bank storage and return flows and the influence on river water chemistry in the upper Barwon River, Australia. Applied Geochemistry, 101, 31-41. https://doi.org/10.1016/j.apgeochem.2018.12.026

International Agricultural Research Consortium database. Consortium for Spatial Information (CGIAR-CSI)-SRTM data. http://srtm.csi.cgiar.org/srtmdata/ (Accessed 13 July 2020).

Jasechko, S., Kirchner, J.W., Welker, J.M., McDonnell, J.J., 2016. Substantial proportion of global streamflow less than three months old. Nature Geoscience, 9, 126-129.https://doi.org/10.1038/ngeo2636

Kalbus, E., Reinstorf, F., Schirmer, M., 2006.Measuring methods for groundwater? surface water interactions: a review. Hydrology and Earth System Sciences, 10, 873-887. https://doi.org/10.5194/hess-10-873-2006

Lamontagne, S., Cook, P.G., 2007. Estimation of hyporheic water residence time in situ using ^{222}Rn disequilibrium. Limnology and Oceanography: Methods, 5, 407-416. https://doi.org/10.4319/lom.2007.5.407

Lamontagne, S., Taylor, A.R., Cook, P.G., Crosbie, R.S., Brownbill, R., Williams, R.M., Brunner, P., 2014. Field assessment of surface water–groundwater connectivity in a semi-arid river basin (Murray–Darling, Australia). Hydrological Processes, 28, 1561-1572. https://doi.org/10.1002/hyp.9691

Lerner, D.N., Issar, A.S., Simmers, I., 1990. Groundwater recharge: a guide to understanding and estimating natural recharge, Rep. 8, International Association of Hydrogeologist, Kenilworth, 1990. https://doi.org/10.2134/jeq1992.00472425002100030036x

Chapter 2

Liang, X., Zlotnik, V.A., Zhang, Y.K., Xin, P., 2020. Diagnostic Analysis of Bank Storage Effects on Sloping Floodplains. Water Resources Research, 56, e2019WR026385. https://doi.org/10.1029/2019WR026385

Martinez, J.L., Raiber, M., Cox, M.E., 2015. Assessment of groundwater–surface water interaction using long-term hydrochemical data and isotope hydrology: Headwaters of the Condamine River, Southeast Queensland, Australia. Science of the Total Environment, 536, 499-516. https://doi.org/10.1016/j.scitotenv.2015.07.031

McCallum, J.L., Cook, P.G., Berhane, D., Rumpf, C., McMahon, G.A., 2012. Quantifying groundwater flows to streams using differential flow gauging and water chemistry. Journal of Hydrology, 416, 118-132. https://doi.org/10.1016/j.jhydrol.2011.11.040

McCallum, J.L., Cook, P.G., Brunner, P., Berhane, D., 2010. Solute dynamics during bank storage flows and implications for chemical base flow separation. Water Resources Research, 46, W07541. https://doi.org/10.1029/2009WR008539

McMahon, T.A., Peel, M.C., 2019. Uncertainty in stage–discharge rating curves: application to Australian Hydrologic Reference Stations data. Hydrological Sciences Journal, 64, 255-275. https://doi.org/10.1080/02626667.2019.1577555

Morgenstern, U., Taylor, C.B., 2009. Ultra low-level tritium measurement using electrolytic enrichment and LSC. Isotopes in Environmental and Health Studies, 45, 96-117. https://doi.org/10.1080/10256010902931194

Morgenstern, U., Stewart, M.K., Stenger, R., 2010. Dating of stream water using tritium in a post nuclear bomb pulse world: continuous variation of mean transit time with streamflow. Hydrology and Earth System Sciences, 14, 2289-2301. https://doi.org/10.5194/hess-14-2289-2010

Chapter 2

Mullinger, N.J., Binley, A.M., Pates, J.M., Crook, N.P., 2007. Radon in Chalk streams: Spatial and temporal variation of groundwater sources in the Pang and Lambourn catchments, UK. Journal of Hydrology, 339, 172-182. https://doi.org/10.1016/j.jhydrol.2007.03.010

Mullinger, N.J., Pates, J.M., Binley, A.M., Crook, N.P., 2009. Controls on the spatial and temporal variability of ^{222}Rn in riparian groundwater in a lowland Chalk catchment. Journal of Hydrology, 376, 58-69. https://doi.org/10.1016/j.jhydrol.2009.07.015

Negulescu, M., Rojanski, V., 1969. Recent research to determine reaeration coefficient. Water Research, 3, 189-202. https://doi.org/10.1016/0043-1354(69)90058-X

O'Connor, D.J., Dobbins, W.E., 1958. Mechanism of reaeration in natural streams. Transactions of the American Society of Civil Engineers, 123, 641-666. https://doi.org/10.1061/JSEDAI.0000050

Ortega, L., Manzano, M., Custodio, E., Hornero, J., Rodríguez-Arévalo, J., 2015. Using ^{222}Rn to identify and quantify groundwater inflows to the Mundo River (SE Spain). Chemical Geology, 395, 67-79. https://doi.org/10.1016/j.chemgeo.2014.12.002

Oxtobee, J.P., Novakowski, K. S., 2003. Ground water/surface water interaction in a fractured rock aquifer. Groundwater, 41, 667-681. https://doi.org/10.1111/j.1745-6584.2003.tb02405.x

Peterson, T.J., Saft, M., Peel, M.C., John, A., 2021. Watersheds may not recover from drought. Science, 372,745-749. https://doi.org/10.1126/science.abd5085

Rhodes, K.A., Proffitt, T., Rowley, T., Knappett, P.S., Montiel, D., Dimova, N., Miller, G.R., 2017. The importance of bank storage in supplying baseflow to rivers flowing through compartmentalized, alluvial aquifers. Water Resources Research, 53, 10539-10557. https://doi.org/10.1002/2017WR021619

Chapter 2

Riis, T., Kelly-Quinn, M., Aguiar, F.C., Manolaki, P., Bruno, D., Bejarano, M.D., Dufour, S., 2020. Global overview of ecosystem services provided by riparian vegetation. BioScience, 70, 501-514. https://doi.org/10.1093/biosci/biaa041

Robinson, N., Rees, D., Reynard, K., Imhof, M., Boyle, G., Martin, J., Giles, S., 2006. A land resource assessment of the Wimmera region. Victoria Department of Jobs, Precincts and Regions. http://vro.agriculture.vic.gov.au/

Sawyer, A.H., Cardenas, M.B., 2009. Hyporheic flow and residence time distributions in heterogeneous cross-bedded sediment. Water Resources Research, 45, W08406. https://doi.org/10.1029/2008WR007632

Segura, C., Noone, D., Warren, D., Jones, J.A., Tenny, J., Ganio, L.M., 2019. Climate, landforms, and geology affect baseflow sources in a mountain catchment. Water Resources Research, 55, 5238-5254. https://doi.org/10.1029/2018WR023551

Shanafield, M., Bourke, S.A., Zimmer, M.A., Costigan, K.H., 2021. An overview of the hydrology of non-perennial rivers and streams. Wiley Interdisciplinary Reviews: Water, 8, e1504. https://doi.org/10.1002/wat2.1504.

Simpson, H.J., Herczeg, A.L., 1991. Salinity and evaporation in the River Murray basin, Australia. Journal of Hydrology, 124, 1-27. https://doi.org/10.1016/0022-1694(91)90003-Z.

Smerdon, B.D., Gardner, W.P., Harrington, G.A., Tickell, S.J., 2012. Identifying the contribution of regional groundwater to the baseflow of a tropical river (Daly River, Australia). Journal of Hydrology, 464, 107-115. https://doi.org/10.1016/j.jhydrol.2012.06.058

Sophocleous, M., 2002. Interactions between groundwater and surface water: the state of the science. Hydrogeology Journal, 10, 52-67. http://dx.doi.org/10.1007/s10040-014-1215-0

Chapter 2

Squillace, P.J., 1996. Observed and simulated movement of bank-storage water. Ground Water, 34, 121-135. https://doi.org/10.1111/j.1745-6584.1996.tb01872.x

Tadros, C.V., Hughes, C.E., Crawford, J., Hollins, S.E., Chisari, R., 2014. Tritium in Australian precipitation: A 50-year record. Journal of Hydrology, 513, 262-273. https://doi.org/10.1016/j.jhydrol.2014.03.031.

Tetzlaff, D., Soulsby, C., 2008. Sources of baseflow in larger catchments–Using tracers to develop a holistic understanding of runoff generation. Journal of Hydrology, 359, 287-302. https://doi.org/10.1016/j.jhydrol.2008.07.008

Tonina, D., Buffington, J.M., 2011. Effects of stream discharge, alluvial depth and bar amplitude on hyporheic flow in pool-riffle channels. Water Resources Research, 47, W08508. https://doi.org/10.1029/2010WR009140

Unland, N.P., Cartwright, I., Cendón, D.I., Chisari, R., 2014. Residence times and mixing of water in river banks: implications for recharge and groundwater-surface water exchange. Hydrology and Earth System Sciences, 18, 5109-5124. https://doi.org/10.5194/hess-18-5109-2014

Unland, N.P., Cartwright, I., Rau, G.C., Reed, J., Gilfedder, B.S., Atkinson, A.P., Hofmann, H., 2013. Investigating the spatio-temporal variability in groundwater and surface water interactions: a multi-technique approach. Hydrology and Earth System Sciences, 17, 3437-3453. https://doi.org/10.5194/hess-17-3437-2013

Van Dijk, A.I., Beck, H.E., Crosbie, R.S., de Jeu, R.A., Liu, Y.Y., Podger, G.M., Viney, N.R., 2013. The Millennium Drought in southeast Australia (2001–2009): Natural and human causes and implications for water resources, ecosystems, economy, and society. Water Resources Research, 49, 1040-1057. https://doi.org/10.1002/wrcr.20123.

Chapter 2

Vertessy, R., Barma, D., Baumgartner, L., Bond, N., Mitrovic, S., Sheldon, F., 2019. Independent assessment of the 2018-19 fish deaths in the lower Darling.

Western, A.W., O'Neill, I.C., Hughes, R.L., Nolan, J.B., 1996. The behavior of stratified pools in the Wimmera River, Australia. Water Resources Research, 32, 3197-3206. https://doi.org/10.1029/96WR01336

Wimmera Catchment Management Authority., 2013. Wimmera Waterway Strategy 2014-2022. Government of Victoria Wimmera Catchment Management Authority. http://wcma.vic.gov.au

Yu, M.C.L., Cartwright, I., Braden, J.L., De Bree, S.T., 2013. Examining the spatial and temporal variation of groundwater inflows to a valley-to-floodplain river using ^{222}Rn, geochemistry and river discharge: The Ovens River, southeast Australia. Hydrology and Earth System Sciences, 17, 4907. https://doi.org/10.5194/hess-17-4907-2013

Zarnetske, J.P., Haggerty, R., Wondzell, S.M., Baker, M.A., 2011. Dynamics of nitrate production and removal as a function of residence time in the hyporheic zone. Journal of Geophysical Research: Biogeosciences, 116, G01025. https://doi.org/10.1029/2010JG001356

Chapter 2

Tables

Table 2.1. Streamflow and geochemistry of stream water from the upper Wimmera River

Site number[1]	Sample ID	Streamflow	Distance[2]	EC	^{222}Rn	Cl	Na	^{3}H
		m^3/day	km	μS/cm	Bq/m^3	mg/L	mg/L	TU
	July 2019							
1	Elmhurst		0	1109	1740	369	190	2.69
2	Elm Town		2	1395	1130	505	239	
3	Eversley 2		7	1790	1340	618	286	
4	Eversley 1	16210	15	1497	869	510	255	
5	CE1		20	1666	366	578	275	1.85
6	CE2		24	2210	677	763	413	
7	Joel 1		32	2880	603	1073	547	
8	Joel 2		39	2870	421	993	493	2.76
9	Joel 3		44	2710	577	952	271	
10	Joel 4		50	2714	507	985	529	
11	Joel 5		53	3220	642	1187	590	
12	37 PAR		56	2610	437	886	457	
13	OLB		58	1890	468	592	316	
14	GC 1		65	2005	436	711	363	
15	GC 2	71100	70	2346	372	793	431	
16	Camb		81	2235	195	804	424	3.00
17	GSR		87	2245	194	779	428	
18	Glenorchy	135000	93	2612	348	894	507	2.41
19	HS1		98	3500	217	1285	712	
20	HS2		103	2265	266	723	400	
21	HS3		106	775	145	202	110	
22	CB		110	294	228	56	54	
23	FB		120	337	148	79	41	
	September 2019							
1	Elmhurst		0	670	1650	198	107	2.67
2	Elm Town		2	685	1210	204	104	
3	Eversley 2		7	920	264	282	143	
4	Eversley 1	9040	15	991	609	298	154	
5	CE1		20	1014	556	310	174	2.58
6	CE2		24	1127	685	351	194	
7	Joel 1		32	1626	678	542	301	
8	Joel 2		39	1779	712	547	326	2.48
9	Joel 3		44	1666	700	539	299	
10	Joel 4		50	1600	727	537	303	
11	Joel 5		53	1610	922	517	283	
12	37 PAR		56	1550	446	520	276	
13	OLB		58	1521	383	502	274	
14	GC 1		65	1455	338	455	256	
15	GC 2	24580	70	1466	432	461	264	
16	Camb		81	1411	402	450	224	2.78
17	GSR		87	1359	249	461	251	
18	Glenorchy	31110	93	1235	304	380	260	2.88
19	HS1		98	1157	175	357	214	

20	HS2		103	1143	229	346	206	
21	HS3		106	1129	223	345	207	
22	CB		110	1117	306	317	202	
23	FB		120	1063	240	329	194	
	November 2019							
1	Elmhurst		0	981	2860	312	164	2.55
2	Elm Town		2	967	1380	300	154	
3	Eversley 2		7	nm[3]	nm	nm	nm	
4	Eversley 1	203	15	1755	477	575	325	
4	CE1		20	1552	591	480	279	2.34
5	CE2		24	2055	442	723	392	
7	Joel 1		32	2443	753	871	467	
8	Joel 2		39	2870	1140	1027	554	2.26
9	Joel 3		44	2760	1470	979	538	
10	Joel 4		50	2250	1120	790	435	
11	Joel 5		53	2191	561	757	427	
12	37 PAR		56	2085	282	719	408	
13	OLB		58	2087	220	705	400	
14	GC 1		65	2129	463	730	413	
15	GC 2	133	70	2148	1160	732	426	
16	Camb		81	2239	160	771	443	2.58
17	GSR		87	2199	477	744	433	
18	Glenorchy	620	93	1925	203	639	378	2.69
19	HS1		98	1871	370	627	367	
20	HS2		103	1876	642	612	364	
21	HS3		106	1821	225	609	359	
22	CB		110	1810	664	605	358	
23	FB		120	1823	601	607	364	

1. Sites on Fig.1.
2. Distance downstream from Elmhurst
3. nm = not measured

Table 2.2. Geochemistry of groundwater from the upper Wimmera River area

Site letter[1]	Bore ID	Formation	Depth	EC	^{222}Rn	Cl	Na	^{3}H
			m	μS/cm	Bq/m^3	mg/L	mg/L	TU
A	5396	Devonian Granite	35	3520	23900	1244	605	
B	5252	Incised Alluvium	7	9670	20100	3381	1896	
C	5242	White Hills Gravel	23	6000	31500	2041	1222	0.16
	5243	White Hills Gravel	18	5010	24600	1699	1012	0.25
D	5244	Incised Alluvium	60	3410	nm[2]	965	694	
	5245	Incised Alluvium	20	1633	21700	459	297	
	5246	Incised Alluvium	9	1924	28100	554	323	
E	5248	Incised Alluvium	3	14500	26100	5205	3140	
F	5227	Incised Alluvium	28	3150	37300	847	395	0.04
	5228	Incised Alluvium	14	3090	80500	946	430	0.06
G	5226	Incised Alluvium	23	1044	19000	313	156	
H	5229	St Arnaud Group	37	18500	46000	1308	475	0.03
	5230	St Arnaud Group	14	4980	17400	6582	4281	0.25
I	5232	Incised Alluvium	32	8080	99700	2591	1564	0.02
J	5234	Incised Alluvium	43	4440	19400	1431	814	0.02
	5235	Incised Alluvium	30	2473	14500	699	396	bd[3]
	5236	Incised Alluvium	12	6650	35200	2032	1658	0.45
K	5377	Alluvium	15	11700	65800	4170	2577	
L	5379	White Hills Gravel	7	7730	23900	2224	1948	bd
M	5381	White Hills Gravel	9	5370	3700	1846	1206	
N	5383	Alluvium	18	20390	3900	8414	480	
	5384	Alluvium	9	20750	8440	8106	440	
O	2541	Alluvium	13	6420	nm	2046	1305	
	2542	Alluvium	17	5300	26600	1701	1118	0.02
P	113123	Alluvium	16	11320	21600	3719	2527	
	Mean			7482	30389	2581	1238	
	SD			5729	23225	2285	1026	
	95% Cl			2365	10043	943	424	

1. Sites on Fig.1.
2. nm = not measured

3. bd=below detection

Table 2.3. Radon emanations from the upper Wimmera River alluvial sediments

Site[1]	Sample ID	E_m (Bq/kg)	γ (Bq/m^3/Day)	γ/λ(Bq/m^3)
4	Eversley 1-1	3.6	2617	14457
4	Eversley 1-2	4.3	3121	17243
4	Eversley 1-3	4.6	3343	18472
4	Eversley 1-4	13.2	9656	53351
4	Eversley 1-5	6.8	4961	27409
5	CE1-1	9.4	6859	37893
5	CE1-2	8.6	6271	34644
7	Joel 1-1	2.2	1574	8694
7	Joel 1-2	2.4	1786	9869
7	Joel 1-3	1.7	1258	6949
10	Joel 4-1	3.7	2704	14938
10	Joel 4-2	2.2	1585	8758
13	OLB-1	1.7	1214	6705
13	OLB-2	3.7	2744	15160
13	OLB-3	2.4	1724	9523
13	OLB-4	5.4	3986	22022
13	OLB-5	2.7	2005	11079
14	GC1-1	10.5	7659	42317
14	GC1-2	7.4	5425	29970
14	GC1-3	9.4	6858	37889
17	GSR-1	4.9	3596	19870
17	GSR-2	6.9	5068	27999
17	GSR-3	17.2	12624	69747
17	GSR-4	10.8	7916	43737
18	Glenorchy-1	5.5	4063	22450
18	Glenorchy-2	1.9	1361	7521
21	HS3-1	1.7	1250	6907
21	HS3-2	6.2	4563	25211
22	CB-1	12.3	9002	49735
22	CB-2	6.9	5060	27957
23	FB-1	5.3	3881	21445
23	FB-2	1.4	1041	5751
	Mean		4274	23615
	SD		2872	15866
	95% Cl		1035	5720

1. Sites on Fig.1.

Table 2.4. Parameters used for calculating net baseflow influxes by water mass balance (I_{net}) with net uncertainty (σ_t) between different gauges and comparison to ^{222}Rn mass balance (I_{RMB})

Parameter[1]	**EVER-GLYN**[2] **Jul 19**	**EVER-GLYN Sep 19**	**EVER-GLYN Nov 19**
Q_u (m^3/day)	16210	9040	203
Q_d (m^3/day)	71100	24580	133
P (m^3/day)	1361	294	176
E_{net} (m^3/day)	1040	1411	3045
Q_t (m^3/day)	11690	7640	70
I_{net} (m^3/day)	42879±3342	9017±703	2729±213
I_{RMB} (m^3/day)	43251	10183	3086

1. Parameters in Eq. (6)

2. Locations and abbreviations on Fig.1.

Chapter 3

Chapter 3 Sources and mean transit times of stream water in an intermittent river system: the upper Wimmera River, southeast Australia

Hydrol. Earth Syst. Sci., 26, 4497–4513, 2022
https://doi.org/10.5194/hess-26-4497-2022

Hydrology and Earth System Sciences
Open Access

Sources and mean transit times of stream water in an intermittent river system: the upper Wimmera River, southeast Australia

Zibo Zhou[1], **Ian Cartwright**[1], **and Uwe Morgenstern**[2]

[1]School of Earth, Atmosphere and Environment, Monash University, Clayton, VIC 3800, Australia
[2]GNS Science, Lower Hutt 5040, New Zealand

Correspondence: Zibo Zhou (zibo.zhou@monash.edu)

Received: 12 January 2022 – Discussion started: 31 January 2022
Revised: 10 August 2022 – Accepted: 24 August 2022 – Published: 9 September 2022

Abstract. Determining the mean transit times (MTTs) and water sources in catchments at different flow conditions helps better understand river functioning, and manage river health and water resources. Despite being common in a range of environments, the MTTs and water sources in intermittent streams are much less well understood compared to perennial streams. Major ion geochemistry, stable isotopes, ^{14}C, and ^{3}H were used in this study to identify water sources and MTTs of the periodically intermittent upper Wimmera River from southeast Australia at different flow conditions, including zero-flow periods. The disconnected pool waters during the zero-flow period in the summer months of 2019 had ^{3}H activities of 0.64 to 3.29 TU. These and the variations in total dissolved solids and stable isotopes imply that these pools contained a mixture of older groundwater and younger stream water impacted by evaporation. ^{3}H activities during the high-flow period in July 2019 were 1.85 to 3.00 TU, yielding MTTs of up to 17 years. The ^{3}H activities at moderate and low-flow conditions in September and November 2019 ranged from 2.26 to 2.88 TU, implying MTTs of 1.6 to 7.8 years. Regional groundwater near the Wimmera River had ^{3}H activities of < 0.02 to 0.45 TU and ^{14}C activities of 57 to 103 pMC, and was not recharged by the river at high flows. The Wimmera River and other intermittent streams in southeast Australia are sustained by younger catchment waters from relatively small near-river stores than comparable perennial streams, which have older deeper regional groundwater inputs. This results in these intermittent streams being more susceptible to short-term changes in climate and necessitates the protection of near-river corridors to maintain the health of the riverine systems.

1 Introduction

Understanding the timescales of water flow through catchments to rivers at different hydrological conditions is vital for effective water resources management, protecting riverine systems, and predicting the changes in river functioning due to climate variability, changes in land use, and water utilisation (Sophocleous, 2002; Cook, 2013; Van Dijk et al., 2013; Gleeson et al., 2016; Segura et al., 2019). Mean transit times (MTTs) represent the average time for precipitation to be transmitted from a recharge area through a catchment to where it discharges into rivers or streams (Cook and Bohlke, 2000; McDonnell et al., 2010; Morgenstern et al., 2010). Transit time distributions (i.e. the frequency of water of different ages in the sample) potentially provide better information on catchment processes than MTTs. In particular, they allow better understanding of finer-scale catchment processes (e.g. the release of water from different stores as catchments wet up and dry down) (Hrachowitz et al., 2010; Benettin et al., 2015; Birkel et al., 2015). However, MTTs are important for understanding broad catchment behaviour (McGuire and McDonnell, 2006; McDonnell et al., 2010; Blavoux et al., 2013; Duvert et al., 2016; Howcroft et al., 2018) such as the average age of the water stores contributing to streams at different flow conditions. Documenting MTTs is also important for understanding the resilience of catchments. Streams with long MTTs are sustained by larger volumes reservoirs of water from within the catchments (e.g. Morgenstern et al., 2010; Gusyev et al., 2016; Howcroft et al., 2018), and thus are less sensitive to short-term climate variability (e.g. droughts lasting years to decades). In addition, the MTTs may control water salinity, water tempera-

Chapter 3

Abstract

Determining the mean transit times (MTTs) and water sources in catchments at different flow conditions helps better understand river functioning, and manage river health and water resources. Despite being common in a range of environments, the MTTs and water sources in intermittent streams are much less well understood compared to perennial streams. Major ion geochemistry, stable isotopes, ^{14}C, and ^{3}H were used in this study to identify water sources and MTTs of the periodically-intermittent upper Wimmera River from southeast Australia at different flow conditions, including zero-flow periods. The disconnected pool waters during the zero-flow period in the summer months of 2019 had ^{3}H activities of 0.64 to 3.29 TU. These and the variations in total dissolved solids and stable isotopes imply that these pools contained a mixture of older groundwater and younger stream water impacted by evaporation. ^{3}H activities during the high-flow period in July 2019 were 1.85 to 3.00 TU, yielding MTTs of up to 17 years. The ^{3}H activities at moderate and low-flow conditions in September and November 2019 ranged from 2.26 to 2.88 TU, implying MTTs of 1.6 to 7.8 years. Regional groundwater near the Wimmera River had ^{3}H activities of < 0.02 to 0.45 TU and ^{14}C activities of 57 to 103 pMC and was not recharged by the river at high flows. The Wimmera River and other intermittent streams in southeast Australia are sustained by younger catchment waters from relatively small near-river stores than comparable perennial streams, which have older deeper regional groundwater inputs. This results in these intermittent streams being more susceptible to short-term changes in climate and necessitates the protection of near-river corridors to maintain the health of the riverine systems.

Chapter 3

3.1 Introduction

Understanding the timescales of water flow through catchments to rivers at different hydrological conditions is vital for effective water resources management, protecting riverine systems, and predicting the changes in river functioning due to climate variability, changes in land use and water utilization (Sophocleous, 2002; Cook., 2013; Van Dijk et al., 2013; Gleeson et al., 2016; Segura et al., 2019). Mean transit times (MTTs) represent the average time for precipitation to be transmitted from a recharge area through a catchment to where it discharges into rivers or streams (Cook and Bohlke, 2000; McDonnell et al, 2010; Morgenstern et al., 2010). Transit time distributions (i.e. the frequency of water of different ages in the sample) potentially provide better information on catchment processes than MTTs. In particular, they allow better understanding of finer-scale catchment processes (e.g., the release of water from different stores as catchments wet up and dry down) (Hrachowitz et al., 2010; Benettin et al., 2015; Birkel et al., 2015). However, MTTs are important for understanding broad catchment behaviour (McGuire and McDonnell, 2006; McDonnell et al, 2010; Blavoux et al., 2013; Duvert et al., 2016; Howcroft et al., 2018) such as the average age of the water stores contributing to streams at different flow conditions. Documenting MTTs is also important for understanding the resilience of catchments. Streams with long MTTs are sustained by larger volumes reservoirs of water from within the catchments (e.g., Morgenstern et al., 2010; Gusyev et al., 2016; Howcroft et al., 2018) and thus are less sensitive to short-term climate variability (e.g., droughts lasting years to decades). In addition, the MTTs may control water salinity, water temperature, microbial activity, and the attenuation and dispersion input of nutrients and other contaminants to rivers (Kirchner et al., 2000; Hare et al., 2021).

The water that sustains river flow may have residence times ranging from a few days to several centuries. Younger water may be derived from stores in the shallow near-river environment (such as surface runoff, water stored in the soil, and interflow), while regional groundwater represents a large store of older water (Soulsby et al., 2000; McGuire and McDonnell, 2006; Stewart et al., 2010; Cartwright and Morgenstern, 2015; Duvert et al., 2016; Jung et al., 2019). However, relatively little is known about the timescale of water flow in most catchments and whether water of different ages and from different stores contributes to rivers at different flow conditions. Numerous studies have focused on perennial streams and have revealed the presence of long-lived water stores contributing to streamflow especially during low-flow periods (Rice and Hornberger, 1998; Soulsby et al., 2006; Hrachowitz et al., 2009; Cartwright and Morgenstern, 2015; Gusyev et al., 2016; Howcroft et al., 2018; Cartwright et al., 2020). There has been less attention on intermittent streams, which represent > 50% of global rivers and are especially important in semi-arid areas (Datry et al., 2014; Costigan et al., 2015; Gutiérrez-Jurado et al., 2019, Shanafield et al., 2021). The connection between intermittent streams and regional groundwater may be less important than for perennial streams, especially during the periodic cease-to-flow times when the water table falls and water from near-river stores become dominant (e.g., Zimmer and McGlynn, 2017). Determining MTTs of intermittent streams will improve our understanding of groundwater -surface water interaction in these catchments.

3.1.1 Documenting mean transit times

Several approaches can be used to estimate MTTs in rivers. MTTs may be determined by using lumped parameter models (LPMs) that describe the distribution of water with different ages or tracer concentrations in homogeneous aquifers with simple geometries and consistent recharge rates (Maloszewski and Zuber, 1982; Maloszewski, 2000; Zuber et al., 2004; McGuire and McDonnell, 2006).

LPMs may be based on the attenuation of $\delta^{18}O$ values or Cl concentration variabilities in rainfall at the catchment outlet. This approach requires frequent (generally at least monthly but preferably shorter spaced if the details of hydrological processes are to be captured) long-term tracer records in rainfall and stream water (Kirchner et al., 2004; McGuire and McDonnell, 2006), and such datasets are available only in a small number of catchments globally. Because intermittent streams only flow for part of the year, it is more difficult to use LPMs based on continuous ^{18}O or Cl measurements than in perennial streams. In addition, this approach assumes that the catchment is at steady state, which is unlikely to be the case (Kirchner, 2016b). It is also not viable where MTTs are greater than 4 to 5 years due to attenuation of the input record to below the resolution at which the tracers can be measured (Stewart et al. 2010), which is commonly the case in southeast Australia (Cartwright et al., 2020). Techniques such as ensemble hydrographs (Kirchner, 2019; Knapp et al., 2019), flux tracking (Hrachowitz et al., 2013), and StoreAge Selection Functions (Rinaldo et al., 2015) can determine transit times from shorter time-series and do not assume steady-state conditions. However, these methods still require frequent tracer data for rainfall and streams that are not commonly available.

Tritium (^3H) has a half-life of 12.32 years and is part of the water molecule. Unlike tracers such as chlorofluorocarbons, and SF_6, ^{14}C, and ^3He, its abundance is not affected by degassing or geochemical or biogeochemical reactions. This allows ^3H to be used to estimate MTTs of shallow groundwater, water from the unsaturated zone and stream water (e.g., Morgenstern et al., 2010; Duvert et al., 2016; Jung et al., 2019). Due to atmospheric nuclear tests, ^3H activities in rainfall reached a peak in the 1950s and 1960s (the “bomb pulse”). In the southern hemisphere, the remnant bomb pulse ^3H activities are now lower than those in modern rainfall (Morgenstern et al., 2010; Tadros et al., 2014). This makes it possible to estimate MTTs from a single ^3H measurement in a similar way to how other radioisotopes such as ^{14}C and ^{36}Cl are used to determine residence times of older groundwater (e.g., Clark, 2015; Cartwright et al., 2017; Howcroft et al., 2019). Low-level ^{3}H measurements allow MTTs of up to ~150 years to be determined, although the relative precision of the estimates decreases at longer MTTs.

MTT estimates made using ^{3}H have several uncertainties. The decline of the bomb pulse ^{3}H activities in the southern hemisphere makes it impossible to assess the suitability of an LPM by time-series ^{3}H measurements that commence now (Cartwright and Morgenstern, 2015). Assigning LPMs is therefore based on catchment attributes (e.g., the geometry of the flow system) or information from previous studies in similar catchments. Although it represents an uncertainty, MTTs are less sensitive to the choice of LPMs than in the northern hemisphere (Morgenstern et al., 2010; Blavoux et al., 2013). In addition, where multiple water sources (e.g., groundwater, soil water, or water from multiple tributaries) with different MTTs contribute to rivers (aggregation), it is difficult to estimate MTTs (Suckow, 2014; Kirchner, 2016a; Stewart et al., 2017). The heterogeneous hydraulic conductivities of aquifers also contribute to uncertainties in MTT calculations (Weissmann et al., 2002; McCallum et al., 2015). However, where the scale of heterogeneity is small relative to the size of the aquifer, the MTTs are similar to those predicted by the LPMs (Cartwright et al., 2018). Lastly, the seasonal variability of ^{3}H activities in rainfall could lead to uncertainty in MTT estimates. Where strong seasonal recharge occurs, ^{3}H activities of rainfall that recharges the catchment may be different from those of annual rainfall, which is usually used as the ^{3}H input (e.g., Morgenstern et al., 2010). Although these factors introduce uncertainties in MTT calculations, water in the southern hemisphere with lower ^{3}H activities invariably has longer MTTs, which allows relative relationships to be determined. This also permits the understanding of the changing sources of water contributing to streams during different flow conditions (Duvert et al., 2016; Howcroft et al., 2018; Cartwright et al., 2018, 2020).

Previous studies of perennial streams in southeast Australia (summarized in Cartwright et al., 2020) noted that the runoff coefficient (the proportion of annual rainfall exported by the stream) had an inverse correlation with MTTs. This relationship probably reflects the high evapotranspiration rates in some catchments which results in less of the rainfall being exported as runoff. Those catchments will also have low recharge rates and slower groundwater flow, and consequently the water discharging to the streams will have longer MTTs. The runoff coefficient represents a more viable first-order proxy for MTTs than catchment attributes such as slope, drainage density, or major ion concentrations in those catchments. Whether a similar relationship between MTTs and runoff coefficients occurs in intermittent catchment is not known.

3.1.2 Understanding water sources

As noted above, rivers are potentially fed by a range of water stores from within catchment, including soil water, interflow, bank return flow, shallow riparian groundwater, and deeper regional groundwater (e.g., Peters et al., 2014; Duvert et al., 2016; Cartwright and Morgenstern, 2018; Howcroft et al., 2019). Due to mineral dissolution, the breakdown of organic matter and evapotranspiration, water stored within catchments commonly has a higher salinity than surface runoff (Herczeg et al., 2001; Edmunds, 2009). Variable operation of these processes may result in differences in major ion geochemistry between the water sources. For example, soil water may have high nitrate or organic carbon concentrations due to breakdown of organic matter. There may also be differences in the stable isotope geochemistry of these waters reflecting seasonal recharge, evapotranspiration, or long-term changes to rainfall stable isotope ratios (Hughes and Crawford, 2012). Not all catchments, however, contain water stores with distinct geochemistry. This is commonly the case in southeast Australia where high evapotranspiration rates mask the effects of mineral dissolution (Herczeg et al., 2001; Cartwright and Morgenstern, 2015; Howcroft et al., 2018; Barua et al., 2022). In those catchments, documenting MTTs allows the inputs of older and younger catchment water to be assessed.

3.1.3 Objectives

This study determines the mean transit time and water sources at different flow conditions (including zero flows) in the seasonally-intermittent upper Wimmera River in southeast Australia using ^{3}H, ^{14}C, stable isotopes, and major ion geochemistry. A previous study (Zhou and Cartwright, 2021) used similar tracers to understand the locations of groundwater inflow to the river; however, did not specifically address the timescale of water flow in the catchment or the volumes of the water stores that sustain streamflow. We hypothesized that: 1) mean transit times in the Wimmera River are younger than in comparable perennial streams from southeast Australia; 2) younger near-river water stores (such as shallow riparian groundwater and bank return flows) are more important than regional groundwater in sustaining the river at all flow conditions; and 3) due to the river containing alternate gaining and losing reaches, the runoff coefficient will not be a reliable indicator of mean transit times. As with many rivers globally (Shanafield et al., 2020; Messager et al., 2021), the upper Wimmera River has become more intermittent over recent years due to climate change. The results from this study are important in understanding and managing catchment behaviour in intermittent streams more generally. We also assess what tracers are useful in distinguishing between water sources, which will help inform studies on similar catchments.

Chapter 3

3.2 Study area

Located in southeast Australia, the Wimmera River is an intermittent river in the southern Murray-Darling Basin. The Wimmera catchment has an area of approximately 24,000 km^2 and the middle and lower parts of the river are important for agriculture (Fletcher, 2015; Department of Environment, Land, Water and Planning, 2021). In the summers of all but the wettest years, the Wimmera River ceases to flow and comprises a series of disconnected pools (Western et al., 1996). Since the 1980s, the Wimmera River has experienced a decline in streamflow and an increase in intermittency (Department of Environment, Land, Water and Planning, 2021) especially between 1996 to 2009 when southeast Australia experienced a large reduction in rainfall and streamflow during the Millennium Drought (Bureau of Meteorology, 2021). The study area is located in the upper Wimmera River catchment (Fig. 3.1) which has an area of approximately 3000 km^2. Dryland pasture with remnant native eucalypt woodlands is the dominant vegetation coverage in the upper catchment (Fletcher, 2015; Department of Environment, Land, Water and Planning, 2021) and there is only minor groundwater and river water use (Robinson et al., 2006; Wimmera Catchment Management Authority, 2013; Fletcher, 2015).

The upper catchment of the Wimmera River comprises a Palaeozoic basement of metamorphosed shales and schists of the St Arnaud Group, indurated sandstones of the Glenthompson and Grampians Groups, and Devonian granites (Fig. 3.1: Department of Jobs, Precincts and Regions, 2021). Alluvial and lacustrine Palaeogene to Recent sediments that were deposited by the precursors of the current rivers overlie the basement. These sediments consist of rounded gravels, coarse sands, silts and clays (Robinson et al., 2006). The dominant topography in the upstream reaches of the upper Wimmera River is a broad valley while the downstream part is a flat alluvial flood plain (Robinson et al., 2006; Department of Environment, Land, Water and Planning, 2021).

There is a decreasing trend of average annual rainfall from the southeast (709 mm) to northwest (505 mm) in this area (Bureau of Meteorology, 2021), and the winter and spring months (May to August) are the wettest (Fig. 3.2a). Evapotranspiration rates are also much higher in summer (up to 1.8 mm day^{-1}: Fig. 3.2a). The combination of rainfall and evapotranspiration variations leads to high river flows occurring in the winter and spring (Department of Environment, Land, Water and Planning, 2021; Fig. 3.2b).

Groundwater in the upper Wimmera recharges on the margins of catchment and flows northwards, with flow paths converging on the river (Radke and Howard, 2007; Fig. 3.1). River water geochemistry demonstrates that groundwater discharge locally occurs in the upper and middle reaches of the upper Wimmera River driven by relatively steep topography and high hydraulic gradients, whereas the lower reaches have lower groundwater inflows due to subdued topography (Zhou and Cartwright, 2021). From the downstream trends in Cl and ^{222}Rn and the high ^{3}H activities, the study concluded that near-river stores were important contributors to streamflow.

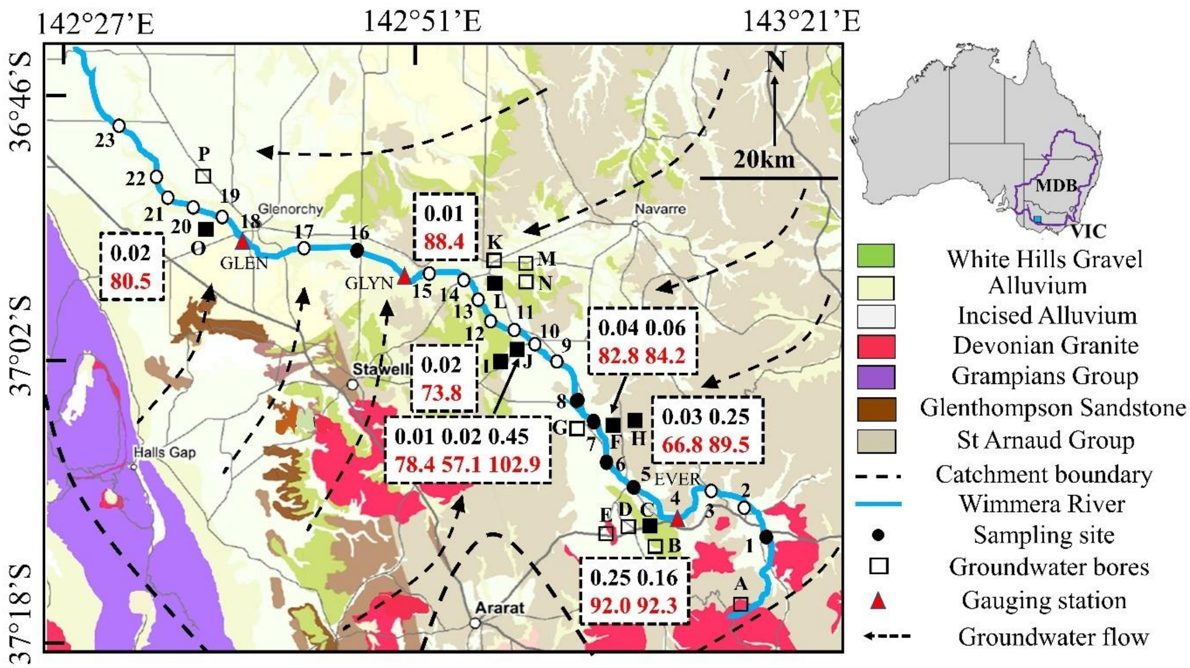

Figure 3.1. Summary geological and hydrogeological map of the upper Wimmera River. Stream water sampling sites and groundwater bores are indicated by numbers and letters, respectively. The sites that have radioactive isotope data are shown in solid symbols. Gauging stations with site number are Eversley (EVER; 415207), Glynwylln (GLYN; 415206), and Glenorchy (GLEN; 415201). Background geological map from Department of Jobs, Precincts and Regions (2021) (© State Government of Victoria 1996-2021); other information from Robinson et al. (2006), Department of Environment, Land, Water and Planning (2021), and Zhou and Cartwright (2021). Boxes show ^{14}C (red) and ^{3}H activities (black) of groundwater (data from Table 3.2).

3.3 Materials and methods

3.3.1 Sampling

Stream water samples (four rounds in total) were collected between March and November 2019 in the upper Wimmera River (Fig. 3.1, Table S1). River samples were collected from the centre of the river ~1m below the surface, or just above the bed where the river was shallower, using an open sample collector. 15 samples of pool water were taken using an open sample collector in March 2019 when the river consisted of disconnected pools with small flowing sections. These samples were taken from isolated pools, not the flowing reaches. 23 samples were collected in

July, September, and November. July and September were high and moderate flow periods, respectively, whereas November was a low flow period just before the river ceased to flow again. 13 samples of near-river water (NRW) were taken from the top of the saturated zone within 3m of the river. Due to Covid-19, the NRW samples were collected in April 2021 but the conditions were similar to March 2019. Groundwater samples were taken in November 2019 from groundwater-monitoring bores installed on the river bank and floodplain using an impeller pump (Fig. 3.1, Table S2). In excess of three volumes of water were extracted prior to sampling or the bores were pumped dry and allowed to recover.

There are three gauging stations along the river that continuously measure streamflow including Eversley, Glynwylln and Glenorchy on Fig. 3.1. (Department of Environment, Land, Water and Planning, 2021). Linear interpolation and extrapolation were used to estimate intermediate streamflow data. Runoff coefficients (the percentage of rainfall that is exported annually by the stream) were estimated using 1993 to 2021 streamflow records from the three gauges (Department of Environment, Land, Water and Planning, 2021). Because insufficient rainfall data exist to calculate area-weighted rainfall amounts upstream of each gauge, runoff coefficients were calculated using the higher and lower annual rainfall from the catchment (505 and 709 mm; Bureau of Meteorology, 2021), which results in a 15% uncertainty at each site. Here, the runoff coefficient is treated as a catchment attribute reflecting average flows rather than the flow at any one time.

3.3.2 Analytical techniques

^{3}H activities were analysed at the Institute of Geological and Nuclear Sciences (GNS) in New Zealand by liquid scintillation in Quantulus ultra-low-level counters following vacuum distillation and electrolytic enrichment (Morgenstern and Taylor, 2009). ^{3}H activities are expressed in Tritium

Units (TU) and the detection limit is 0.02 TU with relative uncertainties (1σ) of approximately ±2%. ^{14}C activities of groundwater were measured at GNS in New Zealand by accelerator mass spectrometer (AMS). CO_2 in groundwater was extracted using orthophosphoric acid and then converted into a graphite target after being purified under vacuum. ^{14}C activities are expressed as percent modern carbon (pMC), where the ^{14}C activity of modern carbon is 95% of the ^{14}C activity of the NBS oxalic acid standard in 1950 (Stewart et al., 2004).

EC values were measured in the field using a calibrated TPS meter and electrode. A ThermoFischer quadrupole ICP-OES at Monash University was used to measure cation concentrations on samples that were filtered through 0.45μm cellulose nitrate filters and acidified to pH<2. Anion concentrations were measured using a Thermo Fischer ion chromatograph at Monash University on filtered, unacidified samples. Based on replicate analyses, the precision (σ) of major ion concentrations ranges from 2 to 5 %. Stable isotope ratios were analysed at Monash University using a ThermoFinnigan Delta Plus Advantage mass spectrometer. $\delta^{18}O$ values of water were measured in a ThermoFinnigan Gas Bench by equilibration with He-CO_2 at 32°C for 24-48 hours. $\delta^{2}H$ values of water were measured following reduction by Cr at 850°C in a Finnigan MAT H/Device. $\delta^{18}O$ and $\delta^{2}H$ values were normalised following Coplen (1988) and are expressed relative to V-SMOW. Precision (σ) based on replicate analyses is 0.15‰ for $\delta^{18}O$ and 1‰ for $\delta^{2}H$. The geochemistry data is in the Supplement.

3.3.3 Mean transit times

MTTs were calculated from single measurements of ^{3}H using lumped parameter model (LPMs) implemented in the TracerLPM Excel workbook (Jurgens et al., 2012). The ^{3}H activity of stream water at time t (C_0 (t)) is related to the input of ^3H (C_i) in rainfall overtime via the convolution integral:

$$C_0(t) = \int_0^{\infty} C_i\,(t-\tau)g(t)e^{-\lambda\tau}d\tau \tag{1}$$

In equation (1), τ is the transit time, t-τ is the time that the water was recharged, λ is the decay constant of ^3H (0.0563 yr^{-1}), and g(t) is a function that describes the distribution of flow paths and transit times in the flow system. The ^3H input was from the annual weighted average ^3H activities of rainfall in Melbourne (Tadros et al., 2014). Modern rainfall in central Victoria is predicted to have average annual ^3H activities in the range of 2.8 to 3.2 TU (Tadros et al., 2014); measured ^3H activities of rainfall in Victoria are within the range of the Tadros et al. (2014) estimates (Cartwright and Morgenstern, 2015; Cartwright et al., 2018; Howcroft et al., 2018; Barua et al., 2022).

Several LPMs were used. The dispersion model (DM) stems from the one-dimensional advection-dispersion transport equation and can be applied to a variety of aquifer configurations (Zuber and Maloszewski, 2001; McGuire and McDonnell, 2006; Jurgens et al., 2012). The dispersion parameter (DP), which is the ratio of dispersion to advection, needs to be defined when using this model. For kilometre-scale flow systems such as in this study, DP values of 0.05 to 0.5 are suitable (Maloszewski, 2000; Zuber and Maloszewski, 2001). The Exponential Mixing Model (EMM) represents a flow system with a simple exponential distribution of flow paths. The Exponential Piston Flow Model (EPM) describes flow systems that have both exponential and piston-flow sections. It is an appropriate model for unconfined aquifers with vertical recharge through the unsaturated zone and exponential flow in the saturated zone (Maloszewski, 2000; Morgenstern et al., 2010; Howcroft et al., 2019). The EPM ratio is the relative contribution of piston to exponential flow and values of 0.33 and 1, which represent 75% and 50% exponential flow were used. MTTs were estimated by matching the ^{3}H activities predicted by the LPMs to the measured ^{3}H activities. While the estimates of MTTs are based on single samples, these LPMs have successfully reproduced long-term time-series ^{3}H activities of stream water in other regions (Maloszewski and Zuber, 1982; Blavoux et al., 2013; Morgenstern et al., 2015).

The same lumped parameter models were used to calculate the predicted ^{14}C vs. ^{3}H trends and MTTs of groundwater. For ^{14}C, the input function is based on activities of atmospheric CO_2 (McCormac et al., 2004; Reimer et al., 2013). Calcite in these aquifers is mainly cements and veins, which are likely to have variable δ^{13}C values (Cartwright and Morgenstern, 2012; Cartwright et al., 2013; Clark, 2015; Meredith et al., 2016), precluding the use of isotope mass-balance to estimate the degree of closed-system calcite dissolution. However, the aquifers are siliceous and close-system calcite dissolution is expected to be minor (< 10%) (Clark, 2015).

3.3.4 Volumes of groundwater

The groundwater volumes (V in m^3) that contribute to the river are related to MTT and streamflow (Q in m^3 yr^{-1}) via:

$$V = Q \times \mathrm{MTT} \tag{2}$$

(Maloszewski and Zuber, 1982, 1992; Morgenstern et al., 2010).

3.4 Results

3.4.1 Streamflow

The variations of streamflow at the three gauging stations (Fig. 3.1) along the upper Wimmera River in 2019 are shown in Fig. 3.2b. Although streamflow of up to 50 m^3 day^{-1} was recorded at Glynwylln during the summer months (January to March), the river largely consisted of disconnected pools with only minor flowing sections. Based on the streamflow at this and the Eversley and Glenorchy gauges (Fig. 3.2b), the river is estimated to have commenced flowing continuously in early to mid-April. There was a significant increase in streamflow from June following autumn rains (Fig. 3.2a) and it reached a peak in August (up to 6.1×10^{5} m^{3} day^{-1} at Glenorchy). Streamflow then decreased over spring and summer and the river ceased to flow continuously in late November. Runoff coefficients have ranges of 4.0 to 5.4% at Eversley, 2.3 to 3.2% at Glynwylln, and 2.2 to 3.0% at Glenorchy.

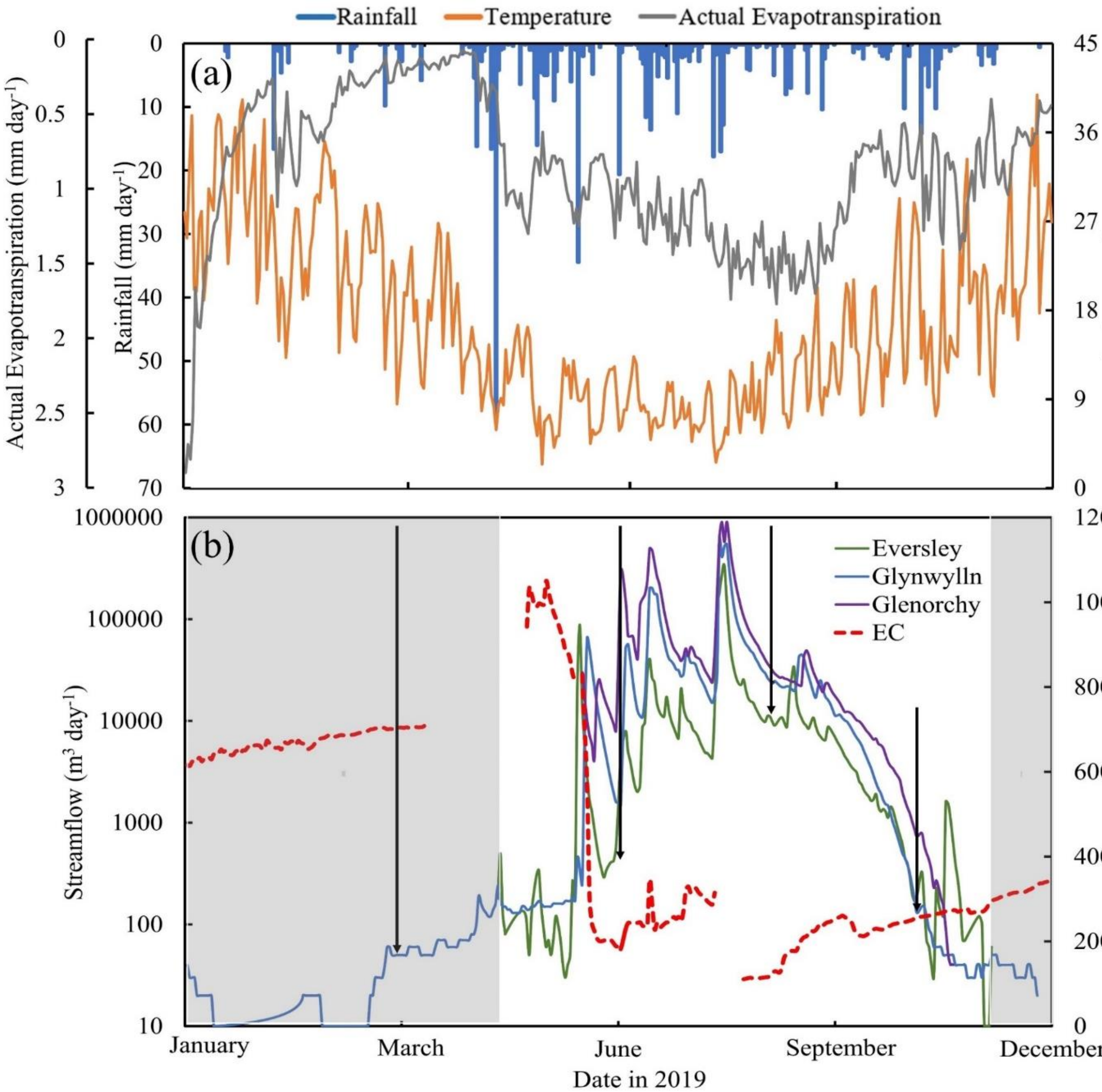

Figure 3.2. (a) Variations in daily rainfall, daily actual evapotranspiration, and temperature and (b) EC at Glynwylln (missing data are caused by measurement errors of equipment) and streamflow at Eversley, Glynwylln, and Glenorchy (Fig. 3.1) in the upper Wimmera River in 2019. Variations in EC at Glynwylln (missing data are caused by measurement errors of equipment) and streamflow at Eversley, Glynwylln, and Glenorchy (Fig.3.1) in the upper Wimmera River in 2019. Sampling times are indicated by arrowed lines. Shaded areas represent the zero-flow periods. Data from Department of Environment, Land, Water and Planning (2021) and Bureau of Meteorology (2021).

3.4.2 EC and major ion geochemistry

EC values in 2019 at the Glynwylln gauging station increased during the summer months, peaked at 10,500 μS cm^{-1} in late May, and decreased to 1780 μS cm^{-1} in June (Fig. 3.2b). Overall, EC values were broadly inversely correlated with streamflow. TDS concentrations of stream water in the upper Wimmera River varied from 360 to 2490 mg L^{-1} (Table S1) and were also higher during the low flow period in November 2019. Na is the most abundant cation in the stream water (74-83% on a molar basis) with lower abundances of Ca (3-7%), Mg (12-19%), and K (1-2%). Cl is the most common anion (82-99% on a molar basis) in the stream water (Fig. 3.3). During the zero-flow period in March 2019, the pool water was much more saline with EC values of 2430-15,330 μS cm^{-1} and TDS concentrations (up to 11,420 mg L^{-1}) (Table S1). Near-river water (NRW) from the zero-flow period in 2021 had EC values of 1035 to 6080 μS cm^{-1}. TDS concentrations of regional groundwater from monitoring bores in this region ranged from 550 to 13,720 mg L^{-1} (mean = 4900 ± 3770 mg L^{-1}: Table S2) and there is no correlation between TDS and depth. Na and Cl are again the dominant cations and anions in the groundwater (Fig. 3.3, Table S2). Overall, the major ion geochemistry of the groundwater, stream water from the different flow conditions, pool water and, NRW are similar (Fig. 3.3).

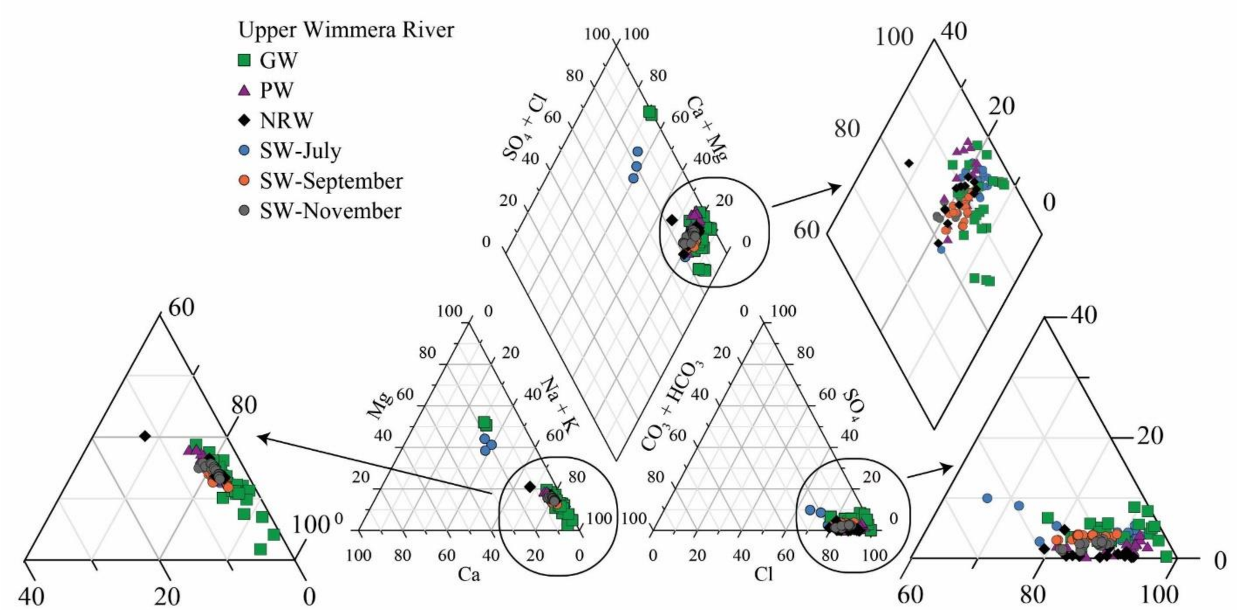

Figure 3.3. Trilinear diagram summarising molar major ion ratios of the different water sources in the upper Wimmera River (data from Table S1 and S2). GW=groundwater; PW= Pool Water; NRW=Near River Water; SW=Stream Water. Inserts show details of the data.

3.4.3 Stable isotopes

The $\delta^{18}O$ and δ^2H values of the stream water differed between the sampling rounds (Tables S1 and S2, Fig. 3.4). The δ^2H and $\delta^{18}O$ values of the pool water were -24 ‰ to +37 ‰ and -3.3 ‰ to +10.3 ‰, respectively and define an array to the right of Melbourne meteoric water line with a slope of 4.2 which implies that evaporation has occurred (Gonfiantini, 1986; Clark and Fritz, 1997). The pool water array intercepts the Melbourne meteoric water line at lower $\delta^{18}O$ and δ^2H values (-5.6 ‰ and -31 ‰) than those of average rainfall in Melbourne ($\delta^{18}O$ = -4.98 ‰, δ^2H = -28.4 ‰; Hollins et al., 2018), probably due to the Wimmera region being further inland. $\delta^{18}O$ and δ^2H values of river water in July and September cluster close to the Melbourne meteoric water line. $\delta^{18}O$ and δ^2H values in July 2019 were -3.6 to -7.2 ‰ (mean= -6.1 ± 0.7 ‰) and -29 to -43 ‰ (mean= -35 ± 3.8 ‰), respectively, whereas in September 2019, $\delta^{18}O$ and δ^2H values were -3.9 to -6.1 ‰ (mean= -5.3 ± 0.4 ‰) and -29 to -32 ‰ (mean= -31 ± 0.9 ‰), respectively (Table S1).

$\delta^{18}O$ and $\delta^{2}H$ values during the low streamflow period in November 2019 ranged from -2.7 to -4.8 ‰ and -20 to -26 ‰, respectively, while those of the NRW were -0.5 to -3.1‰ and -8 to -29 ‰, respectively. Both the November river samples and the near-river waters define similar evaporative trends to the pool waters. Groundwater has $\delta^{18}O$ and $\delta^{2}H$ values of -4.4 to -6.7 ‰ (mean = -5.4 ± 0.6 ‰) and -28 to -38 ‰ (mean= -31 ± 2.7 ‰) respectively that overlap with those of the stream water in July and September (Fig. 3.4; Table S1).

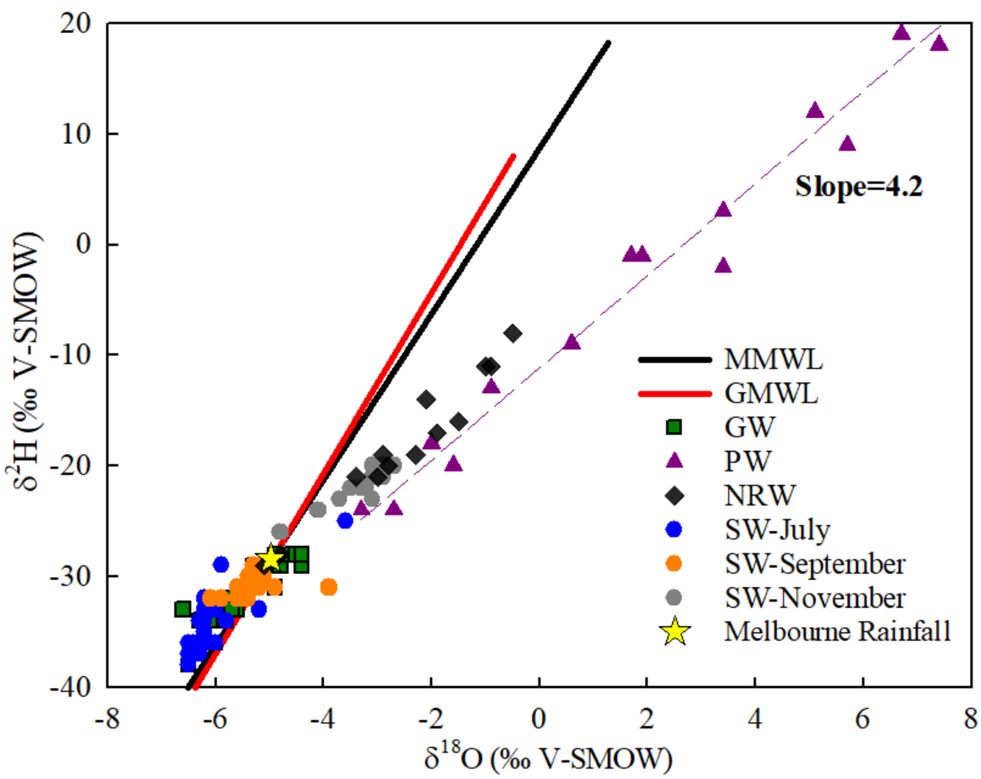

Figure 3.4. Stable isotope ratios of water samples in the upper Wimmera River. GMWL=Global Meteoric Water Line ($\delta^{2}H = 8.2 \times \delta^{18}O + 11.3$ ‰, as defined by Rozanski et al., 1993); MMWL= Melbourne Meteoric Water Line ($\delta^{2}H = 7.4 \times \delta^{18}O + 8.6$ ‰, as defined by Hughes and Crawford, 2012). GW=regional groundwater; PW=pool water; NRW=Near-river water; SW=stream water. The dashed line is the best fit for the pool water data. Data from Table S1 and S2.

3.4.4 ^3H and ^{14}C activities

3.4.4.1 Regional groundwater

^3H activities of regional groundwater were < 0.02 to 0.45 TU (Table 3.2), which are significantly lower than the predicted average ^3H activity of annual modern rainfall in this area (3.0 ± 0.2 TU: Tadros et al., 2014). The higher ^3H activities were from shallow groundwater (<18 m depth) in the upper and middle catchment, whereas deep groundwater (>30 m depth) had ^3H activities <0.02 TU. Groundwater close to the river does not generally have high ^3H activities (Fig. 3.1). ^{14}C activities of regional groundwater ranged between 57.1 and 103 pMC (Table 3.2). The highest ^{14}C activities (up to 103 pMC) are again from the shallow groundwater in the upper and middle catchment. The trend of ^3H vs. ^{14}C activities (Fig. 3.5) are similar to those predicted for an aquifer system that does not show mixing between shallow younger groundwater and deeper older groundwater (i.e., where the activities of the two radioisotopes are controlled by their input functions and decay rates).

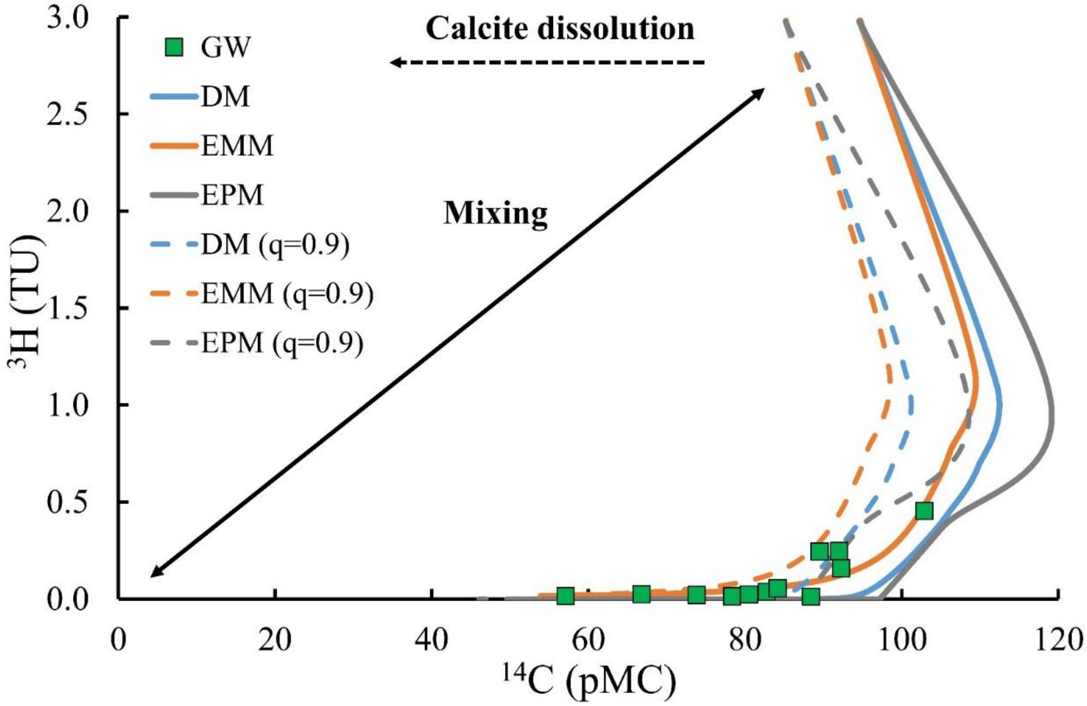

Figure 3.5. ^{3}H activities vs. ^{14}C activities of groundwater from the upper Wimmera River. Curved lines are the predicted covariance in the radioisotopes predicted by the Exponential Mixing, Exponential-Piston (EPM ratio = 1), and Dispersion (DP=0.5) lumped parameter models. Solid arrowed lines show schematically the effects of mixing between old regional groundwater (low ^{14}C and ^{3}H free) and modern or recently recharged water (high ^{14}C and ^{3}H). Calcite dissolution lowers the predicted ^{14}C activities (dashed lines are used to display 10% calcite dissolution).

3.4.4.2 River water

The ^{3}H activities of pool water varied from 0.64 to 3.29 TU (Fig. 3.6; Table 3.1). The highest ^{3}H activity (3.29 TU), which is higher than that of average annual rainfall, was from an area of subdued topography in the lower reaches. In contrast, ^{3}H activities were lowest (down to 0.64 TU) where the river is located near steeper hillslopes and flows through coarse sediments. There is a strong positive correlation (R^2 = 0.94) between ^{3}H activities of pool water and δ^2H values (Fig. 3.6a). Pool waters have a wide range of ^{3}H activities with variable TDS concentrations, ranging from 2237 to 4639 mg L^{-1}. The stream water was less saline with a range of TDS 433-2038 mg L^{-1} (Fig. 3.6b).

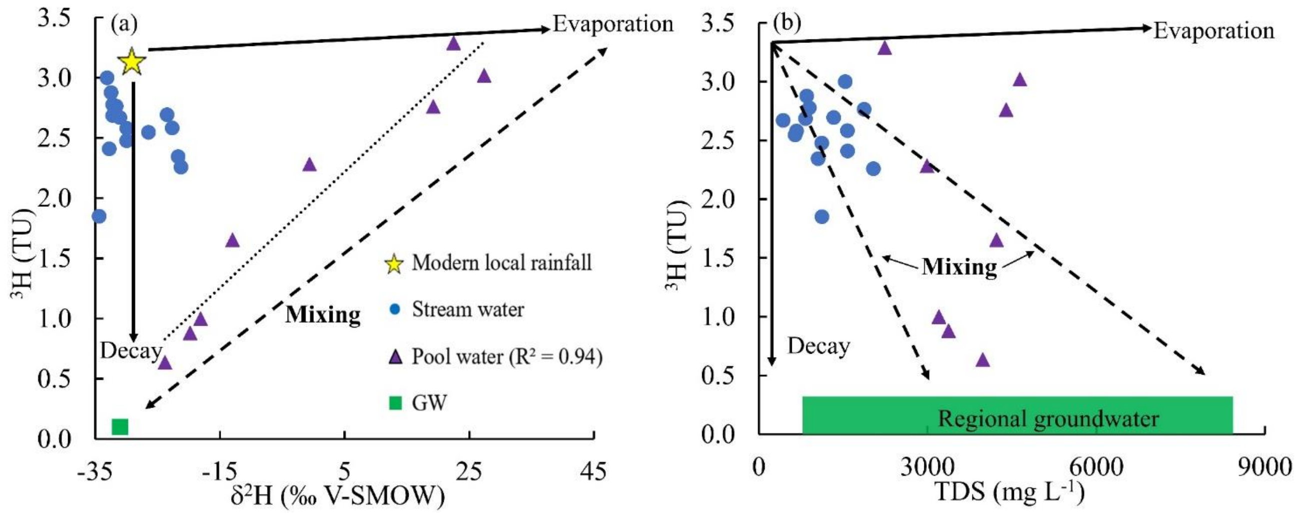

Figure 3.6. (a) Variation of ^3H activities and δ^2H values and (b) ^3H activities and TDS of stream water, pool water and groundwater (GW) in the upper Wimmera catchment. arrows show trends expected from evaporation and mixing. Data from Table S1 and S2.

The ^3H activities of stream water during the periods when the river was flowing were generally lower than those of rainfall and had a range of 1.85 to 3.00 TU in July, 2.48 to 2.88 TU in September, and 2.26 to 2.69 TU in November (Table 3.1). During the high streamflow in July, the ^3H activities of river water were more variable than in September and November (Figs. 3.6, 3.7). Both lowest and highest values of ^3H activities were recorded in the high flow period (Fig. 3.7).

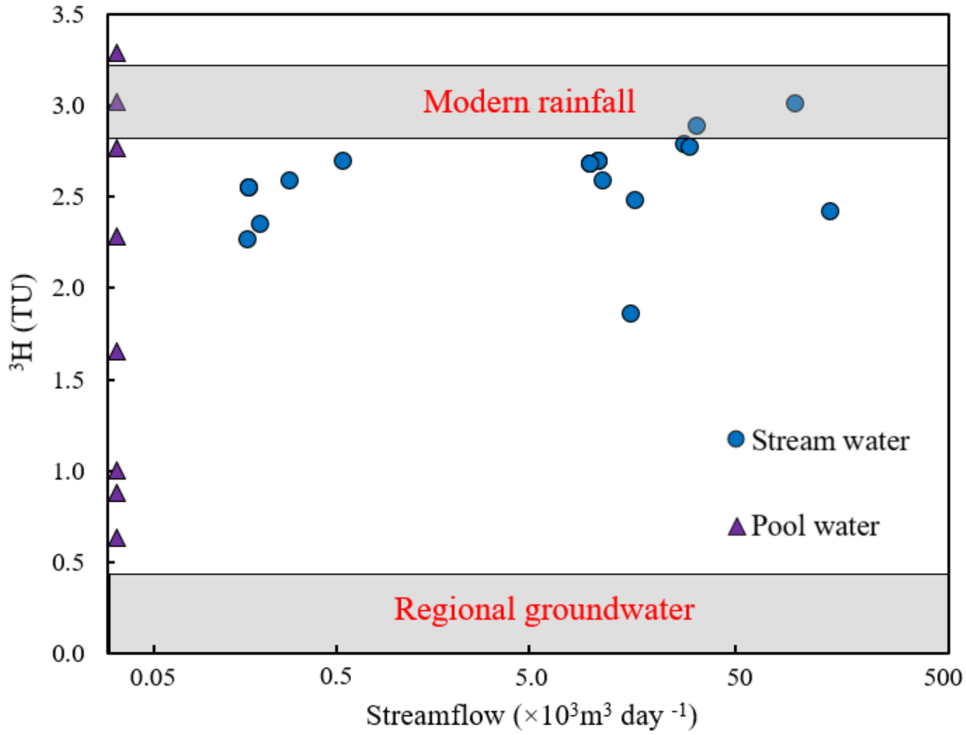

Figure 3.7. Variation of ^{3}H activities and streamflow. Pool water represents a time of zero streamflow. Shaded areas show ^{3}H range of modern rainfall and regional groundwater. Data from Table 3.1.

3.5 Discussion

The combined streamflow, major ion geochemistry, and stable and radioactive isotopes allow the water sources contributing to streamflow and MTTs at different flow conditions to be understood.

3.5.1 Identification of water sources

Pool waters in summer months contain the last remnants of river water from when the river ceases to flow, rainfall and/or groundwater discharging from the underlying aquifers (Cartwright and Morgenstern, 2016; Lamontagne et al., 2021). In the upper Wimmera River, most of the pools are perennial and have a wider range of ^{3}H activities than stream water and groundwater (Fig. 3.7). The variation in ^{3}H activities with δ^2H (Fig. 3.6a) and TDS concentrations (Fig. 3.6b) most likely reflects the mixing between older regional groundwater (saline with lower ^{3}H activities) and younger surface water with lower salinity and higher ^{3}H activities. The variations between δ^{18}O and δ^2H values (Fig. 3.4) and ^{3}H activities and δ^2H values (Fig. 3.6a) imply that the surface water dominated pools have undergone higher degrees of evaporation than those with greater groundwater inflows. Conceivably, the pools that are better connected to the groundwater are throughflow systems, which would limit evaporation whereas other pools may trap surface water which then evaporates. Some of the pool water has higher ^{3}H activities (up to 3.29 TU) than were recorded at the low flows that immediately precede the formation of the pools (Fig. 3.7). Summer rainfall in southeast Australia, however, generally has ^{3}H activities close to the annual average (Tadros et al., 2014), and the input of summer rainfall cannot readily explain the locally high ^{3}H activities. Late winter and spring rainfall has higher ^{3}H activities than those of average rainfall due to stratosphere-to-troposphere moisture exchange (Tadros et al., 2014). The upper Wimmera River is locally losing at high streamflows, such as commonly occur in late winter and early spring (Fig. 3.2) allowing bank storage to occur. Subsequent drainage of bank water back to the river potentially explains the local high ^{3}H activities in the pools. Alternatively, these high ^{3}H activities may reflect the input of young water from perched aquifers in the riparian zone as documented in intermittent streams elsewhere in western Victoria (Barua et al., 2022).

The ^{3}H activities of stream water when the upper Wimmera River is flowing is much higher than that of groundwater (Figs. 3.6, 3.7), implying that the river is largely fed by young water. This is the case even during the low flow periods, which is when rivers are most likely to be sustained by long-lived water stores (e.g., Gusyev et al., 2016; Cartwright et al., 2020). The much lower TDS concentrations of the river water compared with the groundwater (Fig. 3.6b) and irregulated downstream trends in major ion concentrations (Table S1) are also consistent with the input of water from mainly near-river sources. The one lower ^{3}H activity (1.85 TU) during high flow conditions in July 2019 (Table 1, Fig. 3.7) may reflect very local input of regional groundwater or older near-river waters being flushed into the stream during the early stages of rainfall by hydraulic loading. This has been documented in other Australian catchments (e.g., the Tambo River: Unland et al., 2015) and is a common feature in many river systems (sometimes referred to as the old water paradox: Kirchner, 2003; Cartwright and Morgenstern, 2018). Unlike in some catchments (Tsujimura et al., 2007; Birks et al., 2019; Jung et al., 2019), the major ion and stable isotope geochemistry of regional groundwater and near-river water are similar (Figs. 3.3 and 3.4; Tables S1 and S2). The geochemistry of the stream also does not vary with flow. This precludes using these tracers to distinguish water sources or as a proxy for ^{3}H activities (e.g., Peters et al., 2014; Cartwright and Morgenstern, 2015; Beyer et al., 2016; Cartwright et al., 2020). The large difference in ^{3}H activities between regional groundwater and rainfall, however, explicitly allows the input of older groundwater to be assessed.

3.5.2 Mean transit times of river water

The estimates of mean transit time assume that there is a single flow system within the catchment. The pool waters probably represent discrete mixing between older groundwater and younger water (Fig. 3.6). It is not possible to calculate the MTTs of these waters using a single LPM and there is insufficient data to use binary LPM calculations. In common with other studies of MTTs, it is assumed that when the river is flowing it is sustained by a single store of water with MTTs that vary as the catchment dries down and wets up. As discussed above, most of the water sustaining the river when it is flowing is envisaged to be derived from near-river stores with little input from regional groundwater.

The MTTs in the upper Wimmera River when it was flowing ranged from < 1 to 17 years and are mostly less than 7 years (Table 1). The different LPMs yielded slightly different MTTs and the range of MTTs increases with decreasing ^{3}H activities. The highest estimates of MTTs are from the EMM and the lowest are from the DM with D_p 0.05. During the high flow period in July 2019, MTTs were generally higher (<1 to 16.8 years). By contrast, the range of MTTs at moderate and low flow conditions was 1.6 to 7.8 years (Table 3.1).

The MTTs are subject to several uncertainties. The uncertainty arising from the choice of LPMs is greater at ^{3}H activities <2.5 TU with an average uncertainty of 22% (Table 3.1). The influence of uncertainties in the ^{3}H activities of modern rainfall (± 0.2 TU: Tadros et al., 2014) may be demonstrated using the EPM with an EPM ratio of 0.33 (the effects are similar in other models) (Fig. 3.8a). Varying the ^{3}H activities between 2.8 TU and 3.2 TU translates into uncertainties of ±6 to 7% (Fig. 3.8a). Applying a similar 10% uncertainty to the entire ^{3}H input function produces uncertainties of 9 to 21%, with the largest difference when ^{3}H activities were greater than 1 TU (Fig. 3.8b). Uncertainties arising from the precision of the ^{3}H analyses are <0.8 years. Mixing of multiple water sources with different MTTs (aggregation) may result in actual MTTs being lower than calculated MTTs (Suckow, 2014; Kirchner, 2016a; Stewart et al., 2017). Aggregation has the most impact when there is binary mixing between water with very different MTTs. Mixing between multiple water stores with a range of MTTs has less impact on the MTTs calculated using ^{3}H as that scenario is similar to what is modelled using the LPMs (Cartwright and Morgenstern, 2016). In the case of the upper Wimmera River, the smaller range of MTTs implies that aggregation may not be as significant as in other catchments in southeast Australia where the range of MTTs in the catchment waters is much larger. Considering the uncertainties from the different LPMs, the analytical uncertainty, and the tritium activities of modern and historical rainfall, the range of MTTs for a ^3H activity of 1.5 TU was 15.2 to 25.5 years, which is a relative uncertainty of -24 to +27%. For water with 0.5 TU, the MTTs ranged 92.6 to 108 years, which is an uncertainty of -9 % to +15%. Although these are substantial, it does not alter the conclusion that the upper Wimmera River is fed by relatively young water at all stages of flow.

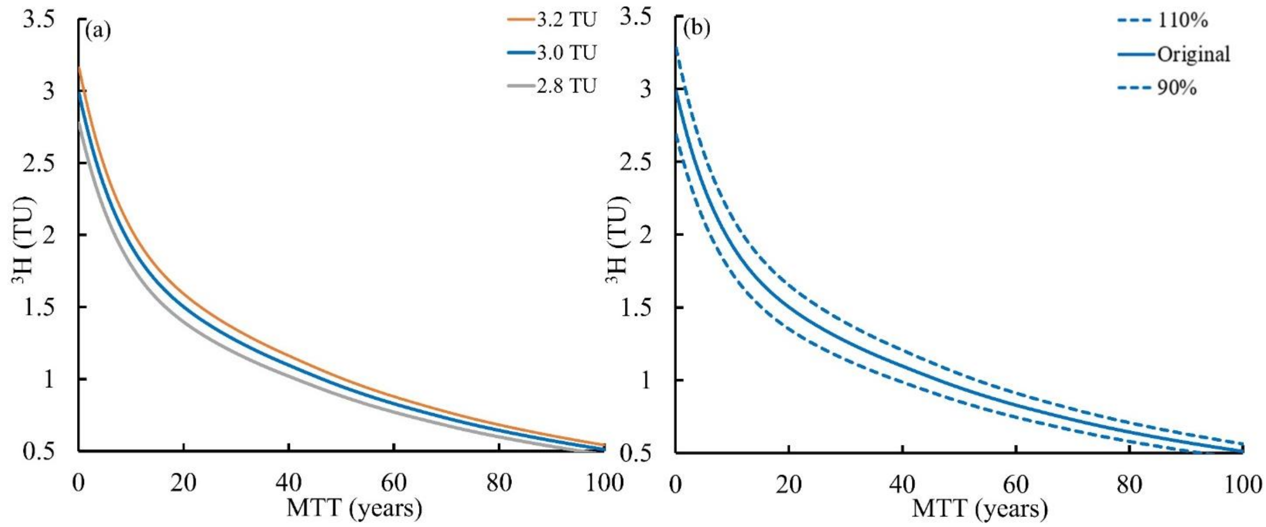

Figure 3.8. (a) Impacts of varying the ^3H activity of modern rainfall from 2.8 to 3.2 TU on MTTs calculated using the Exponential-Piston Flow Model (EPM ratio = 0.33). (b) Impacts of varying ^3H activity of rainfall between 90% and 110% of its assumed values on mean transit time calculated using the Exponential-Piston Flow Model (EPM ratio = 0.33).

The average annual rainfall ^3H activities were used in the MTTs calculations. However, if there is strong seasonal recharge due to summer rainfall being lost by evapotranspiration, the ^3H activities of the recharging water may be different to the average annual ^3H activity (Morgenstern et al., 2010; Blavoux et al., 2013). Monthly variations in rainfall ^3H activities are less than 1 TU and the ^3H activities of summer rainfall are close to annual rainfall values (e.g., Tadros et al., 2014). Considering the general uncertainty in the ^3H input function, uncertainties that originate from adopting the average annual ^3H activity are minor.

The volume of water store that sustained the streamflow calculated from the MTTs (Eq. (2)) ranged from 3.2×10^5 m^3 to 2.6×10^8 m^3 (Fig. 3.9b). The estimated volume of water stored in the riparian zone of the river is 3.1×10^5 m^3, which was calculated from the estimated river length (120,000 m), the width and depth of the riparian zone (6.5 m and 2 m, respectively), and an assumed porosity of 0.2. This value is three orders of magnitude smaller than that of the calculated volume of water needed to generate streamflow during the high flow period, implying that the streamflow was generated from water derived from the broad landscape. By contrast, the volume of water in the riparian zone is similar to the volume needed to generate streamflow at low flow conditions, which indicates that it may be derived from near-river stores.

3.5.3 Groundwater transit times

Groundwater MTTs were calculated using the EPM model (EPM ratio = 0.33; Table 3.2). This model is applicable to groundwater flow systems where the bores sample deeper groundwater flow paths but not the short near-surface flow paths (Maloszewski and Zuber, 1982). MTTs of groundwater with ^3H activities >0.25 TU were calculated using ^3H. For groundwater with lower ^3H activities, the ^{14}C activities were used. As discussed above, the proportion of DIC from closed system calcite dissolution in these siliceous aquifers is likely to be minor and MTTs were calculated assuming up to 10% addition of ^{14}C-free carbon. The estimated MTTs of groundwater were between 120 and 5690 years (Table 3.2). The relative uncertainties on these estimates are similar to those discussed above. Groundwater within a few 10s to 100s meters of the river, such as at locality I and J in Fig. 1, had MTTs of up to 5690 years and the ^{14}C and ^3H activities show little evidence of mixing (Fig. 3.5), implying that there is limited recharge of regional groundwater by stream water even when the river is losing. The large contrast between the MTTs of groundwater and river water also implies that the regional groundwater flow system is distinct from local near-river flow system.

3.5.4 Comparison with perennial streams

In southeast Australia, the ^{3}H activities at low flows in the upper Wimmera River and other intermittent streams are higher than in perennial streams of comparable size from catchment with similar geology and landuse (Fig. 3.9). Perennial streams elsewhere in Australia and New Zealand also locally have low ^{3}H activities at low flows (Stewart et al., 2010; Duvert et al., 2016). This implies that intermittent streams at low streamflows are sustained by much younger water than perennial streams. This is concluded to be caused by a much weaker connection between intermittent streams and deeper older regional groundwater than is the case for perennial streams. Because evapotranspiration rates, local vegetation types and rainfall influence both how much of rainfall is exported via the stream and the MTTs. ^{3}H activities in perennial streams from southeast Australia correlate with the runoff coefficient (Fig. 3.9a). There is a broad correlation (R^2=0.58) between ^{3}H and runoff coefficients from multiple perennial catchments in southeast Australia (including the Ovens, Latrobe, Gellibrand, and Yarra catchments: Fig. 3.9a) and the correlations in individual catchment are higher (R^2 of 0.72 to 0.94: Cartwright et al., 2020). By contrast, the ^{3}H activities in the Wimmera and other intermittent streams are much higher at comparable runoff coefficients and are poorly correlated (Fig. 3.9a). This may be due to the alternating gaining and losing conditions in intermittent streams.

The volumes of the stores of water in the catchment that contributes to streamflow in the upper Wimmera River (3.2×10^5 m^3 to 2.6×10^8 m^3: Fig. 3.9b) are 1-2 orders of magnitude smaller at similar streamflows than those in perennial streams from southeast Australia (up to 8.3×10^9 m^3 in the Ovens catchment) (Fig. 3.9b) but are similar to other intermittent streams (Deep Creek and Gatum catchments). These differences are also due to the intermittent streams being less well-connected to the deeper groundwater, which has larger volumes.

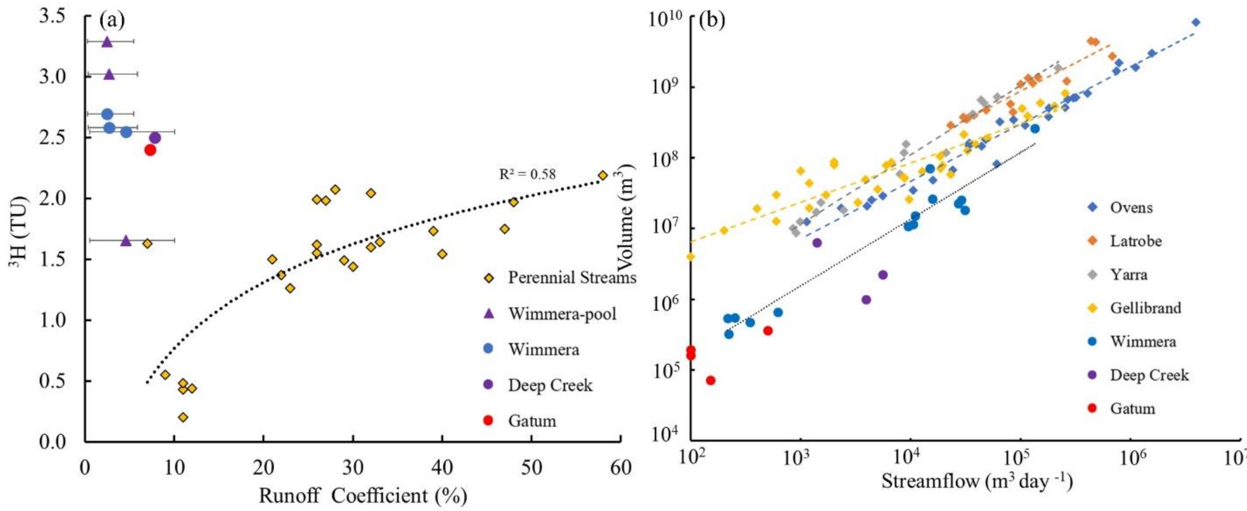

Figure 3.9. (a) Comparison of ^{3}H activities and runoff coefficients at low and zero flow conditions and (b) volumes of water sustaining streamflows between the upper Wimmera River and other intermittent and perennial streams in southeast Australia. Error bars represent the uncertainty of annual rainfall in the upper Wimmera Catchment. Perennial streams are the Ovens, Latrobe, Yarra, and Gellibrand (data from Cartwright et al., 2020); intermittent streams are Deep Creek and Gatum (data from Cartwright and Morgenstern, 2016 and Barua et al., 2022).

3.6 Conclusions

Currently about 51 to 60% of global rivers have ceased to flow at least one day per year and intermittency of streams is forecasted to increase due to climate change and rising water usage (Messager et al., 2021). Thus, investigation of intermittent streams that commonly occur in semi-arid regions with scarce surface water resources is vital. However, our understanding of the functioning of intermittent catchments remains incomplete (e.g., Datry et al., 2014; Shanafield et al., 2020, 2021). Integrating mean transit time estimates into studies of intermittent catchments will allow a better general understanding of this important group of rivers.

The upper Wimmera River and other intermittent streams in southeast Australia are connected to younger stores of near-river water with limited connections to deeper regional groundwater. Because those stores are smaller, intermittent rivers will be more vulnerable to short-term variability of rainfall and respond more quickly to land use changes than comparable perennial rivers. This is evident in the Wimmera River where flow has decreased and intermittency has increased following the onset of the Millennium drought in the mid-1990s. In comparison, most of the perennial rivers summarised in Cartwright et al. (2021) currently have similar flow regimes as prior to the Millennium drought. The fact that intermittent streams receive inputs from near-river water stores also has implications for their protection and management. They are probably less vulnerable to contamination via inputs of regional groundwater; however, protection of the near-river environment is crucial to maintain river health. The pools at zero flow conditions in the Wimmera and other intermittent streams have some groundwater inputs (Lamontagne et al., 2014, 2021; Cartwright and Morgenstern, 2016). Even where these are not substantial, connection with the regional groundwater is important for preventing the stream from drying up completely. Reduction in groundwater elevations due to climate change or pumping may have serious impacts on these pools that are commonly important water sources for local ecosystems in dry summers.

This study also illustrates the general use of radioisotopes such as ^3H to understand water stores that contribute to river flow. Major ion geochemistry and stable isotopes may be able to discern the sources of river water; however, in many catchments (both intermittent and perennial), this is not possible. Estimating mean transit time estimates allows a direct understanding of where in the catchment the water is derived from. In the southern hemisphere, ^3H allows mean transit times to be readily estimated in relatively large catchments and this will be the case in the northern hemisphere in the near future (Morgenstern et al., 2010).

Chapter 3

References

Barua, S., Cartwright, I., Dresel, P. E., Morgenstern, U., McDonnell, J. J., and Daly, E., 2022. Sources and mean transit times of intermittent streamflow in semi-arid headwater catchments, Journal of Hydrology, 604, 127208, https://doi.org/10.1016/j.jhydrol.2021.127208

Benettin, P., J. W. Kirchner, A. Rinaldo, and G. Botter., 2015. Modeling chloride transport using travel time distributions at Plynlimon, Wales, Water Resources. Research, 51, 3259-3276, https://doi.org/10.1002/2014WR016600.

Beyer, M., Jackson, B., Daughney, C., Morgenstern, U., and Norton, K., 2016. Use of hydrochemistry as a standalone and complementary groundwater age tracer, Journal of Hydrology, 543, 127-144, https://doi.org/10.1016/j.jhydrol.2016.05.062.

Birkel, C., Soulsby, C., Tetzlaff, D., 2015. Conceptual modelling to assess how the interplay of hydrological connectivity, catchment storage and tracer dynamics controls nonstationary water age estimates, Hydrological Processes, 29, 2956-2969, https://doi.org/10.1002/hyp.10414.

Birks, S. J., Fennell, J. W., Gibson, J. J., Yi, Y., Moncur, M. C., and Brewster, M., 2019. Using regional datasets of isotope geochemistry to resolve complex groundwater flow and formation connectivity in northeastern Alberta, Canada, Applied Geochemistry, 101, 140-159, https://doi.org/10.1016/j.apgeochem.2018.12.013.

Blavoux, B., Lachassagne, P., Henriot, A., Ladouche, B., Marc, V., Beley, J. J., and Olive, P., 2013. A fifty-year chronicle of tritium data for characterising the functioning of the Evian and Thonon (France) glacial aquifers, Journal of Hydrology, 494, 116-133, https://doi.org/10.1016/j.jhydrol.2013.04.029.

Bureau of Meteorology Australian landscape water balance: Commonwealth of Australia, available at: http://www.bom.gov.au/water/landscape/, last access: 20 July 2021.

Chapter 3

Cartwright, I. and Morgenstern, U., 2018. Using tritium and other geochemical tracers to address the “old water paradox” in headwater catchments. Journal of Hydrology, 563, 13-21, https://doi.org/10.1016/j.jhydrol.2018.05.060.

Cartwright, I. and Morgenstern, U., 2012. Constraining groundwater recharge and the rate of geochemical processes using tritium and major ion geochemistry: Ovens catchment, southeast Australia. Journal of Hydrology, 475, 137-149, https://doi.org/10.1016/j.jhydrol.2012.09.037, 2012.

Cartwright, I. and Morgenstern, U., 2015. Transit times from rainfall to baseflow in headwater catchments estimated using tritium: The Ovens River, Australia, Hydrology and Earth System Sciences, 19, 3771-3785, https://doi.org/10.5194/hess-19-3771-2015.

Cartwright, I. and Morgenstern, U., 2016. Using tritium to document the mean transit time and sources of water contributing to a chain-of-ponds river system: implications for resource protection. Applied Geochemistry, 75, 9-19, https://doi.org/10.1016/j.apgeochem.2016.10.007.

Cartwright, I., Fifield, L. K., and Morgenstern, U., 2013. Using ^{3}H and ^{14}C to constrain the degree of closed-system dissolution of calcite in groundwater, Applied Geochemistry, 32, 118-128, https://doi.org/10.1016/j.apgeochem.2012.10.023.

Cartwright, I., Hofmann, H., Currell, M. J., and Fifield, L. K., 2017. Decoupling of solutes and water in regional groundwater systems: The Murray Basin, Australia, Chemical Geology, 466, 466-478, https://doi.org/10.1016/j.chemgeo.2017.06.035.

Cartwright, I., Irvine, D., Burton, C., and Morgenstern, U., 2018. Assessing the controls and uncertainties on mean transit times in contrasting headwater catchments, Journal of Hydrology, 557, 16-29, https://doi.org/10.1016/j.jhydrol.2017.12.007.

Chapter 3

Cartwright, I., Morgenstern, U., Howcroft, W., Hofmann, H., Armit, R., Stewart, M., and Irvine, D., 2020. The variation and controls of mean transit times in Australian headwater catchments. Hydrological Processes, 34, 4034-4048, https://doi.org/10.1002/hyp.13862.

Clark, I.D. and Fritz, P., 1997. Environmental Isotopes in Hydrogeology, Lewis, New York, p. 328.

Clark, I.D., 2015. Groundwater geochemistry and isotopes, CRC Press Boca Raton, FL, USA.

Cook, P. G. and Bohlke, J. K.,2000. Determining timescales for groundwater flow and solute transport. In Environmental tracers in subsurface hydrology, Springer, Boston, MA, p. 1-30, 2000.

Cook, P.G.: Estimating groundwater discharge to rivers from river chemistry surveys, Hydrological Processes, 27, 3694-3707, https://doi.org/10.1002/hyp.9493, 2013.

Coplen, T. B., 1988. Normalization of oxygen and hydrogen isotope data, Chemical Geology, 72, 293-297, https://doi.org/10.1016/0168-9622(88)90042-5.

Costigan, K.H., Jaeger, K.L., Goss, C.W., Fritz, K.M., and Goebel, P.C., 2015. Understanding controls on flow permanence in intermittent rivers to aid ecological research: integrating meteorology, geology and land cover, Ecohydrology., 9, 1141-1153. https://doi.org/10.1002/eco.1712.

Datry, T., Larned, S.T., and Tockner, K., 2014. Intermittent rivers: a challenge for freshwater ecology. BioSciences., 64, 3, 229-235, https://doi.org/10.1093/biosci/bit027.

Department of Environment Land Water and Planning: State Government Victoria, available at: http://data.water.vic.gov.au/monitoring.htm, last access: 20 August 2021.

Department of Jobs, Precincts and Regions, Energy and Earth Resources: State Government Victoria, available at: http://www.energyandresources.vic.gov.au/earth-resources/maps-reports-and-data/geovic, last access: 20 August 2021.

Chapter 3

Duvert, C., Stewart, M.K., Cendón, D.I., and Raiber, M., 2016. Time series of tritium, stable isotopes and chloride reveal short-term variations in groundwater contribution to a stream, Hydrology and Earth System Sciences, 20, 257-277, https://doi.org/10.5194/hess-20-257-2016.

Edmunds, W.M., 2009. Geochemistry's vital contribution to solving water resource problems. Applied Geochemistry. 24, 1058-1073, https://doi.org/10.1016/j.apgeochem.2009.02.021.

Fletcher, G.,2015. Environmental Water Management Plan-Wimmera River System. Government of Victoria Wimmera Catchment Management Authority. http://wcma.vic.gov.au.

Gleeson, T., Befus, K.M., Jasechko, S., Luijendijk, E., and Cardenas, M.B., 2016. The global volume and distribution of modern groundwater, Nature Geoscience, 9, 161-167, https://doi.org/10.1038/ngeo2590.

Gonfiantini, R., 1986. Environmental isotopes in lake studies, Handbook of environmental isotope geochemistry, 2, 113-168.

Gusyev, M. A., Morgenstern, U., Stewart, M. K., Yamazaki, Y., Kashiwaya, K., Nishihara, T., and Iwami, Y., 2016. Application of tritium in precipitation and baseflow in Japan: a case study of groundwater transit times and storage in Hokkaido watersheds, Hydrology and Earth System Sciences, 20(7), 3043-3058, https://doi.org/10.5194/hess-20-3043-2016.

Gutiérrez-Jurado, K.Y., Partington, D., Batelaan, O., Cook, P., and Shanafield, M., 2019. What triggers streamflow for intermittent rivers and ephemeral streams in low-gradient catchments in Mediterranean climates, Water Resources. Research, 55, 9926-9946, https://doi.org/10.1029/2019WR025041.

Hare, D. K., Helton, A. M., Johnson, Z. C., Lane, J. W., and Briggs, M. A., 2021. Continental-scale analysis of shallow and deep groundwater contributions to streams. Nature communications, 12, 1-10, https://doi.org/10.1038/s41467-021-21651-0.

Chapter 3

Herczeg, A. L., Dogramaci, S. S., and Leaney, F. W., 2001. Origin of dissolved salts in a large, semi-arid groundwater system: Murray Basin, Australia. Marine and Freshwater Resources, 52, 41-52. https://doi.org/10.1071/MF00040.

Hollins, S. E., Hughes, C. E., Crawford, J., Cendón, D. I., and Meredith, K. T., 2018. Rainfall isotope variations over the Australian continent–Implications for hydrology and isoscape applications, Science the Total Environment, 645, 630-645, https://doi.org/10.1016/j.scitotenv.2018.07.082.

Howcroft, W., Cartwright, I., and Cendón, D.I., 2019. Residence times of bank storage and return flows and the influence on river water chemistry in the upper Barwon River, Australia. Applied Geochemistry, 101, 31-41, https://doi.org/10.1016/j.apgeochem.2018.12.026.

Howcroft, W., Cartwright, I., and Morgenstern, U., 2018. Mean transit times in headwater catchments: insights from the Otway Ranges, Australia, Hydrology and Earth System Sciences, 22, 635-653, https://doi.org/10.5194/hess-22-635-2018.

Hrachowitz, M., C. Soulsby, D. Tetzlaff, I. A. Malcolm, and G. Schoups., 2010. Gamma distribution models for transit time estimation in catchments: Physical interpretation of parameters and implications for time-variant transit time assessment, Water Resources Research, 46, W10536, https://doi.org/10.1029/2010WR009148.

Hrachowitz, M., Savenije, H., Bogaard, T. A., Tetzlaff, D., and Soulsby, C., 2013. What can flux tracking teach us about water age distribution patterns and their temporal dynamics?, Hydrology and Earth System Sciences, 17, 533-564, https://doi.org/10.5194/hess-17-533-2013.

Hrachowitz, M., Soulsby, C., Tetzlaff, D., Dawson, J. J. C., and Malcolm, I. A., 2009. Regionalization of transit time estimates in montane catchments by integrating landscape controls, Water Resources Research, 45, https://doi.org/10.1029/2008WR007496.

Chapter 3

Hughes, C. E. and Crawford, J., 2012. A new precipitation weighted method for determining the meteoric water line for hydrological applications demonstrated using Australian and global GNIP data, Journal of Hydrology, 464, 344-351, https://doi.org/10.1016/j.jhydrol.2012.07.029.

Jung, Y. Y., Koh, D. C., Yoon, Y. Y., Kwon, H. I., Heo, J., Ha, K., and Yun, S. T., 2019. Using stable isotopes and tritium to delineate groundwater flow systems and their relationship to streams in the Geum River basin, Korea, Journal of Hydrology, 573, 267-280, https://doi.org/10.1016/j.jhydrol.2019.03.084.

Jurgens, B. C., Bohkle, J. K., and Eberts, S. M., 2012. TracerLPM (Version 1): An Excel® workbook for interpreting groundwater age distributions from environmental tracer data, United States Geological Survey, Techniques and Methods Report 4- F3, United States Geological Survey, Reston, USA, 60 pp., https://doi.org/10.3133/tm4F3.

Kirchner, J. W., Feng, X., and Neal, C., 2000. Fractal stream chemistry and its implications for contaminant transport in catchments. Nature, 403, 524-527, https://doi.org/10.1038/35000537.

Kirchner, J. W., Feng, X., Neal, C., and Robson, A. J., 2004. The fine structure of water-quality dynamics: the (high-frequency) wave of the future, Hydrological Processes, 18, 1353-1359, https://doi.org/10.1002/hyp.5537.

Kirchner, J. W., 2003. A double paradox in catchment hydrology and geochemistry, Hydrological processes, 17, 871-874, https://doi.org/10.1002/hyp.5108.

Kirchner, J. W., 2016a. Aggregation in environmental systems–Part 1: Seasonal tracer cycles quantify young water fractions, but not mean transit times, in spatially heterogeneous catchments, Hydrology and Earth System Sciences, 20, 279-297, https://doi.org/10.5194/hess-20-279-2016.

Chapter 3

Kirchner, J. W., 2016b. Aggregation in environmental systems–Part 2: Catchment mean transit times and young water fractions under hydrologic nonstationarity, Hydrology and Earth System Sciences, 20, 299-328, https://doi.org/10.5194/hess-20-299-2016.

Kirchner, J. W., 2019. Quantifying new water fractions and transit time distributions using ensemble hydrograph separation: theory and benchmark tests, Hydrology and Earth System Sciences, 23, 303-349, https://doi.org/10.5194/hess-23-303-2019.

Knapp, J. L., Neal, C., Schlumpf, A., Neal, M., and Kirchner, J. W., 2019. New water fractions and transit time distributions at Plynlimon, Wales, estimated from stable water isotopes in precipitation and streamflow, Hydrology and Earth System Sciences, 23, 4367-4388, https://doi.org/10.5194/hess-23-4367-2019.

Lamontagne, S., Kirby, J., and Johnston, C., 2021. Groundwater–surface water connectivity in a chain-of-ponds semiarid river, Hydrological Processes, 35, e14129, https://doi.org/10.1002/hyp.14129.

Lamontagne, S., Taylor, A.R., Cook, P.G., Crosbie, R.S., Brownbill, R., Williams, R.M., and Brunner, P., 2014. Field assessment of surface water–groundwater connectivity in a semi-arid river basin (Murray–Darling, Australia). Hydrological Processes, 28, 1561-1572. https://doi.org/10.1002/hyp.9691.

Małoszewski, P. and Zuber, A., 1982. Determining the turnover time of groundwater systems with the aid of environmental tracers: 1. Models and their applicability, Journal of Hydrology, 57, 207-231, https://doi.org/10.1016/0022-1694(82)90147-0.

Maloszewski, P., 2000. Lumped-parameter models as a tool for determining the hydrological parameters of some groundwater systems based on isotope data, in: Tracer and Modelling in

Hydrogeology – Proceetings of the TraM'2000 Conference, IAHS Publ. no. 262, Liege, Belgium, 271-276.

McCallum, J. L., Cook, P. G., and Simmons, C. T., 2015. Limitations of the use of environmental tracers to infer groundwater age, Groundwater., 53, 56-70, https://doi.org/10.1111/gwat.12237.

McCormac, F. G., Hogg, A. G., Blackwell, P. G., Buck, C. E., Higham, T. F., and Reimer, P. J., 2004. SHCal04 Southern Hemisphere calibration, 0-11.0 cal kyr BP, Radiocarbon, 46, 1087-1092, https://doi.org/10.1017/S0033822200033014.

McDonnell, J. J., McGuire, K., Aggarwal, P., Beven, K. J., Biondi, D., Destouni, G., and Wrede, S., 2010. How old is streamwater? Open questions in catchment transit time conceptualization, modeling and analysis, Hydrological Processes, 24, 1745-1754, https://doi.org/10.1002/hyp.7796.

McGuire, K. J. and McDonnell, J. J., 2006. A review and evaluation of catchment transit time modelling, Journal of Hydrology, 330, 543-563, https://doi.org/10.1016/j.jhydrol.2006.04.020.

Meredith, K.T., Han, L.F., Hollins, S.E., Cendón, D.I., Jacobsen, G.E., and Baker, A., 2016. Evolution of chemical and isotopic composition of inorganic carbon in a complex semi-arid zone environment: consequences for groundwater dating using radiocarbon. Geochimica et Cosmochimica Acta, 352-367, https://doi.org/10.1016/j.gca. 2016.06.011.

Messager, M. L., Lehner, B., Cockburn, C., Lamouroux, N., Pella, H., Snelder, T., and Datry, T., 2021. Global prevalence of non-perennial rivers and streams, Nature, 594, 391-397, https://doi.org/10.1038/s41586-021-03565-5.

Morgenstern, U. and Taylor, C.B., 2009. Ultra low-level tritium measurement using electrolytic enrichment and LSC. Isotopes in Environmental and Health Studies, 45, 96-117. https://doi.org/10.1080/10256010902931194.

Chapter 3

Morgenstern, U., Daughney, C. J., Leonard, G., Gordon, D., Donath, F. M., and Reeves, R., 2015. Using groundwater age and hydrochemistry to understand sources and dynamics of nutrient contamination through the catchment into Lake Rotorua, New Zealand, Hydrology and Earth System Sciences, 19, 803-822, https://doi.org/10.5194/hess-19-803-2015.

Morgenstern, U., Stewart, M.K., and Stenger, R., 2010. Dating of stream water using tritium in a post nuclear bomb pulse world: continuous variation of mean transit time with streamflow, Hydrology and Earth System Sciences, 14, 2289-2301, https://doi.org/10.5194/hess-14-2289-2010.

Peters, N. E., Burns, D. A., and Aulenbach, B. T., 2014. Evaluation of high-frequency mean streamwater transit-time estimates using groundwater age and dissolved silica concentrations in a small forested watershed, Aquatic Geochemistry, 20, 183-202, https://doi.org/10.1007/s10498-013-9207-6.

Radke, L. C. and Howard, K. W. F., 2007. Influence of groundwater on the evaporative evolution of saline lakes in the Wimmera of south-eastern Australia, Hydrobiologia, 591, 185-205, https://doi.org/10.1007/s10750-007-0797-0.

Reimer, P. J., Bard, E., Bayliss, A., Beck, J. W., Blackwell, P. G., Ramsey, C. B., and Van Der Plicht, J., 2013. IntCal13 and Marine13 radiocarbon age calibration curves 0-50,000 years cal BP. radiocarbon, 55, 1869-1887, https://doi.org/10.2458/azu_js_rc.55.16947.

Rice, K. C. and Hornberger, G. M., 1998. Comparison of hydrochemical tracers to estimate source contributions to peak flow in a small, forested, headwater catchment, Water Resources. Research, 34, 1755-1766, https://doi.org/10.1029/98WR00917.

Rinaldo, A., Benettin, P., Harman, C. J., Hrachowitz, M., McGuire, K. J., Van Der Velde, Y., and Botter, G., 2015. Storage selection functions: A coherent framework for quantifying how catchments store and release water and solutes, Water Resources Research, 51, 4840-4847, https://doi.org/10.1002/2015WR017273.

Robinson, N., Rees, D., Reynard, K., Imhof, M., Boyle, G., Martin, J., and Giles, S., 2006. A land resource assessment of the Wimmera region. Victoria Department of Jobs, Precincts and Regions. http://vro.agriculture.vic.gov.au/.

Rozanski, K., Araguás-Araguás, L., and Gonfiantini, R., 1993. Isotopic Patterns in Modern Global Precipitation, in: Climate Change in Continental Isotopic Records, edited by: Swart, P. K., Lohmann, K. C., Mckenzie, J., and Savin, S., 1–36, American Geophysical Union, Washington, D.C., USA.

Segura, C., Noone, D., Warren, D., Jones, J.A., Tenny, J., and Ganio, L.M., 2019. Climate, landforms, and geology affect baseflow sources in a mountain catchment, Water Resources. Research, 55, 5238-5254, https://doi.org/10.1029/2018WR023551.

Shanafield, M., Bourke, S.A., Zimmer, M.A., and Costigan, K.H., 2021. An overview of the hydrology of non-perennial rivers and streams. Wiley Interdisciplinary Reviews: Water, 8, e1504, https://doi.org/10.1002/wat2.1504.

Shanafield, M.,Godsey, S.,Datry, T.,Hale, R.,Zipper, S. C.,Costigan, K.,Krabbenhoft, C. A.,Dodds, W. K.,Zimmer, M.,Allen, D. C.,Bogan, M.,Kaiser, K. E.,Burrows, R. M.,Hammond, J. C.,Busch, M.,Kampf, S.,Mims, M. C.,Burgin, A., and Olden, J. D., 2020. Science gets up to speed on dry rivers, Eos, 101, https://doi.org/10.1029/2020EO139902.

Sophocleous, M., 2002. Interactions between groundwater and surface water: the state of the science, Hydrogeological Journal, 10, 52-67, http://dx.doi.org/10.1007/s10040-014-1215-0.

Soulsby, C., Malcolm, R., Helliwell, R., Ferrier, R. C., and Jenkins, A., 2000. Isotope hydrology of the Allt a'Mharcaidh catchment, Cairngorms, Scotland: implications for hydrological pathways and residence times, Hydrological Processes, 14, 747-762, https://doi.org/10.1002/(SICI)1099-1085(200003)14:4<747::AID-HYP970>3.0.CO;2-0.

Soulsby, C., Tetzlaff, D., Rodgers, P., Dunn, S., and Waldron, S., 2006. Runoff processes, stream water residence times and controlling landscape characteristics in a mesoscale catchment: An initial evaluation, Journal of Hydrology, 325, 197-221, https://doi.org/10.1016/j.jhydrol.2005.10.024.

Stewart, M. K. and Morgenstern, U., 2016. Importance of tritium-based transit times in hydrological systems, Wiley Interdisciplinary Reviews: Water, 3, 145-154, https://doi.org/10.1002/wat2.1134.

Stewart, M. K., Morgenstern, U., and McDonnell, J. J., 2010. Truncation of stream residence time: how the use of stable isotopes has skewed our concept of streamwater age and origin, Hydrological Processes, 24, 1646-1659, https://doi.org/10.1002/hyp.7576.

Stewart, M. K., Morgenstern, U., Gusyev, M. A., and Małoszewski, P., 2017. Aggregation effects on tritium-based mean transit times and young water fractions in spatially heterogeneous catchments and groundwater systems, Hydrology and Earth System Sciences, 21, 4615-4627, https://doi.org/10.5194/hess-21-4615-2017.

Stewart, M. K., Thomas, J. T., Norris, M., and Trompetter, V., 2004. Paleogroundwater in the Moutere gravel aquifers near Nelson, New Zealand. Radiocarbon, 46, 517-529, https://doi.org/10.1017/S0033822200035578.

Suckow, A., 2014. The age of groundwater–Definitions, models and why we do not need this term, Applied Geochemistry, 50, 222-230, https://doi.org/10.1016/j.apgeochem.2014.04.016.

Chapter 3

Tadros, C.V., Hughes, C.E., Crawford, J., Hollins, S.E., and Chisari, R., 2014. Tritium in Australian precipitation: A 50-year record, Journal of Hydrology, 513, 262-273, https://doi.org/10.1016/j.jhydrol.2014.03.031.

Tsujimura, M., Abe, Y., Tanaka, T., Shimada, J., Higuchi, S., Yamanaka, T., Oyunbaatar, D., 2007. Stable isotopic and geochemical characteristics of groundwater in Kherlen River basin, a semi-arid region in eastern Mongolia, Journal of Hydrology, 333, 47-57, https://doi.org/10.1016/j.jhydrol.2006.07.026.

Unland, N. P., Cartwright, I., Daly, E., Gilfedder, B. S., Atkinson, A. P., 2015. Dynamic river-groundwater exchange in the presence of a saline, semi-confined aquifer, Hydrological Processes, 29, 4817-4829, https://doi.org/10.1002/hyp.10525.

Van Dijk, A.I., Beck, H.E., Crosbie, R.S., de Jeu, R.A., Liu, Y.Y., Podger, G.M., and Viney, N.R., 2013. The Millennium Drought in southeast Australia (2001–2009): Natural and human causes and implications for water resources, ecosystems, economy, and society, Water Resources Research, 49, 1040-1057, https://doi.org/10.1002/wrcr.20123.

Weissmann, G. S., Zhang, Y., LaBolle, E. M., and Fogg, G. E., 2002. Dispersion of groundwater age in an alluvial aquifer system, Water Resources Research, 38, 16-1, https://doi.org/10.1029/2001WR000907.

Western, A.W., O'Neill, I.C., Hughes, R.L., Nolan, J.B., 1996. The behavior of stratified pools in the Wimmera River, Australia. Water Resources Research, 32, 3197-3206. https://doi.org/10.1029/96WR01336.

Wimmera Waterway Strategy 2014-2022: Government of Victoria Wimmera Catchment Management Authority, available at: http://wcma.vic.gov.au, 2013.

Chapter 3

Zhou, Z. and Cartwright, I., 2021. Using geochemistry to identify and quantify the sources, distribution, and fluxes of baseflow to an intermittent river impacted by climate change: The upper Wimmera River, southeast Australia, Science of the Total Environment, 149725, https://doi.org/10.1016/j.scitotenv.2021.149725.

Zimmer, M. A. and McGlynn, B. L., 2017. Ephemeral and intermittent runoff generation processes in a low relief, highly weathered catchment, Water Resources Research, 53, 7055-7077, https://doi.org/10.1002/2016WR019742.

Zuber, A. and Maloszewski, P., 2001. Lumped parameter models, in: chap. 2, vol 6: Modelling in Environmental Isotopes in the Hydrological Cycle: Principles and Applications, Technical Documents in Hydrology, edited by: Mook, W. G. and Yurtsever, Y., UNESCO, Paris, France, 39, 5-35.

Zuber, A., Weise, S. M., Motyka, J., Osenbrück, K., and Różański, K., 2004. Age and flow pattern of groundwater in a Jurassic limestone aquifer and related Tertiary sands derived from combined isotope, noble gas and chemical data, Journal of Hydrology, 286, 87-112, https://doi.org/10.1016/j.jhydrol.2003.09.004.

Chapter 3

Tables

Table 3.1. ^3H activities and calculated mean transit times (MTTs) from pool water and stream water of upper Wimmera River

Site number[1]	Sample ID	Streamflow	^3H	MTTs (years)				
		m^3 day^{-1}	TU	DM (0.05)	DM (0.5)	EPM (0.33)	EPM (1.0)	EMM
	March 2019							
1	Elmhurst	0	1.65	nc[2]	nc	nc	nc	nc
4	Ever 1	0	0.88	nc	nc	nc	nc	nc
5	CE1	0	1.00	nc	nc	nc	nc	nc
6	CE2	0	2.28	nc	nc	nc	nc	nc
7	Joel 1	0	2.76	nc	nc	nc	nc	nc
8	Joel 2	0	0.64	nc	nc	nc	nc	nc
16	Campbell	0	3.02	nc	nc	nc	nc	nc
18	Glenorchy	0	3.29	nc	nc	nc	nc	nc
	July 2019							
1	Elmhurst	10500	2.69	2.8	3.1	3.0	2.9	3.1
5	CE1	14919	1.85	10.9	14.9	13.0	11.3	16.8
8	Joel 2	28949	2.76	2.4	2.5	2.4	2.4	2.5
16	Campbell	91617	3.00	0.1	0.1	0.1	0.1	0.1
18	Glenorchy	135000	2.41	4.8	5.7	5.3	5.0	5.8
	September 2019							
1	Elmhurst	9500	2.67	3.0	3.3	3.1	3.0	3.3
5	CE1	10898	2.58	3.6	4.0	3.8	3.6	4.0
8	Joel 2	15698	2.48	4.3	5.0	4.6	4.4	5.1
16	Campbell	27077	2.78	2.2	2.4	2.3	2.2	2.4
18	Glenorchy	31110	2.88	1.6	1.7	1.6	1.6	1.7
	November 2019							
1	Elmhurst	220	2.55	3.8	4.3	4.0	3.9	4.3
5	CE1	250	2.34	5.4	6.5	6.0	5.6	6.7
8	Joel 2	215	2.26	6.0	7.6	6.9	6.3	7.8
16	Campbell	343	2.58	3.6	4.0	3.8	3.6	4.0
18	Glenorchy	620	2.69	2.8	3.1	2.9	2.8	3.1

1. Sites on Fig. 1.
2. nc = not calculated

Table 3. 2. ^{3}H, ^{14}C activities, and calculated MTTs by EPM (ratio=0.33) of groundwater from the upper Wimmera River

Site letter[1]	**Bore ID**	**Depth**	^{3}**H**	^{14}**C**	**MTTs-**^{3}**H**	**MTTs-**^{14}**C**	**MTTs-**^{14}**C**[2]
		m	TU	pMC	years	years	years
C	5242	23	0.16	92.3	197	nc[3]	nc
	5243	18	0.25	92.0	176	nc	nc
F	5227	28	0.04	82.8	nc	1591	691
	5228	14	0.06	84.2	nc	1436	551
H	5229	37	0.03	66.8	nc	3826	2671
	5230	14	0.25	89.5	176	nc	nc
I	5232	32	0.02	73.8	nc	2726	1681
J	5234	43	0.02	57.1	nc	5691	4421
	5235	30	bd[4]	78.4	nc	2111	1141
	5236	12	0.45	102.9	121	nc	nc
L	5379	7	bd	88.4	nc	1016	221
	2542	17	0.02	80.5	nc	1851	921

1. Sites on Fig. 1
2. MTTs estimated by ^{14}C activities with 10% calcite dissolutions
3. nc= not calculated

Chapter 4

Chapter 4 Integrating major ion geochemistry, stable isotopes (^{18}O, ^{2}H) and radioactive isotopes (^{222}Rn, ^{14}C, ^{36}Cl, ^{3}H) to understand the interaction between catchment waters and an intermittent headwater stream: the upper Avoca River, southeast Australia

Chapter 4

Abstract

Determining the locations and sources of baseflow and the transit times of water that sustains river flow at different hydrologic conditions are important for water management and understanding catchment behaviour and functioning. Major ion geochemistry, stable isotopes (^{18}O and ^{2}H), and radioisotopes (^{222}Rn, ^{3}H, ^{14}C, and ^{36}Cl) were used to investigate the sources and transit times of water in the upper catchment of the intermittent Avoca River from the Murry-Darling Basin in southeast Australia. The along stream variations in ^{222}Rn activities and Cl concentrations imply that the headwaters of the Avoca River receive significant baseflow inflows. The distribution of baseflow inputs was mainly controlled by local topography with higher baseflow in areas of steep topography and higher hydraulic gradients in the upper reaches. Cl concentrations fluctuate along the river, implying that low salinity near-river water was an important component of baseflow. During the summer months, the Avoca River ceased to flow and comprised laterally-disconnected water pools. The ^{3}H activities of pool waters were 1.64 to 5.11 TU. The higher of these values exceed those of average annual rainfall (2.8-3.2 TU), probably due to the input of later winter to spring rainfall. The stream water when the river is flowing had ^{3}H activities ranging from 2.21 to 2.40 TU in July and 2.39 to 2.77 TU in August, which yield mean transit times of 4.0 to 7.0 years and 1.4 to 4.8 years respectively. These ^{3}H activities were significantly higher than those of regional groundwater (^{3}H activities < 0.1TU) implying that the Avoca River is largely sustained by young near-river sources of water at all flow conditions. Regional groundwater had ^{14}C activities of 34 to 98 pMC, which yield mean residence times of up to 12,900 years. $R^{36}Cl$ values of regional groundwater ($50.9\text{-}61.9 \times 10^{-15}$) were higher than those of modern rainfall, probably reflecting the $R^{36}Cl$ values of recharge. Similar $R^{36}Cl$ values of the pool and stream water ($33.3\text{-}58.7 \times 10^{-15}$) imply that some Cl is derived from the influx of regional groundwater. As with other

intermittent streams in southeast Australia, because the upper Avoca River was mainly sustained by younger relatively small water stores, it will be vulnerable to short-term changes in climate and land use.

Chapter 4

4.1 Introduction

A holistic understanding interaction between rivers and waters stored within their catchments is essential for understanding regional hydrogeology, determining catchment water balance, predicting the hydrological response to changes in climate and land use, and effective water resources management (Sophocleous, 2002; Fleckenstein et al., 2010; Cook et al., 2018; Lewandowski et al., 2020, Barua et al., 2022; Messager et al., 2021; Fowler et al., 2022). There are a number of water sources that potentially contribute to rivers at different flow conditions (e.g., McCallum et al, 2010; Peters et al., 2014; Rhodes et al., 2017; Cartwright and Irvine, 2020; Zhou et al., 2022). Deep regional groundwater represents the oldest and largest water store in most catchments. Younger and smaller water stores include water from riparian zone, soil water, bank storage and return flows, and interflow. Collectively, these waters contribute baseflow to rivers and are important in sustaining streamflow, especially between high flow events generated by rainfall. The sources of water determine how rivers respond to short and long-term changes to climate and land use (e.g., Duvert et al., 2016; Cook et al., 2018; Richardson et al., 2020). For example, if the river is connected to a large reservoir of long-lived groundwater, it is likely to be resilient to yearly to decadal variations in rainfall whereas streamflow in rivers sustained dominantly by smaller short-lived stores is likely to be more variable (Brunner et al., 2011; Fuchs et al., 2019).

Because the different sources of water may have different geochemistry, geochemical techniques have been successfully used to locate and quantify the inputs of baseflow into streams (McCallum et al., 2012; Zhang et al., 2013; Miller et al., 2015; Cartwright, 2022). Due to evapotranspiration, mineral dissolution, and the breakdown of organic matter, the salinity of baseflow is generally higher than that of surface runoff (Herczeg et al., 2001; Edmunds, 2009) and thus, baseflow inputs are commonly marked by increases in stream salinity. ^{222}Rn is an intermediate isotope in the 238U to 206Pb decay series. Because of the high concentration of U in minerals compared with those in surface water, groundwater ^{222}Rn activities are commonly 2 to 3 orders of magnitude higher than those in surface water, making ^{222}Rn a useful tracer to locate and quantify baseflow inputs (Cecil and Green, 2000; Burnett and Dulaiova, 2006; Burnett et al., 2010). ^{222}Rn decays with a half-life of 3.8 days and degasses to the atmosphere, hence high ^{222}Rn activities occur only around zones of baseflow input (Genereux and Hemond, 1992; Cook, 2013).

Geochemistry may also be used to discern origins of water in the streams. For example, soil water may have high nitrate or organic carbon as a result of organic matter breakdown (Stelzer et al., 2014). Due to seasonal recharge, evaporation, and long-term changes of stable isotope ratios of rainfall (Hughes and Crawford, 2012), the different water sources may have different stable isotope ratios. Differences between downstream trends in stream water salinity and ^{222}Rn activities may also be able to distinguish between the inputs of water near-river sources (which is likely to have high ^{222}Rn activities but low salinities) and regional groundwater (high ^{222}Rn activities and higher salinities) (Yu et al., 2013; Ortega et al., 2015; Zhou and Cartwright, 2021).

Because the different water stores in a catchment have different residence times, radioactive isotopes such as ^{3}H or other residence time indicators (e.g., the chlorofluorocarbons) are useful to understand the contributions of different potential water sources to streamflow at different locations or times. In the southern hemisphere, ^{3}H activities of rainfall during the 1950s and 1960s (the “bomb-pulse”) were far lower than in the northern hemisphere and have now decayed to values lower than those of modern rainfall (Morgenstern et al., 2010; Tadros et al., 2014). This results in transit or residence times being more readily estimated from ^{3}H activities and older water invariably having lower ^3H activities than younger water, which is invaluable in determining relative residence times.

^{36}Cl, which has a half-life of 301,000 years, has traditionally been used to estimate the residence time of very old groundwater (up to 1 Ma: e.g., Phillips, 2000; Labotka et al., 2015). However, as with all the cosmogenic radioisotopes, elevated $R^{36}Cl$ values were recorded during the bomb-pulse period (Bentley et al., 1982; Phillips, 2000). In addition, the $R^{36}Cl$ value of precipitation and dry deposition varies with climate; in particular $R^{36}Cl$ values of rainfall increase with distance from the ocean (Keywood et al., 1998), which has varied as sea levels have changed during the Holocene. From 110 ka, sea levels around Australia declined irregularly to a maximum of ~120 m below present day mean sea level and then rose to reach present day sea level between 7 and 3 ka (Chappell, 2009; Lewis et al., 2013). During that period, the upper Avoca region would have been further from the coast than at present. The temporal changes in the $R^{36}Cl$ values of precipitation account for $R^{36}Cl$ values of groundwater in southeast Australia with ^{14}C residence times of up to 20 ka being higher than those of modern precipitation (Howcroft et al., 2019). Because of the long half-life, the $R^{36}Cl$ values of water recharged over the last few ka will be little changed and different water sources in the catchment may have a range of $R^{36}Cl$ values. This makes ^{36}Cl a potentially useful tracer of the water stores that sustain streamflow, however, it has rarely been employed in this way. Where groundwater has significantly higher Cl concentrations than surface water, ^{36}Cl may be able to detect small fluxes of groundwater that may not be apparent from other tracers.

While intermittent rivers account for more than 50% of global rivers, their hydrology is less well understood than perennial streams (Datry et al., 2014; Gutiérrez-Jurado et al., 2019; Shanafield et al., 2021; Barua et al., 2022; Zhou et al., 2022). Perennial streams that have continuous flow throughout the year may be connected to regional groundwater, which provides a substantial reservoir of water to sustain streamflow, especially during low flow periods (Tetzlaff and Soulsby, 2008; Cartwright et al., 2014, 2018; Duvert et al., 2016). However, the connection between stream water and regional groundwater in intermittent streams is likely to be limited especially during the cease-to-flow periods in dry seasons when the water table may have dropped to below the streambed along many reaches (e.g., Rhodes et al., 2017; Zhou and Cartwright, 2021). Most of the water in intermittent streams may come from near-river stores. While these stores could provide a buffer zone between the rivers and contaminated regional groundwater and lessen the impacts of groundwater pumping, the small volume of those stores implies that intermittent rivers are vulnerable to short-term climate and land use changes.

This study integrates major ion geochemistry, stable isotopes (^{18}O, ^{2}H), and radioactive isotopes (^{222}Rn, ^{14}C, ^{3}H, and ^{36}Cl) to understand the different water sources in the intermittent upper Avoca River in southeast Australia. In particular, it explores the use of ^{36}Cl in distinguishing the sources of solutes and water in rivers. The results from this study will improve our understanding of the functioning of intermittent streams and are vital to their protection and management.

4.2 Study area

The Avoca River is located in northwest Victoria and is an intermittent river in the Murray-Darling Basin with a catchment area of approximately 14,000 km^2. The river originates from the Great Dividing Ranges near Amphitheatre (Fig. 4.1), flows north for 280 km and terminates in Lake Bael Bael and the Avoca Marshes near the Murray River (Lorimer and Rowan, 1982; Smith, 1995). The river occupies a confined valley from its headwaters to Charlton (Fig.4.1) with a wider floodplain downstream that has many wetland areas. The study area is located in the upper catchment of the Avoca River between the headwaters and Charlton (Fig.4.1). The upper catchment is dominantly covered by dryland pasture with larger stands of native woodlands along the floodplain and native plantation forests in the headwaters (North Central Catchment Management Authority, 2007; Department of Environment, Land, Water and Planning, 2022). The geology of the upper Avoca catchment includes a basement of Palaeozoic metamorphosed turbidites (the Castlemaine Group and St Arnaud Group) and Devonian Granites. These are overlain by small basaltic lava plains of the Newer Volcanic Group and fluviatile sediments that have rounded gravels, coarse sands, silts and clays (Lorimer and Rowan, 1982).

The average annual rainfall in the upper Avoca catchment decreases northwards from 536 mm at Amphitheatre to 420 mm at Charlton (Bureau of Meteorology, 2022). Winter (June to August) is the wettest season while the summer months have the lowest rainfall (Bureau of Meteorology, 2022). Streamflow is higher in the winter and spring and the Avoca River ceases to flow during the summer months, forming a series of persistent pools. The average annual streamflow between 2000 and 2020 ranged from 1.1×10^5 to 1.2×10^8 m^3/year at Amphitheatre and 1.3×10^5 to 2.3×10^8 m^3/year at Coonooer (Department of Environment, Land, Water and Planning, 2022).

Most tributaries along the river are ephemeral and dry except immediately after major rainfall. Amphitheatre and Fentons Creeks are the largest of the tributaries in the upper Avoca catchment (Fig. 4.1). These flow for longer periods of the year, although their discharge is much lower than the main river (Department of Environment, Land, Water and Planning, 2022). Groundwater is recharged on the higher ground at the catchment margins and flows from south to north (North Central Catchment Management Authority, 2007). The total dissolved solids (TDS) of the groundwater varies from <560 mg/L in some of the basalts to 3360 mg/L in some of lower areas (Heislers, 1993; Department of Environment, Land, Water and Planning, 2022). Surface water and groundwater in the upper Avoca catchment are locally used for domestic and irrigation purposes (North Central Catchment Management Authority, 2007).

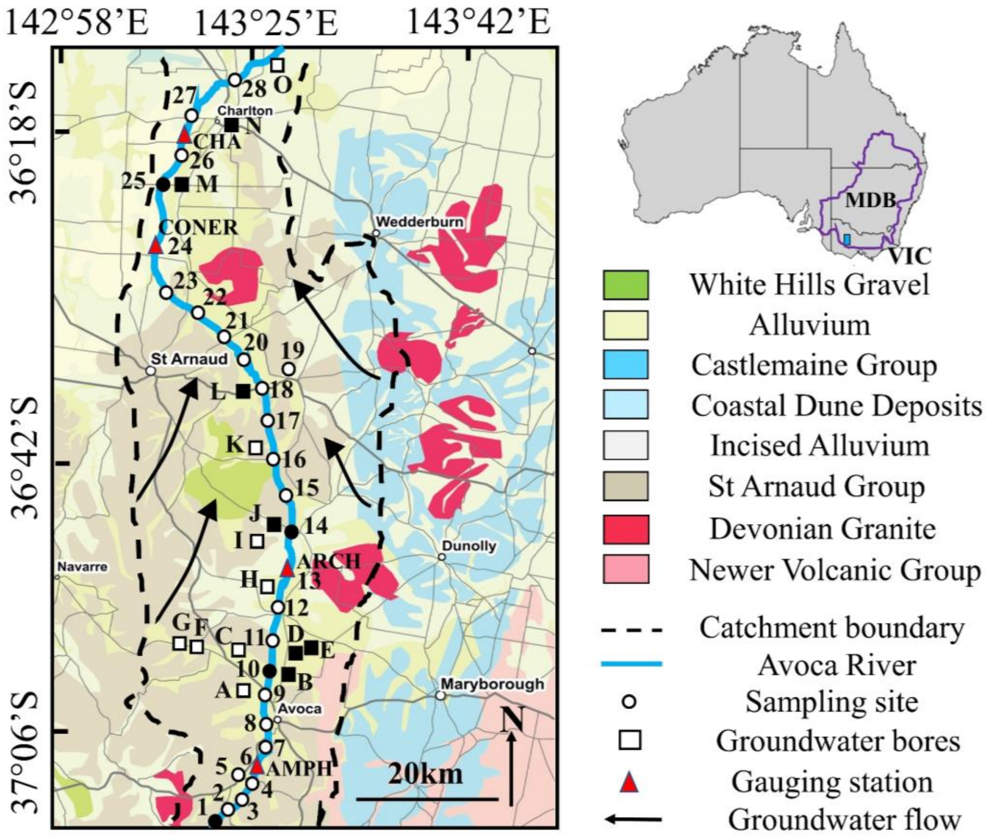

Figure 4.1. Summary geological and hydrogeological map of the upper Avoca River. Stream water sampling sites and groundwater bores are indicated by numbers and letters, respectively. The inset shows the location in Victoria (VIC) and the Murry-Darling Basin (MDB). The sites that have ^{14}C, ^{3}H, and/or ^{36}Cl data are shown in solid symbols. Gauging stations with site numbers are Amphitheatre (AMPH; 408202), Archdale Junction (ARCH; 408206), and Coonooer (CONER; 408200). Background geological map from Department of Jobs, Precincts and Regions (2022).

4.3 Materials and methods

4.3.1 Sampling

Twenty-six samples of pool water were collected from laterally disconnected pools (Fig. 4.1) in March 2019 when the upper Avoca River had ceased to flow during the summer months (Fig. 4.2). Two rounds of stream water sampling (28 samples each round) were conducted between July and

August 2019 when the upper Avoca River was flowing (Fig. 4.1, Table S3). Samples were also collected from Amphitheatre Creek and Fentons Creek (Fig. 4.1) at their confluences with the main river; in March 2019 these tributaries also consisted of laterally-disconnected pools. An open sample collector was used for river water sampling from the centre of the river. Continuous streamflow and electrical conductivity are measured at Amphitheatre and Coonooer (Figs 4.1, 4.2; Department of Environment, Land, Water and Planning, 2022). Continuous streamflow is also measured at Archdale Junction and river depth (but not streamflow) is measured at Charlton (Fig 4.1; Department of Environment, Land, Water and Planning, 2022). Groundwater was sampled in May 2019 from groundwater monitoring bores, which are installed on the river bank and floodplain (Fig. 4.1). During the sampling campaign, several volumes of water were purged from the bore prior to sampling using an impellor pump or the bores were pumped dry and sampled following recovery.

4.3.2 Analytical techniques

A calibrated TPS meter and electrode were used to measure Electrical Conductivity (EC) values in the field. Cation and anion concentrations were determined at Monash University using a Thermo Fischer quadrupole ICP-OES and a Thermo Fischer ion chromatograph, respectively. Samples were filtered through 0.45μm cellulose nitrate filters and acidified to $pH<2$ for cation measurements and filtered and unacidified for anion measurements. Overall precision (σ) of major ion concentrations is 2-5% based on replicate analyses. Stable isotope analyses were performed at Monash University using a Thermo Finnigan Delta Plus Advantage mass spectrometer. $\delta^{18}O$ values were analysed via equilibration with He-CO_2 at 32°C for 24-48 hours in a Thermo Finnigan Gas Bench. δ^2H values were determined following reduction of H_2O by Cr at 850°C in a Finnigan MAT H/Device. Values of $\delta^{18}O$ and δ^2H were normalised as described by Coplen (1988) and are expressed relative to V-SMOW. Precision (σ) based on replicate analyses is 0.15‰ for $\delta^{18}O$ and 1‰ for $\delta^{2}H$.

^{222}Rn activities were measured in the field using portable radon-in-air detectors (Durridge Corporation RAD-7). ^{222}Rn was degassed from 500 ml of water for 5 min into a closed air loop of known volume and counting times were 2 hrs for surface water and 30 mins for groundwater. ^{222}Rn activities are reported as Bq/m^3 (becquerels per m^3) with a precision of ~3% at 10,000 Bq/m^3 and ~10% at 100 Bq/m^3.

^{3}H activities were analysed at the Institute of Geological and Nuclear Sciences (GNS) in New Zealand by liquid scintillation in Quantulus ultra-low-level counters following vacuum distillation and electrolytic enrichment (Morgenstern and Taylor, 2009). ^{3}H activities are reported in Tritium Units (TU) where 1 TU corresponds to ^{3}H / H = 10-18 with a 0.02 TU detection limit and relative uncertainties (1σ) ~ ±2%. ^{14}C activities of groundwater were determined by using accelerator mass spectrometer (AMS) at GNS in New Zealand. Orthophosphoric acid was used for CO_2 extraction from the groundwater and the extracted CO_2 was converted into a graphite target after being purified under vacuum. ^{14}C activities are expressed as percent modern carbon (pMC), where the ^{14}C activity of modern carbon is 95% of the ^{14}C activity of the NBS oxalic acid standard in 1950 (Stewart et al., 2004). ^{36}Cl analyses were conducted by using 14UD accelerator at the Australian National University as described by Fifield et al. (2013). ^{36}Cl activities are reported as $R^{36}Cl$ ($^{36}Cl/Cl \times 10^{-15}$). $R^{36}Cl$ uncertainties ranged from 5 to 6%. The complete geochemistry dataset is in the Supplement (Tables S3 and S4).

4.3.3 Mean residence and mean transit times

Mean transit times (MTTs), which represent the time taken for water to flow through the catchment from where it recharged to where it discharges into the stream, were calculated using lumped parameter model (LPMs) from the river ^3H activities. The convolution integral:

$$C_0(t) = \int_0^\infty C_i\,(t-\tau)g(t)e^{-\lambda\tau}d\tau \quad (1)$$

relates the input of ^3H (C_i) in rainfall overtime to the ^3H activity of stream water sampled at time t (C_0 (t)). In equation (1), t-τ is the time that the water was recharged, τ is the transit time, λ is the decay constant of ^3H (0.0563 yr $^{-1}$)., and the function g(t) describes the distribution of flow paths and transit times in the flow system. Annual weighted ^3H activities of rainfall in Melbourne (Tadros et al., 2014) were used as the ^3H input. Predicted present-day ^3H activities of annual rainfall in central Victoria are 2.8 to 3.2 TU (Tadros et al., 2014) and the measured ^3H activities in that region are within that range (Cartwright and Morgenstern, 2015, 2018; Howcroft et al., 2018; Barua et al., 2022).

The LMPs used are implemented in the TracerLPM Excel workbook (Jurgens et al., 2012). The Exponential Mixing Model (EMM) represents flow systems with simple exponential distributions of transit times. The Exponential Piston Flow Model (EPM) describes aquifers with both exponential and piston-flow sections. It is commonly used for unconfined aquifers that have vertical recharge through the unsaturated zone and exponential flow below the water table (Maloszewski, 2000; Morgenstern et al., 2010; Howcroft et al., 2019). The EPM ratio describes the relative ratio of piston and exponential flow; here EPM ratios of 0.33 (75% exponential flow) and 1 (50% exponential flow) were used. The dispersion model (DM) is based on the one-dimensional advection-dispersion transport equation and can be applied to a variety of aquifer configurations (Zuber and Maloszewski, 2001; McGuire and McDonnell, 2006; Jurgens et al., 2012). This model includes the dispersion parameter (D_P) which is the ratio of dispersion to advection. D_P values of 0.05 to 0.5 are suggested for kilometre-scale flow systems (Maloszewski, 2000; Zuber and Maloszewski, 2001) and were used here. The estimates of MTTs are based on single samples. While the much lower bomb-pulse ^{3}H activities preclude testing of the LPMs using time-series measurements that commenced over recent years (Cartwright and Morgenstern, 2015), this approach has reproduced stream water time-series ^{3}H activities elsewhere (Maloszewski and Zuber, 1982; Blavoux et al., 2013; Morgenstern et al., 2015).

The same lumped parameter models were used to calculate the mean residence times (MRTs) and the predicted ^{14}C vs. ^{3}H trends in groundwater. The ^{14}C activities of atmospheric CO_2 were used as the input function (McCormac et al., 2004; Reimer et al., 2013). These aquifers locally contain calcite cements and veins. These are likely to have variable δ^{13}C values (Cartwright et al., 2013; Clark, 2015; Meredith et al., 2016) and isotope mass balance is not viable to estimate closed-system calcite dissolution. However, the aquifers are siliceous and closed-system calcite dissolution is probably < 10% (Clark, 2015). In these calculations, values of q (the fraction of DIC derived from the recharging water) between 1 (all DIC derived from recharge) and 0.9 (10% contribution of ^{14}C-free DIC from the aquifer matrix) were used.

4.4 Results

4.4.1 Streamflow

The variations of streamflow and EC at the Amphitheatre and Coonooer (Fig. 4.1) in 2019 are shown in Fig. 4.2. Streamflow at Archdale Junction and water levels at Charlton (Fig. 4.1) show similar patterns. A short period of relatively high streamflow (up to 6980 m^3/day) was recorded at Coonooer in early 2019 following rainfall in late 2018. However, the upper Avoca River largely comprised laterally-disconnected water pools during the summer months from January to April.

The river started to flow from early May 2019 and streamflow reached a peak in June (up to 2.5×10^5 m^3/day at Amphitheatre and 5.6×10^5 m^3/day at Coonooer). Streamflow then gradually decreased from August and the river ceased to flow in later October. During the sampling periods in July and August, the daily streamflow values were 5900 m^3/day and 2806 m^3/day at Amphitheatre and 1.3×10^5 m^3/day and 3.6×10^4 m^3/day at Coonooer (Fig. 4.2).

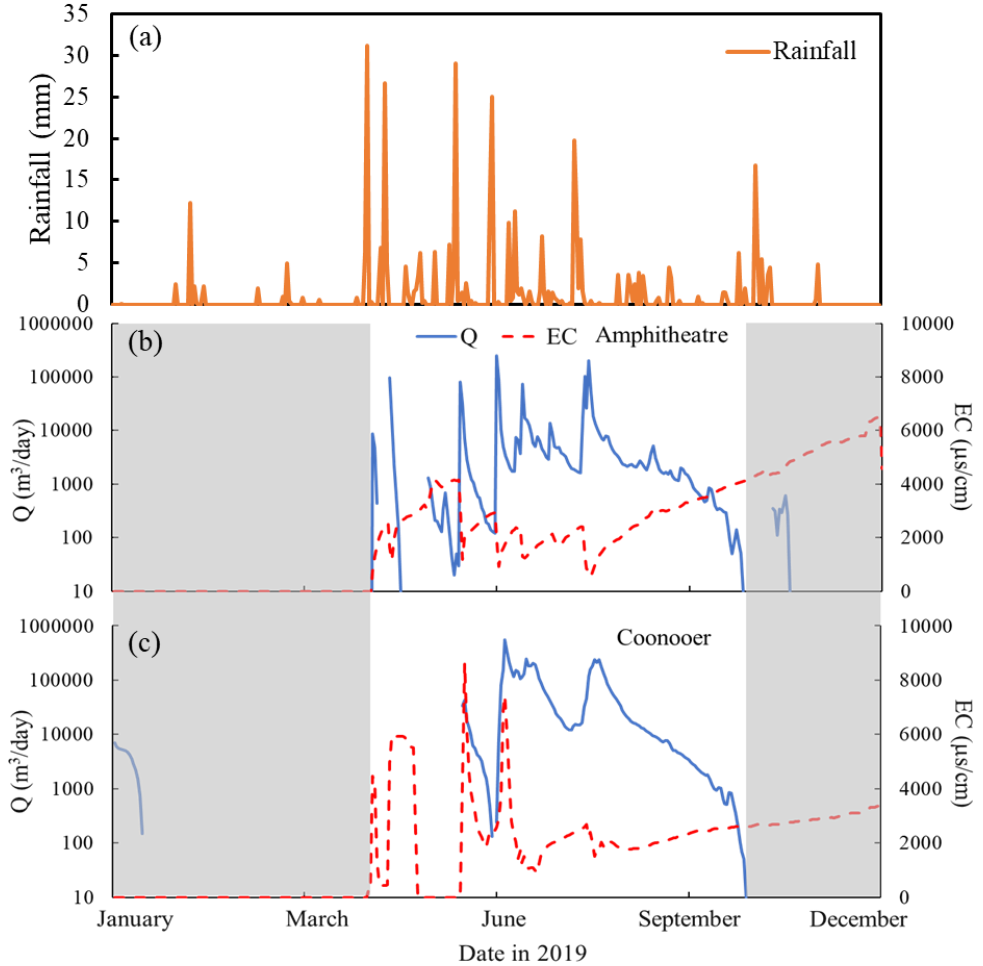

Figure 4.2. (a) Variations in rainfall in the upper Avoca River and EC and Q (streamflow) at Amphitheatre (b) and Coonooer (c) (Fig. 4.1) in the upper Avoca River in 2019 (missing data during the flow period are caused by equipment failure). Shaded areas indicate the cease-to-flow period. Data from Department of Environment, Land, Water and Planning (2022) and Bureau of Meteorology (2022).

4.4.2 Major ion geochemistry and radon (^{222}Rn)

EC values of stream water in 2019 in the headwaters at Amphitheatre were generally lower (1000-4000 μS/cm) than further downstream at Coonooer (up to 8629 μS/cm) (Fig. 4.2). EC values at both gauges were variable but were generally lower during the high winter flows (Fig. 4.2). Na and Cl are the most abundant cation (78-86% on a molar basis) and anion (85-98% on a molar basis), respectively, in the stream water (Table S3). During July and August when the upper Avoca River was flowing, Cl concentrations were between 230 and 1640 mg/L (Fig. 4.3b). Unlike many rivers where Cl concentrations increase downstream due to groundwater inflows (Yu et al., 2013; Ortega et al., 2015), there is no consistent downstream trend in Cl concentrations. ^{222}Rn activities (Fig. 4.3a) were up to 2920 Bq/m^3 in the headwaters and generally decreased downstream to <1000 Bq/m^3. Locally higher ^{222}Rn activities were recorded between 8 and 36 km (Fig. 4.3a).

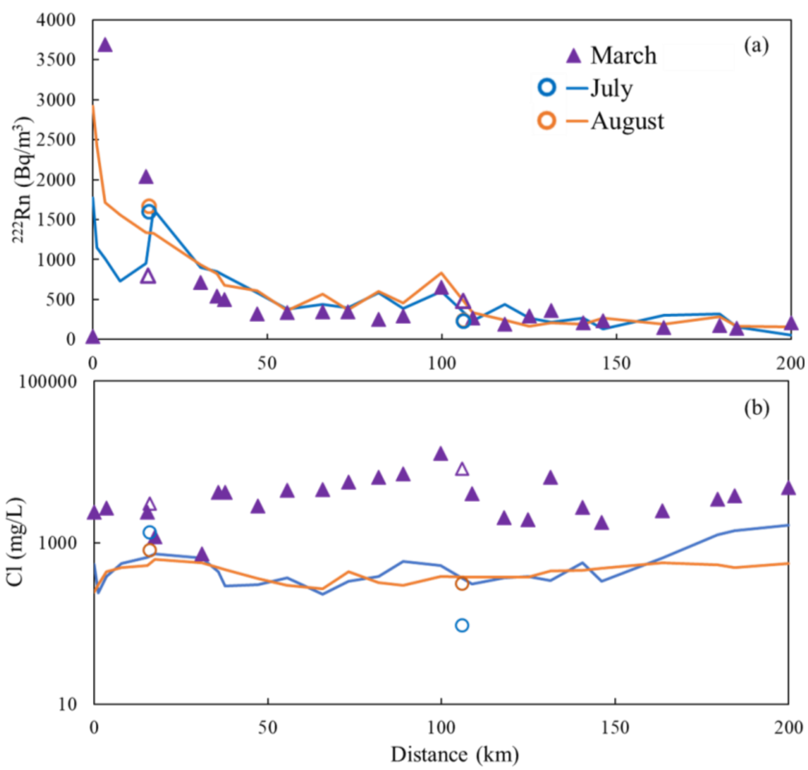

Figure 4.3. Downstream variations in ^{222}Rn (a) and Cl concentrations (b) during different flow conditions in the Avoca River. Solid symbols represent pool water samples and open symbols were tributaries samples.

The water from the laterally-disconnected pools in the summer months is much more saline than when the river was flowing, with EC values of 2220-14,070 μS/cm (Table S3). Cl concentrations during the cease-to-flow period were 726 to 12,7723 mg/L and were higher in the middle and lower reaches of the river (Fig. 4.3). The concentrations of the other major ions have similar spatial and temporal variations to Cl (Table S3). The major ion geochemistry and ^{222}Rn activities of the major tributaries (Amphitheatre Creek and Fentons Creek) are similar to the main river near their confluences (Table S3, Fig. 4.3).

Regional groundwater had EC values of 1643-12060 μS/cm (mean=5763 ± 1581 μS/cm). Na concentrations were 362 to 4578 mg/L (mean = 1883 ± 589 mg/L) and Cl concentrations were between 489 and 6832 mg/L (mean=2998 ± 953 mg/L). The concentrations of these and other major ions were correlated EC (Table S4). ^{222}Rn activities in the regional groundwater ranged from 2470 to 107,000 Bq/m^3 with a mean value of 29,912 ± 29,620 Bq/m^3 (and a 95% confidence interval (Cl) of 15230 Bq/m^3). There is no difference in the major ion geochemistry of groundwater from the different formations (Table 4.2, Fig. S3). The major ion ratios of the pool water and river water overlap. However, the groundwater has slightly higher relative Na concentrations (Fig. 4.4).

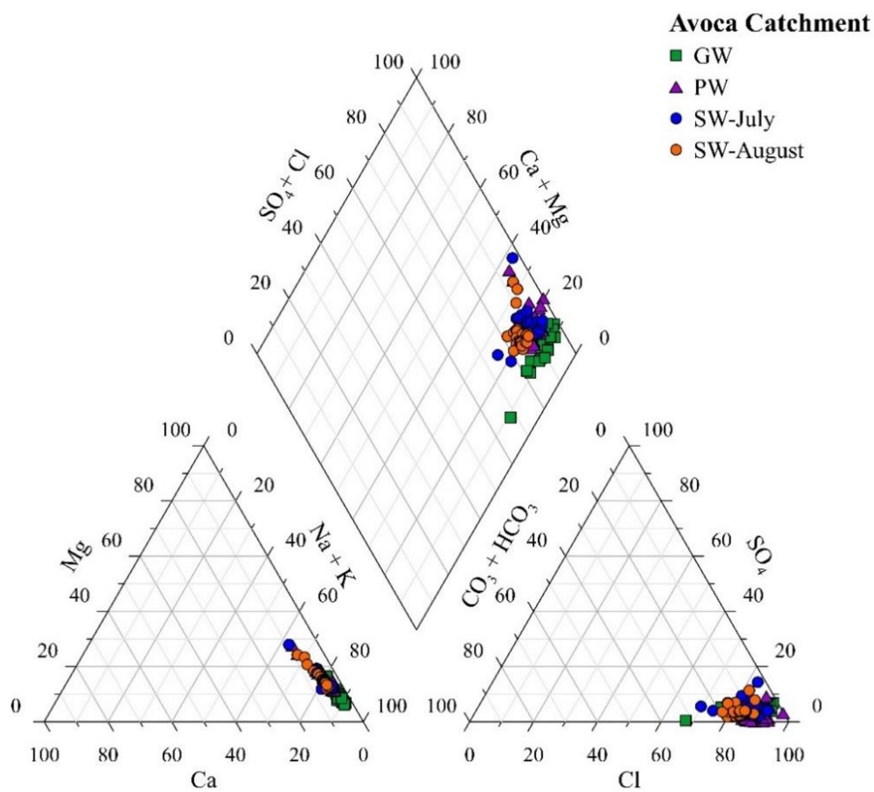

Figure 4.4. Trilinear diagram summarising molar major ion ratios of the different water sources in the Avoca River (data from Table S3 and S4). GW=groundwater; PW= pool water; SW=stream water.

4.4.3 Stable isotopes

Water from the laterally-disconnected pools had a wide range of δ^2H and $\delta^{18}O$ values that varied from -23 ‰ to +44 ‰ and -4.1 ‰ to +12.3 ‰, respectively (Tables S3 and S4, Fig. 4.5). These values define an array with a slope of 4.1 to the right of Melbourne meteoric water line that reflects evaporation during the summer months. (Gonfiantini, 1986; Clark and Fritz, 1997). This array intercepted the Melbourne meteoric water line close to the weighted average $\delta^{18}O$ and δ^2H values of Melbourne rainfall ($\delta^{18}O$ = -4.98 ‰, δ^2H = -28.4 ‰; Hollins et al., 2018). The upper Avoca River in July and August had $\delta^{18}O$ and δ^2H values that plot on the Melbourne meteoric water line and cluster around those of average Melbourne rainfall. $\delta^{18}O$ and δ^2H values in July ranged from -3.3 to -6.1 ‰ (mean= -4.7 ± 0.2 ‰) and -17 to -33 ‰ (mean= -23 ± 1.9 ‰), respectively, whereas in August, the values were -2.6 to -5.3 ‰ (mean= -4.6 ± 0.2 ‰) and -11 to -30 ‰ (mean= -26 ±

1.5 ‰), respectively (Table S3). The $\delta^{18}O$ and $\delta^{2}H$ values of groundwater were slightly lower (-4.1 to -7.7 ‰, mean = -5.5 ± 0.4 ‰ and -27 to -52 ‰, mean= -34 ± 2.2 ‰) than those of the river water and the pool waters (Fig. 4.5; Table S4).

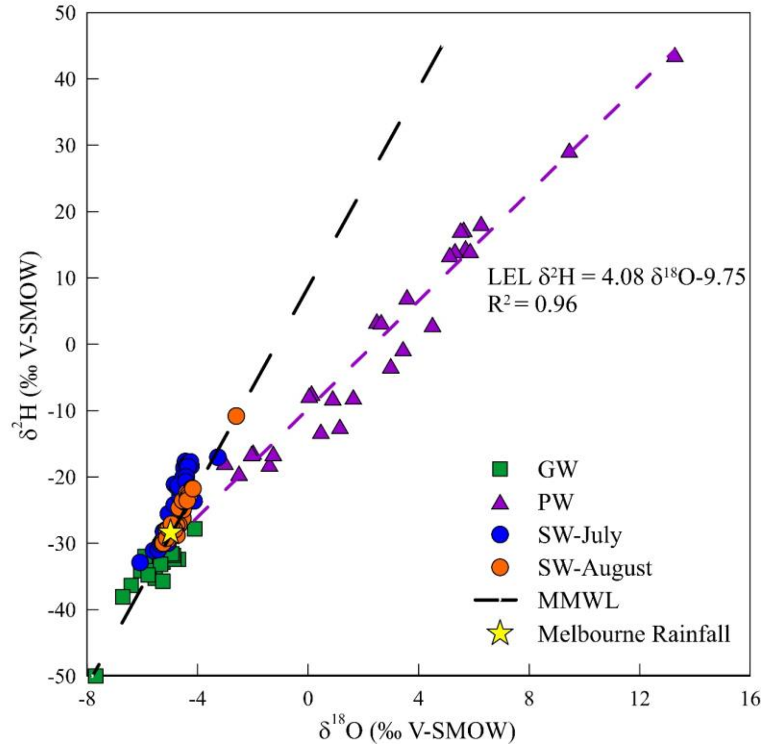

Figure 4.5. Stable isotope ratios of water samples in the Avoca catchment. MMWL= Melbourne Meteoric Water Line ($\delta^2H = 7.4 \times \delta^{18}O + 8.6$ ‰, as defined by Hughes and Crawford, 2012). GW=regional groundwater; PW=pool water; SW=stream water. The dashed line is the best fit for the pool water data. LEL=local evaporation line. Data from Table S4.

4.4.4 Radioactive isotopes (^{3}H, ^{14}C, and ^{36}Cl)

4.4.4.1 Regional groundwater

^{3}H activities of regional groundwater ranged from below detection (< 0.02 TU) to 1.08 TU (Table 4.1). These are much lower than the weighted average ^{3}H activity of modern rainfall in this area (3.0 ± 0.2 TU: Tadros et al., 2014). There is no decreasing trend of ^{3}H activities with depth in the groundwater. Groundwater from sites J and M (Fig. 4.1) that have ^{3}H activities > 0.1 TU are within 100 m of the Avoca River (Fig. 4.1 and Table 4.2). ^{14}C activities of regional groundwater were 34.0-98.1 pMC (Table 4.1). Groundwater with the highest ^{14}C activity (98.1 pMC) had a ^{3}H

activity of 0.29 TU. Groundwater that does not undergo mixing within aquifers following recharge has predictable ^{14}C and ^{3}H activities governed by the relative decay rates of those two isotopes (Fig. 4.6b) (Le Gal La Salle et al., 2001; Cartwright et al., 2019). Mixing of young (high ^{14}C and ^{3}H) and old (low ^{14}C and ^{3}H-free) water in aquifers produces groundwater with low to moderate ^{14}C activities but measurable ^{3}H activities (shown schematically in Fig. 4.6b). The majority of groundwater samples from the upper Avoca catchment have ^{14}C and ^{3}H activities that imply that significant mixing has not occurred. Only 60 m deep groundwater from Archdale Reserve (bore 8003933 from site J: Fig. 4.1) shows evidence of mixing (Fig. 4.6b). This groundwater sample was about 200 m from the Avoca River.

Table 4.1. ^{3}H, ^{14}C activities, and calculated MTTs by exponential piston-flow model (EPM; ratio=0.33) of groundwater from the upper Avoca River Catchment. letters in brackets represent location site in Fig 4.1.

Bore ID	**Depth** m	**$R^{36}Cl$** 10^{-15}	**^{3}H** TU	**^{14}C** pMC	**MTT-^{3}H** Years	**MTT-^{14}C** Years
8003924 (B)	42	60.6	0.06	34.04	nc[1]	12900
8003936 (D)	12	50.9	bd[2]	93.87	nc	500
8003934 (E)	58	51.1	bd	70.23	nc	3201
8003932 (J)	17	61.9	0.04	73.63	nc	2700
8003933 (J)	60	59.1	1.08	61.59	mixed[3]	mixed
109570 (L)	30	53.6	bd	58.42	nc	5401
110184 (M)	30	58.5	0.16	93.50	201	nc
110185 (M)	13	56.5	0.29	98.05	151	nc
119378 (N)	11	54.7	0.06	88.94	nc	1000

1 nc=not calculated
2 bd=below detection
3 sample showing mixing between old and young water (Fig. 4.6)

$R^{36}Cl$ values of the groundwater had a range of 50.9-61.9 × 10^{-15} (Fig. 4.5 and Table 4.1), which is higher than those of local modern rainfall in northern Victoria (15-35 × 10^{-15}: Davie et al., 1989; Cartwright et al., 2017; Howcroft et al., 2019). This is similar to the Barwon catchment in southeast Australia where $R^{36}Cl$ values of groundwater were up to 53.7 × 10^{-15} and those of the local rainfall were 14 to 20 × 10^{-15} (Howcroft et al., 2019). $R^{36}Cl$ values do not correlate with ^{14}C and ^{3}H activities (Fig. 4.5) or Cl concentrations.

4.4.4.2 Stream water

During the cease-to-flow period in the summer, ^{3}H activities of pool water varied from 1.64 to 5.11TU (Fig. 4.5; Table 4.2), which are higher than all of the groundwater ^{3}H activities. The pool waters with ^{3}H activities higher than the average of local modern rainfall (3.0 ± 0.2 TU) were downstream of Logan Reserve (109 km). The ^{3}H activities when the river was flowing were 2.21 to 2.67 TU in July and 2.39 to 2.77 TU in August, which were lower than those of average rainfall and again higher than those of the groundwater (Table 4.1).

Table 4.2. ^{3}H activities, $R^{36}Cl$ values and calculated mean transit times (MTTs) from pool water and stream water of upper Avoca River. Numbers in brackets represent location site in Fig 4.1.

Sample ID	**Distance**	**^{3}H**	**$R^{36}Cl$**	**MTTs (years)**				
March 2019	km	TU	10^{-15}	DM[1] (0.05)	DM (0.5)	EPM[2] (0.33)	EPM (1.0)	EMM[3]
Headwaters (1)	0	2.36	31.9	nc[4]	nc	nc	nc	nc
Amphitheatre (6)	15	1.64	45.6	nc	nc	nc	nc	nc
Bealiba (10)	38	2.79	42.1	nc	nc	nc	nc	nc
Arch Res (14)	73	1.89	57.7	nc	nc	nc	nc	nc
Logan Res (18)	109	4.57	66.9	nc	nc	nc	nc	nc
Coonooer (24)	146	5.11	60.8	nc	nc	nc	nc	nc
Seven Mile (25)	164	5.03	57.2	nc	nc	nc	nc	nc
Boort (28)	191	4.42	56.6	nc	nc	nc	nc	nc
July 2019								
Headwaters (1)	0	2.40	33.3	4	4.6	4.2	4	4.6
Amphitheatre (6)	15	2.21	58.5	5.5	6.8	6.2	5.7	7
Archdale Res (14)	73	2.23	55.1	5.4	6.6	6	5.6	6.7
Logan Res (18)	109	nm[5]	42.1					
Coonooer (24)	146	nm	59.2					
Seven Mile (25)	164	2.22	58.7	5.6	6.7	6.1	5.7	6.8
August 2019								
Headwaters (1)	0	2.67	36.4	2.1	2.2	2.1	2.1	2.2
Amphitheatre (6)	15	2.39	42.6	4.1	4.7	4.4	4.2	4.8
Archdale Res (14)	73	2.77	54.3	1.4	1.5	1.4	1.4	1.5
Logan Res (18)	109	nm	54.1					
Coonooer (24)	146	nm	47.9					
Seven Mile (25)	164	2.57	50.3	2.8	3	2.9	2.8	3

1 DM=dispersion model
2 EPM=exponential piston-flow model
3 EMM=exponential mixing model
4 nc=not calculated (due to mixing of water in the pools)
5 nm=not measured

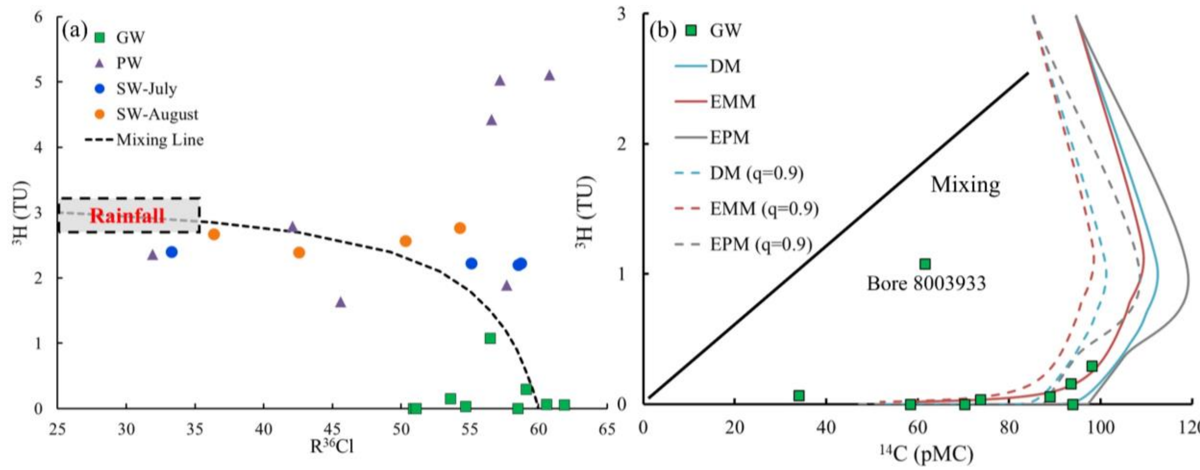

Figure 4.6. (a) ^{3}H activities vs. R^{36}Cl of groundwater (GW), pool water (PW), and stream water (SW) from the upper Avoca River and modern rainfall in the region. The curved line shows schematically the effects of mixing between young and old water end members. The shaded area represents the modern rainfall in the region. (b) ^{3}H activities vs. ^{14}C activities of groundwater from the upper Avoca River. Curved lines are the predicted covariance in the radioisotopes predicted by the Exponential Mixing (EMM), Exponential-Piston-Flow (EPM; EPM ratio = 1), and Dispersion (DM; D_P=0.5) lumped parameter models. Solid line shows schematically the effects of mixing between old regional groundwater (low ^{14}C and ^{3}H free) and modern or recently recharged water (high ^{14}C and ^{3}H). Calcite dissolution lowers the predicted ^{14}C activities (dashed lines display trends with 10% calcite dissolution).

R^{36}Cl values were lowest in the headwaters ($< 40 \times 10^{-15}$) and increased downstream to 40-60 × 10^{-15} (Fig. 4.7b; Table 4.2). There is no significant difference between the R^{36}Cl values of the pool water and the river water from July and August, and the highest R^{36}Cl values overlapped with those of the groundwater (Fig. 4.6a). Most of samples have ^{3}H activities and R^{36}Cl values that lie along a mixing trend between rainfall and regional groundwater.

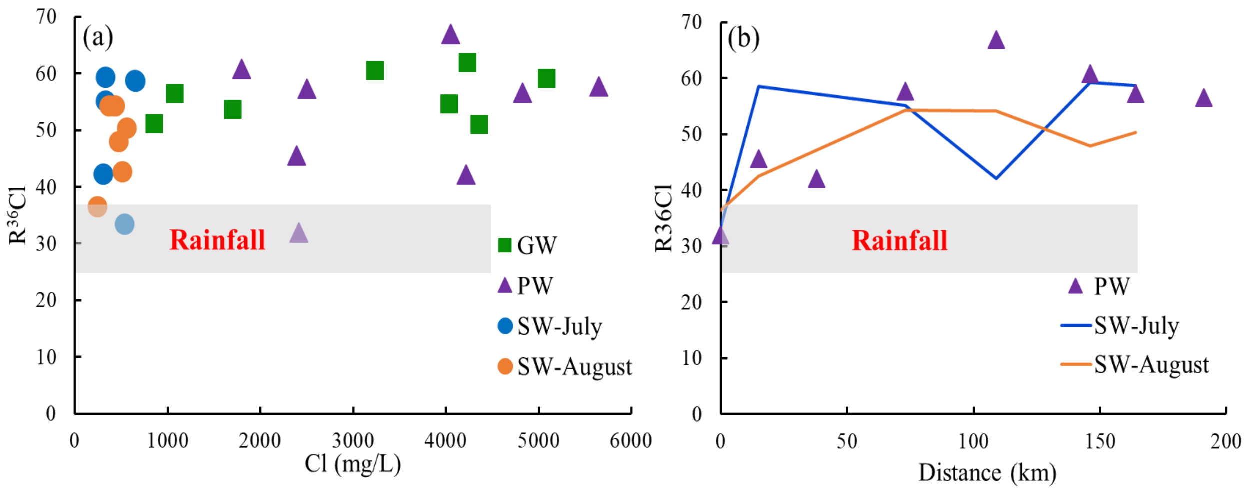

Figure 4.7. (a) $R^{36}Cl$ vs. Cl concentrations of groundwater (GW), pool water (PW), and stream water (SW) in July and August from the upper Avoca River. (b) $R^{36}Cl$ vs. distance in PW and SW. Shaded areas represent the range of $R^{36}Cl$ values in modern rainfall.

4.5 Discussion

The stable and radioactive isotopes together with major ion geochemistry can be used to determine baseflow locations, water sources, and MTTs in the upper Avoca River and MRTs of the groundwater.

4.5.1 Baseflow discharge to the river

Baseflow represents regional groundwater and other younger water sources including water from the riparian zone, bank storage and return flows, soil water, and interflow (McCallum et al., 2010; Cartwright et al., 2014; Cook et al., 2018; Zhou and Cartwright, 2021). In ideal circumstances ^{222}Rn activities may be used to calculate baseflow fluxes; however, they may be also used qualitatively to identify the reaches with high relatively baseflow inputs (e.g., Ortega et al., 2015). In the upper Avoca River, the higher ^{222}Rn activities in August compared with July imply higher relative baseflow inputs (Fig. 4.3a). This is likely to be a result of the regional water table rising after multiple rainfall events (Fig. 4.2a), which promotes increased baseflow discharge by hydraulic loading (Voltz et al., 2013). The higher ^{222}Rn activities (up to 2920 Bq/m^3) in the headwaters between 0 to 31km (Fig. 4.3a) may be due to high relative baseflow inputs caused by the steep topography and consequently high hydraulic gradient in this region. This is consistent with the increase in Cl concentrations in the headwaters (Fig. 4.3b). The ^{222}Rn activities in the middle and lower reaches of the river of less than 1000 Bq/m^3 suggest lower baseflow inputs probably as a result of decreased hydraulic gradients in flat alluvial floodplains. Cl concentrations in rivers with groundwater inflows are expected to increase downstream (Yu et al., 2013; Ortega et al., 2015). The Cl concentrations in the upper Avoca River fluctuate, especially in the middle and lower reaches (Fig. 4.3b). This fluctuation suggests that the river also receives water from low-salinity near-river sources such as bank storage and return flow, surface runoff, and/or interflow. Similar behaviour has been documented elsewhere in southeast Australian rivers (e.g., Yu et al., 2013; Barua et al., 2022; Zhou et al., 2022).

4.5.2 Sources of water contributing to streamflow

In common with rivers elsewhere (e.g., the Maribyrnong catchment, in southeast Australia: Cartwright and Gilfedder, 2015; the Coyote Creek, in northern California, USA: Bogan et al., 2019) that contain permanent pools in dry seasons, the persistence of the pools suggests that the upper Avoca River receives water from within the catchment over the summer months. The ^{222}Rn activities of the pool water were 38-9480 Bq/m^3 (Fig. 4.3a), which are generally higher than if the pools were only fed by surface water (e.g., from sporadic rainfall) (Cook et al., 2018). The high ^3H activities (1.64 to 5.11 TU) recorded in the pool water, however, suggests limited contributions of old regional groundwater (Fig. 4.6a) indicating much of the water is from younger near-river sources. This conclusion is consistent with the observation that major ion and stable isotope geochemistry of the pool water overlapped with that of the stream water but was different to the groundwater (Figs. 4.4, 4.5). The locally higher ^3H activities (up to 5.11 TU) that were recorded at localities downstream of Logan Reserve (Fig. 4.1) may reflect the input of water derived from late winter and spring rainfall in southeast Australia that has high ^{3}H activities due to moisture exchange from the stratosphere-to-the troposphere (Tadros et al., 2014).

Higher ^{3}H activities of stream water than those of groundwater (Fig. 4.6a) and a difference between the stable isotope and major ion geochemistry (Figs. 4.4, 4.5) also imply that the river is mainly fed by young water when it is flowing. This is consistent with the Cl and ^{222}Rn trends discussed above, which are not consistent with the input of only saline regional groundwater. Lower ^{3}H activities of stream water during the high flow period in July compared to intermediate flow conditions in August (Table 4.2) may be caused by local inputs of regional groundwater or older water from elsewhere in the catchment (e.g., from the soil or the regolith) that was flushed into the river at the early stage of rainfall events. Input of older water at the onset of flow event has been reported in other Australian catchments and elsewhere (Uhlenbrook et al., 2002; Kirchner, 2003; Unland et al., 2015; Tweed et al., 2016; Cartwright and Morgenstern, 2018; Barua et al., 2022)

4.5.3 $R^{36}Cl$ as a tracer of the solutes

Based on ^{14}C and ^{3}H activities (discussed below), the regional groundwater in the upper Avoca River had MRTs of up to 12900 years. This timescale is too short for significant decay of ^{36}Cl, and the $R^{36}Cl$ values will largely reflect those when the groundwater was recharged. The $R^{36}Cl$ values of groundwater overlapped with the stream and pool water and were higher than those of rainfall in the region (Fig. 4.6a). $R^{36}Cl$ values in Australian rainfall increase inland due to variations of Cl deposition rates (Keywood et al., 1998; Howcroft et al., 2019) and the high $R^{36}Cl$ values are probably due to the groundwater being recharged during the Holocene when sea levels were lower, and the area had a more continental climate. High $R^{36}Cl$ values were also produced during the bomb pulse period; however, relatively low ^{14}C activities (34-98 pMC: Table 4.1) imply that there is no bomb pulse recharge in the groundwater. An increase of $R^{36}Cl$ downstream from the headwaters (Fig. 4.7b) may reflect groundwater entering the river.

Although regional groundwater is not generally well connected to intermittent streams (e.g., Larsen and Woelfle‑Erskine, 2018; Zhou et al., 2022), there will still be some localities (e.g., in some areas that have steep riverbanks with high hydraulic gradients) where some groundwater inflows occur. Because of the high salinity of the groundwater (Table S4), the fluxes of groundwater required to change the $R^{36}Cl$ values of the river are probably small.

4.5.4 Mean transit and residence times

4.5.4.1 Mean transit times of stream water

The estimates of MTTs in the river water assumed that a single flow system in the catchment contributed to the stream. Mixing rainfall and water from within the catchment in the pools of the upper Avoca River in dry seasons means that single lumped parameter models (LPMs) cannot be used to calculate MTTs. While it is possible to use binary LPMs, there is insufficient data to accurately constrain mixing proportions and the ^{3}H activity of the end-members.

As with other studies (Morgenstern et al., 2010; Cartwright and Morgenstern, 2015; Cartwright et al., 2018), MTT estimates for when the river was following assume that river is maintained by a single store of water that varies in age as the catchment dries down and wets up. As discussed above, the stream water in the upper Avoca River is mainly fed by young water from near-river stores and the contribution from groundwater is limited, which is consistent with that conceptualisation.

The MTTs in the upper Avoca River when it was flowing ranged from 1.4 to 7.0 years (Table 4. 2). MTTs were generally higher in July (4.0 to 7.0 years) and were 1.4 to 4.8 years in August (Table 4.2). There are several uncertainties in the MTT calculations (e.g., as discussed in detail by

Morgenstern et al., 2010 and Cartwright and Morgenstern, 2016). The different LPMs result in different estimated MTTs. For the upper Avoca River, the highest MTTs (1.5 to 7.0 years) are from the EMM and the lowest (1.4 to 5.5 years) are from the DM with D_p 0.05. This is a relative uncertainty of 17%. Uncertainties and variations of the average annual ^3H activities of modern rainfall (± 0.2 TU: Tadros et al., 2014) also contribute to uncertainties in the MTT calculations. Varying the average annual ^3H activities of modern rainfall between 2.8 TU and 3.2 TU produced uncertainties in MTTs of -33% to 21%. A similar uncertainty (± 10%) in the ^3H input function translated to a -39% to 46% uncertainty in the MTTs for these samples.

Mixing of multiple water sources with different MTTs (aggregation) may result in actual MTTs being lower than calculated MTTs (Suckow, 2014; Kirchner, 2016a; Stewart et al., 2017). Aggregation has the most impact when there is binary mixing between water with very different MTTs. Mixing between multiple water stores with a range of MTTs has less impact on the MTTs calculated using ^3H as that scenario is similar to what is modelled using the LPMs (Cartwright and Morgenstern, 2016). In the case of the upper Avoca River, the relatively small range of MTTs implies that the effects of aggregation may not be significant.

Although the uncertainties hamper the precise estimates of MTTs, they do not change the conclusion that the upper Avoca River is mainly sustained by relatively young water even when streamflow ceases over summer.

4.5.4.2 Mean residence times of regional groundwater

Mean residence times of groundwater were estimated using the EPM model (EPM ratio = 0.33; Table 2). The EPM model can be used for groundwater where the bores sample the deeper longer flow paths but not the short near surface flow paths (Maloszewski and Zuber, 1982). MRTs were calculated using ^3H activities when these were > 0.1 TU (i.e., significantly above the lowest detection limit) and the ^{14}C activities for the rest of the samples. The estimated MRTs of groundwater were between 151 and 12900 years (Table 1). There is no systemic increase of MRTs with changes in depth and distance between the bore location and the Avoca River.

Similar uncertainties to those discussed above apply to the MRT estimates and the unknown degree of calcite dissolution adds an additional uncertainty; however, the groundwater is demonstrably several hundreds to thousands of years old. As discussed earlier, the variation in ^{14}C and ^{3}H activities (Fig. 4.5b) implies that there is limited mixing between regional groundwater and younger recently recharged water even close to the Avoca River. Only one sample (bore 8003933 from site J: Fig. 4.1) at 60 m depth and 200 m from the river shows mixing between young and old water components. This could be a result of local geology, such as faults or interconnected high permeability layers. However, generally, the Avoca River, which may be locally losing especially at high streamflows, does not appear to recharge the regional groundwater. That conclusion is also consistent with the differences in major ion and stable isotope geochemistry between the river and the groundwater (Figs 4.4, 4.5).

4.6 Conclusions and summary

Intermittent streams may become more prevalent globally in the future due to climate change and extraction of near-river groundwater (Messager et al., 2021); however, our understanding of these important systems is far less complete than that of perennial streams (Datry et al., 2014; Shanafield et al., 2021). Catchment intermittency has increased in southeast Australia following the Millennium Drought in the mid-1990s (1996-2010) and the streamflow in many catchments has still not recovered to pre-drought levels (e.g., Peterson et al., 2021).

The combination of major ions, stable isotopes, and radioisotopes highlighted the importance of young near-river water stores in maintaining the streamflow of the intermittent upper Avoca River.

This is similar to other intermittent streams in southeast Australia (e.g., Yihdego and Webb, 2013; Dresel et al., 2018; Barua et al., 2022) that are also maintained largely by young near-river water stores. In contrast, perennial headwater streams in southeast Australia are sustained by catchment waters that are typically decades and up to several hundreds of years old (summarised in Cartwright et al., 2020). At similar streamflows, the volume of the reservoir contributing to the river is proportional to the MTT (Małoszewski and Zuber, 1982). The smaller reservoir contributing to these intermittent streams makes them more susceptible to short-term variations in climate and changes to land use. Because the contribution from regional groundwater in intermittent streams in southeast Australia are limited and young and fresh near-river stores are dominant. In this case, the near-river stores are likely to act as a buffer zone that may prevent potentially regional contaminated groundwater entering the river and the effects of groundwater pumping on streamflow could also be less as a result of this weak connection. Thus, maintaining the health of near-river corridor is important in protecting intermittent streams and their ecosystems.

The results of this study also illustrate the application of multiple tracers in detecting baseflow discharges and the input from water stores with different residence time. This allows the effects of land use, topography, rainfall, and geology on catchment behaviour to be assessed and better understands what waters in the catchments come from. The utilization of ^{36}Cl as an environmental tracer for small fluxes of regional groundwater rather than as a residence time indicator represents a potentially important use of this tracer in river catchments. However, to achieve this a more comprehensive understanding of how R^{36}Cl values have varied over time is needed as well as good characterisation of R^{36}Cl values in the various stores of water within catchments.

Chapter 4

References

Barua, S., Cartwright, I., Dresel, P. E., Morgenstern, U., McDonnell, J. J., Daly, E., 2022. Sources and mean transit times of intermittent streamflow in semi-arid headwater catchments, Journal of Hydrology, 604, 127208, https://doi.org/10.1016/j.jhydrol.2021.127208.

Bentley, H.W., Phillips, F.M., Davis, S.N., Gifford, S., Elmore, D., Tubbs, L.E., Gove, H.E., 1982. Thermonuclear ^{36}Cl pulse in natural water. Nature, 300, 737-740, https://doi.org/10.1038/300737a0.

Bogan, M. T., Leidy, R. A., Neuhaus, L., Hernandez, C. J., Carlson, S. M., 2019. Biodiversity value of remnant pools in an intermittent stream during the great California drought. Aquatic Conservation: Marine and Freshwater Ecosystems, 29, 976-989, https://doi.org/10.1002/aqc.3109.

Brunner, P., Cook, P. G., Simmons, C. T., 2011. Disconnected surface water and groundwater: from theory to practice. Groundwater, 49, 460-467, https://doi.org/10.1111/j.1745-6584.2010.00752.x.

Bureau of Meteorology Australian landscape water balance: Commonwealth of Australia, available at: http://www.bom.gov.au/water/landscape/, last access: 20 July 2022.

Cartwright, I., 2022. Implications of variations in stream specific conductivity for estimating baseflow using chemical mass balance and calibrated hydrograph techniques. Hydrology and Earth System Sciences, 26, 183-195, https://doi.org/10.5194/hess-26-183-2022.

Cartwright, I., Atkinson, A. P., Gilfedder, B. S., Hofmann, H., Cendón, D. I., Morgenstern, U., 2018. Using geochemistry to understand water sources and transit times in headwater streams of a temperate rainforest. Applied geochemistry, 99, 1-12, https://doi.org/10.1016/j.apgeochem.2018.10.018.

Chapter 4

Cartwright, I., Gilfedder, B., 2015. Mapping and quantifying groundwater inflows to Deep Creek (Maribyrnong catchment, SE Australia) using 222Rn, implications for protecting groundwater-dependant ecosystems. Applied Geochemistry, 52, 118–129. https://doi.org/10.1016/j.apgeochem.2014.11.020.

Cartwright, I., Morgenstern, U., 2015. Transit times from rainfall to baseflow in headwater catchments estimated using tritium: The Ovens River, Australia, Hydrology and Earth System Sciences, 19, 3771-3785, https://doi.org/10.5194/hess-19-3771-2015.

Cartwright, I., Gilfedder, B., Hofmann, H., 2013. Chloride imbalance in a catchment undergoing hydrological change: Upper Barwon River, southeast Australia. Applied geochemistry, 31, 187-198. https://doi.org/10.1016/j.apgeochem.2013.01.003

Cartwright, I., Gilfedder, B., Hofmann, H., 2014. Contrasts between estimates of baseflow help discern multiple sources of water contributing to rivers. Hydrology and Earth System Sciences, 18, 15-30, https://doi.org/10.5194/hess-18-15-2014.

Cartwright, I., Hofmann, H., Currell, M. J., Fifield, L. K., 2017. Decoupling of solutes and water in regional groundwater systems: The Murray Basin, Australia. Chemical Geology, 466, 466-478, https://doi.org/10.1016/j.chemgeo.2017.06.035.

Cartwright, I., Hofmann, H., Sirianos, M. A., Weaver, T. R., Simmons, C. T., 2011. Geochemical and 222Rn constraints on baseflow to the Murray River, Australia, and timescales for the decay of low-salinity groundwater lenses. Journal of hydrology, 405, 333-343, https://doi.org/10.1016/j.jhydrol.2011.05.030.

Cartwright, I., Irvine, D., 2020. The spatial extent and timescales of bank infiltration and return flows in an upland river system: Implications for water quality and volumes. Science of the Total Environment, 140748. https://doi.org/10.1016/j.scitotenv.2020.140748.

Cartwright, I., Morgenstern, U., 2016. Contrasting transit times of water from peatlands and eucalypt forests in the Australian Alps determined by tritium: implications for vulnerability and the source of water in upland catchments. Hydrology and Earth System Sciences, 20, 4757-4773, https://doi.org/10.5194/hess-20-4757-2016.

Cartwright, I., Morgenstern, U., Howcroft, W., Hofmann, H., Armit, R., Stewart, M., Irvine, D., 2020. The variation and controls of mean transit times in Australian headwater catchments. Hydrological Processes, 34, 4034-4048, https://doi.org/10.1002/hyp.13862.

Cartwright, I., Werner, A. D., Woods, J. A., 2019. Using geochemistry to discern the patterns and timescales of groundwater recharge and mixing on floodplains in semi-arid regions. Journal of Hydrology, 570, 612-622, https://doi.org/10.1016/j.jhydrol.2019.01.023.

Chappell, J.M., 2009. Sea Level Change, Quaternary. In: Gornitz, V. (eds) Encyclopedia of Paleoclimatology and Ancient Environments. Encyclopedia of Earth Sciences Series. Springer, Dordrecht. https://doi.org/10.1007/978-1-4020-4411-3_208

Clark, I.D., Fritz, P., 1997. Environmental Isotopes in Hydrogeology, Lewis, New York, p. 328.

Clark, I.D., 2015. Groundwater geochemistry and isotopes, CRC Press Boca Raton, FL, USA.

Cook, P.G., 2013. Estimating groundwater discharge to rivers from river chemistry surveys. Hydrological Processes, 27, 3694–3707. https://doi.org/10.1002/hyp.9493.

Cook, P.G., Rodellas, V., Stieglitz, T.C., 2018. Quantifying Surface Water, Porewater, and Groundwater Interactions Using Tracers: Tracer Fluxes, Water Fluxes, and End-member Concentrations. Water Resources Research, 54, 2452-2465. https://doi.org/10.1002/2017WR021780.

Coplen, T. B., 1988. Normalization of oxygen and hydrogen isotope data, Chemical Geology, 72, 293-297, https://doi.org/10.1016/0168-9622(88)90042-5.

Chapter 4

Datry, T., Larned, S.T., Tockner, K., 2014. Intermittent rivers: a challenge for freshwater ecology. BioScience, 64, 3, 229-235. https://doi.org/10.1093/biosci/bit027.

Department of Environment Land Water and Planning: State Government Victoria, available at: http://data.water.vic.gov.au/monitoring.htm, last access: 20 August 2022.

Department of Jobs, Precincts and Regions, Energy and Earth Resources: State Government Victoria, available at: http://www.energyandresources.vic.gov.au/earth-resources/maps-reports-and-data/geovic, last access: 20 August 2022.

Dresel, P. E., Dean, J. F., Perveen, F., Webb, J. A., Hekmeijer, P., Adelana, S. M., Daly, E., 2018. Effect of Eucalyptus plantations, geology, and precipitation variability on water resources in upland intermittent catchments. Journal of hydrology, 564, 723-739, https://doi.org/10.1016/j.jhydrol.2018.07.019.

Duvert, C., Stewart, M.K., Cendón, D.I., Raiber, M., 2016. Time series of tritium, stable isotopes and chloride reveal short-term variations in groundwater contribution to a stream, Hydrology and Earth System Sciences, 20, 257-277, https://doi.org/10.5194/hess-20-257-2016.

Edmunds, W.M., 2009. Geochemistry's vital contribution to solving water resource problems. Applied Geochemistry, 24, 1058-1073, https://doi.org/10.1016/j.apgeochem.2009.02.021.

Fifield, L. K., Tims, S. G., Stone, J. O., Argento, D. C., De Cesare, M., 2013. Ultra-sensitive measurements of 36Cl and 236U at the Australian National University. Nuclear Instruments and Methods in Physics Research Section B: Beam Interactions with Materials and Atoms, 294, 126-131.

Fleckenstein, J. H., Krause, S., Hannah, D. M., Boano, F., 2010. Groundwater-surface water interactions: New methods and models to improve understanding of processes and dynamics. Advances in Water Resources, 33, 1291-1295, https://doi.org/10.1016/j.advwatres.2010.09.011.

Chapter 4

Fowler, K., Peel, M., Saft, M., Peterson, T., Western, A., Band, L., Nathan, R., 2022. Explaining changes in rainfall-runoff relationships during and after Australia's Millennium Drought: a community perspective. Hydrology and Earth System Sciences Discussions, 1-56, https://doi.org/10.5194/hess-2022-147.

Fuchs, E. H., King, J. P., Carroll, K. C., 2019. Quantifying disconnection of groundwater from managed-ephemeral surface water during drought and conjunctive agricultural use. Water Resources Research, 55, 5871-5890, https://doi.org/10.1029/2019WR02494.

Gonfiantini, R., 1986. Environmental isotopes in lake studies, Handbook of environmental isotope geochemistry, 2, 113-168.

Gutiérrez-Jurado, K.Y., Partington, D., Batelaan, O., Cook, P., Shanafield, M., 2019. What triggers streamflow for intermittent rivers and ephemeral streams in low-gradient catchments in Mediterranean climates. Water Resources Research, 55, 9926-9946. https://doi.org/10.1029/2019WR025041

Heislers D., 1993. Groundwater in the Central Victorian Highlands. Report No. 87, Department of Conservation and Natural Resources, Water Division, Melbourne.

Herczeg, A. L., Dogramaci, S. S., Leaney, F. W., 2001. Origin of dissolved salts in a large, semi-arid groundwater system: Murray Basin, Australia. Marine and Freshwater Resour., 52, 41-52. https://doi.org/10.1071/MF00040.

Hollins, S. E., Hughes, C. E., Crawford, J., Cendón, D. I., Meredith, K. T., 2018. Rainfall isotope variations over the Australian continent–Implications for hydrology and isoscape applications, Science the Total Environment, 645, 630-645, https://doi.org/10.1016/j.scitotenv.2018.07.082.

Chapter 4

Howcroft, W., Cartwright, I., Cendón, D.I., 2019. Residence times of bank storage and return flows and the influence on river water chemistry in the upper Barwon River, Australia. Applied Geochemistry., 101, 31-41, https://doi.org/10.1016/j.apgeochem.2018.12.026.

Howcroft, W., Cartwright, I., Morgenstern, U., 2018. Mean transit times in headwater catchments: Insights from the Otway Ranges, Australia. Hydrology and Earth System Sciences, 22, 635-653, https://doi.org/10.5194/hess-22-635-2018.

Hughes, C. E., Crawford, J., 2012. A new precipitation weighted method for determining the meteoric water line for hydrological applications demonstrated using Australian and global GNIP data, Journal of Hydrology, 464, 344-351, https://doi.org/10.1016/j.jhydrol.2012.07.029.

Jurgens, B. C., Bohkle, J. K., Eberts, S. M., 2012. TracerLPM (Version 1): An Excel® workbook for interpreting groundwater age distributions from environmental tracer data, United States Geological Survey, Techniques and Methods Report 4-F3, United States Geological Survey, Reston, USA, 60 pp., https://doi.org/10.3133/tm4F3.

Keywood, M.D., Fifield, L.K., Chivas, A.R., Cresswell, R.G., 1998. Fallout of chlorine 36 to the Earth's surface in the southern hemisphere. Journal of Geophysical Research, 103 (D7), 8281-8286, https://doi.org/10.1029/97JD03125.

Kirchner, J. W., 2003. A double paradox in catchment hydrology and geochemistry, Hydrological. Processes, 17, 871–874, https://doi.org/10.1002/hyp.5108.

Kirchner, J. W., 2016. Aggregation in environmental systems–Part 1: Seasonal tracer cycles quantify young water fractions, but not mean transit times, in spatially heterogeneous catchments, Hydrology and Earth System Sciences, 20, 279-297, https://doi.org/10.5194/hess-20-279-2016

Labotka, D. M., Panno, S. V., Locke, R. A., Freiburg, J. T., 2015. Isotopic and geochemical characterization of fossil brines of the Cambrian Mt. Simon Sandstone and Ironton–Galesville

Formation from the Illinois Basin, USA. Geochimica et Cosmochimica Acta, 165, 342-360, https://doi.org/10.1016/j.gca.2015.06.013

Larsen, L. G., Woelfle‐Erskine, C., 2018. Groundwater is key to salmonid persistence and recruitment in intermittent Mediterranean‐climate streams. Water Resources Research, 54, 8909-8930, https://doi.org/10.1029/2018WR023324.

Le Gal La Salle, C., Marlin, C., Leduc, C., Taupin, J.D., Massault, M., Favreau, G., 2001. Renewal rate estimation of groundwater based on radioactive tracers (^{3}H, ^{14}C) in an unconfined aquifer in a semi-arid area, Iullemeden Basin. Niger. Journal of Hydrology 254, 145–156. https://doi.org/10.1016/S0022-1694(01)00491-7.

Lewandowski, J., Meinikmann, K., Krause, S., 2020. Groundwater–surface water interactions: Recent advances and interdisciplinary challenges. Water, 12, 296, https://doi.org/10.3390/w12010296.

Lewis, S. E., Sloss, C. R., Murray-Wallace, C. V., Woodroffe, C. D., Smithers, S. G., 2013. Post-glacial sea-level changes around the Australian margin: a review. Quaternary Science Reviews, 74, 115-138. https://doi.org/10.1016/j.quascirev.2012.09.006.

Lorimer, M. S., Rowan, J. N., 1982. A Study of the Land in the Catchment of the Avoca River. Soil Conservation Authority.

Maloszewski, P., 2000. Lumped-parameter models as a tool for determining the hydrological parameters of some groundwater systems based on isotope data, in: Tracer and Modelling in Hydrogeology-Proceetings of the TraM'2000 Conference, May 2020, Liege, Belgium, IAHS Publ. no. 262, 271–276, ISBN 190150221X.

Małoszewski, P., Zuber, A., 1982. Determining the turnover time of groundwater systems with the aid of environmental tracers: 1. Models and their applicability, Journal of Hydrology, 57, 207–231, https://doi.org/10.1016/0022-1694(82)90147-0, 1982.

McCallum, J.L., Cook, P.G., Berhane, D., Rumpf, C., McMahon, G.A., 2012. Quantifying groundwater flows to streams using differential flow gauging and water chemistry. Journal of Hydrology, 416, 118-132. https://doi.org/10.1016/j.jhydrol.2011.11.040.

McCallum, J.L., Cook, P.G., Brunner, P., Berhane, D., 2010. Solute dynamics during bank storage flows and implications for chemical base flow separation. Water Resources Research, 46, W07541. https://doi.org/10.1029/2009WR008539

Meredith, K. T., Han, L. F., Hollins, S. E., Cendón, D. I., Jacobsen, G. E., & Baker, A. (2016). Evolution of chemical and isotopic composition of inorganic carbon in a complex semi-arid zone environment: Consequences for groundwater dating using radiocarbon. Geochimica et Cosmochimica Acta, 188, 352-367, https://doi.org/10.1016/j.gca.2016.06.011.

Messager, M. L., Lehner, B., Cockburn, C., Lamouroux, N., Pella, H., Snelder, T., Datry, T., 2021. Global prevalence of non-perennial rivers and streams, Nature, 594, 391-397, https://doi.org/10.1038/s41586-021-03565-5.

Miller, M. P., Johnson, H. M., Susong, D. D., Wolock, D. M., 2015. A new approach for continuous estimation of baseflow using discrete water quality data: Method description and comparison with baseflow estimates from two existing approaches. Journal of Hydrology, 522, 203-210, https://doi.org/10.1016/j.jhydrol.2014.12.039.

Morgenstern, U. Taylor, C.B., 2009. Ultra low-level tritium measurement using electrolytic enrichment and LSC. Isotopes in Environmental and Health Studies, 45, 96-117. https://doi.org/10.1080/10256010902931194.

Morgenstern, U., Stewart, M. K., Stenger, R.,2010. Dating of streamwater using tritium in a post nuclear bomb pulse world: continuous variation of mean transit time with streamflow, Hydrology and Earth System Sciences, 14, 2289–2301, https://doi.org/10.5194/hess-14-2289-2010.

North Central Catchment Management Authority., 2007. Avoca Catchment Local Management Plan.

Oh, Y. H., Koh, D. C., Kwon, H. I., Jung, Y. Y., Lee, K. Y., Yoon, Y. Y., Ha, K. (2021). Identifying and quantifying groundwater inflow to a stream using 220Rn and 222Rn as natural tracers. Journal of Hydrology: Regional Studies, 33, 100773, https://doi.org/10.1016/j.ejrh.2021.100773

Ortega, L., Manzano, M., Custodio, E., Hornero, J., Rodríguez-Arévalo, J., 2015. Using 222Rn to identify and quantify groundwater inflows to the Mundo River (SE Spain). Chemical Geology, 395, 67–79. https://doi.org/10.1016/j.chemgeo.2014.12.002.

Peters, N. E., Burns, D. A., Aulenbach, B. T., 2014. Evaluation of high-frequency mean streamwater transit-time estimates using groundwater age and dissolved silica concentrations in a small forested watershed, Aquatic Geochemistry, 20, 183-202, https://doi.org/10.1007/s10498-013-9207-6.

Peterson, T.J., Saft, M., Peel, M.C., John, A., 2021. Watersheds may not recover from drought. Science 372, 745–749. https://doi.org/10.1126/science.abd5085.

Phillips, F.M., 2000. Chloribe-36. In: Cook, P., Herczeg, A. (Eds.), Environmental Tracers in Subsurface Hydrology. Kluwer Academic Publishers, Boston, pp. 299-348.

Rhodes, K.A., Proffitt, T., Rowley, T., Knappett, P.S., Montiel, D., Dimova, N., Miller, G.R., 2017. The importance of bank storage in supplying baseflow to rivers flowing through compartmentalized, alluvial aquifers. Water Resources Research, 53, 10539-10557. https://doi.org/10.1002/2017WR021619

Chapter 4

Richardson, C. M., Zimmer, M. A., Fackrell, J. K., Paytan, A., 2020. Geologic controls on source water drive baseflow generation and carbon geochemistry: Evidence of nonstationary baseflow sources across multiple subwatersheds. Water Resources Research, 56, e2019WR026577, https://doi.org/10.1029/2019WR026577.

Shanafield, M., Bourke, S.A., Zimmer, M.A., Costigan, K.H., 2021. An overview of the hydrology of non-perennial rivers and streams. Wiley Interdisciplinary Reviews: Water, 8, e1504. https://doi.org/10.1002/wat2.1504.

Smith, N., 1995. Recent hydrological changes in the Avoca River catchment, Victoria. Australian Geographical Studies, 33, 6-18, https://doi.org/10.1111/j.1467-8470.1995.tb00681.x.

Sophocleous, M., 2002. Interactions between groundwater and surface water: the state of the science. Hydrogeology Journal, 10, 52-67. http://dx.doi.org/10.1007/s10040-014-1215-0

Stelzer, R. S., Thad Scott, J., Bartsch, L. A., Parr, T. B., 2014. Particulate organic matter quality influences nitrate retention and denitrification in stream sediments: evidence from a carbon burial experiment. Biogeochemistry, 119, 387-402, https://doi.org/10.1007/s10533-014-9975-0.

Tadros, C. V., Hughes, C. E., Crawford, J., Hollins, S.E., Chisari, R., 2014. Tritium in Australian precipitation: A 50-year record, Journal of Hydrology, 513, 262–273, https://doi.org/10.1016/j.jhydrol.2014.03.031.

Tweed, S., Munksgaard, N., Marc, V., Rockett, N., Bass, A., Forsythe, A.J., Bird, M.I., Leblanc, M., 2016. Continuous monitoring of stream $\delta^{18}O$ and $\delta^{2}H$ and stormflow hydrograph separation using laser spectrometry in an agricultural catchment. Hydrological Processes, 30, 648-660, https://doi.org/10.1002/hyp.10689.

Chapter 4

Uhlenbrook, S., Frey, M., Leibundgut, C., Maloszewski, P., 2002. Hydrograph separations in a mesoscale mountainous basin at event and seasonal timescales. Water Resources Research, 38, 311-3114, https://doi.org/10.1029/2001WR000938.

Unland, N. P., Cartwright, I., Daly, E., Gilfedder, B. S., Atkinson, A. P., 2015. Dynamic river-groundwater exchange in the presence of a saline, semi-confined aquifer, Hydrological Processes, 29, 4817– 4829, https://doi.org/10.1002/hyp.10525

Voltz, T., Gooseff, M., Ward, A. S., Singha, K., Fitzgerald, M., Wagener, T., 2013. Riparian hydraulic gradient and stream-groundwater exchange dynamics in steep headwater valleys. Journal of Geophysical Research: Earth Surface, 118, 953-969, https://doi.org/10.1002/jgrf.20074.

Yihdego, Y., Webb, J., 2013. An empirical water budget model as a tool to identify the impact of land-use change in stream flow in southeastern Australia. Water resources management, 27, 4941-4958, https://doi:10.1007/s11269-013-0449-2.

Yu, M. C. L., Cartwright, I., Braden, J. L., De Bree, S. T., 2013. Examining the spatial and temporal variation of groundwater inflows to a valley-to-floodplain river using 222 Rn, geochemistry and river discharge: the Ovens River, southeast Australia. Hydrology and Earth System Sciences, 17, 4907-4924, https://doi.org/10.5194/hess-17-4907-2013.

Zhang, R., Li, Q., Chow, T. L., Li, S., Danielescu, S., 2013. Baseflow separation in a small watershed in New Brunswick, Canada, using a recursive digital filter calibrated with the conductivity mass balance method. Hydrological Processes, 27, 2659-2665, https://doi.org/10.1002/hyp.9417.

Zhou, Z., Cartwright, I., 2021. Using geochemistry to identify and quantify the sources, distribution, and fluxes of baseflow to an intermittent river impacted by climate change: The upper

Wimmera River, southeast Australia, Science of the Total Environment, 801, 149725, https://doi.org/10.1016/j.scitotenv.2021.149725.

Zhou, Z., Cartwright, I., Morgenstern, U., 2022. Sources and mean transit times of stream water in an intermittent river system: the upper Wimmera River, southeast Australia. Hydrology and Earth System Sciences, 26, 4497-4513, https://doi.org/10.5194/hess-26-4497-2022.

Chapter 5 Summary and conclusions

Intermittent streams constitute more than 50% of global river network and are common in semi-arid areas (Messager et al., 2021). However, despite their importance in sustaining often fragile ecosystems and providing water for human use, their hydrogeology is far less well understood than that of perennial streams (Datry et al., 2014; Costigan et al., 2016; Shanafield et al., 2021). Understanding the functioning of intermittent catchments is important for their management and protection, especially as intermittency is predicted to increase globally due to land use changes, climate change, and the increased use of groundwater and surface water (Messager et al., 2021). In comparison to perennial streams, intermittent streams are less likely to be connected to regional groundwater systems and younger near-river sources are more likely to be important in sustaining streamflow.

5.1 Research aims and methods

The main aim of this study was to understand the interaction between two intermittent streams from the Murray-Darling Basin in southeast Australia (the upper Wimmera and Avoca Rivers) and waters stored within their catchments. In order to achieve this, three main objectives were addressed. The first objective was to identify and quantify the sources, distributions, and fluxes of baseflow inflows to these intermittent streams at different hydrological conditions (Chapters 2 and 4). The second and third objectives concentrated on documenting the timescale of water flow through the catchments (the transit times) and how diverse water sources with different ages contribute to streamflow during different flow conditions (Chapters 3 and 4).

The study integrated major ion geochemistry, stable isotopes (^{2}H and ^{18}O), and radioisotopes (^{222}Rn, ^{3}H, ^{14}C, and ^{36}Cl) with streamflow data, Google Earth imagery, and GIS. Multiple rounds of sampling at high flows, low flows, and cease-to-flow periods allowed an understanding of processes at different hydrological conditions.

5.1.1 Integration of environmental tracers to understand intermittent streams

Due to contrasts in geochemistry, environmental tracers have been successfully applied to study the locations and sources of baseflow discharge into rivers, transit or residence times of river water and groundwater, and the river recharge of groundwater (Oxtobee and Novakowski, 2003; Kalbus et al., 2006; Morgenstern et al., 2010; Cook, 2013; Atkinson et al., 2015; Barua et al., 2022; Zhou et al, 2022). This study used environmental tracers to study these processes in intermittent streams, which are not as well understood as perennial streams.

^{222}Rn helped to understand the location of and quantity of baseflow discharge into the upper Wimmera River and Avoca River at different flow conditions (discussed in Chapters 2 and 4). As with streams worldwide (e.g., Ortega et al., 2015; Tan et al., 2021), the locations of high baseflow inputs are identified by elevated ^{222}Rn activities along the river. However, while ^{222}Rn allows the pattern and amount of total baseflow to be understood, it does not define where in the catchment the water comes from nor how long it takes to flow into the river. Multiple water stores with different ages may sustain the streamflow of these streams and the water sources may be different at variable flow conditions. By using a range of tracers including other radioisotopes (^{3}H, ^{14}C, and ^{36}Cl), stable isotopes, and major ions (discussed in Chapters 2, 3 and 4), a better understanding of the sources of baseflow is possible. In addition, the use of ^{3}H and ^{14}C allows the mean transit times of the water contributing to streamflow to be made, as well as understanding the residence times of groundwater and whether the river water recharges the groundwater system.

Due to the fact that intermittent streams only flow for parts of the year, it is not viable to estimate mean transit times using lumped parameter models based on time-series of chloride or ^{18}O as these methods require continuous datasets in rainfall and stream water (Kirchner et al., 2004; McGuire and McDonnell, 2006). Other techniques, such as StorAge Solutions and Flux Tracking (Hrachowitz et al., 2013; Rinaldo et al., 2015) may be used with shorter discontinuous time-series of these tracers but still require frequent (ideally daily) measurements in rainfall and stream water, which are logistically difficult and costly to obtain. They are also less effective where transit times are longer than a few years, which is commonly the case in Australian catchments (Cartwright et al., 2020), as the temporal variations in the tracer signal are severely attenuated (Stewart et al., 2010). Due to the much lower bomb-pulse ^{3}H activities in the Southern Hemisphere (Tadros et al., 2014), ^{3}H is invaluable in determining transit and residence times of surface water and groundwater where these are less than 100 years (Morgenstern et al., 2010; Cartwright and Morgenstern, 2018).

Additionally, this study highlighted the use of ^{36}Cl as a tracer of small inflows of saline regional groundwater. Because $R^{36}Cl$ values of precipitation increase inland (Keywood et al., 1998; Howcroft et al., 2019), $R^{36}Cl$ values of groundwater recharged during the Holocene when sea levels were lower and the coastline was further away were higher than those of modern rainfall. Because of the long half-life of ^{36}Cl (301,000 years), these variations in initial $R^{36}Cl$ values are preserved and the catchment waters may have a wide range of $R^{36}Cl$ values. Waters recharged during the 1950s and 1960s are likely to have very high $R^{36}Cl$ values due to the atmospheric nuclear tests; these too will be preserved. A better understanding of the distribution of $R^{36}Cl$ values in the different water stores in catchments would improve the utility of this tracer.

5.1.2 Limitations of environmental tracers

While environmental tracers are useful tools for discerning water sources in the river flow, there are limitations. For example, difficulties in quantifying the rate of degassing to the atmosphere (e.g., Cook, 2013) hamper ^{222}Rn-based baseflow discharge estimates. In addition, ^{222}Rn and other tracers such as Cl are problematic to use in streams with losing reaches, which may be more prevalent in intermittent streams (e.g., Avery et al., 2018; Adyasari et al., 2023). Using environmental tracers to quantify the water sources contributing to rivers requires the geochemistry of the potential sources to be well understood (Cartwright and Morgenstern, 2016; Duvert et al., 2016; Tan et al., 2021). In larger catchments it is difficult to constrain the geochemistry of all the water stores across the catchment, especially if the geochemistry is heterogeneous, making such quantification difficult. In the Avoca catchment, a lack of constraints on the geochemistry of near-river waters hampered the quantification of the water balance in the pools (Chapter 4).

Calculating transit times and residence times is also subject to uncertainties. These include: uncertainties in the input function of the tracers and the value of modern rainfall; assumptions as to the geometry of the flow system (i.e., the most suitable lumped parameter model to use); whether seasonal recharge has occurred; and the possibility that macroscopic mixing (aggregation) has occurred (Kirchner, 2016). For residence times estimated using ^{14}C, the input of ^{14}C-free DIC from the aquifer matrix is an additional uncertainty (Clark, 2015).

5.2 Baseflow discharge in intermittent streams

Baseflow sustains rivers and their ecosystem, especially when surface runoff declines following reduced precipitation (Kalbus et al., 2006; Cartwright and Morgenstern, 2016; Zimmer and McGlynn, 2017). Baseflow estimates calculated by ^{222}Rn mass balance and water mass balance (also referring as differential flow gauging) in the upper Wimmera River were higher (up to 1.3 m^3/m/day) during wetter periods (high flow conditions) and lower (up to 0.1 m^3/m/day) during low flow periods. Similar conclusions were drawn from the upper Avoca River that high baseflow inputs were promoted by multiple rainfall events and decreased after high flow conditions. The spatial variations in baseflow inputs were mainly controlled by local topography that influences hydraulic gradients. For example, in the upper Wimmera River, higher baseflow fluxes were recorded in the upper and middle reaches where the river flows through relatively steep topography with higher hydraulic gradients. The lower reaches that were occupied with flat alluvial floodplains had less baseflow inputs due to smaller hydraulic gradients. Higher baseflow inflows in regions of steep topography are reported elsewhere (Voltz et al., 2013; Yu et al., 2013; Rudnick et al., 2015). However, several observations imply that in the upper Wimmera and Avoca catchments, young and transient near-river water stores (e.g., bank storage and return waters, soil water, and/or interflow) are more important sources of baseflow than regional groundwater. In streams that receive substantial inputs of saline groundwater, concentrations of Cl and other major ions are expected to increase downstream (e.g., The Gellibrand River in southeast Australia: Atkinson et al., 2015). However, Cl concentrations in the upper Wimmera and Avoca fluctuate downstream (Chapters 2 and 4), implying that some of the baseflow must be derived from other sources. These fluctuations in Cl concentrations also restrict the use of Cl and proxies such as EC in quantifying baseflow inflows. In the Avoca River, the river water stable isotope and major ion geochemistry are different to that of groundwater at all flow conditions, including in the pools at cease-to-flow conditions (Chapter 4). In addition, in both catchments, the ^{3}H activities of the river water are relatively high implying a significant input from relatively young sources (Chapters 3 and 4). Notably, some of the pool waters in the Avoca catchment had ^{3}H activities greater than those of average annual rainfall, probably indicating a substantial input of winter and spring rainfall stored in the catchment.

Thus, the connection of the Wimmera and Avoca Rivers with deeper and older regional groundwater is relatively weak during most of flow periods and much of the baseflow is probably derived from near-river stores that have a lower salinity than the regional groundwater. This situation is likely to be common in intermittent streams where the connection between regional groundwater and the streams is limited, especially during the cease-to-flow periods. This is different to comparable perennial streams where regional groundwater is an important water source maintaining the streamflow, especially during the low flow periods and rivers commonly receive more inputs from regional groundwater downstream (McCallum et al., 2012; Atkinson et al., 2015; Ortega et al., 2015).

5.3 Timescales of water flow in intermittent streams

Rivers are sustained by inflows of water that range in age from a few days to millennia (McGuire and McDonnell, 2006; Morgenstern et al., 2010; Duvert et al., 2016). Near-river water stores, including riparian water, bank return water, and soil water are much younger compared than regional groundwater (Cartwright and Irvine, 2020; Zhou et al., 2022). Mean transit times in the upper Wimmera and Avoca Rivers determined by ^{3}H are up to 15 years in the upper Wimmera and 7 years in the upper Avoca River. The longer MTTs (15 and 7 years, respectively) at the onset of flow following autumn rainfalls may reflect local inputs of regional groundwater mobilized by hydraulic loading or older near-river water that is flushed into the stream by rainfall. During both the high and low flow periods, the shorter MTTs (less than 6 years in both rivers) imply that young water contributes most to streamflow. These intermittent streams cease to flow and comprise laterally-disconnected water pools during summer. Elsewhere, pools commonly have inputs of regional groundwater (Cartwright and Morgenstern, 2016; Bourke et al., 2023); however, in both the upper Wimmera and upper Avoca catchments, the high ^{3}H activities, major ion, and stable isotope geochemistry imply that pools contain a substantial amount of young near-river water. Mean residence times (MRTs) of groundwater in these catchments are up to 12,900 years) and the lack of evidence for recharge of the groundwater by river water at most localities again demonstrates the limited connection with regional groundwater in these rivers.

5.4 Implications for water resources management

Intermittent streams account for more than 50% of the global river system and intermittency is predicted to increase in the future due to climate change, surface water usage, and groundwater use (Messager et al., 2021). This study demonstrated that there is a limited connection between these intermittent rivers and the deeper regional groundwater and emphasized the importance of smaller younger reservoirs in the riparian zone (such as soil water, interflow, and bank storage) as the water sources that maintained streamflow at most flow conditions. Similar findings that near-river sources are important for sustaining the streamflow of intermittent streams have been made by Barua et al. 2022. While perennial streams are more likely to be connected to regional groundwater, near river-river water is also locally important in those catchments (e.g. Yu et al., 2013; McCallum et al., 2010; 2012; Rhodes et al., 2017). Those conclusions also agree with the results of a recent study that deeper groundwater contributes less than 0.1% of global river discharge (Ferguson et al., 2023) and the findings of Jasechko et al. (2016) that a substantial of river water globally is less than a few months old.

The fact that these intermittent catchments in southeast Australia are connected to younger water stores has broad implications for managing and protecting water resources and riverine ecosystem in this region. Firstly, the influences of regional groundwater extractions on the river flows may be less. Secondly, the near-river waters could also act as a buffer zone to prevent inflows of potentially contaminated regional groundwater from coming into the river. Finally, the volume of the water stores contribution to stream flow is generally proportional to the mean transit times (Małoszewski and Zuber, 1982). Unlike perennial streams in southeast Australia that receive contributions from older (MTTs of up to 250 years) larger water stores, especially at low flow conditions (Cartwright et al., 2020), small near-river water stores with MTTs of only a few years to decades maintains the streamflow in these and other intermittent streams (e.g., Cartwright and Morgenstern, 2016; Barua et al., 2022). These small water stores will be likely susceptible to short-term variations in rainfall and changes to land use. This makes the intermittent streams more likely to have short-term fluctuations in streamflow, as is apparent in the upper Wimmera River where streamflows declined significantly during and following the Millennium drought (Chapter 2). The difference in MTTs may also impact nutrient transport to the streams as denitrification is likely to be more complete in older waters (e.g., Romeijn, 2019).

5.5 Future research directions

A holistic understanding of catchment functioning is required to manage and protect river systems. Compared to perennial streams, our understanding of how intermittent streams function is limited. There are very few estimates of the mean transit times of intermittent streams, making it difficult to generalize conclusions as to water sources and vulnerability. Transit time distributions (TTDs) estimates that describe all the transit times of the water parcels in the streamflow would provide better information about catchment processes such as how different water stores are released in catchments during the wet and dry periods (McGuire and McDonnell, 2006; Birkel et al., 2015). Considering this research usually requires detailed and frequent sampling of radioisotopes or stable isotopes, it may be most feasible to conduct in small catchments (Stewart et al., 2021). Future studies could also concentrate on better quantifying the contribution of near-river water stores such as bank storage, soil water, and interflow at different flow conditions. Differences in baseflow estimates from streamflow measurements and chemical mass balance may be able to estimate contributions of interflow or bank storage (Cartwright et al., 2014) as could distinguishing multiple components of delayed flow from the hydrographs (Stoelzle et al., 2020). However, a better understanding of the geochemistry of the near-river waters would be ideal to achieve this aim. In most catchments, geochemical data are largely from regional groundwater and surface water. Sampling the near river waters would require intensive infrastructure to sample soil water or interflow and again this would be more feasible in smaller catchments. Additionally, this study has demonstrated that integrating a diverse range of geochemical parameters is required to understand the multiple water sources in rivers, which results in high total analytical costs.

The results of this study also help to make decisions regarding water resources management for the Murray-Darling Basin to be made. In particular, highlighting that the near-river water resources in intermittent catchments are equally important to river protection as understanding changes to the regional groundwater.

References

Adyasari, D., Dimova, N. T., Dulai, H., Gilfedder, B. S., Cartwright, I., McKenzie, T., Fuleky, P., 2023. Radon-222 as a groundwater discharge tracer to surface waters. Earth-Science Reviews, 104321, https://doi.org/10.1016/j.earscirev.2023.104321

Atkinson, A. P., Cartwright, I., Gilfedder, B. S., Hofmann, H., Unland, N. P., Cendón, D. I., Chisari, R., 2015. A multi-tracer approach to quantifying groundwater inflows to an upland river; assessing the influence of variable groundwater chemistry. Hydrological Processes, 29, 1-12, https://doi.org/10.1002/hyp.10122.

Avery, E., Bibby, R., Visser, A., Esser, B., Moran, J., 2018. Quantification of groundwater discharge in a subalpine stream using radon-222. Water, 10, 100, https://doi.org/10.3390/w10020100.

Barua, S., Cartwright, I., Dresel, P. E., Morgenstern, U., McDonnell, J. J., Daly, E., 2022. Sources and mean transit times of intermittent streamflow in semi-arid headwater catchments, Journal of Hydrology, 604, 127208, https://doi.org/10.1016/j.jhydrol.2021.127208.

Birkel, C., Soulsby, C., Tetzlaff, D., 2015. Conceptual modelling to assess how the interplay of hydrological connectivity, catchment storage and tracer dynamics controls nonstationary water age estimates. Hydrological Processes, 29, 2956-2969, https://doi.org/10.1002/hyp.10414.

Bourke, S. A., Shanafield, M., Hedley, P., Chapman, S., Dogramaci, S., 2023. A hydrological framework for persistent pools along non-perennial rivers. Hydrology and Earth System Sciences, 27, 809-836, https://doi.org/10.5194/hess-27-809-2023.

Cartwright, I., Gilfedder, B., Hofmann, H., 2014. Contrasts between estimates of baseflow help discern multiple sources of water contributing to rivers. Hydrology and Earth System Sciences, 18, 15-30. https://doi.org/10.5194/hess-18-15-2014.

Cartwright, I., Irvine, D., 2020. The spatial extent and timescales of bank infiltration and return flows in an upland river system: Implications for water quality and volumes. Science of the Total Environment, 140748. https://doi.org/10.1016/j.scitotenv.2020.140748

Cartwright, I., Morgenstern, U., 2016. Using tritium to document the mean transit time and sources of water contributing to a chain-of-ponds river system: implications for resource protection. Applied Geochemistry, 75, 9-19, https://doi.org/10.1016/j.apgeochem.2016.10.007.

Cartwright, I., Morgenstern, U., 2018. Using tritium and other geochemical tracers to address the "old water paradox" in headwater catchments. Journal of hydrology, 563, 13-21, https://doi.org/10.1016/j.jhydrol.2018.05.060.

Cartwright, I., Morgenstern, U., Howcroft, W., Hofmann, H., Armit, R., Stewart, M., Irvine, D., 2020. The variation and controls of mean transit times in Australian headwater catchments. Hydrological Processes, 34, 4034-4048, https://doi.org/10.1002/hyp.13862.

Clark, I.D., 2015. Groundwater geochemistry and isotopes, CRC Press Boca Raton, FL, USA.

Cook, P.G., 2013. Estimating groundwater discharge to rivers from river chemistry surveys. Hydrological Processes, 27, 3694–3707. https://doi.org/10.1002/hyp.9493.

Costigan, K.H., Jaeger, K.L., Goss, C.W., Fritz, K.M., Goebel, P.C., 2015. Understanding controls on flow permanence in intermittent rivers to aid ecological research: integrating meteorology, geology and land cover, Ecohydrology., 9, 1141-1153. https://doi.org/10.1002/eco.1712.

Datry, T., Larned, S.T., Tockner, K., 2014. Intermittent rivers: a challenge for freshwater ecology. BioScience, 64, 3, 229-235. https://doi.org/10.1093/biosci/bit027.

Duvert, C., Stewart, M.K., Cendón, D.I., Raiber, M., 2016. Time series of tritium, stable isotopes and chloride reveal short-term variations in groundwater contribution to a stream. Hydrology and Earth System Sciences, 20, 257-277. https://doi.org/10.5194/hess-20-257-2016.

Chapter 5

Ferguson, G., McIntosh, J. C., Jasechko, S., Kim, J. H., Famiglietti, J. S., McDonnell, J. J., 2023. Groundwater deeper than 500 m contributes less than 0.1% of global river discharge. Communications Earth & Environment, 4, 48, https://doi.org/10.1038/s43247-023-00697-6.

Howcroft, W., Cartwright, I., Cendón, D.I., 2019. Residence times of bank storage and return flows and the influence on river water chemistry in the upper Barwon River, Australia. Applied Geochemistry., 101, 31-41, https://doi.org/10.1016/j.apgeochem.2018.12.026.

Hrachowitz, M., Savenije, H., Bogaard, T. A., Tetzlaff, D., Soulsby, C., 2013. What can flux tracking teach us about water age distribution patterns and their temporal dynamics?. Hydrology and Earth System Sciences, 17, 533-564, https://doi.org/10.5194/hess-17-533-2013.

Jasechko, S., Kirchner, J.W., Welker, J.M., McDonnell, J.J., 2016. Substantial proportion of global streamflow less than three months old. Nature Geoscience, 9, 126-129.https://doi.org/10.1038/ngeo2636.

Kalbus, E., Reinstorf, F., Schirmer, M., 2006. Measuring methods for groundwater? surface water interactions: a review. Hydrology and Earth System Sciences, 10, 873-887. https://doi.org/10.5194/hess-10-873-2006.

Keywood, M.D., Fifield, L.K., Chivas, A.R., Cresswell, R.G., 1998. Fallout of chlorine 36 to the Earth's surface in the southern hemisphere. Journal of Geophysical Research, 103 (D7), 8281-8286, https://doi.org/10.1029/97JD03125.

Kirchner, J. W., Feng, X., Neal, C., Robson, A. J., 2004. The fine structure of water-quality dynamics: the (high-frequency) wave of the future, Hydrological Processes, 18, 1353-1359, https://doi.org/10.1002/hyp.5537.

Chapter 5

Kirchner, J. W., 2016. Aggregation in environmental systems–Part 1: Seasonal tracer cycles quantify young water fractions, but not mean transit times, in spatially heterogeneous catchments, Hydrology and Earth System Sciences, 20, 279-297, https://doi.org/10.5194/hess-20-279-2016

Małoszewski, P., Zuber, A., 1982. Determining the turnover time of groundwater systems with the aid of environmental tracers: 1. Models and their applicability, Journal of Hydrology, 57, 207-231, https://doi.org/10.1016/0022-1694(82)90147-0.

McCallum, J. L., Cook, P. G., Berhane, D., Rumpf, C., McMahon, G. A., 2012. Quantifying groundwater flows to streams using differential flow gaugings and water chemistry. Journal of Hydrology, 416, 118-132, https://doi.org/10.1016/j.jhydrol.2011.11.040.

McGuire, K. J., McDonnell, J. J., 2006. A review and evaluation of catchment transit time modelling, Journal of Hydrology, 330, 543-563, https://doi.org/10.1016/j.jhydrol.2006.04.020.

Messager, M. L., Lehner, B., Cockburn, C., Lamouroux, N., Pella, H., Snelder, T., Datry, T., 2021. Global prevalence of non-perennial rivers and streams, Nature, 594, 391-397, https://doi.org/10.1038/s41586-021-03565-5.

Morgenstern, U., Stewart, M. K., Stenger, R.,2010. Dating of streamwater using tritium in a post nuclear bomb pulse world: continuous variation of mean transit time with streamflow, Hydrology and Earth System Sciences, 14, 2289–2301, https://doi.org/10.5194/hess-14-2289-2010.

Ortega, L., Manzano, M., Custodio, E., Hornero, J., Rodríguez-Arévalo, J., 2015. Using 222Rn to identify and quantify groundwater inflows to the Mundo River (SE Spain). Chemical Geology, 395, 67–79. https://doi.org/10.1016/j.chemgeo.2014.12.002.

Oxtobee, J. P., Novakowski, K. S., 2003. Ground water/surface water interaction in a fractured rock aquifer. Groundwater, 41, 667-681, https://doi.org/10.1111/j.1745-6584.2003.tb02405.x.

Rinaldo, A., Benettin, P., Harman, C. J., Hrachowitz, M., McGuire, K. J., Van Der Velde, Y., Botter, G., 2015. Storage selection functions: A coherent framework for quantifying how catchments store and release water and solutes, Water Resources Research, 51, 4840-4847, https://doi.org/10.1002/2015WR017273.

Romeijn, P., 2019. Microbial metabolic activity and nutrient turnover at groundwater-surface water interfaces (Doctoral dissertation, University of Birmingham).

Rudnick, S., Lewandowski, J., Nützmann, G., 2015. Investigating groundwater-lake interactions by hydraulic heads and a water balance. Groundwater, 53, 227-237, https://doi.org/10.1111/gwat.12208.

Shanafield, M., Bourke, S.A., Zimmer, M.A., Costigan, K.H., 2021. An overview of the hydrology of non-perennial rivers and streams. Wiley Interdisciplinary Reviews: Water, 8, e1504. https://doi.org/10.1002/wat2.1504.

Stewart, M. K., Morgenstern, U., Cartwright, I., 2021. Comment on “A comparison of catchment travel times and storage deduced from deuterium and tritium tracers using StorAge Selection functions” by Rodriguez et al. (2021), Hydrology and Earth System Sciences, 25, 6333–6338, https://doi.org/10.5194/hess-25-6333-2021.

Stewart, M. K., Morgenstern, U., McDonnell, J. J., 2010. Truncation of stream residence time: how the use of stable isotopes has skewed our concept of streamwater age and origin, Hydrological Processes, 24, 1646-1659, https://doi.org/10.1002/hyp.7576.

Stoelzle, M., Schuetz, T., Weiler, M., Stahl, K., Tallaksen, L. M., 2020. Beyond binary baseflow separation: a delayed-flow index for multiple streamflow contributions. Hydrology and Earth System Sciences, 24, 849-867, https://doi.org/10.5194/hess-24-849-2020.

Chapter 5

Tadros, C. V., Hughes, C. E., Crawford, J., Hollins, S. E., Chisari, R., 2014. Tritium in Australian precipitation: A 50 year record. Journal of hydrology, 513, 262-273, https://doi.org/10.1016/j.jhydrol.2014.03.031.

Tan, H., Chen, X., Shi, D., Rao, W., Liu, J., Liu, J., Wang, J., 2021. Base flow in the Yarlungzangbo River, Tibet, maintained by the isotopically-depleted precipitation and groundwater discharge. Science of The Total Environment, 759, 143510, https://doi.org/10.1016/j.scitotenv.2020.143510.

Voltz, T., Gooseff, M., Ward, A. S., Singha, K., Fitzgerald, M., Wagener, T., 2013. Riparian hydraulic gradient and stream-groundwater exchange dynamics in steep headwater valleys. Journal of Geophysical Research: Earth Surface, 118, 953-969, https://doi.org/10.1002/jgrf.20074.

Yu, M. C. L., Cartwright, I., Braden, J. L., De Bree, S. T., 2013. Examining the spatial and temporal variation of groundwater inflows to a valley-to-floodplain river using 222 Rn, geochemistry and river discharge: the Ovens River, southeast Australia. Hydrology and Earth System Sciences, 17, 4907-4924, https://doi.org/10.5194/hess-17-4907-2013.

Zhou, Z., Cartwright, I., Morgenstern, U., 2022. Sources and mean transit times of stream water in an intermittent river system: the upper Wimmera River, southeast Australia. Hydrology and Earth System Sciences, 26, 4497-4513, https://doi.org/10.5194/hess-26-4497-2022.

Zimmer, M. A., McGlynn, B. L., 2017. Ephemeral and intermittent runoff generation processes in a low relief, highly weathered catchment. Water Resources Research, 53, 7055-7077, https://doi.org/10.1002/2016WR019742.

Appendix

S1-Geochemistry of stream water (SW), pool water (PW), and near-river water (NRW) in the upper Wimmera River

Sample ID	EC	HCO_3	F	Cl	Br	NO_3	SO_4	Na	K	Ca	Mg	Si	Li	Sr	TDS	^3H	^{18}O	^2H
	μs/cm	mg/L	mg/L	mg/L	mg/L	mg/L	mg/L	mg/L	mg/L	mg/L	mg/L	mg/L	mg/L	mg/L	mg/L	TU	SMOW	SMOW
PW																		
Elmhurst	6140	300	0.47	2431	6.60	0.82	58.9	993	5.3	151	265	12.20	0.019	1.87	4225	1.65	-0.9	-13
Eversley 2	4010	376	0.39	1357	4.07	0.16	7.8	684	10.7	84	165	2.19	0.013	0.98	2692		3.4	-2
Eversley 1	4900	520	0.54	1555	4.85	0.49	90.7	874	9.1	82	173	6.47	0.025	1.02	3317	0.88	-1.6	-20
CE1A	4630	326	0.63	1613	5.29	0.46	114.9	876	5.9	70	172	14.87	0.037	0.87	3200		-3.3	-24
CE1B	3150	356	0.64	961	3.13	0.15	63.3	576	6.1	48	105	18.18	0.03	0.58	2139	1.00	-2.0	-18
CE2	4600	196	0.37	1607	4.60	0.55	113.6	804	9.0	83	165	5.12	0.022	0.89	2990	2.24	1.9	-1
Joel 1	4560	326	0.50	2893	8.39	0.27	90.1	815	9.0	83	166	5.08	0.015	1.57	4397	2.76	6.7	19
Joel 2	3840	368	0.45	2001	6.84	0.94	165.2	1049	7.1	112	258	12.12	0.022	1.52	3982	0.64	-2.7	-24
Joel 3	9160	285	0.38	4408	12.60	1.82	232.9	1626	13.1	201	432	4.87	0.013	2.41	7221		0.6	-9
Joel 4	5600	179	0.44	2125	5.82	1.06	188.4	976	11.4	96	214	7.24	0.011	1.10	3805		1.7	-1
Joel 5	5010	170	0.44	1807	4.90	0.70	122.5	888	10.7	80	186	4.13	0.013	0.96	3276		3.4	3
37 PAR	6580	194	0.53	2558	6.98	0.64	222.6	1164	14.2	111	249	3.50	0.017	1.28	4525		5.1	12
GC 1	15330	433	0.72	6208	15.43	1.62	698.1	2956	22.5	334	744	1.67	0.025	3.91	11421		5.7	9
GC 2	10050	377	0.59	3879	10.95	0.74	251.5	1710	21.7	213	453	3.68	0.022	2.71	6924		7.4	18
Camb	6420	460	0.72	2607	7.38	0.26	41.1	1180	15.7	101	223	1.73	0.011	1.48	4639	3.02	9.7	27
Glen	3400	228	0.44	1148	3.31	0.66	43.0	631	13.5	54	113	1.29	0.007	0.68	2237	3.29	8.3	22
SW-7																		
Elmhurst	1109	161	0.13	369	0.77	7.40	34.0	190	3.5	19	33	7.30	0.008	1.76	827	2.69	-6.2	-32
Elm Town	1395	46	0.14	505	1.11	5.14	43.8	239	4.8	30	51	8.35	0.011	2.67	936		-6.2	-33
Eversley 2	1790	102	0.25	618	1.56	2.35	63.9	286	5.5	36	63	7.72	0.009	3.47	1190		-6.2	-36

Appendix

Eversley 1	1497	70	0.23	510	1.24	3.43	53.8	255	5.3	31	56	7.36	0.007	3.03	996		-6.5	-36
CE1	1666	81	0.22	578	1.35	2.42	67.9	275	6.1	33	61	6.48	0.008	3.19	1115	1.85	-6.5	-38
CE2	2210	154	0.33	763	2.02	2.71	81.6	413	6.9	37	79	7.11	0.01	3.83	1549		-5.8	-34
Joel 1	2880	73	0.29	1073	2.70	3.18	111.5	547	9.0	35	97	5.61	0.008	3.67	1961		-6.5	-37
Joel 2	2870	137	0.38	993	2.76	4.36	104.3	493	8.5	32	86	5.40	0.008	3.51	1869	2.76	-5.9	-32
Joel 3	2710	92	0.79	952	2.62	7.39	98.7	271	5.5	18	52	6.62	0.007	3.47	1510		-5.9	-29
Joel 4	2714	107	0.33	985	2.69	2.52	109.9	529	7.6	43	101	6.53	0.007	4.66	1901		-6.0	-36
Joel 5	3220	93	0.37	1187	3.24	1.40	123.7	590	8.2	51	117	7.51	0.009	5.57	2188		-6.0	-36
37 PAR	2610	99	0.30	886	2.37	2.72	99.8	457	8.1	36	89	5.96	0.007	3.91	1690		-6.3	-37
OLB	1890	81	0.30	592	1.53	2.65	76.2	316	7.0	23	58	4.81	0.005	2.66	1165		-6.5	-37
GC 1	2005	55	0.23	711	1.68	2.85	96.8	363	8.2	29	68	6.43	0.007	2.98	1346		-7.2	-42
GC 2	2346	56	0.24	793	1.91	2.73	126.0	431	9.3	36	83	6.43	0.008	3.78	1550		-7.2	-43
Camb	2235	110	0.23	804	2.31	4.49	70.8	424	7.7	30	71	4.34	0.007	3.40	1532	3.00	-6.0	-33
GSR	2245	66	0.28	779	2.24	4.97	72.0	428	7.1	31	68	4.92	0.005	3.48	1466		-6.2	-35
Glen	2612	92	0.36	894	2.53	3.44	111.7	507	7.8	40	84	4.99	0.007	4.93	1752	2.41	-5.2	-33
HS1	3500	176	0.32	1285	3.88	3.93	111.2	712	9.4	56	112	5.02	0.009	6.33	2479		-3.6	-25
HS2	2265	153	0.24	723	1.99	4.35	77.7	400	7.8	39	70	4.73	0.007	4.02	1485		-5.3	-31
HS3	775	70	0.17	202	0.50	6.07	36.3	110	46.3	142	183	4.63	0.004	1.58	803		-6.4	-36
CB	294	35	0.19	56	0.11	7.18	22.8	54	31.3	61	80	4.87	0.002	0.71	355		-6.3	-34
FB	337	38	0.17	79	0.19	6.91	25.7	41	34.6	66	66	4.84	0.003	0.66	362		-6.2	-35
SW-9																		
Elmhurst	670	71	0.14	198	0.42	0.75	19.4	107	2.0	12	19	2.2	0.006	0.133	433	2.67	-5.4	-31
Elm Town	685	74	0.14	204	0.41	0.71	19.9	104	2.0	12	19	1.7	0.006	0.129	438		-3.9	-31
Eversley 2	920	77	0.17	282	0.56	0.50	35.8	143	5.6	18	26	6.0	0.004	0.177	594		-4.9	-31
Eversley 1	991	79	0.18	298	0.69	0.67	28.2	154	2.6	19	31	1.6	0.007	0.207	614		-5.6	-31
CE1	1014	94	0.20	310	0.77	0.68	30.0	174	3.1	20	35	2.4	0.007	0.208	670	2.58	-5.1	-30

Appendix

CE2	1127	99	0.19	351	0.83	0.41	34.3	194	3.3	21	38	4.7	0.008	0.242	747		-5.4	-30
Joel 1	1626	116	0.21	542	1.41	1.64	57.7	301	4.6	24	58	4.9	0.008	0.267	1112		-5.1	-30
Joel 2	1779	87	0.21	547	1.42	0.99	57.6	326	4.8	26	62	4.9	0.008	0.291	1118	2.48	-5.2	-30
Joel 3	1666	124	0.21	539	1.39	0.72	56.5	299	4.4	25	58	4.7	0.008	0.277	1114		-5.3	-29
Joel 4	1600	106	0.22	537	1.43	1.42	56.6	303	4.8	25	58	4.8	0.007	0.268	1099		-5.2	-29
Joel 5	1610	105	0.22	517	1.31	0.86	54.9	283	4.5	24	54	4.8	0.007	0.269	1050		-5.2	-29
37 PAR	1550	94	0.22	520	1.33	1.23	56.6	276	4.9	23	53	5.1	0.006	0.233	1035		-5.2	-31
OLB	1521	107	0.22	502	1.32	1.68	55.5	274	4.5	23	52	5.1	0.007	0.252	1027		-5.4	-31
GC 1	1455	99	0.21	455	1.18	1.34	52.6	256	4.9	21	48	5.6	0.007	0.236	944		-5.3	-31
GC 2	1466	65	0.21	461	1.19	1.68	54.6	264	4.7	21	49	5.8	0.006	0.243	928		-5.3	-31
Camb	1411	101	0.22	450	1.20	1.90	51.1	224	5.4	18	38	6.3	0.006	0.236	897	2.78	-5.9	-32
GSR	1359	104	0.24	461	1.25	1.94	54.6	251	5.0	20	43	6.3	0.005	0.217	948		-6.1	-32
Glen	1235	84	0.21	380	1.05	1.73	45.2	260	5.2	20	45	6.3	0.005	0.212	849	2.88	-5.6	-32
HS1	1157	98	0.21	357	0.94	1.59	42.8	214	5.6	17	36	6.3	0.005	0.199	780		-5.4	-32
HS2	1143	89	0.21	346	0.94	1.72	41.4	206	4.8	16	34	6.1	0.004	0.185	746		-5.4	-32
HS3	1129	96	0.21	345	0.89	1.92	41.3	207	5.5	16	34	6.2	0.005	0.189	756		-5.5	-32
CB	1117	88	0.20	317	0.84	1.79	37.9	202	5.0	16	33	6.2	0.004	0.182	708		-5.5	-31
FB	1063	90	0.22	329	0.87	1.72	39.9	194	5.8	15	32	6.1	0.004	0.181	715		-5.6	-32
SW-11																		
Elm 1	981	90	0.18	312	0.85	0.60	10.1	164	1.9	23	36	5.66	0.006	0.224	644	2.55	-4.8	-26
Elm Town	967	107	0.17	300	0.85	0.69	10.8	154	2.5	23	33	4.20	0.006	0.212	637		-4.1	-24
Eversley 2	nm	nm	nm	nm	nm	nm	nm	nm	nm	nm	nm	nm	nm	nm	nm	nm	nm	nm
Eversley 1	1755	209	0.25	575	1.56	0.78	26.9	325	4.0	40	74	5.06	0.01	0.402	1261		-2.9	-21
CE1	1552	170	0.25	480	1.11	1.17	22.3	279	3.9	34	61	1.75	0.009	0.336	1055	2.34	-3.5	-22
CE2	2055	155	0.26	723	2.22	1.45	45.1	392	3.9	41	82	5.16	0.013	0.412	1451		-3.3	-22
Joel 1	2443	154	0.24	871	2.46	2.97	63.6	467	5.9	41	98	2.57	0.008	0.441	1709		-2.9	-20

Appendix

Joel 2	2870	194	0.25	1027	2.77	1.66	69.9	554	5.5	54	124	4.03	0.008	0.585	2038	2.26	-3.0	-21
Joel 3	2760	206	0.27	979	2.81	0.92	57.7	538	5.7	51	119	4.48	0.007	0.560	1966		-3.1	-21
Joel 4	2250	171	0.24	790	2.16	2.08	53.0	435	5.5	40	93	3.26	0.007	0.431	1595		-3.0	-21
Joel 5	2191	162	0.26	757	2.53	1.38	54.9	427	5.7	39	91	3.42	0.007	0.412	1546		-3.1	-20
37 PAR	2085	144	0.24	719	2.02	0.92	56.1	408	5.8	37	85	2.01	0.007	0.382	1460		-3.1	-20
OLB	2087	142	0.28	705	2.01	3.12	52.8	400	6.5	36	83	1.09	0.007	0.381	1432		-2.7	-20
GC 1	2129	140	0.23	730	1.80	1.15	70.1	413	5.9	39	87	3.72	0.007	0.398	1492		-3.2	-22
GC 2	2148	159	0.27	732	2.22	1.97	53.8	426	6.5	39	87	3.95	0.007	0.412	1513		-3.0	-21
Camb	2239	156	0.25	771	2.00	1.49	66.3	443	6.0	39	87	2.42	0.007	0.422	1575	2.58	-3.1	-23
GSR	2199	155	0.26	744	2.21	1.58	61.6	433	6.9	39	84	2.38	0.007	0.427	1530		-3.3	-22
Glen	1925	133	0.22	639	1.81	1.83	58.0	378	6.3	34	73	3.03	0.006	0.363	1329	2.69	-3.7	-23
HS1	1871	138	0.26	627	1.68	3.21	51.8	367	6.9	33	70	3.42	0.006	0.351	1303		-3.2	-22
HS2	1876	162	0.26	612	1.81	2.15	42.9	364	7.2	34	69	3.81	0.005	0.361	1299		-3.0	-21
HS3	1821	160	0.26	609	1.73	1.64	47.1	359	6.9	33	68	3.08	0.005	0.352	1290		-3.0	-21
CB	1810	171	0.25	605	1.48	1.65	44.3	358	6.7	33	68	1.89	0.005	0.359	1292		-2.9	-21
FB	1823	122	0.25	607	1.59	2.85	49.0	364	7.0	34	67	2.67	0.005	0.357	1258		-3.1	-21
NRW																		
Elmhurst	1853	216	0.18	619	1.90	2.39	5.2	294	4.5	92	98	13.65	0	0.817	1350		-5.1	-29
Ever1-1	2687	295	0.32	910	2.95	2.41	9.8	292	8.2	29	59	3.37	0	0.705	1613		-1.5	-16
Ever1-2	2720	140	0.36	957	2.63	1.60	7.3	576	12.6	45	106	7.37	0	0.541	1858		-1.9	-17
Ever1-3	3140	134	0.69	1103	3.64	1.04	2.6	694	11.9	60	136	10.00	0	0.471	2158		-3.0	-21
CE1	6080	336	0.67	2615	8.30	3.62	1.4	2228	11.1	162	411	19.10	0	1.013	5800		-4.8	-28
Joel 1-1	4390	406	0.46	2453	7.75	2.19	41.5	1443	12.2	127	310	8.66	0	0.909	4814		-2.3	-19
Joel1-2	5520	336	0.46	1461	4.57	0.97	1.3	1012	6.0	91	202	7.42	0	1.185	3123		-2.8	-20
Joel3-1	3710	296	0.48	1450	5.42	0.63	12.0	818	6.8	80	190	10.46	0	1.097	2873		-2.9	-19
Joel3-2	3890	427	0.38	1423	4.99	2.38	9.5	1075	7.8	100	253	4.35	0	0.93	3309		-3.4	-21

Appendix

OLB-1	1977	198	0.22	621	2.05	0.51	96.3	331	15.6	32	78	4.41	0	0.403	1380		-0.5	-8
OLB-2	1779	78	0.31	576	1.80	0.32	16.9	326	12.5	30	73	5.70	0	0.324	1122		-0.9	-11
OLB-3	1764	109	0.29	586	1.84	0.51	28.4	296	11.7	28	67	5.05	0	0.324	1135		-1.0	-11
Camb	1034	137	0.27	320	1.02	0.60	15.7	188	9.1	20	37	8.09	0	0.214	741		-2.1	-14

nm=not measured

Appendix

S2-Geochmistry of regional groundwater in the Wimmera Catchment

Bore ID	EC	HCO_3	F	Cl	Br	NO_3	SO_4	Na	K	Ca	Mg	Si	Li	Sr	TDS	^{3}H	^{14}C	^{18}O	^{2}H
	μs/cm	mg/L	mg/L	mg/L	mg/L	mg/L	mg/L	mg/L	mg/L	mg/L	mg/L	mg/L	mg/L	mg/L	mg/L	TU	pMC	SMOW	SMOW
5396	3520	32.9	0.05	1244	3.76	1.34	5	605	10.0	30	137	0.56	0.235	0.531	2070			-6.6	-33
5252	9670	148.8	0.15	3381	7.59	1.89	859	1896	18.7	158	475	6.03	0.013	1.513	6955			-6.5	-38
5242	6000	79.3	0.71	2041	6.16	28.60	234	1222	9.0	37	196	30.85	0.017	0.578	3887	0.16	92.26	-5.8	-32
5243	5010	42.7	0.37	1699	4.77	9.28	135	1012	6.9	30	150	30.67	0.026	0.48	3121	0.25	92	-5.6	-33
5244	3410	175.7	0.58	965	3.01	3.19	152	694	10.4	49	70	18.04	0.132	0.303	2142			-6.0	-36
5245	1633	130.5	0.49	459	1.15	1.85	17	297	1.5	14	49	23.14	0.035	0.158	995			-6.1	-34
5246	1924	93.9	0.29	554	1.37	1.54	46	323	0.6	24	64	20.19	0.032	0.27	1130			-6.3	-34
5248	14500	134.2	0.52	5205	17.51	2.72	732	3140	16.3	57	464	61.87	0.212	0.766	9833			-5.3	-29
5227	3150	146.4	0.23	847	2.75	3.44	75	395	5.0	46	110	12.86	0.006	0.629	1644	0.04	82.8	-5.4	-31
5228	3090	102.5	0.09	946	3.17	0.54	55	430	5.3	50	95	15.22	0.008	0.622	1704	0.06	84.2	-5.4	-32
5226	1044	nm	0.11	313	1.09	3.00	13	156	0.8	18	22	22.62	0.006	0.186	550			-5.8	-34
5229	18500	396.5	0.52	1308	4.07	5.10	147	475	72.7	39	15	0.00	0.007	0.989	2464	0.03	66.8	-5.6	-33
5230	4980	1317.6	0.89	6582	23.11	1.47	744	4281	27.6	172	556	9.94	0.009	2.873	13719	0.25	89.5	-4.4	-29
5232	8080	534.4	0.85	2591	8.72	1.50	303	1564	14.6	117	330	8.49	0.022	1.995	5476	0.02	73.8	-4.9	-31
5234	4440	173.2	0.42	1431	4.85	1.25	146	814	7.1	54	152	15.70	0.024	0.916	2800	0.02	57.1	-4.8	-29
5235	2473	150.1	0.33	699	2.22	1.40	60	396	5.1	34	91	18.61	0.01	0.53	1458	bd	78.4	-5.3	-30
5236	6650	589.3	2.53	2032	6.64	3.58	221	1658	3.1	26	93	5.29	0.01	0.443	4640	0.45	102.9	-5.1	-30
5377	11700	240.3	0.88	4170	13.08	3.36	680	2577	26.3	184	392	6.44	0.035	4.686	8299			-5.8	-34
5379	7730	818.6	2.07	2224	6.93	1.04	516	1948	12.1	41	178	4.79	0.002	1.125	5754	bd	88.4	-5.7	-33
5381	5370	319.6	1.20	1846	6.33	1.39	250	1206	16.0	79	175	3.05	0	1.144	3904			-5.2	-29
5383	20390	95.2	2.84	8414	30.53	332.63	1921	480	22.6	443	813	0.00	0.054	6.332	12561			-4.8	-29
5384	20750	120.8	0.26	8106	19.24	7.14	1209	440	20.3	435	808	0.00	0.021	15.13	11182			-4.6	-28
2541	6420	439.2	0.77	2046	6.63	32.51	373	1305	11.5	79	196	27.59	0.004	1.458	4518			-4.5	-28
2542	5300	328.2	0.63	1701	4.08	0.91	228	1118	9.6	69	169	22.00	0.004	1.254	3651	0.02	80.5	-4.4	-28
113123	11320	568.5	1.62	3719	10.77	18.08	661	2527	12.6	138	365	17.31	0.002	2.867	8042			-4.9	-28

nm=not measured

bd=below detection

Appendix

S3-Geochemistry of stream water (SW), pool water (PW) in the upper Avoca River

Sample ID	EC	HCO_3	F	Cl	Br	NO_3	SO_4	Na	K	Ca	Mg	Si	Sr	TDS	^3H	$R^{36}Cl$	^{18}O	^2H	^{222}Rn
	µs/cm	mg/L	mg/L	mg/L	mg/L	mg/L	mg/L	mg/L	mg/L	mg/L	mg/L	mg/L	mg/L	mg/L	TU	10^{-15}	SMOW	SMOW	Bq/m^3
PW																			
Headwaters	4300	257	0.61	2411	6.28	2.31	85.0	825	14.0	189.5	381.1	2.14	1.05	4175	2.36	31.9	9.5	29	38
Pellets	2310	193	0.52	905	2.33	1.09	57.5	439	6.7	38.8	113.8	18.07	0.28	1776			-2.0	-16	
Lonarch	4150	316	0.34	2706	6.70	1.64	26.3	928	4.9	204.6	358.6	10.60	1.18	4564			-3.0	-18	3690
Lexton	nm	nm	nm	nm	nm	nm	nm	nm	nm	nm	nm	nm	nm	nm			nm	nm	nm
Amphitheatre	4590	516	0.69	2389	9.34	0.98	135.1	1123	8.7	125.7	283.9	0.74	1.15	5258	1.64	45.6	0.0	-8	2040
Amph Ck	4730	620	0.64	3030	7.05	1.45	35.2	1147	8.5	100.3	252.7	7.25	0.98	4545			0.1	-7	794
Greenhill	2920	375	0.35	1190	3.55	1.84	81.6	587	7.8	46.5	119.2	6.14	0.45	2418			-4.1	-23	9480
Lions	2220	207	0.29	726	1.79	1.53	22.8	346	8.3	43.7	84.1	2.15	0.38	1444			2.5	3	716
Vale Bridge	8800	444	0.40	4248	9.62	2.85	504.8	1905	22.6	241.2	492.6	10.20	2.35	7881			2.6	3	541
Bealiba	9390	484	0.74	4214	9.32	4.25	615.7	2101	23.9	180.3	442.1	4.10	1.87	7692	2.79	42.1	5.9	14	503
Mills Ln	6970	680	0.91	2858	7.84	2.00	179.0	1630	24.3	100.2	297.3	0.60	1.02	5779			5.6	17	320
River Bend	9000	660	1.09	4424	12.03	1.83	23.6	2304	29.8	109.4	416.2	0.76	1.30	7982			13.3	44	337
Archdale Junc	8610	948	1.09	4564	12.21	2.19	9.5	2394	21.1	143.1	434.9	2.67	2.02	8533			5.5	17	343
Arch Res	10090	913	1.11	5645	16.06	3.00	318.8	2955	22.6	136.2	567.0	2.04	2.91	10579	1.89	57.7	3.6	7	343
Maff	11100	780	0.83	6420	16.49	2.65	350.8	3316	26.2	154.6	601.6	1.14	3.31	11670			5.3	14	250
Dunnoly	9760	795	0.60	7058	18.47	2.13	299.4	3581	27.3	190.9	588.5	1.69	3.32	12563			6.3	18	298
Emu Logan	14070	60	0.03	12773	31.55	1.68	1113.6	5375	79.7	556.9	1123.9	12.99	9.19	21129			5.1	14	653
Fentons Ck	12180	673	0.48	8258	10.97	1.98	229.1	4158	21.8	161.9	370.0	1.71	2.93	7570			0.9	-8	480
Logan Res	7850	400	0.00	4051	21.40	2.56	2318.0	2048	48.6	418.8	835.3	6.79	8.76	16468	4.57	66.9	1.6	-8	266
Gower Logan	5030	547	0.54	2050	5.57	1.24	111.7	1128	17.5	78.1	167.2	2.35	1.34	4109			-1.4	-18	187
Old St A	4630	427	0.38	1931	5.54	1.46	158.3	1105	17.9	96.2	160.4	2.26	1.58	3905			-2.5	-19	293
K16 Res	10700	763	0.58	6420	19.33	4.56	935.0	3785	33.6	274.6	526.0	7.85	5.34	12769			-2.0	-16	366
K 15 Res	5980	658	0.37	2757	8.27	2.74	38.7	1488	19.6	122.9	215.0	10.93	1.74	5321			1.1	-12	209
Coonooer	3990	476	0.30	1797	5.20	0.84	45.9	971	16.8	91.7	152.0	9.61	1.26	3566	5.11	60.8	-1.3	-16	233
7 Mile	5290	559	0.49	2501	7.71	0.95	43.7	1337	20.1	113.4	194.7	9.35	1.49	4788	5.03	57.2	3.0	-3	152
Hoggs Lane	6930	797	0.56	3480	10.60	3.11	26.7	1751	27.4	128.8	250.9	6.22	1.89	6482			4.5	3	173
Charlton Town	7390	466	0.44	3789	10.99	5.08	352.6	2041	24.6	138.1	298.1	4.72	2.02	7131			0.5	-13	144

Appendix

Boort	8590	705	0.50	4826	14.31	2.68	205.9	2567	27.3	181.5	365.9	2.10	3.06	8898	4.42	56.6	3.4	-1	205
SW-7																			
Headwaters	2240	29	0.08	544	1.05	65.89	254.7	238	6.6	62.6	114.2	14.45	0.42	1331	2.40	33.3	-6.1	-33	1771
Pellets	875	148	0.17	241	0.56	2.70	52.3	133	3.3	15.5	36.5	8.39	0.13	642			-5.6	-31	1150
Lonarch	1252	96	0.30	382	0.91	3.31	36.2	198	5.1	29.6	53.4	9.99	0.20	815			-5.4	-31	1010
Lexton	3650	115	0.36	555	1.37	4.57	38.2	284	6.9	40.0	71.5	7.94	0.30	1125			-5.4	-30	732
Amphitheatre	2053	194	0.36	663	3.89	2.86	97.3	323	8.6	79.4	176.3	7.66	0.97	2612	2.21	58.5	-5.3	-30	950
Amph Ck	1657	133	0.33	1337	1.73	3.97	47.6	704	7.1	43.7	84.0	8.12	0.39	1316			-5.1	-30	1670
Greenhill	2196	172	0.32	731	2.01	2.61	61.1	344	6.5	44.3	92.1	7.43	0.45	1463			-5.2	-28	1630
Lions	1424	104	0.24	652	1.87	2.79	38.3	374	6.5	27.2	55.8	5.59	0.27	1269			-5.1	-26	900
Vale Bridge	1047	82	0.21	441	0.89	3.20	33.9	231	6.1	20.9	39.2	5.04	0.20	863			-4.8	-24	853
Bealiba A	982	73	0.21	294	0.76	3.25	40.2	146	5.8	18.5	34.8	4.87	0.18	621			-4.8	-21	797
Mills Ln	1035	60	0.21	303	0.76	4.19	72.3	171	7.1	18.9	38.1	5.13	0.21	680			-4.6	-21	588
River Bend Lane	1264	79	0.21	370	0.90	6.05	117.7	224	8.5	22.4	48.6	4.98	0.26	883			-4.5	-19	381
Archdale Junc	812	66	0.20	229	0.59	3.35	46.5	132	6.0	14.7	28.5	4.06	0.16	531			-4.4	-18	436
Archdale Res	1121	58	0.23	337	0.90	4.89	54.7	188	6.7	20.2	38.8	4.16	0.26	714	2.23	55.1	-4.4	-18	399
Maffescioni	1279	85	0.22	384	0.98	4.85	69.2	227	7.8	22.1	44.0	4.36	0.29	850			-4.4	-18	581
Dunnoly	1536	74	0.27	587	1.56	5.96	104.7	289	8.3	28.4	51.3	4.39	0.38	1155			-4.2	-18	384
Emu-Logan	1458	88	0.26	521	1.23	5.70	96.6	283	8.3	22.5	44.4	4.39	0.38	1075			-4.3	-18	606
Fentons Ck	384	82	0.22	95	0.74	9.32	58.3	57	7.6	18.3	30.7	4.31	0.29	691			-4.6	-23	246
Logan Reserve	1022	48	0.12	309	0.13	7.06	13.8	171	7.5	9.5	9.5	4.71	0.12	253			-4.5	-20	236
Gowar-Logan	1379	62	0.19	371	0.92	5.54	63.9	254	7.6	22.2	40.8	3.85	0.37	832			-4.3	-18	439
Old St Arnaud	1354	65	0.21	382	0.93	6.94	65.1	239	7.4	22.8	41.4	3.91	0.39	834			-4.3	-18	272
K16 Res	1152	55	0.22	338	0.88	7.95	53.9	205	7.2	19.6	32.1	4.12	0.31	725			-4.7	-22	218
K15 Res	1562	98	0.27	562	1.44	7.59	86.8	296	8.5	25.0	44.6	4.24	0.42	1135			-4.4	-20	265
Coonooer	1175	65	0.14	334	0.83	6.95	54.0	209	7.6	19.5	33.4	4.53	0.31	734			-4.7	-21	132
7 Mile	2245	90	0.26	651	1.65	6.21	99.9	430	9.4	31.6	66.0	4.32	0.54	1390	2.22	58.7	-4.4	-21	305
Hoggs Lane	3380	130	0.32	1265	3.23	6.76	172.1	720	13.7	52.6	112.8	4.84	0.92	2481			-4.2	-23	319
Charlton Town	4170	128	0.31	1421	3.58	6.50	188.0	870	14.9	64.5	146.0	4.84	1.14	2848			-4.1	-24	161
Boort	4810	140	0.27	1643	4.26	10.53	194.8	1073	16.6	78.2	179.5	4.62	1.41	3345			-3.3	-17	53
SW-8																			
Headwaters	964	35	0.09	247	0.58	2.60	92.6	108	4.5	24.3	42.2	10.24	0.18	567	2.67	36.4	-5.3	-30	2920

Appendix

Pellets	983	41	0.12	304	0.75	1.81	75.7	142	4.3	24.2	51.0	9.26	0.20	653			-5.3	-30	2420
Lonarch	1253	83	0.27	440	1.40	3.74	39.7	194	4.0	34.1	59.8	9.22	0.26	869			-5.1	-28	1710
Lexton	1596	193	0.28	490	1.26	1.37	29.3	273	5.1	40.1	71.1	5.54	0.34	1110			-4.8	-27	1560
Amphitheatre	1600	226	0.31	520	2.47	2.17	54.7	268	5.7	45.1	103.1	2.91	0.61	1677	2.39	42.6	-4.8	-28	1340
Amph Ck	2298	170	0.29	818	1.39	1.91	33.1	416	5.0	35.4	66.1	3.23	0.34	1105			-4.5	-26	1600
Greenhill	1821	187	0.30	626	1.78	2.19	43.3	322	5.3	38.4	79.8	3.54	0.43	1310			-4.8	-28	1330
Lions	1664	158	0.27	564	1.58	1.47	41.0	277	5.2	33.7	67.3	2.01	0.38	1152			-4.7	-27	932
Vale Bridge	1481	140	0.25	489	1.27	1.68	37.5	242	5.1	30.3	58.2	2.50	0.33	1008			-4.8	-27	824
Bealiba A	1424	140	0.25	468	1.30	1.96	38.4	233	5.0	28.9	55.5	2.71	0.31	975			-4.7	-29	675
Mills Lane	1170	122	0.23	365	0.99	2.38	44.1	189	5.1	22.6	41.9	4.42	0.25	798			-5.1	-29	608
River Bend Ln	971	110	0.22	297	0.73	3.06	47.9	162	5.1	17.4	33.6	5.08	0.20	682			-5.2	-30	362
Archdale Junc	925	94	0.21	267	0.71	2.78	65.0	152	5.3	16.6	31.6	5.07	0.19	640			-5.1	-29	565
Archdale Res	1267	125	0.25	439	1.14	2.85	103.8	218	6.2	25.0	44.7	5.43	0.33	971	2.77	54.3	-4.8	-28	368
Maffescioni	1048	118	0.23	320	0.89	2.85	39.6	171	5.4	20.1	35.2	4.60	0.26	717			-5.1	-28	601
Dunnoly	984	126	0.23	298	0.78	2.69	37.6	161	5.3	18.4	32.4	4.49	0.25	687			-4.9	-27	457
Emu-Logan	1221	116	0.21	382	1.02	2.45	44.2	205	6.2	22.0	39.4	4.89	0.33	824			-4.5	-25	836
Fentons Ck	1054	124	0.22	312	0.95	2.88	42.7	181	6.0	21.9	38.3	4.53	0.32	812			-2.6	-11	231
Logan Reserve	1197	109	0.15	374	0.79	3.86	72.3	197	7.8	21.3	28.6	5.22	0.39	742			-4.7	-25	338
Gowar-Logan	1170	121	0.23	375	0.99	3.29	44.5	200	6.1	22.1	38.1	4.38	0.33	816			-4.5	-24	240
Old St Arnaud	1197	124	0.22	375	1.01	3.05	45.7	206	6.1	21.6	36.9	4.35	0.34	823			-4.4	-23	169
K16 Res	1371	119	0.22	445	1.19	2.94	52.1	240	6.6	24.4	40.7	4.38	0.39	936			-4.5	-24	207
K15 Res	1431	119	0.22	459	1.19	3.50	54.5	245	6.8	25.2	42.2	4.61	0.41	961			-4.4	-22	193
Coonooer	1471	137	0.22	480	1.41	3.85	56.5	255	7.1	26.1	44.0	4.79	0.42	1016			-4.2	-22	272
7 Mile	1669	132	0.21	561	1.52	2.71	68.0	292	7.9	29.7	55.2	5.34	0.49	1155	2.57	50.3	-4.3	-23	192
Hoggs Lane	1611	132	0.21	538	1.39	3.03	71.4	275	8.0	29.3	51.2	5.71	0.49	1116			-4.3	-23	288
Charlton Town	1525	137	0.22	496	1.30	3.44	66.0	264	7.8	26.6	43.7	5.60	0.45	1052			-4.4	-24	168
Boort	1663	133	0.20	557	1.4331	3.5591	72.3	290	8.468	29.7	50.8	5.43	0.51	1152			-4.2	-22	161

nm=not measured

Appendix

S4-Geochemistry of regional groundwater in the Avoca Catchment

Bore ID	Depth	EC	HCO_3	F	Cl	Br	NO_3	SO_4	Na	K	Ca	Mg	Si	Sr	TDS	^3H	^{14}C	^{18}O	^2H	^{222}Rn
	meter	µs/cm	mg/L	mg/L	mg/L	mg/L	mg/L	mg/L	mg/L	mg/L	mg/L	mg/L	mg/L	mg/L	mg/L	TU	pMC	SMOW	SMOW	Bq/m^3
8003930	30	1669	239	0.33	625	1.92	3.18	64	362	3.1	25	79	6.17	0.428	1409			-6.4	-36	18800
8003931	52	1773	475	0.96	580	1.89	0.60	11	490	10.4	20	40	6.73	0.190	1635			-6.1	-34	6510
8003924	42	6460	473	0.84	3239	11.20	4.09	535	2243	28.3	129	199	12.39	1.358	6874	0.06	34.04	-4.1	-28	20700
8003927	18	1643	192	0.44	489	1.49	23.40	74	387	5.9	20	38	5.64	0.273	1236			-5.7	-33	14900
8003936	12	8840	1457	0.92	4361	12.75	3.84	636	3089	42.6	174	379	13.85	2.224	10171	bd	93.87	-5.1	-32	16900
8003937	86	2840	228	0.39	1089	3.10	1.09	45	660	9.8	45	62	6.11	1.143	2150			-5.5	-35	nm
8003934	58	2210	209	0.33	856	2.70	1.35	92	628	7.6	39	52	6.31	1.130	1894	bd	70.23	-5.8	-33	8800
8003935	30	2870	440	0.41	1054	2.98	4.37	195	677	12.5	52	70	7.66	0.604	2516			-5.8	-35	107000
101708	11	5260	278	0.73	2876	9.34	3.81	422	1736	20.4	88	178	8.99	0.605	5621			-5.9	-32	37200
8003928	44	3680	268	0.48	1686	5.01	2.57	209	1052	20.1	90	100	6.23	2.075	3441			-5.3	-33	16200
60091	4	7880	888	0.83	4231	12.90	4.81	501	2723	36.3	148	198	15.87	3.209	8760			-5.3	-33	nm
8003932	17	7090	650	0.71	4038	11.78	2.55	478	2519	26.6	136	199	10.16	3.345	8072	0.04	73.63	-4.9	-32	23200
8003933	60	2281	288	0.34	1079	2.99	3.74	137	718	10.2	41	63	3.88	0.588	2347	1.08	61.59	-6.7	-38	2470
71129	60	9300	675	1.52	5536	20.19	1.32	940	3105	41.4	211	386	13.88	1.641	10931			-7.7	-52	52500
109570	30	12060	471	1.62	6832	20.32	8.17	1236	4578	80.3	229	375	18.60	13.883	13850	bd	58.42	-4.9	-32	93800
110184	30	3680	332	0.43	1701	6.37	3.11	300	1123	19.4	69	135	8.66	1.584	3698	0.16	93.5	-5.6	-33	40600
110185	13	10020	854	1.48	5088	20.10	2.47	687	3168	39.0	183	380	14.20	7.743	10438	0.29	98.05	-5.5	-32	10020
119378	11	6570	272	0.75	4233	10.32	3.87	478	2485	30.8	132	365	14.27	3.010	8024	0.06	88.94	-4.9	-32	27800
95032	80	10060	156	1.41	5810	20.37	4.97	1159	3365	58.6	208	372	14.20	6.260	11170			-5.3	-36	nm
95033	40	9070	234	1.32	4550	16.02	6.78	869	2555	46.8	132	279	15.14	5.306	8705			-4.7	-32	11100

bd=below detection

nm-not measured